UNIVERSIDADE DE LISBOA
FACULDADE DE CIÊNCIAS
DEPARTAMENTO DE GEOLOGIA

Mineralogical and geochemical characterization of drill hole samples of the lithiniferous pegmatite of Aldeia, Ribeira de Pena: Metallogenic implications and their importance for Li exploration

Bruno Filipe Farinha Ferreira

Mestrado em Geologia
Especialização em Geoquímica Mineralogia e Petrologia

Dissertação orientada por:
Luís Miguel Guerreiro Galla Gaspar

2023

ENTITY ACKNOWLEDGEMENTS

O presente trabalho foi financiado pela Atividade 7 do Projeto Mobilizador INOVMINERAL4.0 (Tecnologias Avançadas e Software para os Recursos Minerais), Agência Nacional de Inovação, contando igualmente com o apoio do Instituto Dom Luiz (IDL) através do programa UIDB/50019/2020 - IDL (FCT I.P./MCTES).

The present work was financed by activity 7 of the mobilizing project INOVMINERAL4.0 (Advanced technologies and software for mineral resources), National innovation agency, counting also with support from Instituto Dom Luiz (IDL) through the programme UIDB/50019/2020 - IDL (FCT I.P./MCTES) programme.

PERSONAL ACKNOWLEDGEMENTS

Começo por agradecer ao meu orientador, o Dr. Luis Miguel Guerreiro Galla Gaspar, que foi fundamental para levar este trabalho a bom porto. Foram vastas horas de discussão, teimosia, "crises existenciais", ataques de estupidez crónica, desorganização e conversas sobre NBA que no final culminaram neste trabalho. Agradeço-lhe o incentivo para procurar sempre fazer o melhor possível com os dados obtidos, e o incentivo para nunca perder a curiosidade. Um agradecimento especial ao professor António Mateus pelo tempo disponibilizado, conhecimento transmitido e pelos esforços para que pudesse não só trabalhar com as amostras fornecidas, mas sim conhecer pessoalmente o local em estudo, embora saiba que ouvir "não estou a ver" repetidamente no campo tenha sido uma experiência certamente frustrante para ele. Deixo também nota de agradecimento aos professores, Mário Abel Gonçalves e Isabel Ribeiro da Costa que sempre se mostraram, ao longo de todo o mestrado, disponíveis para responder as minhas incessantes perguntas. Agradeço ainda ao professor Paulo Fonseca por ao longo de toda a licenciatura ter alimentado as minhas "geocuriosidades", à Dra. Ana Jesus por toda a disponibilidade demonstrada independentemente da altura e finalmente ao professor Pedro Costa pela confiança depositada em mim no 1º ano despertando assim o meu interesse na investigação. Em termos laboratoriais, uma palavra de apreço para a Sofia Rodrigues, não só pelo pequeno milagre que fez em termos de produção das lâminas, mas também pelo apoio e incentivo ao longo de toda a tese.

Aos meus colegas de mestrado, Bruno Araújo, Diogo Neves, Francisco Pereira, Leonie Tipp e Nuno Rodrigues aos quais adiciono o nosso "júnior" Tiago Catita, que muito (com bastante ênfase no "muito") me ouviram queixar e reclamar. Obrigado pelas conversas, paciência, momentos de descontração fundamentais para evitar o esgotamento nervoso, as eternas pausas para café no globo serão sempre guardadas com o maior dos apreços.

Aos meus bons amigos, Alexandre Pires, Miguel Rodrigues a quem devo por esta altura o meu volume em copos desmarcados e viagens adiadas um obrigado pela paciência e uma promessa de que serão recompensados. Um especial abraço aos pais do Alexandre, Fernando e Paula pelos vastos serões à conversa sobre os mais variados temas e pelos deliciosos (*pun* intended) convites para jantar.

Seria sem dúvida injusto não agradecer aos meus companheiros de equipa André Costa, Gonçalo Olas, João Monteiro, Paulo Ferrão, Pedro Alves e Simão Lourenço. Destaco entre estes o Paulo que para além de colega e amigo me ajudou com parte do trabalho em python utilizado nesta tese.

Finalmente agradecer à minha família, mãe e pai, por serem sempre exemplos de trabalho árduo e por não me deixarem preguiçar quando eu mais queria. Aos meus avós maternos, Joaquim e Arminda, pelos diversos conselhos e constante preocupação. À minha avó paterna, Vitorina, e Tia Fátima que embora mais distantes sempre se demonstraram preocupadas e interessadas, mesmo quando o assunto era longe dos seus interesses.

Certamente me esqueço de alguém nestes parágrafos, mas peço que me deem alguma abébia, visto que a minha vida tem sido rochas e mais rochas.

ABSTRACT

Aldeia's pegmatite swarm, part of the much larger Barroso-Alvão pegmatitic field, is composed of several spodumene-bearing aplite-pegmatite bodies hosted in a sequence of micaschists and quartzschists belonging to the parautochthonous unit of NE Iberia.

An appraisal of the Li-mineralization was carried out on drillhole samples from both host-rocks and aplite-pegmatite bodies. 30 thin sections were produced. After a detailed petrographic analysis, 17 thin sections were selected for EMPA to assess mineral compositions.

The petrographic analysis revealed that spodumene-bearing aplite-pegmatites are poorly zoned, and show a complex mineral assemblage developed along two main crystallization stages (Stage I and Stage II), with a superimposed later metasomatic event.

Given the metallogenetic and economic implications of the reported variability for the Li-bearing phases within the Barroso-Alvão pegmatitic field, it is important to stress that: 1- although usually deformed, analysed spodumene is extremely fresh, with no evidence of alteration or weathering processes; 2- petalite is absent and there is no suggestion that spodumene results from the decomposition of petalite, since SQI textures are inexistent in studied samples.

All the main mineral phases from both stages (including spodumene) exhibit micro-textures and intra-crystalline high-T deformation features, suggesting deformation under crystallization and cooling conditions, compatible with the regional Variscan deformation patterns observed in the metasedimentary host-rocks.

Based on petrography and mineral chemistry, the studied Aldeia aplite-pegmatites can be classified as Complex Spodumene Rare Element-Li pegmatites. They are texturally and compositionally similar, showing a complex history with two main crystallization stages, with secondary phosphates underlining late metasomatism. From a geochemical standpoint the system stands out due to elevated enrichments in Na. Stage 1 should represent a Li-poor melt, with moderate P and F, and minor Fe, Mn, and Sn. Stage 2, concomitant with spodumene crystallization, should represent a Li-rich and F-poor melt with minor Nb and Ta.

Keywords: Lithium, Spodumene, Aplite-Pegmatite, Portugal, Rare-Element

RESUMO

O norte de Portugal é caracterizado por uma forte abundância de campos aplito-pegmatíticos da família LCT (Lítio, Césio, Tântalo) definida por Černý and Ercit (2005). Estes campos pegmatíticos têm, ao longo dos anos, sido alvo de exaustivos estudos do ponto de vista económico, petrográfico e geoquímico (*e.g.*, Lima, 2000; Farinha and Lima, 2000; Lima *et al.* 2010; Silva 2014). O enxame aplito-pegmatítico de Aldeia, Ribeira de pena encontra-se inserido no campo aplito-pegmatítico do Barroso-Alvão. Este campo é composto por diversos corpos aplito-pegmatíticos enriquecidos localmente em espodumena ($LiAlSi_2O_6$) hospedados numa sequência de micaxistos e xistos quartzosos, pertencentes à unidade parautóctone do NE da península ibérica.

Tradicionalmente, os enxames aplito-pegmatíticos de Barroso-Alvão eram interpretados como resultado de uma evolução magmática contínua associada às frequentes intrusões graníticas parentais abundantes na região. No entanto, ao longo do tempo, essa interpretação tem sido questionada em favor de um modelo anatético que envolve a fusão parcial de material metassedimentar enriquecido em Li (*e.g.*, Deveaud *et al.* 2014).

De modo a avaliar a tipologia e teores da mineralização de lítio recorreram-se a amostras colhidas em testemunhos de uma sondagem. A amostragem foi realizada de modo a compreender não só os dois domínios aplito-pegmatíticos, mas também as rochas encaixantes. A partir da amostragem realizada 30 lâminas delgadas polidas foram produzidas sobre as quais foi realizado um estudo petrográfico detalhado. Com base nas ilações retiradas do estudo petrográfico 17 lâminas foram selecionadas e posteriormente submetidas a estudos de microssonda eletrónica de modo a avaliar as composições químicas, e respetivas variações das mesmas, das fases minerais mais proeminentes.

A análise petrográfica realizada revelou que os corpos aplito-pegmatíticos de Aldeia, se encontram, de modo geral, pouco zonados e apresentam uma mineralogia altamente complexa e variada. Mineralogia a qual se desenvolve ao longo de dois estádios evolutivos bem demarcados aos quais se sobrepõe um evento metassomático tardio.

O primeiro estádio evolutivo é caracterizado pela presença de uma paragénese mineral pegmatítica constituída por plagioclase-microclina-quartzo-moscovite com quantidades acessórias de berilo, apatite e fosfatos de Fe-Mn (Li) e quantidades mínimas de fosfatos de U-REE e esfalerite. A esta mineralogia pegmatítica associa-se uma fase aplítica de composição idêntica, todavia sem a presença de microclina. A presença de texturas mirmequíticas e pertíticas, recristalização de albite exsolvida assim como elevado grão de alteração e deformação da microclina são características distintivas da associação pegmatítica.

O segundo estádio é caracterizado pela presença de uma paragénese mineral pegmatítica constituída por espodumena-albite-quartzo-moscovite com quantidades acessórias de montebrasite e quantidades reduzidas de óxidos de Nb-Ta (*i.e* da série columbite-tantalite). Esta paragénese mineral apresenta uma heterogranularidade assinalável, podendo variar entre domínios aplíticos até domínios francamente pegmatíticos. O contacto entre estádios varia entre difuso e "à faca" e é marcado frequentemente pela recristalização fina de moscovite.

O evento metassomático tardio expressa-se maioritariamente na forma de fosfatos de Fe-Mn secundários substituindo apatite e fosfatos de Fe-Mn (Li) primários.

Devido à elevada variabilidade das fases portadoras de lítio dentro do campo aplito-pegmatítico do Barroso Alvão, que por consequência têm implicações tanto do foro económico como metalogenético, torna-se importante salientar alguns fatores: 1) embora altamente deformada, a

espodumena presente no pegmatito de Aldeia não aparenta qualquer evidencia de alteração ou degradação; 2) ausência completa de petalite, assim como a inexistência de texturas SQI (*spodumene quartz intergrowth*) que possam sugerir que a espodumena presente nestes corpos resulte da decomposição dessa mesma petalite.

Todas as fases minerais principais de ambos os estádios evolutivos apresentam características micro texturais intracristalinas, coincidentes com deformação a alta temperatura ao longo do processo de arrefecimento. Estas texturas são em tudo compatíveis com os padrões típicos de deformação varisca apresentados pela sequência metasedimentar hospedeira dos corpos aplito-pegmatíticos.

As amostras correspondentes à sequência metassedimentar hospedeira são caracterizadas por um forte *fabric* tectono-metamórfico e textura lepidoblástica. Preservam ainda as 3 principais fases de deformação na região. Estes metassedimentos apresentam uma mineralogia heterogénea de quartzo-biotite-moscovite-clorite e ilmenite, ocasionalmente recristalizada e localmente enriquecida em turmalina e quantidades acessórias de apatite, pirite e arsenopirite. Porfiroblastos milimétricos de granada e biotite ocorrem esporadicamente ao longo das amostras analisadas.

Várias ilações podem ser retiradas com base nos dados de química mineral obtidos por microssonda eletrónica:

(1) Os feldspatos alcalinos, microclina e albite, apresentam composições próximas das ideais com uma componente berlinitic moderada (microclina – 0.21 wt.% P_2O_5 em média; albite – 0.15 wt.% P_2O_5 em média)
(2) A espodumena aparenta ser extremamente pura com um valor médio de 3.67 wt.% de Li estimado), com uma pequena componente jadeítica (valores médios de FeO <1wt.% e 0.3% valor médio de wt.% Na_2O)
(3) As moscovites do pegmatito apresentam composições próximas da ideal com uma pequena componente litinífera (valores médios de 0.21 e 0.42 wt.% Li_2O para pegmatito 1 e 2 respetivamente). As moscovites do encaixante, com valores médios de 0.19 wt.% Li_2O, tendem a mostrar uma componente mais fengítica,. As moscovites do encosto metassomatizado (MAZ) apresentam um valor médio de Li_2O superior às moscovites da rocha encaixante não metassomatizada, aproximadamente 0.32 wt.% Li_2O. Importante ainda mencionar valores consideráveis de elementos como Sn, Ta, Nb e Mn.
(4) A biotite, que apenas ocorre nos metassedimentos, apresenta um *trend* composicional entre os termos Fe-Biotite e siderofilite, este último predominante nas amostras mais proximais ao pegmatito.
(5) A apatite, na sua maioria fluorapatite, apresenta ligeiras variações composicionais entre os diferentes domínios identificados petrograficamente, destacando-se ainda valores relevantes de Sr, Na, Fe e Mn.
(6) Os fosfatos primários de Fe-Mn(Li) pertencem ao grupo da trifilite-litiofilite. Os fosfatos de Fe-Mn secundários incluem composições na série da fairfieldite-messelite, frequentemente alterada para ludlamite.
(7) A ilmenite apresenta uma variação composicional sistemática, apresentando-se enriquecidas em Mn quando proximais ao pegmatito, enquanto as mais distais tendem a ser enriquecidas em HFSE (W+Nb+Ta)
(8) Os grãos de granada encontrados não apresenta zonamento composicional evidente e a mesma pode ser classificada como almandina com uma componente de espessartina considerável (66% almandina e 22% espessartina em média)
(9) A turmalina das rochas metasedimentares encaixantes incluem dois grupos composicionais distintos. A turmalina do encaixante cai dentro *X-Vacant Group* e a

turmalina da MAZ recai, no mesmo diagrama classificativo, sob o campo das turmalinas alcalinas.

Com base nos dados de química mineral e na avaliação petrográfica é possível classificar os aplito-pegmatitos de Aldeia como "pegmatitos complexos de espodumena enriquecidos em elementos raros-Li". Com base nas associações minerais, e dados geoquímicos apresentados acima é ainda possível inferir que primeiro estádio evolutivo deverá representar um fluido original pobre em lítio com quantidades moderadas de P e F e quantidades menores de Fe e Mn. O segundo estádio evolutivo será enriquecido em Li com quantidades minoritárias de Nb e Ta. Importante ainda mencionar a presença constante de Na como elemento dominante em todo o sistema.

Com base na combinação de dados petrográficos, de campo e geoquímicos procurou-se responder essencialmente a um conjunto específico de questões:

1) Estabelecer condições aproximadas de temperatura e pressão para a instalação do aplito-pegmatito de aldeia;
2) Estabelecer uma sequência paragenética detalhada;
3) Estabelecer causas genéticas responsáveis pelos dois estádios magmáticos distintos;
4) Identificar assinaturas geoquímicas peculiares dentro do pegmatito, assim como nas rochas encaixantes afetadas pela instalação do mesmo.
5) Comparar diferentes modelos genéticos e procurar nas assinaturas geoquímicas obtidas evidências que apontem para um modelo preferencial, e deste modo contribuir para uma melhoria dos modelos de prospeção utilizados.

Palavras-Chave: Litio, Espodumena, Aplito-Pegmatito, Portugal, Elementos-Raros

INDEX

FIGURE INDEX

TABLE INDEX

ABBREVIATION LIST

Geotectonic Domains

CIZ- Central Iberian Zone

GTMZ- Galicia Trás os Montes Zone

Entities

EU - European Union

FCUL- Faculdade de Ciências da Universidade de Lisboa

IDL- Instituto Dom Luís

LNEG- Laboratório Nacional Energia e Geologia

COLCHICO- Comisión Chilena del Cobre

Mineral Phases

Ab- Albite

Aby- Amblygonite

Alm- Almandine

And- Andradite

Ap- Apatite

Brl- Beryl

Bt- Biotite

Chl- Chlorite

Ecp- Eucryptite

Ffd- Fairfieldite

Grs- Grossular

Grt- Garnet

Het- Heterosite

Lhp- Lithiophilite

Lud- Ludlamtie

Mbs- Montebrasite

Mcc- Microcline

Ms- Muscovite

Msl- Messelite

Pet- Petalite

Pur- Purpurite

Pyr- Pyrite

Qz- Quartz

Spd- Spodumene

Sph- Sphalerite

Sps- Spessartine

Srl- Schorl

Trp- Triphylite

Methods

EDS- Energy-dispersive spectrometer

EMPA- Electron Microprobe Analysis

PPL- Plane-Polarized Light

RL- Reflected Light

WDS- Wavelenght-dispersive spectrometers

XPL- Cross Polarized Light

Units

a.p.f.u- atom per formula unit

cm- centimeter

kbar-kilobar

Km- kilometer

m- meter

mm- millimeter

My -million Year

ppm- parts per million

wt% - weight percentage

μm- micrometer

LCE- Lithium Carbonate Equivalent

Geological Terms

BG- Barroso Granite

BM- Barroso Massif

CBM- Cabeceiras de Basto Massif

D1 – First deformation phase of Variscan Orogeny

D2 – Second deformation phase of Variscan Orogeny

D3 – Third deformation phase of Variscan Orogeny

DPA- Diretic Products of Anatexis

GSG- Gouvães da Serra Granite

HFSE- High Field Strength Elements

LCT- Lithium Cesium Tantalum pegmatite family

NYF- Niobium Ytrium Fluor pegmatite family

PG- Pisões Granite

PSG- Pedras Salgadas Granite

RMG- Residual Melts of Granite Magmatism

S1 – Main foliation resulting from D1

S2- Main foliation resulting from D2

S3 - Main foliation resulting from D3

Var.- Variety

VGr- Vilar Granitoid

VPA- Vila Pouca de Aguiar Massif

VPAG- Vila Pouca de Aguiar Granite

VPG- Vila da Ponte Granite

Others

□- Structural Vacancies

1. INTRODUCTION

Portugal boasts a rich history of mineral exploration, with its mining sector often associated with renowned deposits like those in the Iberian pyrite belt (IPB), such as Neves-Corvo, or the world-famous Panasqueira Sn-W deposit. However, Portugal's mining legacy extends beyond these deposits as it has been a major European producer of lithium. Notable mining concessions contributing to this production include Alijó, Lousas, amongst others, all part of the Barroso Alvão aplite-pegmatite field, which forms the subject of this dissertation.

Despite previous extensive studies on the Barroso Alvão aplite-pegmatite field (*e.g.*, Charoy *et al.*, 1992, 2001; Lima, 2000; Farinha and Lima, 2000; Almeida, 2002; Ribeiro *et al.*, 2007; Noronha *et al.*, 2013), the current panorama, characterized by a growing demand in the lithium-producing industry, underscores the increasing importance of a comprehensive understanding and detailed characterization of metallogenetic processes. Recent research in the past 5 to 10 years on aplite-pegmatites has sparked a debate regarding the origin of economically significant deposits. Anatexis, proposed as an alternative process (*e.g.*, Muller *et al.*, 2017; Knoll, 2023) for the genesis of these deposits, has gained popularity in academic literature. While classic works have traditionally associated the Barroso Alvão aplite-pegmatites with magmatic genesis, specifically the syn-D3 granites, this connection is not straightforward and, at times, contradicts this hypothesis. This emerging perspective suggests the possibility of categorizing the Barroso-Alvão as metamorphic/anatectic pegmatites (*e.g.*, Deveaud *et al.*, 2014) or, at the very least, considering contributions from both magmatic and metamorphic processes. This hypothesis posits a low melting rate of crustal material ascending in consecutive independent batches.

The primary objectives of this dissertation can be summarized as follows: i) characterize drill core samples from both geochemical and petrographic perspectives; ii) identify and analyze the chemical signatures and variations of the main mineral phases; iii) establish a paragenetic sequence for the pegmatitic body; and iv) investigate whether geochemical variability allows for the distinction between purely magmatic processes and contributions from regional metamorphism.

To achieve these objectives, a drill hole core, provided by Savannah Resources, was sampled into 19 segments representative of the main lithologies and textures, which underwent comprehensive macroscopic, petrographic, and geochemical analyses. Mineral chemistry characterization was conducted using the Electron Microprobe System at the Geology Department of Faculdade de Ciências, Universidade de Lisboa (FCUL).

2. SETTING

The purpose of this chapter is to provide the reader with the background of this study. To achieve this goal, this chapter is divided into four subchapters. The first subchapter introduces how the global lithium problem can be addressed in the context of a green energy transition, and how Portugal can become an even more expressive lithium producer, reducing Europe's dependence on external markets (*e.g.,* China). It is followed by a brief introduction to the latest anatomy, classification, and genesis of pegmatites. The third and fourth subchapters serve as the geological background for the subject of the study, starting from a regional perspective all the way to Aldeia's aplite-pegmatite swarm.

2.1. LITHIUM: THE PROBLEMATIC & PORTUGAL AS A SOLUTION

2.1.1. Lithium: The foundation for a green world

The last decade has been marked by an industrial and energetic revolution, the signing of multiple "green deals" to mitigate global warming, such as the 2015 Paris agreement, has pushed the need for new energetic alternatives with special focus on the transition from fossil to the so-called green energies. This has been reflected in the investments made in the energy sector where investments in green energies have doubled the investments in new energy from fossil and nuclear sources (Dwyer and Teske, 2018). It's further noticed when we consider that during the 2007-2017 decade the renewable power capacity more than doubled, with special emphasis on non-hydropower renewables which increased more than sixfold (Dwyer and Teske, 2018). However, the transition to 100% green energy implies an increase in demand of certain essential materials such as: cobalt (mainly used in batteries), silver (used in solar cells due to its excellent conductor abilities), rare earth elements (required to build permanent magnets, used in vehicles and wind turbines), lithium amongst many others. Due to the object of study of this dissertation, focus shall fall mainly on lithium as key-commodity for the desired green transition.

Lithium is an extremely light and reactive metal with a high electrochemical potential. These characteristics make lithium a greatly valuable and sought after commodity essential to produce high energy-density rechargeable lithium-ion batteries (Goonan, 2012). Batteries which in turn are fundamental in various sectors such as electronics and in the growing electric vehicle market. Despite lithium usage being most relevant in the latter industry this trend is relatively new, only ten years ago the main usage of lithium was in the ceramics industry (Jaskula, 2013; Jaskula 2023). The shift in lithium usage is quite evident as seen in figure 2.1.

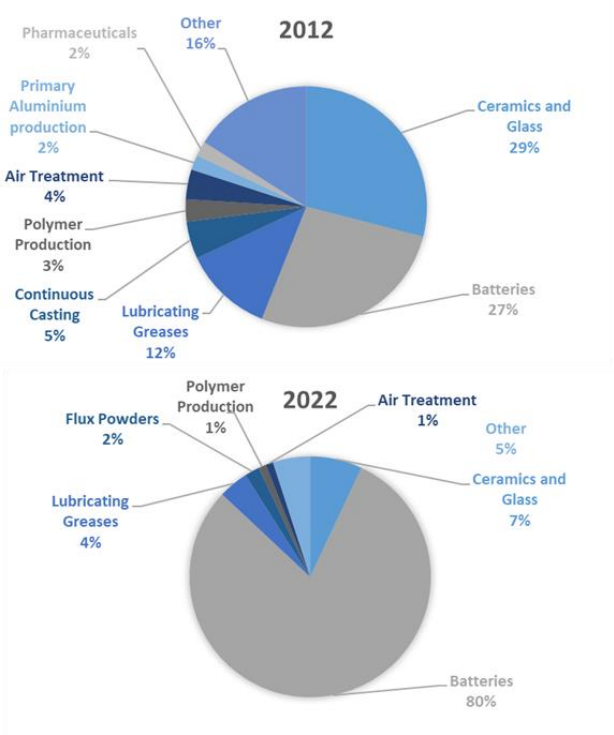

Figure 2.1 Lithium usage per industry in percentage in 2012 and 2022. Data shows a clear increment in lithium usage in battery production data compiled from Jaskula (2013, 2023) respectively.

2.1.2. Demand and supply: Predictions and data

According to Giurco *et al*. (2019) the annual demand for lithium should exceed production rates by 2022, and data provided by COLCHICO (2021), later compiled by Statista, expects the demand to rise almost ten-fold from 2019 to 2030 (Figure 2.2). Based on several studies of this nature and on the evident geopolitical necessity from third-party (non-EU) countries the European Commission included lithium in the 2020 critical raw materials, stating that in order to achieve the climate neutrality scenarios proposed for 2050 the EU would need up to 18 times more lithium in 2030 and almost 60 times more lithium in 2050, when compared to the current supply to the whole EU economy (European Comission, 2020). These projections imply an immediate need for new sources of lithium as well as new ways to recycle the existing one.

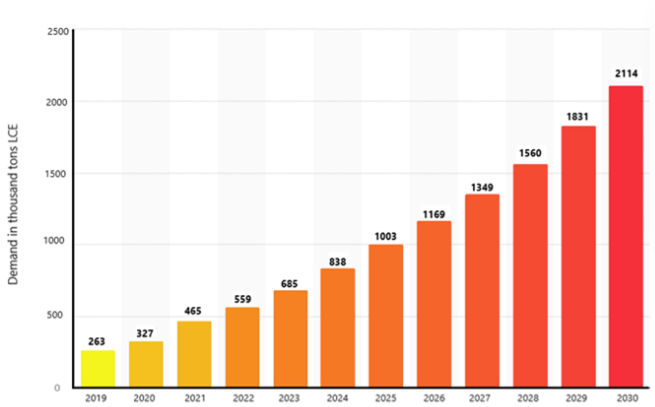

Figure 2.2 Lithium Carbonate equivalent (LCE) requirements from 2019-2030. Data from COLCHICO (2021).

As mentioned previously, lithium supply is controlled by countries outside of the European Union. South America (Chile and Argentina) hosts 70% of the lithium resources, despite representing only about 40% of the world production (Sterba *et al.* 2019.). Data provided by the Jaskula (2023) shows that production is dominated by Australia, China, and Chile. Reserves follow this trend, with these countries alongside with Argentina hosting the main world lithium reserves (approximately 78%). European Union production is pretty much limited to Portugal. However, resources have been identified in Germany, Czechia, Spain, and Austria.

Lithium is extracted from three main deposit typologies: brines and related evaporites, pegmatites, and sedimentary rocks. According to Gruber *et al.* (2011) lithium-rich brines make up 66% of the world's lithium resources, followed by pegmatites (26%), and sedimentary rocks (clay and lacustrine evaporites 8%). Despite much lower tonnages than brine deposits, the widespread occurrence of Li pegmatites make them a valuable asset both in production and in the geographic broadening of that same production (Kessler, 2012).

2.1.3. Portugal as an alternative

Portugal has a rich history of mineral exploration, with world-known deposits of copper, zinc, tungsten, and tin. In recent years, due to the previously mentioned reasons, lithium deposits in Portugal have been a matter of special attention and controversy. According to Oliveira *et al.* (2018) 9 regions are recognized to have known lithium mineralizations: 1) Serra de Arga; 2) Barroso-Alvão; 3) Seixoso-Veiros; 4) Almendra; 5) Barca de Alva-Escalhão; 6) Massueime; 7) Guarda; 8) Argemela; 9) Segura (Figure 2.3). The mineralized structures are typically hosted in Neoproterozoic to Silurian metasedimentary sequences, except for the Guarda region where (aplite)-pegmatites are mainly hosted in granitic rocks (Oliveira *et al.* 2018). The current metallogenetic interpretation for these structures points towards a strong genetic relationship with the sin- to tardi-variscan granitic intrusions (320-290 My) (*e.g.*, Farinha and Lima, 2000). These structures are mostly aplite-pegmatite sills and dykes from the LCT family, with various subgroups (*e.g.*, spodumene + albite, petalite + lepidolite) being represented.

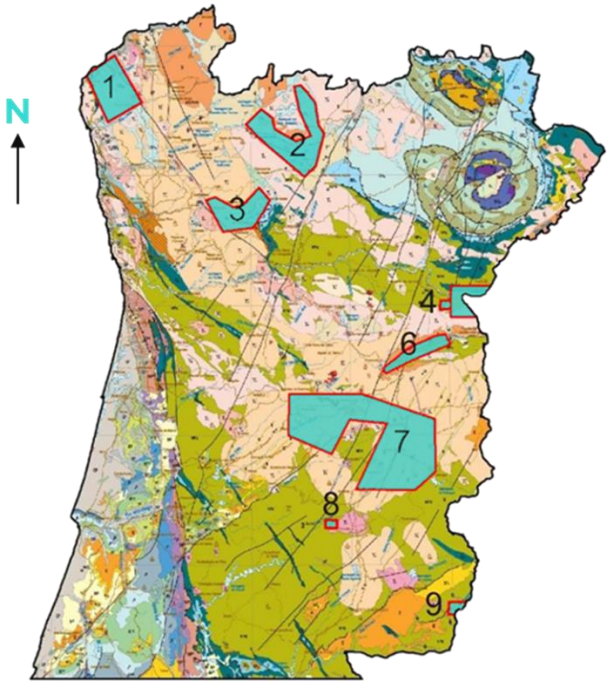

Figure 2.3 Potential areas for lithium mineralizations in Portugal. 1) Serra de Arga; 2) Barroso-Alvão; 3) Seixoso-Veiros; 4) Almendra; 5) Barca de Alva-Escalhão; 6) Massueime; 7) Guarda; 8) Argemela; 9) Segura. Adapted from Oliveira et al. (2018).

From the aforementioned regions it's relevant to highlight the aplite-pegmatite field of Barroso-Alvão, where the study object for this dissertation is included. This fields extends through several counties in northern Portugal (Boticas, Cabeceiras de Basto, Montalegre, Ribeira de Pena and Vila Pouca de Aguiar), and is characterized by an overabundance of dike-like bodies, some of which are mineralized but a considerable amount is barren. Mineralized bodies fall into the LCT family, dominated by the spodumene and petalite subtypes, with minor representation of the lepidolite subtype (Lima, 2000). A more detailed geological setting will be provided in the following section of this chapter. According to Oliveira *et al.* (2018) the combination of the abundant mineralized bodies results in at least 14 million tons of lithium ore at 1% Li_2O, placing these bodies in the inferred mineral resources category.

According to the Jaskula (2023), Portugal was the main European producer of lithium in 2022, being responsible for the production of around 600 metric tons of Li ore. Portuguese reserves are estimated in the 60000 metric tons range, with the possibility of reaching 270000 metric tons as consumption turns previously non-profitable deposits into reserves. This makes Portugal an opportunity for Li exploration in Europe, fact which is reflected by the concession requests and already authorized in Portugal (Figure 2.4)

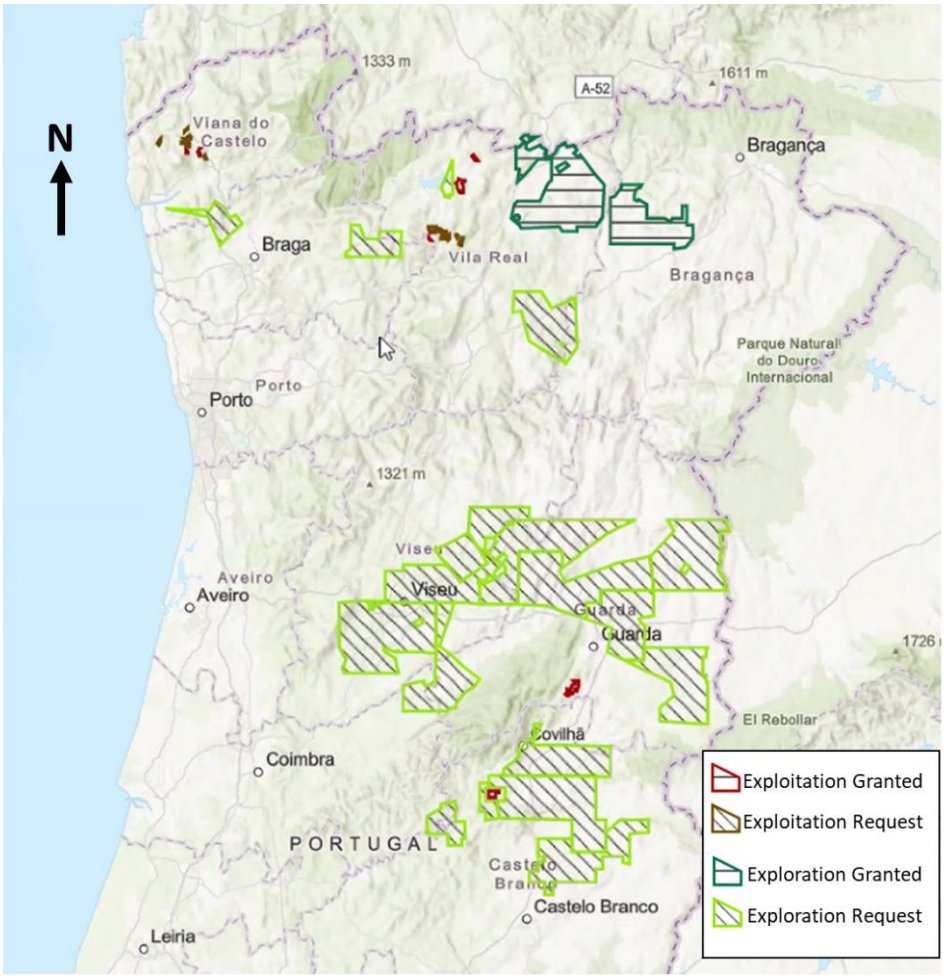

Figure 2.4 Lithium exploitation and exploration applications requested and granted. Source: DGEG

These new exploration concessions have been met with heavy protest by environmental associations, local authorities, and the overall population. These groups regard lithium exploitation as an environmental disaster and accuse companies of withholding information about the impact of such

projects (*e.g.*, Dunlap and Riquito, 2023). On the other hand, the Portuguese government sees lithium exploitation as a way for Portugal to assume a leading role in EU's "green transition". In 2016 a "Lithium work group" was created to: 1) identify and characterize the economic activities related to lithium; 2) hierarchize the priorities of industry in order to maximize economic benefit; 3) establish a program for the production of lithium compounds; 4) propose and create measures to validate the building of a lithium processing unit for extracted minerals (República Portuguesa, 2017)

2.2. A BRIEF INTRODUCTION TO PEGMATITES

2.2.1. What are pegmatites?

Pegmatites are highly complex, coarse-grained, heterogeneous intrusive igneous rocks typically of granitic composition (therefore enriched in quartz, feldspar, and mica) characterized by a combination of extremely large but also extremely variable crystal size (from millimeters to meters in length), accentuated crystal orientation anisotropism, spatial zonation of minerals, presence of various crystal intergrowth habits such as skeletal, radial, or graphic intergrowth (London, 2008). Although one of these textural features allows for identification of pegmatitic bodies, they typically occur together resulting in an extremely complex textural arrangement. Despite being typically of granitic composition, there are pegmatites of sienitic (*e.g.*, Andersen *et al.* 2010) and gabbroic composition (*e.g.*, Beard *et al.* 2002), making pegmatite chemical compositions extremely variable. Therefore, the term pegmatite in its essence focusses more on the textural arrangement of the rock than in its composition. Granitic pegmatites are generally considered to represent residual fractions of magmatic fractionation processes and/or resulting from late-stage magmatic-hydrothermal activity (London, 2008). These processes can lead to an enrichment in incompatible elements, which is later reflected in its mineralogy, characterized by the incorporation of volatiles (B, Cl, F, OH) and rare metals (Li, Be, Rb, Nb, Sn, Cs, REE, Ta, U, etc). This diverse and complex mineralogic assemblage allows for the establishment of chemical-mineralogical zonation fundamental for the classification of pegmatitic systems (*e.g.*, Černý, 1991a).

Pegmatites are known sources for a variety of economic commodities including both industrial (*e.g.*, London and Kontak, 2012) and strategic metals (*e.g.*, Linnen et.al 2012). Pegmatites are also a major source for "industrial" minerals such as feldspar, quartz, mica, clay minerals and Li-silicate minerals (*e.g.*, spodumene), essential in the production of ceramics, electronics, lubricants, amongst many others as described in further detail by Glover *et al.* (2012). In respect of gemstones, pegmatites are sources of several precious and semi-precious stones such as beryl var. emerald, beryl var. aquamarine, spodumene var. kunzite, etc. (Simmons *et al.* 2012)

2.2.2. Pegmatite anatomy

Pegmatites can be seen as segregations that like many other igneous bodies, occur in pods, dikes, or sills. Dikes and sills are used with the same connotation as in other igneous context, describing planar bodies of igneous composition. Typically dikes and sills preserve the original orientation of consolidation since most pegmatite-forming events are either anorogenic or occur at the final stages of tectonic events (London, 2008). Pods on the other end refer to pegmatitic bodies that lack a planar continuity and in its place form lenticular bodies (London, 2008). The shift between dikes and sills to pods is considered by many authors a result of differences in mechanical competence of host rocks, which in turn results from changes in composition, with dikes and sills appearing in more competent hosts (*e.g.*, Gneiss) while pods tend to form in less competent hosts (*e.g.*, schists) (London, 2008).

Pegmatite's internal zoning has been debated since mid-20th century and is nowadays considered a relatively settled problematic with the zoning scheme proposed by Cameron *et al.* (1949) being the most

widely accepted today, dividing pegmatites into Border Zone, Wall Zone, Intermediate Zones and Core (Figure 2.5), described, individually, below.

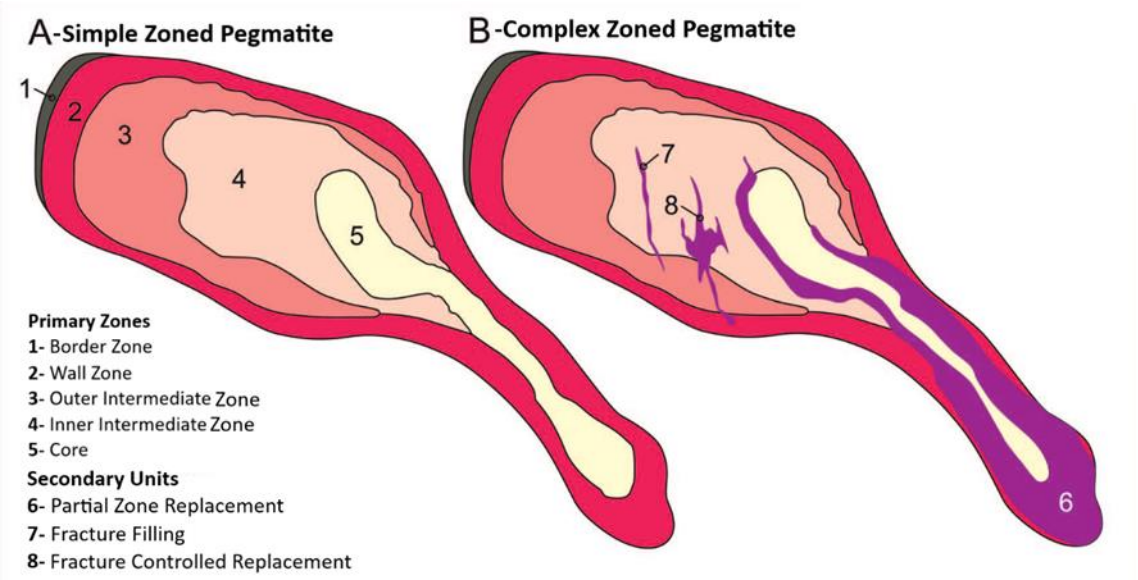

Figure 2.5 Schematization of pegmatite zonation. (A) Simple zoned pegmatite. (B) Complex zoned pegmatite with replacement units/zones named as secondary units. Adapted from Simmons et al. (2003).

2.2.2.1. Border Zone

According to London (2014) the border zone can be described as a thin "shell" (mm to cm in thickness) that surrounds the pegmatite, marking the contact between pegmatites and host rocks. Is typically marked by fine-grained minerals (~2-5 mm) and the texture is typically hypidiomorphic granular. Border zones mineralogical assemblage is very diverse, in addition to plagioclase and quartz which are the dominant phases, border zones can contain in variable amounts muscovite, apatite, beryl, biotite, K-Feldspar, garnet, tourmaline, and columbite.

2.2.2.2. Wall Zone

Wall zones just like border zones typically envelop the pegmatitic bodies roughly completely. In the same note, the mineralogy presented by these zones is essentially the same as the one seen in the border zone. Compared to border zones, wall zones are generally thicker (cm up to several meters thick), coarser-grained (1cm up to several m) and marked by an anisotropic orientation of interiorly elongated crystals (London, 2014).

2.2.2.3. Intermediate Zone

Intermediate zones are, according to (London, 2014), marked by a rapid increase in crystal size and a less variable mineralogical assemblage dominated by a few minerals, such as, in LCT pegmatites microcline, plagioclase, muscovite, lepidolite, spodumene, petalite, all in association with massive quartz. Contrary to the wall zone, the intermediate zones may be discontinuous and symmetrically or asymmetrically distributed through the pegmatite. Intermediate zones tend to vary in thickness in agreement with pegmatite thickness, being thicker in zones where the pegmatite is thicker and vice-versa.

2.2.2.4. Core

According to London (2014) core represents the innermost part of the pegmatitic body, and it can be a single mass or a multiple repetition of the same mineralogical assemblage at the same structural

position. The ratio between core and the remaining zones can be highly variable. Typically, cores are monomineralic composed of massive quartz.

It is also important to mention the existence of replacement bodies, which represent the substitution of the original pegmatitic body into a metasomatic rock. Pseudomorphism is one of the pieces of evidence for the processes that cannot be explained via igneous processes (London, 2014).

2.2.3. Classic classification of pegmatites

Several classification schemes for pegmatites have been proposed (*e.g.*, Niggli (1920), Schneiderhöhn (1961), Černý and Ercit (2005)). The currently most accepted and used classification scheme is the one proposed by Černý and Ercit (2005). This classification scheme distinguishes between five pegmatite classes, ten subclasses, thirteen types and seven subtypes. Classes are ruled by the pressure temperature conditions in which pegmatites are formed and were classified into Abyssal, Muscovite, Muscovite–Rare-Element, Rare-Element, and Miarolitic pegmatite classes. Within each category, subdivision into subclasses is based on geochemical characteristics. The third level of classification, pegmatite types, is based on mineral paragenesis. Concurrently accepted is the pegmatite family classification suggested by Černý (1991a). This classification system is based on the most distinctive elements that are enriched in the pegmatitic body. This classification results in three different families summarily described in the following subchapters.

2.2.3.1. LCT Family

Standing for pegmatites enriched in Li, Cs, and Ta, the LCT family is generally considered to be related geochemically to S-type granites. In addition to the three elements that give name to this family, these pegmatites tend to be enriched in Be, B, F, P, Mn, Ga, Rb, Nb, Sn and Hf. According to Černý *et al.* (2012) this enrichment is expressed by mineral assemblages with abundant muscovite, feldspar – many times with an important berlinitic component (London, 1999) – garnet, tourmaline, beryl, sillimanite and/or andalusite amongst others. Lithium is incorporated into mineral phases such as lepidolite, eucryptite, petalite, spodumene, and in minerals from the phosphate series amblygonite–montebrasite and lithiophilite–triphylite. Cesium can be incorporated into micas and beryl and can sometimes reach high enough concentrations to crystallize pollucite. Tantalum appears enriched in oxides of the columbite-tantalite series (Linnen *et al.* 2012). Adding to the described paragenesis it's common to find various secondary phosphates, resulting from metasomatic/hydrothermal alteration of primary phosphate phases (Nizamoff *et al.* 1999). According to London (2008) the abundance of phosphorus in the system is a crucial characteristic to distinguish between LCT pegmatites protoliths, with phosphorus enriched LCT's being typically associated with a metasedimentary protolith, while low P-contents are most likely associated with igneous protoliths.

2.2.3.2. NYF Family

Standing for pegmatites enriched in Nb, Y and F, is a pegmatite family typically associated with A-type granites (*e.g.*, Eby,1990). These pegmatites are believed to be associated with granite magmatism from deep crustal melting in intra-continental rifting zones with more or less contribution from mantle sources (Martin and Devito, 2005). In addition to Nb, Y, and F, these pegmatites tend to be enriched in HREE, Be, Ti, Sc and Zr. According to Černý *et al.* (2012), this enrichment is expressed by mineral assemblages with abundant fluorite and/or topaz (reflecting the elevated F concentrations in the system), aegirine, riebeckite, and Fe-rich biotite, the former two representing the peralkaline character of these type of pegmatites. Another distinguishing feature of this family is the abundant presence K-feldspar var. amazonite (Martin *et al.* 2008). It is also important to refer the extreme depletion of phosphorous in NYF pegmatites as well as the absence of tourmaline (Černý *et al.* 2012)

2.2.3.3. NYF-LCT mix

An intermingling of the above-described processes can originate NYF+LCT mixed pegmatites (Černý and Ercit, 2005). The LCT component is usually less well represented, when compared with the NYF counterpart, and it is commonly materialized by typical LCT trace-element content of rock-forming minerals and as accessory LCT mineral phases in highly differentiated members of NYF populations.

2.2.4. New classification scheme

Despite the proposal by Černý and Ercit (2005) being the prominent classification scheme a recent work by Müller *et al.* (2022) points out the need for new and updated multi-criteria classification schemes, highlighting several issues in the former schemes such as:

1. Usage of inferred criteria (*e.g.*, depth of crystallization);

2. Classification schemes combine several criteria per classification level (*e.g.*, mineralogical data and structural criteria), breaking a basic rule of one criterion per level;

3. An increasing number of aplite-pegmatite bodies do not fit into any classification scheme (*e.g.*, the highly variable NYF-type pegmatites);

4. The absence of a well-defined "NYF-endmember composition".

5. Confusion over the quantitative aspects of mineralogical classification, seeing that it is unclear if it's based on macroscopical or microscopical observation.

6. Overcomplex and under complex definitions, such as rare element pegmatites and abyssal pegmatites, respectively

7. Barren pegmatites and abyssal pegmatites specially complicated to apply due to the lack of macroscopically visible rare element minerals.

8. Undefined mineral quantity marking the boundary between pegmatites (*e.g.*, on what % spodumene it is considered a spodumene pegmatite.

9. Current classification schemes do not attend to the possibility of LCT pegmatites derived from direct anatexis.

10. Muscovite pegmatites is a misleading term seeing that muscovite is presentt in most aplite-pegmatite bodies.

11. The difference between certain classes is not evident via field observation.

12. Classifications based on mineralogy may be misleading due to the absence of the mineral giving name to the class (*e.g.*, Beryl type pegmatites).

Wise *et al.* (2022) proposed a new classification scheme that strongly relies on the minor to rare accessory mineralogical assemblage which can be genetically related to individual types of associated rocks, placing less importance on textural features such as miarolitic cavities, economical relevant minerals, geochemical families, subtypes, depth of emplacement and rare metal enrichment. The classification scheme proposed by Wise *et al.* (2022) considers three different groups, summarily described in the subchapters below.

2.2.4.1. Group 1

Pegmatites are typically enriched in B, Be, Cs, F, Ga, Li, P, Sn and Ta > Nb. Three different types are regularly recognized: a) Li-rich spodumene- or petalite-dominant types; b) bodies with

lepidolite and or elbaite as the principal Li phase; c) beryl ± phosphate-bearing types; pegmatites from this group might present variable degrees of rare-element fractioning resulting in one or more of the following rare-element mineral assemblages: i) albite+ spodumene; ii) beryl + spodumene; iii) spodumene + lepidolite + elbaite; iv) spodumene + lepidolite; v) spodumene + amblygonite; vi) beryl + columbite; vii) beryl with no evidence of Li, Nb, Ta, or Sn mineralization; viii) beryl + columbite + triphylite.

2.2.4.2. Group 2

Pegmatites are mineralogically similar to pegmatites from group 1, nonetheless they are distinguishable from the first group via small but significant amounts of accessory minerals, such as, fluorite, magnetite, or hyalite opal.

2.2.4.3. Group 3

Pegmatites that are strongly peraluminous, with essential quartz, K-feldspar, plagioclase and accessory muscovite, biotite, garnet and/or tourmaline. The distinguishing feature of this group is the presence of: either: i) primary andalusite, sillimanite, kyanite or cordierite; ii) Borum mineralization (*e.g.*, borasilite); iii) chrysoberyl or surinamite rather than beryl/phenakite as Be retainers.

2.2.5. Genesis of Pegmatites: Magmatic vs Anatectic orgin

These 3 groups can be further related to the two most common genetic models for pegmatites: residual melts of granite magmatism (RMG) and direct products of anatexis (DPA). The former pegmatites are directly associated with the fractionation of slightly peralkaline, metaluminous and peraluminous granites, resultant from S-A or I-type granitic melts, as opposed to the latter which have no relation with parental granites and are interpreted as result from partial melting of metapelites, amphibolite, gneisses and migmatites in amphibolitic to granulitic metamorphic facies (Wise *et al.*, 2022). The comparison of these genetic models is presented in figure 2.6.

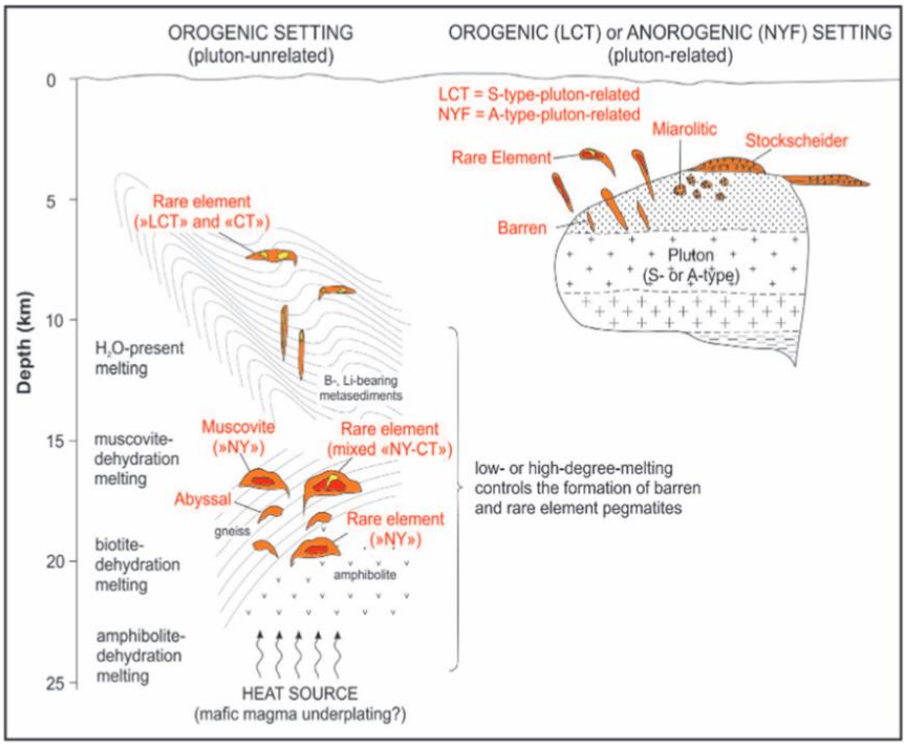

Figure 2.6 Schematic illustration of the crustal profile contrasting the two different genetic models for pegmatites. LCT referring to Lithium, Cesium and Tantalum and NYF for Niobium Ytrium and Fluorine. CT refers to a possible lack of Li in pluton unrelated. Same for NY referring to the lack of F. Adapted from Müller et al. (2017)

2.2.5.1. Magmatic Origin

It's overall accepted that the majority of pegmatitic bodies are formed via fractional crystallization of larger batches of granitic melts (*e.g.*, Černý 1991a,b). This close genetic relationship derives from the observation that pegmatitic swarms often occur within or distributed across the surroundings of granite intrusions and, furthermore, the fact that some of these swarms present a chemical zoning congruent with an evolution from a parental pluton which via fractional crystallization produces residual batches more and more enriched in incompatible and volatile elements (Müller *et al.* 2017).

2.2.5.2. Anatectic Origin

Recent studies (*e.g.*, Simmons and Webber, 2008, Müller *et al.*,2017; Lv *et al.*, 2021) have shown that mechanisms other than fractional crystallization may be involved in the genesis of pegmatitic bodies, one of which is anatexis. This process consists of partial melting of crustal and/or mantellic rocks, which for low partial melting can result in leucocratic melts typically enriched in incompatible elements (London, 2008). This is particularly true in convergent tectonic settings where sedimentary/metasedimentary sequences can contain considerable amounts of incompatible elements, as well as fluxing elements such as B, Li, and P, that will be segregated into the newly formed pegmatitic melt during partial melting (Simmons and Webber, 2008).

2.3. Geological Setting

2.3.1. General Setting

The Barroso-Alvão aplite-pegmatite field, where aldeia's prospect is included, is located in the Galicia Trás-Os-Montes Zone (GTMZ), which represents, along with the Central Iberian Zone (CIZ), the centermost part of the Iberian Variscan orogen (Figure 2.7).

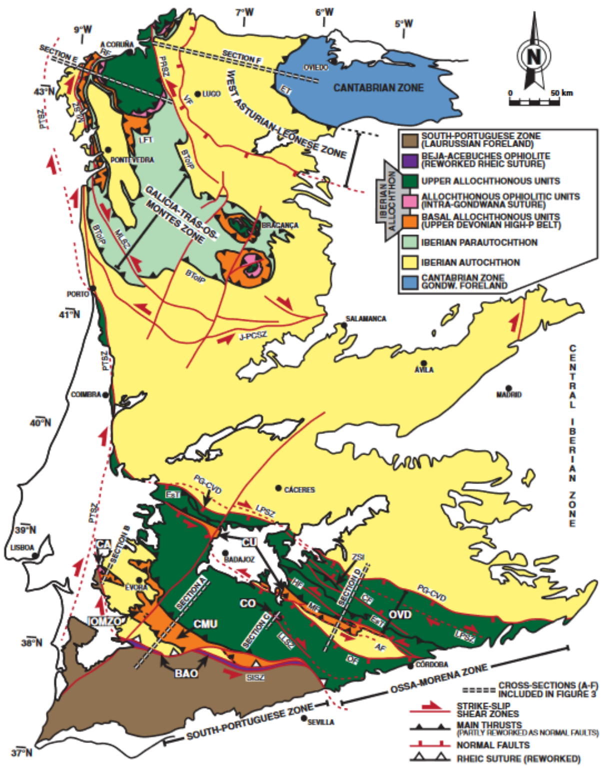

Figure 2.7 Geological schematization of the different geotectonic units from Iberia. bbreviations: AF — Azuaga Fault; BToIP — Basal Thrust of the Iberian Parautochthon; BAO — Beja–Acebuches Ophiolite; CA — Carvalhal Amphibolites; CF — Canaleja Fault; CMU — Cubito–Moura Unit; CO — Calzadilla Ophiolite; CU — Central Unit; EsT — Espiel Thrust; ET

Espina Thrust; HF— Hornachos Fault; IOMZO — Internal Ossa-Morena Zone Ophiolites; J–PCSZ — Juzbado-Penalva do Castelo Shear Zone; LFT — Lalín-Forcarei Thrust; LPSZ — Los Pedroches Shear Zone; LLSZ — Llanos Shear Zone; MLSZ — Malpica–Lamego Shear Zone; MF — Matachel Fault; OF — Onza Fault; OVD — Obejo–Valsequillo Domain; PG–CVD — Puente Génave–Castelo de Vide Detachment; PRSZ— Palas de Rei Shear Zone; PTSZ — Porto–Tomar Shear Zone; RF — Riás Fault; SISZ — South Iberian Shear Zone; VF — Viveiro Fault; ZSI — Zalamea de la Serena Imbricates. (adapted from Díez Fernández et al. 2016)

It represents an area of 300-350 km^2 (Figure 2.8) running WNW-ESE where for the last five decades a series of Li-rich aplite-pegmatites have been recognized and, in some cases, exploited. These bodies are of the Li-Cs-Ta (LCT) type peraluminous and complex, mostly falling into the spodumene and/or petalite subtypes (Charoy *et al.* 2001), according to the classification scheme proposed by Černy and Ercit (2005). These bodies, despite showing a generally strong deformation and variable form, tend to present a lenticular morphology. According to Silva (2014) they can be divided into three main families: from N0º to N63º, from N64º to N113º, and finally from N114 to N179º. Most aplite-pegmatite bodies in Barroso-Alvão are hosted in an allochthonous Silurian metasedimentary (with a minor metavolcaniclastic component) sequence divided in three distinct units (Sa, Sb and Sc), with particular emphasis on Sb which seems to host most of the mineralized aplite-pegmatite bodies, including the Aldeia prospect. Most of the aplite- pegmatite bodies in Barroso-Alvão field are surrounded by several granitic massifs.

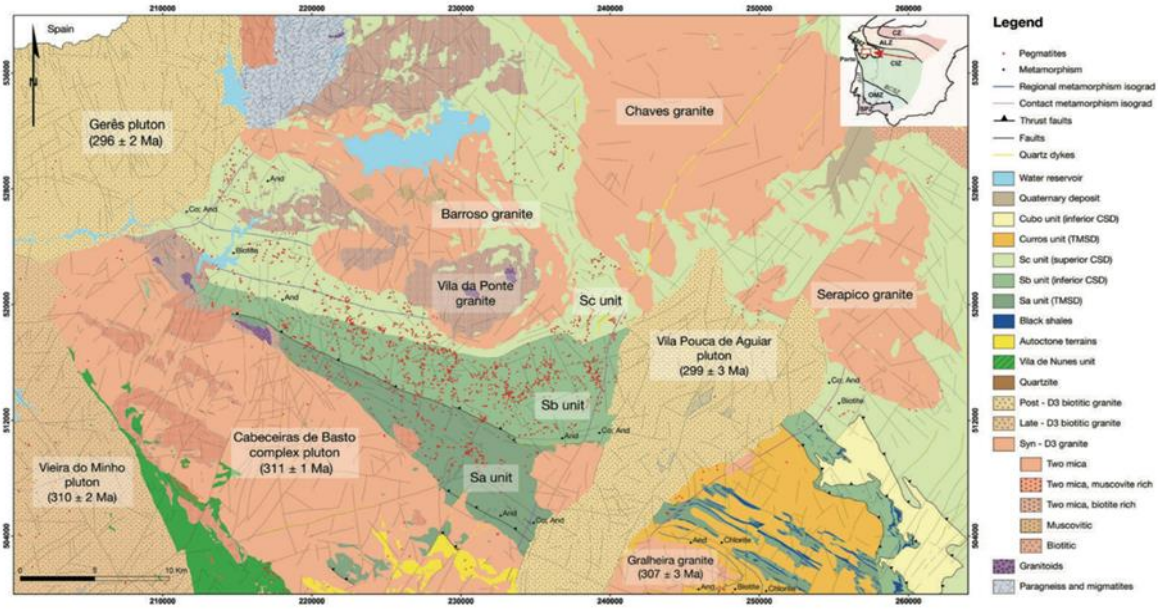

Figure 2.8 Simplified geology of the Barroso-Alvão region, with granite bodies emplacement ages. Adapted from Silva (2014)

2.3.2. Variscan orogeny in Galicia Trás-Os-Montes zone: Synthesis

The Variscan orogen is the result of a continental collision between Laurasia and Gondwana and, in the process, the closing of the Rheic ocean. This collision resulted in three main deformation phases (D1, D2, and D3) distinguished all over the Iberian massif (Ribeiro, 1974, Dias and Ribeiro 1995). The GTMZ is marked by an overabundance of crustal nappes separated by thrust faults, resulting in the overlapping of allochthonous piles over the autochthonous terraines of the CIZ. GTMZ is bounded by a large thrust fault which overlaps all GTMZ units with the autochthonous units in CIZ (Noronha *et al.* 2013). Furthermore, the GTMZ parautochthonous units can be divided into two domains from a lithostratigraphic, structural and lithochemistry point of view, geometrically separated by the Palheiros-Vila Flor Fault. Depending on the authors, different denominations are ascribed to these domains. The Upper Parautochthon and Lower Parautochthon nomenclature suggested by Dias da Silva *et al.* (2016) will be the one used in this work.

The D1 deformation phase, 359-336 My (Dallmeyer *et al.*, 1997), is mostly a compressive phase, resulting in crustal shortening and development of sub-vertical axial plane folds with a predominant NW-SE strike (Noronha *et al.* 2013). Several regional ductile shear zones also developed sin-D1 (Ferreira *et al.* 1987). The D2 deformation phase, 337-316 My (Dallmeyer *et al.*, 1997), is mostly observed in the allochthonous and parautochthonous units, highlighting the SE vergence and resulting in leaning folds with inverted flanks (Noronha *et al.* 2013). The D3 deformation phase, 315-306 My (Dallmeyer *et al.* 1997), seems to affect all terraines (autochthonous, parautochthonous, and allochthonous) originating small amplitude folding with vertical axial plane. During the tardi-D3 and post-D3 phases, ductile-brittle and brittle deformation systems of fractures, mostly orientated NNE-SSW, and it's conjugate NNW-SSE, were formed. The main trends of these fault systems vary from N020º - N030ºE to N-S, and E-W to ENE-WSW (Noronha *et al.* 2013).

All the three main deformation phases resulted into a distinct foliation on CIZ and GTMZ rocks. The D1 deformation phase developed a S1 foliation which is roughly parallel to the bedding (S1//S0) with main orientation N120º (Martins and Lima, 2011). The D2 deformation phase caused the horizontalization of the S1 foliation, producing a crenulation cleavage S2 (Noronha *et al.*, 1981). D3 deformation phase produced a strong penetrative crenulation cleavage (S3), that is associated with ductile shear zones and seems to overprint previous foliations (Noronha *et al.*, 1981). The deformation path from D1 to D3 comprises a regional partial melting event (ca. 320 My) as well as a major episode of crustal shortening (ca. 330-15 My). Both events precede the isostatic rebound of the continental crust and subsequent orogen dismantling dated at around 300Ma (Mateus and Noronha 2010).

2.3.3. Metasedimentary envelope

The metasedimentary sequence hosting the pegmatitic bodies includes 3 Units (Sa, Sb, and Sc). These units belong to the parautochthonous complex of the GTMZ, with ages from late Ordovician to Devonian (Ribeiro *et al.* 2000). The Sa Unit, equivalent to the Fragas Unit mentioned in several works (*e.g.*, Dias, 2016) represents part of the Lower Parautochthonous (also denominated Três Minas Structural Domain), whereas Sb and Sc are comparable to the Rancho subunit and Santa Maria Émeres Unit mentioned in several works (*e.g.*, Oliveira *et al.* 2020) respectively, both included in the Upper Parautochthonous domain (also denominated by Carrazedo Structural Domain) (Silva,2014). The sedimentary envelope is composed of dark greyish pelites intercalated with pale psammitic levels mostly on the range between silt and fine sand. It is sometimes noticeable that the presence of matrix-supported volcaniclastic layers enriched in calc-silicate rocks with quartz enriched levels, being also possible to find feldspar enriched levels (Ribeiro *et al.* 2007). Aldeia's pegmatitic swarm is mainly hosted by the metasedimentary unit Sb.

2.3.3.1. S_a Unit

The Sa unit, of pelitic psammitic nature, is composed of micaschists, quartz-rich micaschists and lidites, all presenting a very distinct and evident foliation parallel to S0. Micaschist mineralogy is dominated by quartz + white mica + biotite with some andalusite, biotite, cordierite, and staurolite porphyroblasts in a poikilitic texture. Lidites are characterised by high contents of organic matter as well as small percentages of white mica and quartz (Ribeiro *et al.* 2000).

2.3.3.2. S_b Unit

This unit is the main hosting of Aldeia's prospect and will be described in further detail. It comprises two main rock types: micaschists and quartzschists resulting from genetic evolution of pelitic and psammitic sedimentary protoliths, respectively (Ribeiro *et al.* 2000).

The Sb unit micaschists are strongly foliated, intersected by tightly folded recrystallized quartz veins, sometimes found in pinch and swell structures, and display a rhythmic fine grained tectono-metamorphic banding affected by various folding phases. The banding consists of an alternation of quartz-enriched layers with mica-enriched layers, where biotite dominates over white mica. It's worth mentioning the presence of two distinct andalusite porphyroblast generations, as well as accessory amounts of garnet. The predominant and earlier andalusite generation is characterized by centimetric porphyroblasts, preserving an internal foliation consistent with the foliation presented by the main rock, and displaying evident effects of rotation/twisting. This first andalusite is sometimes strongly retrograded to white mica and quartz. The second generation is made of better preserved smaller porphyroblasts (typically inferior to 1 cm), which seems to postdate the development of the main rock foliation.

Although millimetric and variably retrograded, garnet blasts are frequent. Garnet relative abundance tends to increase when (chloritized) biotite- and white mica-rich bands are thicker, which is typically close to the interfaces with quartz-rich bands. Closer to the Li-enriched aplite-pegmatite bodies, micaschists present a noticeable enrichment in tourmaline, which often presents linear fabrics with a roughly parallel direction when compared with rock foliation (Mateus *et al.* 2022).

The quartzschists composing the Sb unit also present strong evidence for multiphase folding and display a foliation, less penetrative than the one seen on the micaschists. This foliation affects both the previous fabric and the strongly recrystallized folded quartz veins. From a mineralogical standpoint, the quartzschists present a simpler mineralogical association, dominated by quartz and white mica, matching the description of Ribeiro *et al.* (2000).

2.3.3.3. S_c Unit

Sc is a relatively monotonous sequence dominated by filites, micaschists, and quartz-rich greywackes interlayed with calcossilicated rocks (more abundant here than in previous units). Quartz-albite rocks are much more abundant than in previous units and, although rare, it is also possible to find carbonaceous rocks (Ribeiro *et al.* 2000).

2.3.4. Bordering Granites

As suggested by Lima (2000), in the Barroso-Alvão region we find essential three main outcropping granitic massifs which limit the region: The Barroso massif, the Cabeceiras de Basto massif, and the Vila Pouca de Aguiar massif.

2.3.4.1. Barroso Massif (BM)

Not yet dated with absolute methods, is composed by multiple granitic facies, all of them considered sin to tardi-D3. According to Noronha and Ribeiro (1983) the distinct facies comprise:

a) Barroso Granite (BG) - It's an orientated coarse grained two mica granite (Biotite > Muscovite), with porphyroid tendency. The accessory minerals of this granite are apatite, tourmaline, and opaque minerals.
b) Vila da Ponte Granite (VPG) - Medium grained granite with a porphyroid tendency, characterised by a high abundance of biotite (including ovoid textures). Besides biotite the mineral assemblage is composed of quartz, K-feldspar, plagioclase, and muscovite. The accessory minerals include apatite, rutile, zircon, and opaque minerals.
c) Pisões Granite (PG) - It's a medium to coarse grain two-mica granite that, despite being associated with the BG, is not as coarse nor as porphyritic as the BG. Petrographic studies seem to reveal high deformation rates and high recrystallization rates. The main difference between the Barroso and Pisões granite is that PG is more enriched in albite and muscovite.

d) Vilar Granitoids (VGr) -They are rocks of medium to fine grain characterised by their dark colour due to the high abundance of biotite. Quartz is less abundant than in the previous granites, reaching more quartz-monozitic compositions.

2.3.4.2. Cabeceiras de Basto Massif (CBM)

Is a syn-D3 two-mica granitic body elongated into the direction NW-SE. This massif intruded 311±1Ma ago, according to U-Pb dating in zircon and monazite presented by Almeida (1998). Almeida (1994) identified three main groups of two-mica granites according to grain size:

a) Fine-grained granites where the grain size goes from 0.5 to 1mm;
b) Medium-grained granites where the grain size goes from 2 to 4mm;
c) Coarse-grained granites where the grain size goes from 5 to 7mm sometimes crystals reach rare sizes of 8 to 10mm.

All granitic facies present a hipidiomorphic texture and similar composition, leaving the grain size as the only distinguishing characteristic between granite groups. The main mineralogy comprises quartz, plagioclase, K-feldspar, biotite, and muscovite (always more abundant than biotite). The accessory mineral assemblage includes apatite, zircon, rutile, sillimanite, tourmaline, monazite, and ilmenite. Sporadically some andalusite was found near the contact with the metasedimentary rocks SW of the CBM.

2.3.4.3. Vila Pouca de Aguiar Massif (VPA)

Is a post-D3 massif that limits the aplitopegmatites area to the east. According to Martins and Sant'Ovaia (1998) the emplacement of this massif is controlled by the Régua-Verin fault. It is comprised by three different facies all of them biotitic granites (Lima,2000):

a) Vila Pouca de Aguiar Granite (VPAG)- Is a porphyroid medium grain sized granite, characterized by micro-inclusions of tonalites and granodiorites to these inclusions appears facies of coarse-grained granite. According to Almeida *et al.* (2002) the geochronologic data referring to VPAG point towards a massif intrusion around 299±3Ma based on zircon and monazite U-Pb geochronology.
b) Gouvães da Serra Granite (GSG) – Coarse-grained granite with K-feldspar megacrystals.
c) Pedras Salgadas Granite (PSG)- Slightly more leucocratic granite, with medium to thin grain, tends to occupy the central part of the VPA. Lima (2000) places PSG's age at 295±13Ma, using Rb-Sr in whole rock chemistry.

2.3.4.4. Metallogenetic specialization

Almeida *et al.* (2002) point out that according to standards defined by Tischendorf (1977) only Cabeceiras de Basto granites can be considered specialized with ppm values of Li, Sn and W over the limits defined by the latter author. Almeida *et al.* (2002) also refers that geochemical data for VPAG granites show that they are not strongly differentiated and cannot therefore be considered specialized. However, the authors also refers that despite not specialized VPAG granites are spatially related to important Sn, W and Au mineralizing systems, suggesting that their emplacement might create thermal conditions to generate convection of crustal fluids leading to ore concentration. Furthermore, the lack of systematic trace element studies for Barroso Massif complicates the assessment of the metallogenetic specialization of this massif.

2.3.5. Metamorphism

Both the CIZ and GTMZ experienced widespread granitic plutonism and metamorphism. Martinez *et al.* (1990) delineated the isograds of numerous metamorphic zones for the whole Iberian Massif. According to Martinez *et al.* (1990) the distribution of those isograds is directly related to the regional metamorphism, which in turn is directly related to granite plutonism that has been complicated by subsequent faulting events. The metamorphic zones exhibit crosscutting isograds, which imply the existence of overprinting metamorphic events (Martins, 2009). It is possible to identify in the study area a prograde orogenic/regional metamorphism with conditions analogous to the Abukuma (Low pressure, High Temperature) and Barrovian Type (Medium pressure, High Temperature) described by Miyashiro (1961). Added to the local metamorphism there seems to be some contact metamorphism related to the intrusion of the sintectonic CBM. The isograds are parallel to this granite and to the lithostratigraphic units and result from the Pre to Syn-D3 thermal peak (Noronha and Ribeiro, 1983). Close to the contact with the Cabeceiras de Basto granite there are two different mineralogical associations defining the andalusite isograde (Martins and Lima, 2011):

1. quartz + muscovite + biotite +/- andalusite +/- staurolite;

2. quartz + muscovite + biotite +/- andalusite +/- staurolite +/- garnet +/- plagioclase

Adding to the regional metamorphism, there are some evidence for local hydrothermal alteration related to the aplite-pegmatite or quartz vein emplacement (Ribeiro *et al.* 2007).

2.4. ALDEIA'S APLITE-PEGMATITE SWARM

Aldeia's aplite-pegmatite bodies (Figure 2.9) present a plethora of directions and dips. Drilling campaigns recognized a main family of thick and long bodies, approximately oriented NW-SW and with dips comprised between 20-90º NE/SW. Occasionally, preservation of intrusive almost planar contacts (also variable in dip) is found, typically intersecting late-D2 folds. In some cases, these contacts are replaced by a collection of minor/secondary apophyses of the aplite-pegmatite bodies, often interlayered with S2 foliation and lately affected by D3 folding. These bodies also present late tectonic fabrics, compatible with D3 shearing. This deformation phase is also responsible for some displacement of the aplite-pegmatite bodies. Peripherally to the main cluster it is possible to find three different aplite-pegmatite "sub-groups":

a) Oriented ENE-WSW, dipping up to 25º to the NNW
b) Oriented N-S, vertical to sub-vertical
c) Roughly NE-SW, dipping 65º to SE

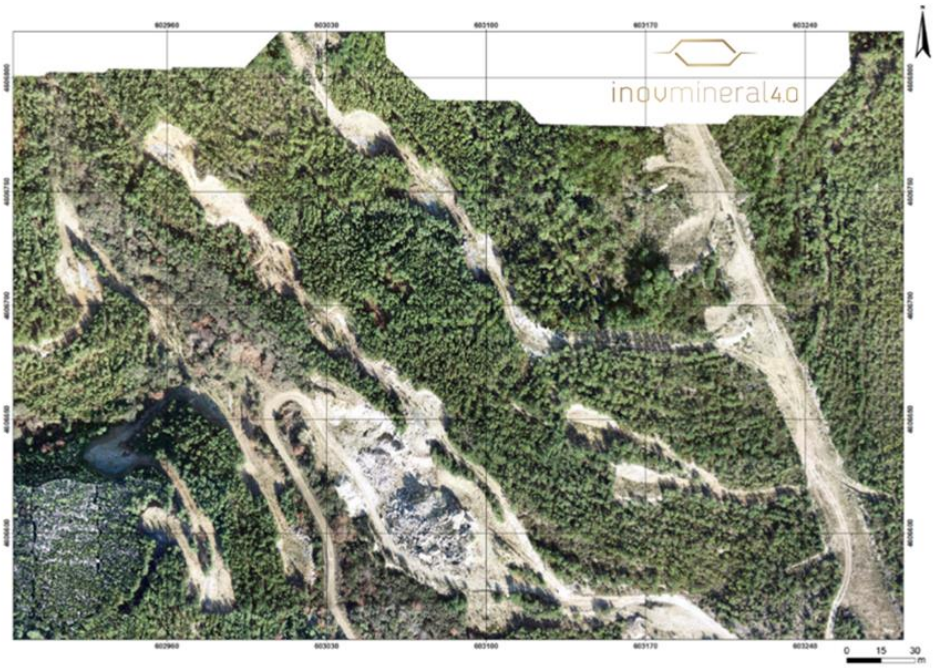

Figure 2.9 Georeferenced aerial view from Aldeia's aplite-pegmatite swarm. Adapted from Mateus et al. *2022.*

Field observation of Li-rich aplite-pegmatite bodies allow to recognize three fusiform morphologically asymmetrical bodies separated by screens of sheared micaschist. The walls of these fusiform bodies display several structural features such as oriented quartz-slickensides, tension gashes recording strain accommodation surrounding the rigid bodies. The enveloping sheared schists, mentioned previously, show an array of different structures such as small dragging folds or pinch-and-swell features. Field work allowed for the identification of local scale tectonic structures cutting and displacing the aplite-pegmatite (Figure 2.10).

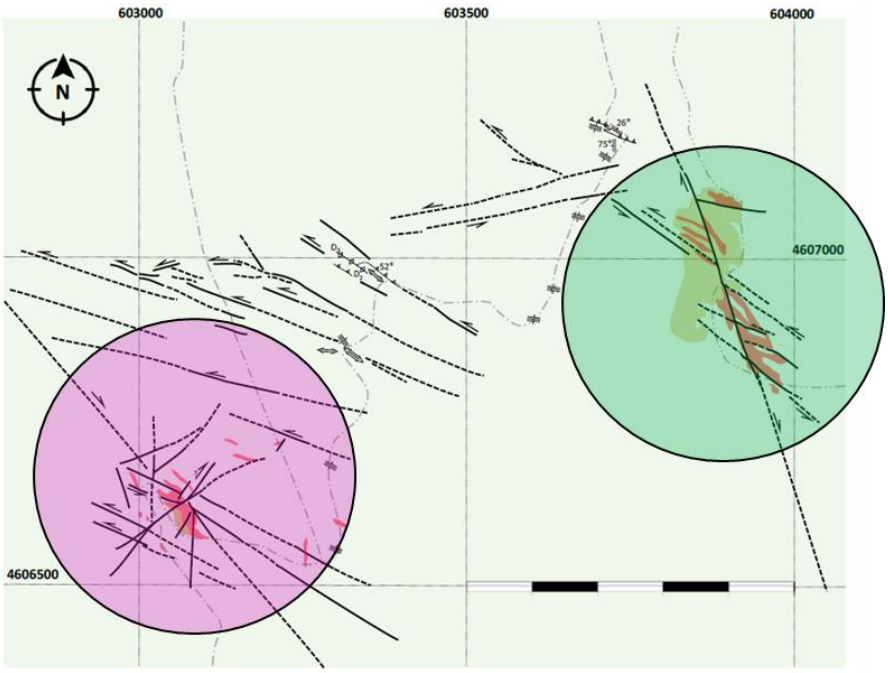

Figure 2.10 Geological scheme of structural features in the area. Pink circle roughly delimiting Aldeia prospect, green circle roughly delimiting Alijó mine. Adapted from (Mateus et al. 2022).

Field observations of the exposures also allowed for the identification of significant mineralogical differences between aplite and pegmatite domains. The aplite is dominated by quartz, albite, and accessory white mica. Whereas pegmatite domains are dominated by quartz, K-Feldspar, and albite locally enriched in spodumene. The contacts between pegmatitic and aplitic domains can be gradual or sharp, sometimes marked by reaction fronts irregular in geometry.

3. METHODOLOGY

The purpose of this chapter is to provide the reader insight into the procedures utilized during this dissertation. This chapter will briefly summarize the processes of sampling, macroscopic analysis, thin section production, petrographic characterization, and electron microprobe analysis.

3.1. SAMPLING

The samples analysed in this work were obtained in the scope of the project INOVMineral4.0 and belong to 1 of the 39 drilling holes performed by Savannah Resources in Aldeia's swarm. Drill hole recovery starts at 88 meters all the way to 177 meters, and intercepts two aplite-pegmatite bodies: pegmatite 1, representing the initial 46 meters; and pegmatite 2 with circa 10 meters thickness (Figure 3.1). Ten samples of pegmatite 1 (#1-#10) and five samples of Pegmatite 2 (#13-17) were collected to include the observed mineral and textural diversity. A metasomatic alteration zone (MAZ) of roughly 5 meters separates the two pegmatite bodies from which two samples were collected (#11-#12). Samples #18 and #19 correspond to the metasedimentary host rocks representing the last 13 recoverable meters.

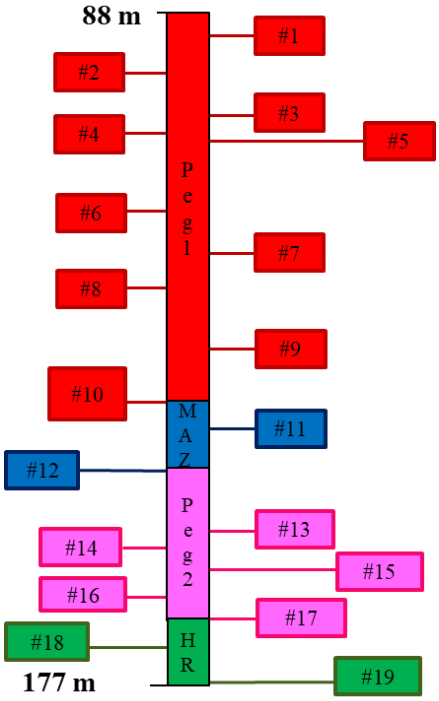

Figure 3.1 Drill hole schematization with identified domains in different colors. Red - Pegmatite 1; Blue- Metasomatic Alteration Zone; Pink- Pegmatite 2; Green- Host Rock

3.2. MACROSCOPIC DESCRIPTIONS

After a macroscopic description (presented in Appendix I) and analysis, 30 rock slabs were selected to produce polished thin sections, considering their mineralogical or textural arrangement characteristics. Prior to cutting the rock slabs a full sample photographic database was created preserving the location of chosen sections (figures in appendix I.I to I.XIX)

3.3. LABORATORY PROCEDURE

The laboratory procedure consisted in: 1) cutting 5x3 cm rock slabs; 2) glue them to an unpolished glass; 3) cutting and grindind to 35 µm thickness; 4) polishing, using polishing diamond paste of 15 µm

,6 μm, 3 μm, and 1 μm. This resulted in 30 polished thin sections from the original 19 samples (Table 3.1). The laboratory procedure was conducted at Faculdade de Ciências da Universidade de Lisboa (FCUL).

Table 3.1 Thin section production based on the sample. Samples analysed with EMPA marked with a checkmark.

Macroscopic Sample	Thin Sections	Geochemical Analyses
#1	1	✓
#2	2a	
	2b	
	2c	✓
#3	3a	
	3b	
#4	4	✓
#5	5	✓
#6	6a	
	6c	
#7	7a	✓
	7b	✓
	7c	
#8	8a	
	8b	✓
#9	9a	
	9b	✓
	9c	✓
#10	10	
#11	11a	
	11b	✓
	11c	✓
#12	12	✓
#13	13	✓
#14	14	✓
#15	15	
#16	16	
#17	17	✓
18	18a	✓
	18b	
19	19	✓

3.4. PETROGRAPHIC CHARACTERIZATION

The petrographic analysis was conducted in a Leica DM2700 P microscope, with a coupled digital camera, which allowed to observe the thin sections in transmitted plane-polarized light (PPL) and cross-polarized light (XPL) as well as in reflected light (RL). Based on this analysis, minerals were selected for further electron microprobe analysis.

3.5. ELECTRON MICROPROBE ANALYSIS

A JEOL JXA 8200 instrument, equipped with 4 wavelength-dispersive spectrometers (WDS), secondary and back-scattered electron detectors, and an energy-dispersive spectrometer (EDS), was employed to chemically analyse the minerals and to identify and characterize textural and mineralogical features not visible at the microscopic scale. EDS was essential, through collection of semi quantitative chemical data, to the identification and characterization of unknown mineral phases prior to their chemical analyses. The JEOL JXA 8200 system running conditions were the following: Acceleration voltage of 15 kV, with a beam size of 5 μm (silicates except feldspars), 8 μm (feldspars), 7 μm (phosphates except ludlamite which was measured with 10 μm) and 1 μm for ilmenite. Counting times were 20 seconds and 5 seconds for background radiation. The correction program ZAF was also applied. The calibration standards, as well as detection limits are reported in appendix II.I. 17 thin sections were selected for geochemical analyses (table 3.1). Analyses focused over the critical mineral phases (Table 3.2) considered relevant for this study possibly providing information of the metallogenetic processes involved in the system. Other mineral phases were studied, however due to analytical problems were not considered for discussion. The mineral microanalysis using these methods was supervised and instructed by Dr. Pedro Rodrigues at the microprobe laboratory of FCUL.

Table 3.2 Main mineral phases submitted to EMPA.

Silicates	**Sulfides**	**Oxides**	**Phosphates**
Spodumene	Pyrite	Ilmenite	Apatite
Albite	Arsenopyrite		Ambligonite- Montbrasite
Microcline	Sphalerite		Triphylite- Lithiophilite
Moscovite			Heterosite-Purpurite
Biotite			Fairfieldite-Messelite
Beryl			Ludlamite
Garnet			
Tourmaline			

4. PETROGRAPHY

The detailed macroscopic and microscopic analysis of the drill hole samples revealed the existence of 4 principal domains: a) pegmatite 1; b) metasomatic alteration zone (MAZ); c) pegmatite 2; and d) host rock. It is important to refer that despite the "pegmatite" denomination both pegmatite domains include aplitic and pegmatitic facies with the former serving many times as the matrix. Despite the division between pegmatite 1 and pegmatite 2 these domains share several similar features. Macroscopic description (Complete in appendix I) allowed to establish an initial mineralogical assemblage for each domain.

Pegmatite domains (Figure 4.1A) being dominated by a typical assemblage of quartz, plagioclase, K-feldspar, muscovite ± spodumene. Microscopic analyses of polished thin sections revealed its presence in 20 thin sections, all representative of pegmatite domains.

MAZ (Figure 4.1B) samples share many of their characteristics with the host rock, however, the presence of clear lixiviation zones and intermingling with pegmatite domains being the principal differentiation factor between them.

Host rocks (Figure 4.1C) in the study area correspond to strongly foliated micaschists displaying a rhythmic fine-grained tectono-metamorphic banding. This layering is marked by mica-enriched (biotite > muscovite) domains and quartz ± muscovite layers. Garnet was identified in one of the samples.

Figure 4.1 Examples of the different domains found in the studied drill hole. ***A)*** *Macroscopic sample of aplite-pegmatite domain;* ***B)*** *Macroscopic sample of metasomatic alteration zone domain;* ***C)*** *Macroscopic sample of the host rock.*

4.1. PEGMATITE

The petrographic analysis of the aplite-pegmatite domains revealed poorly zoned bodies with an extremely complex mineral assemblage developed along two petrographically and mineralogical distinct crystallization stages, later affected by a strong metasomatic event.

Stage I (Figure 4.2A) is characterized by a typical pegmatitic mineralogical assemblage of quartz+ albite + K-feldspar + muscovite with accessory beryl, apatite, and Fe-Mn (Li) phosphates, and residual U-REE phosphates and sulfides (pyrite ± sphalerite). This pegmatitic assemblage is commonly found intermingled with an aplitic phase of identical composition, yet absent in K-spar, which sometimes works as matrix/groundmass for the pegmatitic phase.

Stage II (Figure 4.2B) is characterized by a main assemblage of spodumene, albite, quartz, and muscovite, with accessory montebrasite, and minor Nb (Ta) oxides (*i.e.* minerals from columbo-tantalite series). It is important to underline the absence of K-feldspar in this second crystallization stage, contrary to what happens in stage I. This assemblage, texturally varying from aplitic to pegmatitic, displays either diffuse or sharp contacts with stage I mineral assemblage, frequently underlined by thin muscovite recrystallization (Figure 4.2C). It is not uncommon to find this stage intersecting stage one, which allows the establishment of a chronological relationship between them (*i.e.* Stage I older than Stage II) .

The metasomatic stage is mainly expressed by late secondary alteration of the primary apatite and Fe-Mn (Li) phosphates which are transformed into Li poor Fe-Mn phosphates. The relations between phosphates (*i.e* phosphate A transforms into phosphate B) are not perceptible under the microscope, and the use of backscattering imaging was needed to establish these relations (Figure 4.2D).

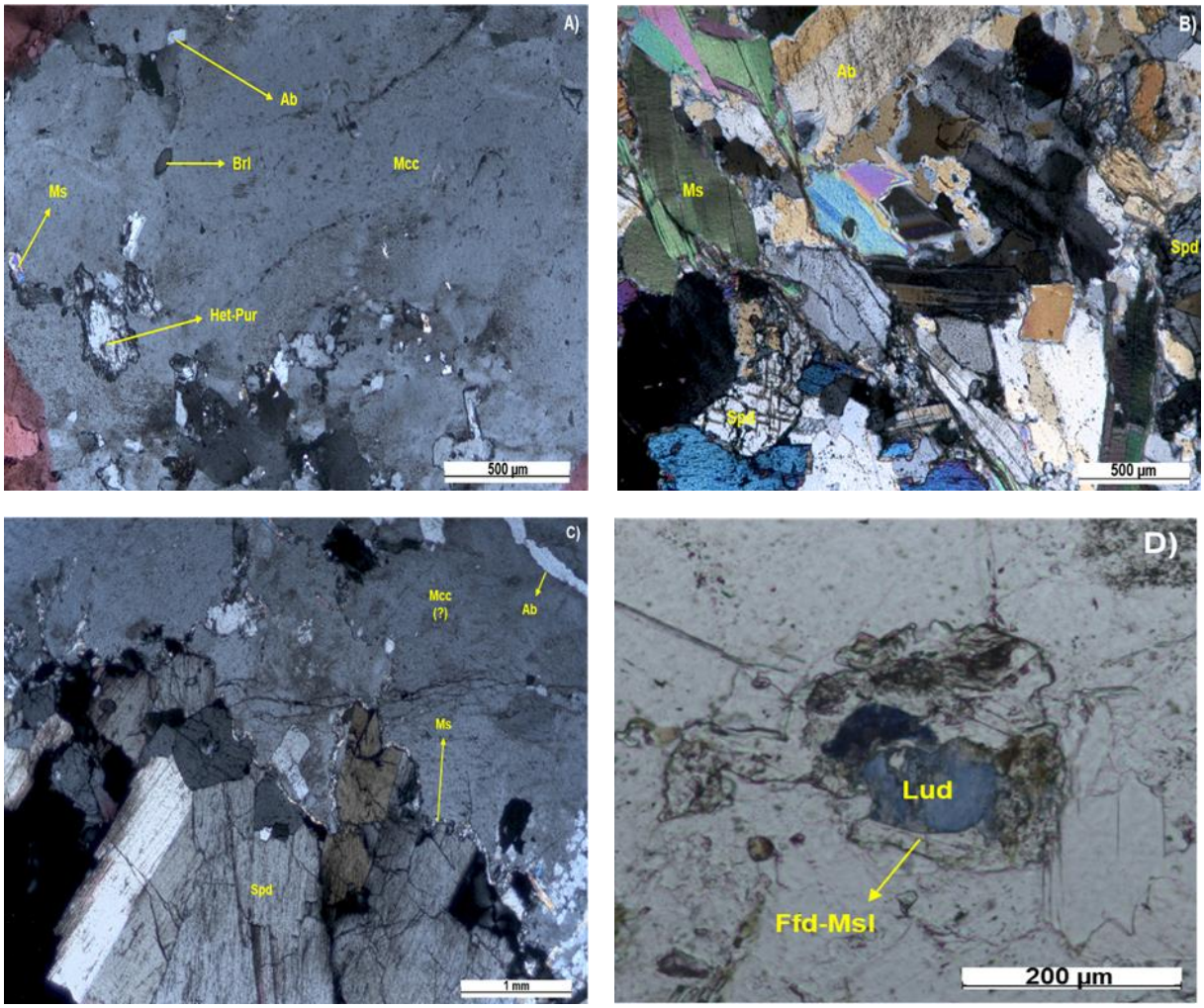

Figure 4.2 Petrographic details of both crystallization stages. ***A)*** *Stage I typical aspect, with prevailing microcline and residual amounts of beryl, albite, muscovite, and phosphates, in this case heterosite-purpurite (XPL);* ***B)*** *Stage II typical aspect, abundance of spodumene, albite and muscovite (XPL);* ***C)*** *Contact between stage I and Stage II underlined by muscovite crystallization (XPL);* ***D)*** *Example of phosphate grain alteration, representative of metasomatic stage (PPL). Mineral abbreviations according to Ward (2021) (see abbreviation list).*

In both magmatic stages quartz appears highly deformed showing abundant wavy extinction (Figure 4.3A) as well as some recrystallization in the zones of stronger deformation. It is worth mentioning the existence of abundant fluid inclusions in quartz crystals, as well as secondary quartz crystals, typically idiomorphic, filling void spaces.

K-feldspar presents abundant perthitic (Figure 4.3B) textures as well as exsolutions of albite, with some small albite regular sections being seen inside the K-feldspar crystal. K-feldspar shows a high degree of alteration appearing most of the time turbid with a brownish tint in PPL. Inclusions of Fe-Mn phosphates (posteriorly identified via EMPA analyses) and/or apatite (Figure 4.3C) is also not uncommon in Aldeia's K-feldspar. The aforementioned phosphate inclusions can be sometimes of sub microscopic dimension only being identified by backscatter electron imaging. K-Feldspar often shows cross-hatched twinning pattern which on its own is sometimes deformed. The presence of this pattern indicates a phase transformation from sanidine/orthoclase to microcline.

Albite seems to accompany the pegmatitic development being present from early stage I forward, until the end of stage II. Four generations of albite were identified: albite presenting myrmekitic textures, only present in stage I and contemporaneous with microcline; albite present in the aplitic ground mass normally less well developed; albite exsolved and recrystallized inside Microcline crystals; and albite present in stage II mineral assemblage. Normally, and independent of generation albite shows polysynthetic twinning (Figure 4.3D) and even mechanical induced twinning, most likely caused by the deformation process. Albite from stage II tends to appear less deformed than albite from Stage I. Furthermore, subsequent EMPA analyses revealed no composicional differences between the different generations of albite.

Muscovite appears in a vast range of dimensions and can be divided into three main groups: common, many times highly deformed, muscovite that appears along with the rest of stage I mineral assemblage (Figure 4.3E); muscovite that underlines the contact between the first and second crystallization stages; common, deformed, muscovite that appears along with the remaining mineral assemblage of stage II. Due to the reduced dimensions of the second group, it was impossible to obtain viable/consistent EMPA analyses. It is also important to mention that muscovite from stage 2 tends to reach bigger dimensions that muscovite from the first stage.

Both beryl and apatite assume a secondary role appearing in typically small (<5mm) dimensions. There doesn't seem to exist a time lag between these mineral phases and the main constituents of stage I. Apatite, as aforementioned, often appears included in mega crystals of Microcline.

Spodumene crystals are highly variable in size reaching centimetric dimensions. Spodumene occurs in three distinct classes: i) sub-euhedral to euhedral crystals of bigger dimension presenting the typical spodumene twinning (Figure 4.3F); ii) anhedral and irregular crystals normally not showing twinning (Figure XG); iii) anhedral very small crystals near the transition between stages. The absence of mineral inclusions suggests that spodumene crystallizes early in the mineral sequence of stage II. It is not rare to run into highly deformed spodumene, sometimes developing slight bending. Given both the metallogenetic and economic implications of the reported variability (*i.e.* albite + spodumene type, petalite + quartz type) for the Li-mineral phases within the Barroso-Alvão aplite-pegmatite field, it is important to stress: i) the absence of both petalite and eucryptite as visible mineral phases ii) the absence, in the studied samples, of spodumene quartz intergrowths (SQI) textures, indicating that spodumene does not result from the decomposition of petalite into spodumene + quartz; iii) despite strongly deformed, spodumene from this stage is extremely well preserved with no evidence of weathering neither alteration

Ambligonite-montebrasite in general occurs associated with anhedral spodumene crystals, appears sporadically, and was exclusively found in pegmatite 1, not being recognized in any samples of pegmatite 2. Typically presents polysynthetic twinning which are slightly thicker than the ones presented by spodumene (Figure 4.3H). The absence of F by subsequent EMPA allowed being identified as montebrasite.

Lithiophilite-triphylite group can be considered a primary phosphate, for stage I, like montebrasite in stage II. The lithium lixiviation that occurs in the late-stage alteration metasomatic episode results in the genesis of secondary Li-deficient phosphates such as fairfieldite-messelite.

Ludlamite is one of the rarest secondary phosphates being only observed in two different thin sections, both corresponding to pegmatite 2 domain. It's the only phosphate that is possible to recognize at the microscope presenting strong pleochroism between colorless and deep blue. Despite being typically green, ludlamite can assume blue colors as mentioned by Neiva (2001). Ludlamite appears typically in the core of multi-phosphate grains being normally bordered by phosphates from the fairfieldite-messelite series.

Fairfieldite-Messelite as mentioned previously it is common to find minerals from this series bordering other phosphate minerals. EMPA analyses revealed that fairfieldite dominates over messelite. Sometimes minerals from this series present a yellowish color without any pleochroism, however due to alteration and reduced dimensions it is not always visible.

As mentioned previously, almost every primary mineral phase, either from stage I or stage II, exhibits micro-textures and intra-crystalline high temperature deformation features (*e.g.*, bending, twinning). These features suggest deformation under crystallization and/or cooling conditions, which is compatible with the regional Variscan deformation patterns observed all over the metasedimentary host rocks.

The contact between the pegmatitic domains and the MAZ is done diffusely with no sharp contacts between domains being found.

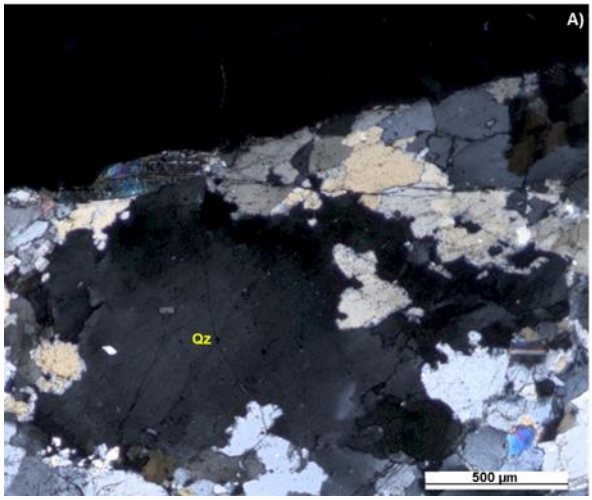

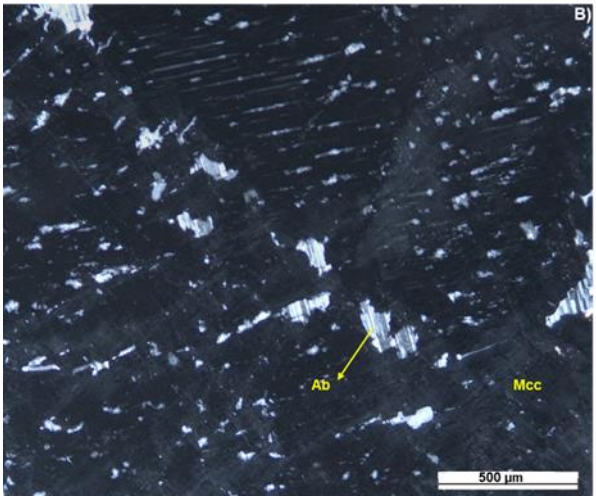

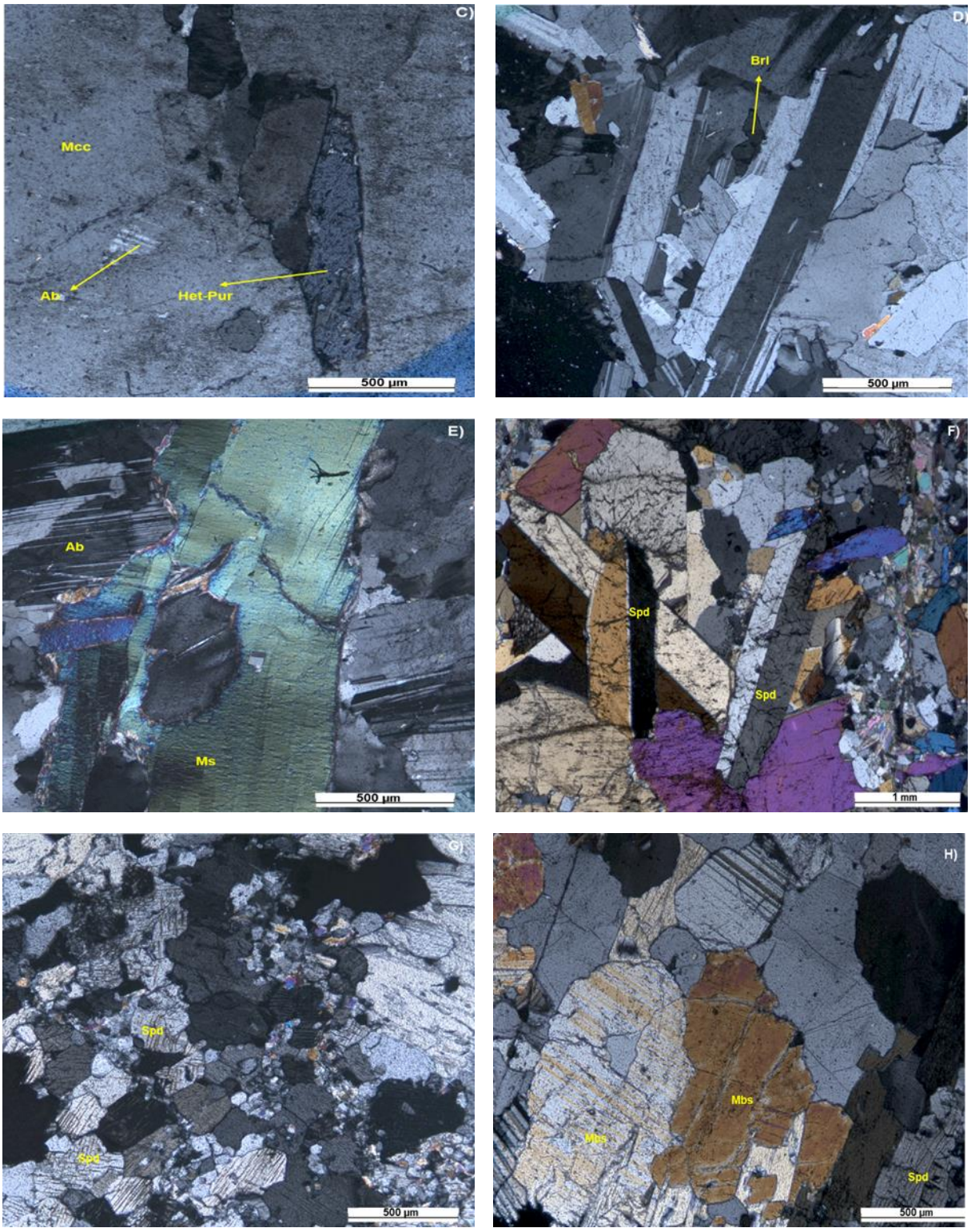

Figure 4.3 Petrographic details from pegmatitic domains. ***A)*** *Wavy extinction on quartz, evidence for strain applied to the aplite-pegmatite bodies (XPL);* ***B)*** *Perhtitic texture in microcline. Worth mentioning the presence of recrystallization of some albite crystals included in microcline (XPL);* ***C)*** *Exsolution of both heterosite-purpurite and albite from microcline (XPL);* ***D)*** *Polysynthetic twinning and slight bending on albite, crystal of beryl highlighted (XPL).* ***E)*** *Example of common muscovite seen in stages I and II, presenting clear evidence of deformation. Also, observable mechanical twinning of albite (XPL);* ***F)*** *Euhedral spodumene crystals showing evident twinning;* ***G)*** *Anhedral/irregular crystals of spodumene, worth to mention the absence of twinning (XPL);* ***H)*** *Montebrasite crystals (twinned) in association with spodumene (XPL). Mineral abbreviations according to Ward (2021) (see abbreviation list).*

4.2. METASOMATIC ALTERATION ZONE

Petrographic analyses of the metasomatic alteration zone domain revealed an intermingling between the mineral assemblage seen in pegmatitic domains and the mineralogical assemblage seen in the host rock domains. MAZ is composed of a heterogeneous quartz, muscovite, chlorite, and tourmaline mineralogical assemblage with minor amounts of sulfides and phosphates. Lepidoblastic domains are present in which sometimes porphyroblasts of biotite and chlorite are present. Pegmatitic domains are also present composed mainly of quartz muscovite with accessory amounts of albite and completely absent spodumene. The contact between these domains is typically marked by the presence of tourmaline Figure 4.4A.

Biotite, contrary to what occurs in host rock samples, does not appear as part of the matrix appearing exclusively in clusters of porphyroblasts (Figure 4.4B).

Chlorite appears as porphyroblasts incorporated in the rock matrix (Figure 4.4C), showing typical anomaly coloration in XPL. Chlorite abundance is especially high in this domain.

Tourmaline tends to appear only in the contact with the pegmatitic domains. Basal sections are quite common and show distinct zonation with the rims being caramel-brown while the cores tend to be a faded shade of that same tonality (Figure 4.4D). EMPA analyses reveal a schorlitic composition for tourmalines from MAZ.

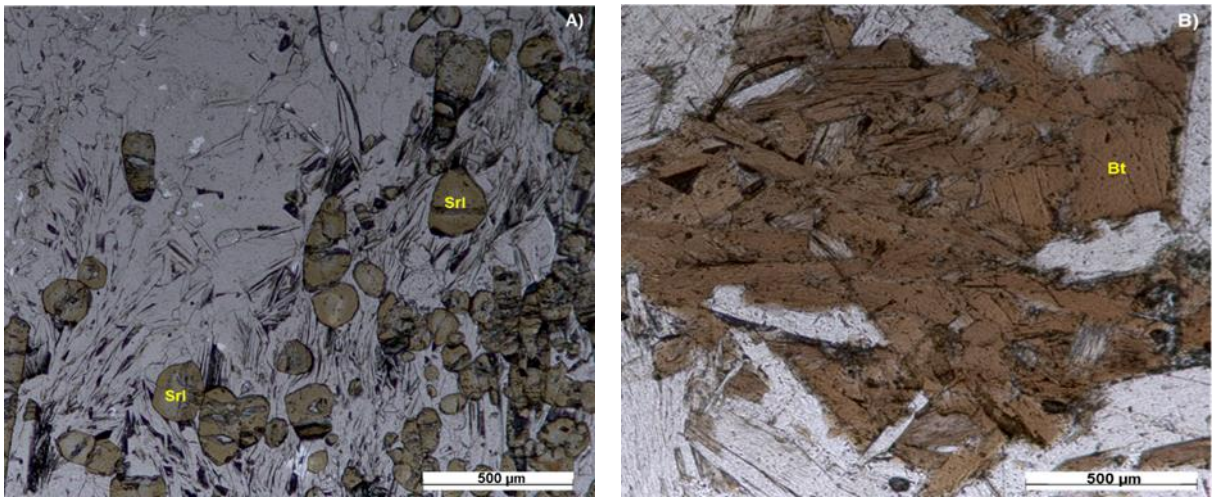

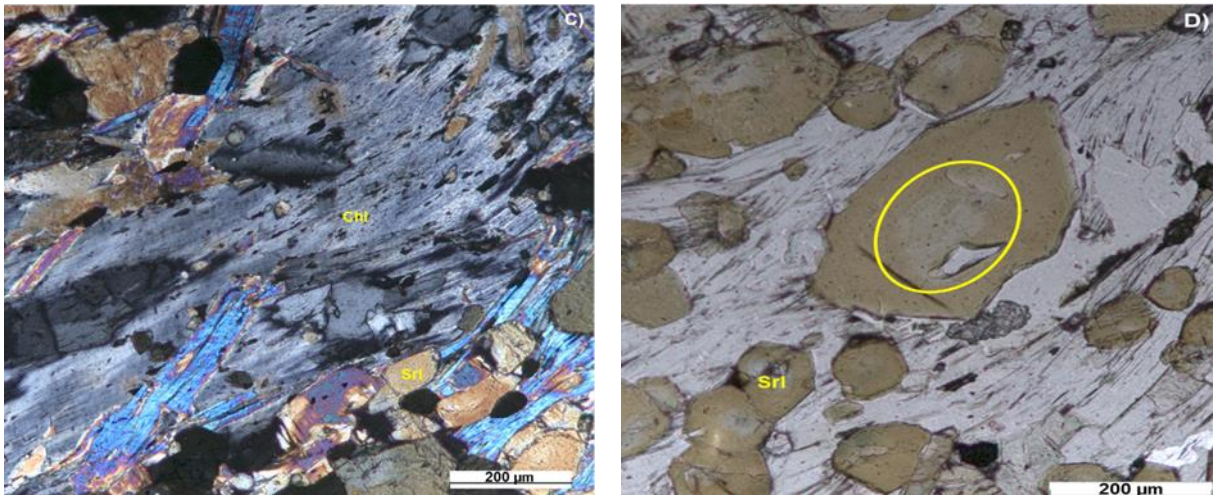

Figure 4.4 Petrographic details from the metasomatic alteration zone domain, ***A)*** *Contact between aplite-pegmatite domain and MAZ, marked diffusely by the presence of tourmaline (PPL);* ***B)*** *Biotite porphyroblast (PPL);* ***C)*** *Chlorite porphyroblasts in the rock matrix, showing blue anomaly colors (XPL);* ***D)*** *Basal section of tourmaline showing a distinct zonation the core (inside the yellow circle) showing a lighter shade than the rims (PPL). Mineral abbreviations according to Ward (2021) (see abbreviation list).*

4.3. HOST ROCK

Petrographic analyses of the host rock domains revealed a strong tectono- metamorphic fabric with a lepidoblastic texture (Figure 4.5A), recording the 3 main deformation phases recognized regionally. As mentioned previously, host rocks are micaschist/quartzschist. Quartz layers appear typically recrystallized in sigmoid like structures (Figure 4.5B). These schists have an heterogenous quartz, biotite, muscovite, chlorite, and ilmenite, mineral assemblage. Assemblage which appears locally enriched in tourmaline with minor quantities of accessory minerals such as apatite, xenotime, arsenopyrite, sphalerite and pyrite. Some domains of the samples present millimetric porphyroblasts of euhedral/sub-euhedral crystals of garnet and biotite.

Biotite, as mentioned above, appears in two distinct size classes: i) common biotite with small needle-like sections part of the matrix marking the foliation (Figure 4.5C); ii) millimetric porphyroblasts of biotite, showing sometimes zircon inclusions (Figure 4.5D). Both classes appear in the typical brown pleochroic color of biotite showing bird eye extinction typical of this mineral. Biotite micafish occur very rarely and exclusively in samples from this domain (Figure 4.5E).

Muscovite in the host rocks appear mostly as thin needles along with biotite being part of the matrix. However, it is not uncommon to find larger crystals of tabular shape contrasting with the typical matrix flow (Figure 4.5F).

Tourmaline in Aldeia's host rock appears in bands over the samples, mixed in the matrix with biotite. Basal sections are quite common and show distinct zonation with the rims being caramel-brown whereas the cores tend to be a faded shade of brown (Figure 4.5G). EMPA analyses reveal a composition between foitite and schorl for the host rock tourmalines.

Both apatite and sulfide appear in the same context, over the matrix in typically in euhedral crystals. These minerals appear very dispersed, typically inconsistent with the foliation, over the sample and rarely reach considerable sizes, making EMPA analyses extremely complicated.

Ilmenite presents a similar behavior as these last two mineral groups, appearing dispersed over the sample normally inconsistent with the foliation in needle like sharp crystals. However, ilmenite also appears as an inclusion inside garnet crystals, normally in rounded crystals of reduced dimension.

Chlorite is abundant in one of the samples, #19, but uncommon in the remaining ones. In sample #19 chlorite appears as thin crystals following the foliation whereas on the remaining samples it appears as porphyroblasts. The chlorite in these samples shows no evidence to result from the alteration of biotite.

Garnet appears in euhedral to sub euhedral crystals (Figure 4.5H), completely isotropic, absent a microscope visible compositional zonation. As mentioned previously, ilmenite crystals are found included in garnet crystals. The Aldeia garnet preserves an internal foliation, not compatible with the foliation of the remaining sample. Adding to that a slight rotation on the largest garnets is evident. Aldeia garnets show some internal fracturing normally not reaching the core of the crystal.

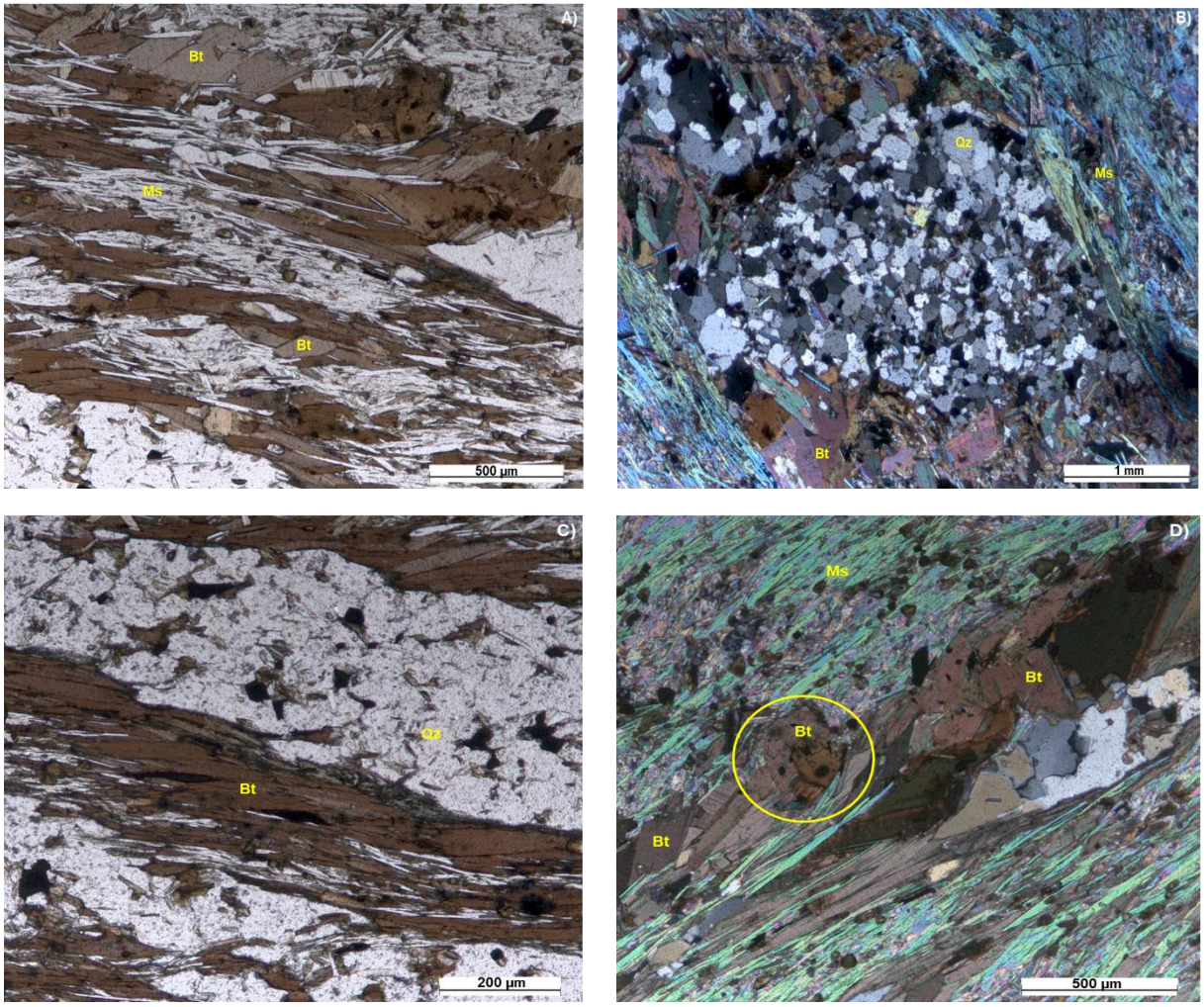

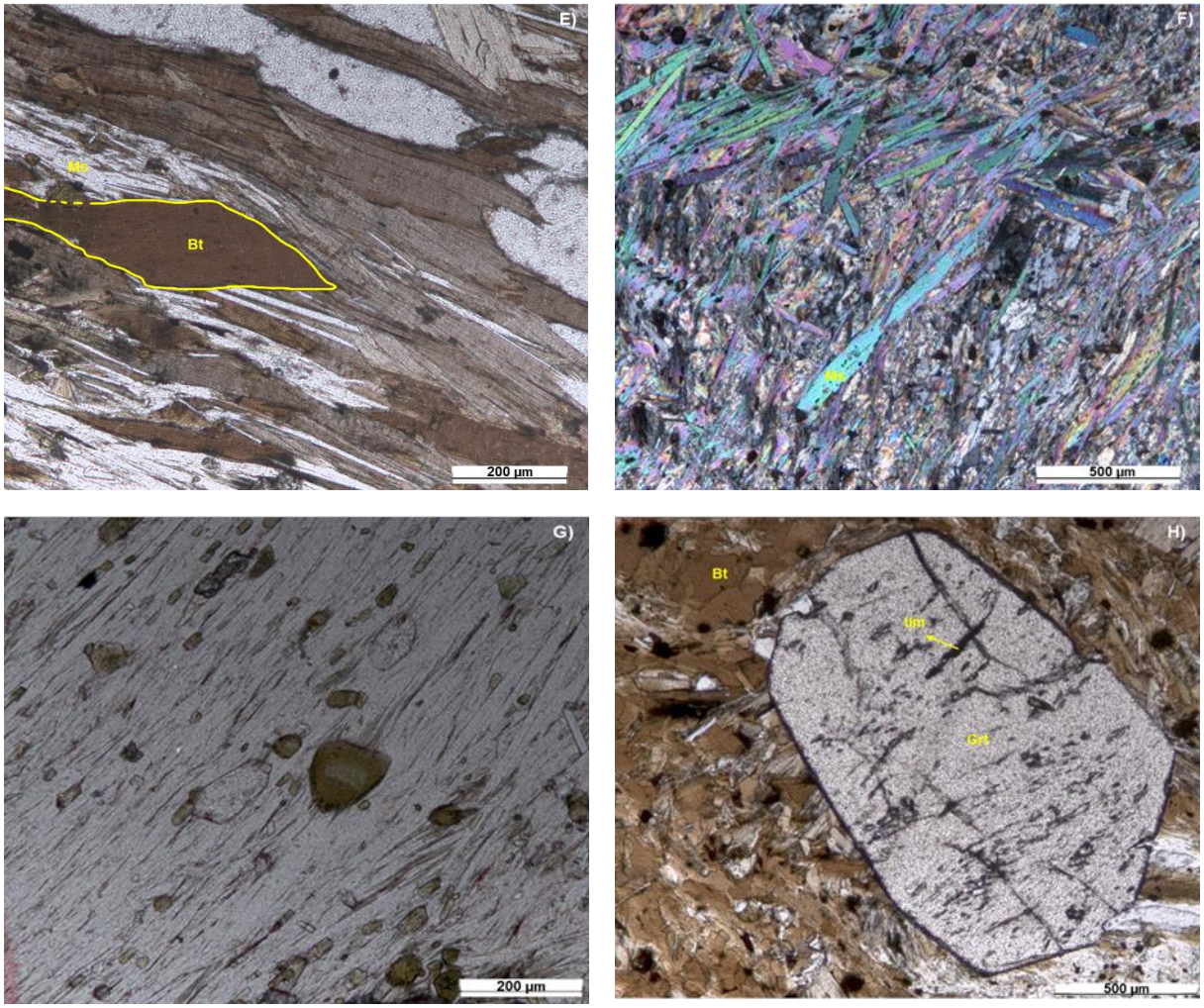

Figure 4.5 Petrographic details from the host rock samples. ***A)*** *Lepidoblastic texture present in host rocks (PPL);* ***B)*** *Recrystallized quartz in pseudo sigmoid shape;* ***C)*** *Quartz and Biotite layers, biotite being part of the matrix marking a foliation (PPL);* ***D)*** *Porphyroblasts of biotite presenting zircon inclusion (inside yellow circle, PPL);* ***E)*** *Biotite micafish present in the host rock foliation (PPL);* ***F)*** *Different morphologies of muscovite crystals, tabular crystals nonconforming with the matrix (XPL);* ***G)*** *Tourmaline crystals emplaced in micaceous matrix. Basal sections zonation with cores showing a lighter shade of the borders (PPL);* ***H)*** *Garnet crystal included in the micaceous matrix, showing evidence for rotation. Also, important to mention the presence of Ilmenite inclusions (PPL). Mineral abbreviations according to Ward (2021) (see abbreviation list).*

5. MINERAL CHEMISTRY

Mineral chemistry studies work as a tool for a detailed characterization of the chemical variability of the mineral phases recognized during the petrographic study. It was also used for the identification of minerals with reduced dimensions which were impossible to identify microscopically. On total 17 thin sections were subjected to EMPA, with 21 different mineral phases being identified. This work resulted in close to 1000 valid EMPA. Nonetheless, a high number of analyses were disregarded due to not complying with the requirements to be considered acceptable. In this chapter only the main mineral phases will be discussed, and on the "Other minerals" subchapter the other mineral phases that were not able to be properly chemically described will only the mentioned. The cationic distribution for each mineral phase is found in appendix II.II. It is important to highlight that the elements Li and Be were not measured in the mineral phases but estimated numerically considering the whole charge balance and cationic distribution per coordination sites.

5.1. SILICATES

5.1.1. Spodumene

Spodumene (figure 5.1) is a lithium pyroxene of ideal composition $LiAlSi_2O_6$ with Al and Li occupying two inequivalent octahedral positions, M1 and M2 respectively (Pap,1969). According to Morimoto (1989) M1 position can be typically occupied by: Al^{3+}, Fe^{3+}, Ti^{4+}, Cr^{3+}, V^{3+}, Ti^{3+}, Zr^{4+}, Sc^{3+}, Zn^{2+}, Mg^{2+}, Fe^{2+}, Mn^{2+}; whereas the M2 position is typically occupied by: Mg^{2+}, Fe^{2+}, Mn^{2+}, Li^{+}, Ca^{2+}, Na^{+}. Aldeia prospect spodumene occurs neither in the host rock samples nor the metasomatic zone samples, but exclusively in pegmatitic samples, as expected. It is overall well represented in the pegmatitic domains of the studied bodies, resulting in 194 EMPA analyses over 11 different samples (appendix II.II.I). Representative samples are summarized in table 5.1.

Table 5.1 Representative samples of spodumene. Full table, with stoichiometric distributions in appendix II.II.I .
Lithium values are estimated

Sample	#1B5		#4B7		#14B1		#17B4	
Zone	Pegmatite 1				Pegmatite 2			
wt%	1	2	1	2	1	2	3	4
SiO_2	63.84	63.89	63.44	63.80	63.73	63.79	63.09	63.25
Al_2O_3	27.49	27.64	27.26	27.23	27.68	27.56	27.37	27.55
Fe_2O_3	0.00	0.00	0.00	0.06	0.00	0.00	0.00	0.00
Mn_2O_3	0.00	0.00	0.00	0.00	0.00	0.00	0.00	0.00
ZnO	0.06	0.00	0.00	0.09	0.00	0.00	0.00	0.00
FeO	0.31	0.31	0.24	0.09	0.18	0.10	0.30	0.28
MnO	0.00	0.00	0.05	0.04	0.00	0.05	0.02	0.03
CaO	0.01	0.00	0.00	0.02	0.00	0.00	0.01	0.01
K2O	0.01	0.01	0.02	0.02	0.00	0.00	0.02	0.01
Na_2O	0.08	0.07	0.06	0.06	0.07	0.07	0.10	0.06
Li_2O*	7.86	7.95	7.84	7.86	8.01	7.99	7.83	7.92
Total	99.65	99.86	98.90	99.28	99.67	99.56	98.73	99.11

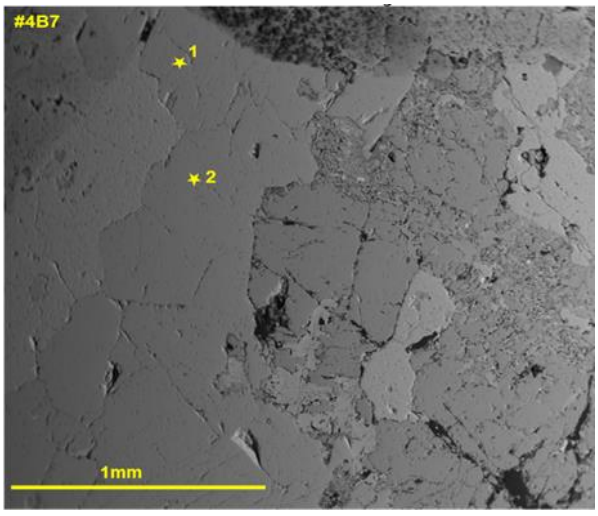

Figure 5.1 Representative backscatter image of spodumene crystals. Point 1 and 2 correspond to analyses presented in table 5.1

Spodumene is compositionally extremely pure (Appendix II.II.I) with an average of 3.67 wt% Li in both pegmatitic bodies, with minor ferrosilitic (FeO < 0.4%) and jadeitic components (Na_2O <0.3%). Li values for Aldeia spodumene are slightly higher than the ones described by Charoy *et al.*

(1992) for spodumenes in the same area. Trace elements present in analysed spodumene display fairly similar distributions independently of the pegmatite body from which they originate (Figure 5.2). Geochemical data also shows no significant difference between the two petrographically identified classes of spodumene (*i.e* coarse grained euhedral spodumene and anhedral corroded spodumene) as it is seen on figure 5.2. Analyses from the fine grain spodumene that appears along stage I and II contact were not conducted.

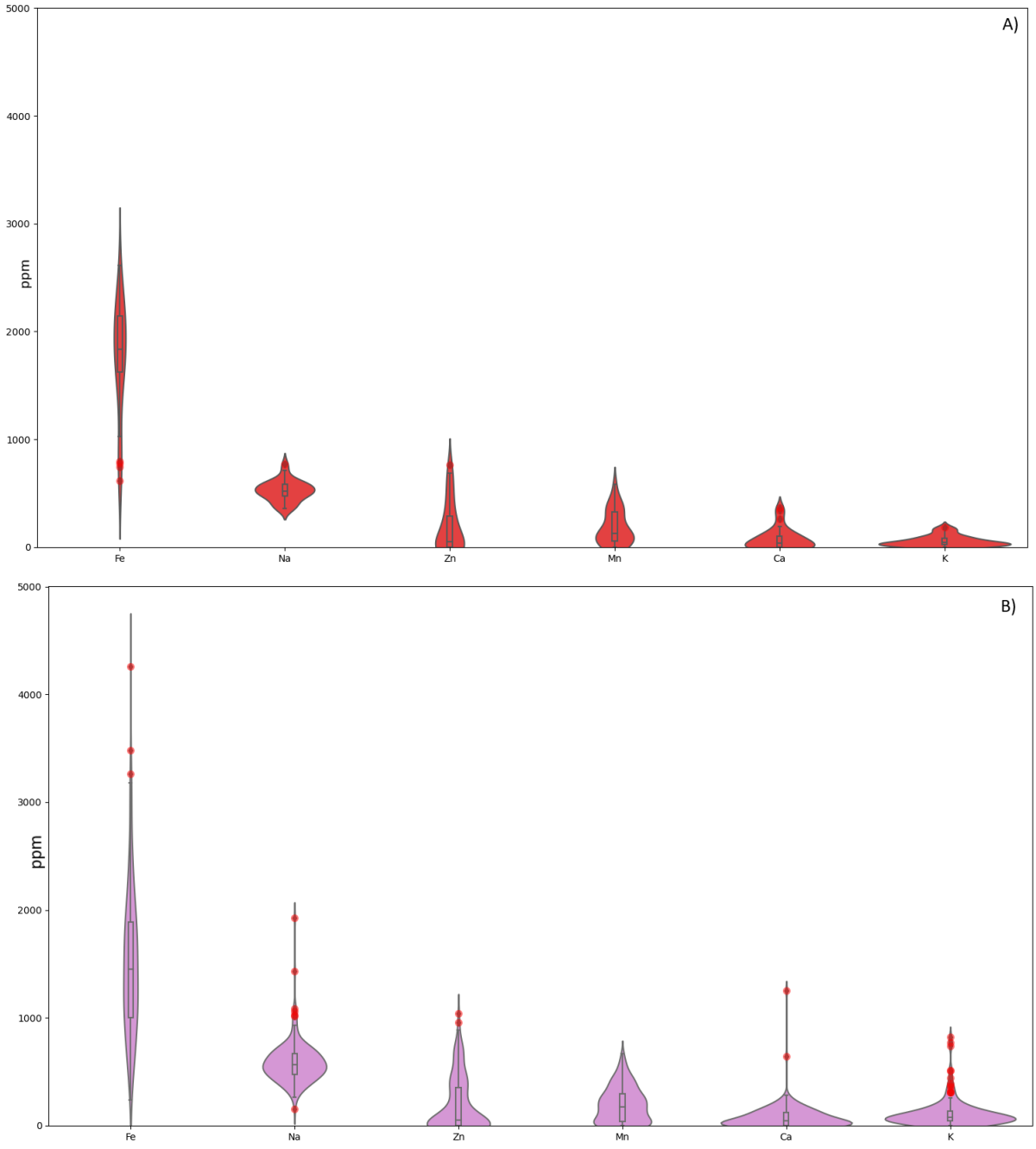

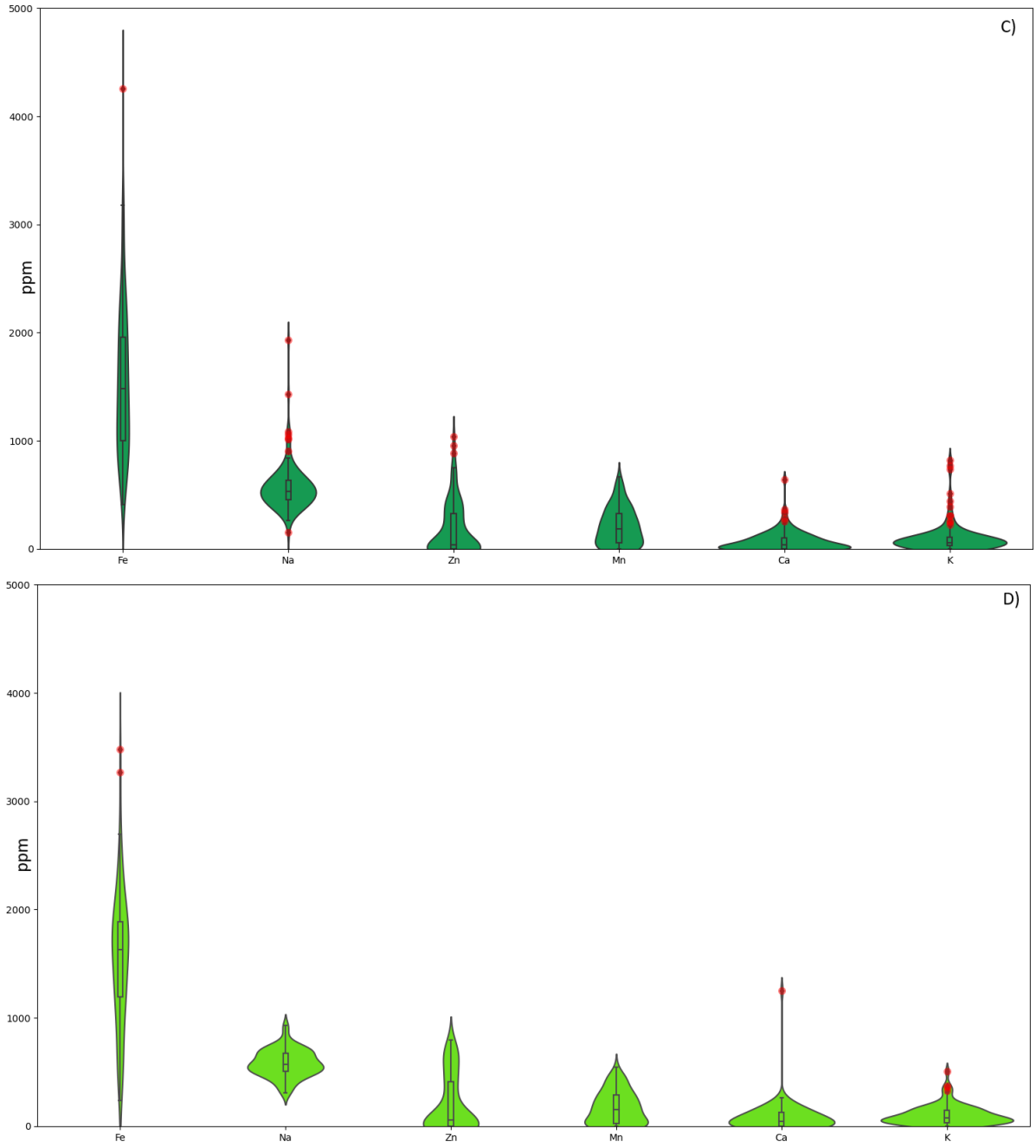

Figure 5.2 Violin plots representing the distribution of trace elements, Fe, Na, Zn, Mn, Ca, and K in different spodumenes. ***A)*** *Spodumene derived from pegmatite 1;* ***B)*** *Spodumene derived from pegmatite 2;* ***C)*** *Corroded/anehedral spodumene;* ***D)*** *Euhedral spodumene.*

5.1.2. Beryl

The beryl group is defined by the general formula $(M^{3+}, M^{2+})_4[Be_6Si_{12}O_{36-z}(OH)_z] \cdot (H_2O)_y A_x$, where A is mostly represented by Na and X rarely exceeds the value of 1. The ideal composition of beryl is $Be_3Al_2Si_6O_{18}$. However, impurities of Na, Fe, Li, Cr, Mn, Zn, Mg are extremely common in beryl from pegmatitic environments (Cerny ,2002; Hawthorne and Cerny, 1977). Fifty-three EMPA analyses were performed in beryl (Figure 5.3) from pegmatite 1 and pegmatite 2 (Appendix II.II.II). Representative analyses of the two sectors are presented in Table 5.2.

Table 5.2 Representative samples of beryl. Full table, with stoichiometric distributions in appendix II.II.II .
**Lithium and Beryllium values are estimated*

Sample	#8bB6		#9cB1		#13B2		#17B2	
Zone	Pegmatite 1				Pegmatite 2			
Wt%	1	2	1	2	1	3	1	2
SiO_2	65.78	65.55	65.48	65.21	65.70	65.03	66.00	65.92
Al_2O_3	18.81	18.87	19.03	18.96	19.17	18.97	19.15	19.06
CaO	0.01	0.02	0.01	0.01	0.00	0.01	0.03	0.04
MnO	0.00	0.01	0.01	0.00	0.00	0.03	0.01	0.02
ZnO	0.00	0.00	0.00	0.03	0.06	0.04	0.00	0.09
MgO	0.00	0.00	0.00	0.00	0.00	0.00	0.00	0.00
FeO	0.25	0.29	0.17	0.19	0.23	0.09	0.24	0.25
Na_2O	0.73	0.96	0.69	1.03	1.02	1.25	0.61	0.81
K_2O	0.03	0.03	0.04	0.03	0.03	0.04	0.03	0.02
SnO_2	0.03	0.00	0.00	0.00	0.01	0.00	0.00	0.01
BaO	0.00	0.02	0.00	0.05	0.00	0.01	0.03	0.00
SrO	0.00	0.05	0.04	0.06	0.00	0.08	0.02	0.02
Cs_2O	0.12	0.12	0.08	0.14	0.07	0.48	0.08	0.06
Li_2O*	0.37	0.48	0.35	0.52	0.51	0.67	0.31	0.41
BeO*	12.98	12.69	12.92	12.56	12.67	12.28	13.05	12.88
CoO	0.00	0.00	0.00	0.00	0.02	0.00	0.02	0.00
Nb_2O_5	0.07	0.03	0.03	0.00	0.06	0.00	0.00	0.01
Ta_2O_5	0.00	0.08	0.05	0.16	0.01	0.00	0.00	0.11
GeO_2	0.00	0.00	0.00	0.00	0.00	0.00	0.00	0.00
Sc_2O_3	0.00	0.00	0.00	0.01	0.00	0.00	0.00	0.00
PbO	0.00	0.01	0.00	0.03	0.00	0.03	0.00	0.03
Cl	0.00	0.01	0.00	0.00	0.01	0.01	0.01	0.00
Total	99.17	99.19	98.90	98.99	99.56	99.01	99.59	99.73

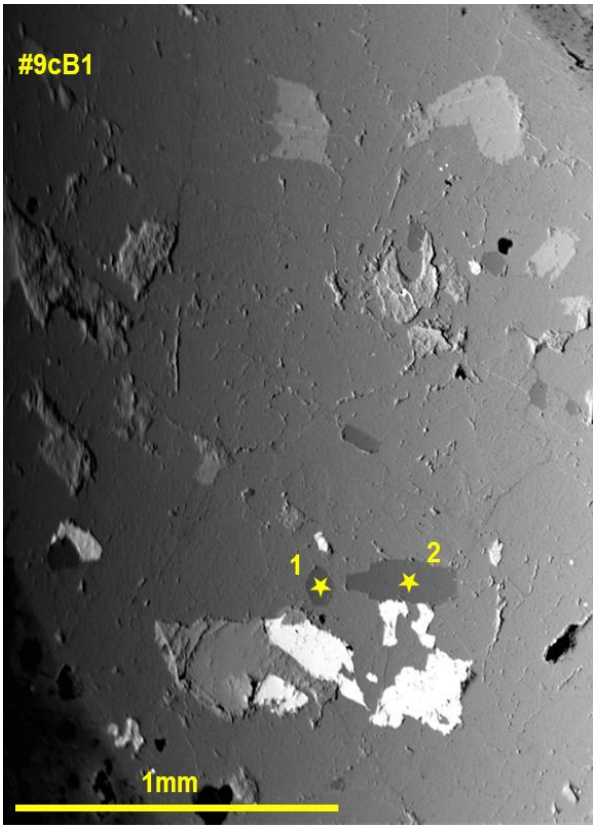

Figure 5.3 Backscatter image of beryl crystals. Point 1 and 2 correspond to analyses presented in table 5.2

In both pegmatites beryl presents considerable concentrations of Na, Li, Fe, and Cs (Appendix II.II.II, Table 5.2) that range between 3350-14350 ppm Na, 1040-1300 ppm Li, 93-2700 ppm Fe, and 104-5075 ppm Cs in pegmatite 1 and between 4050-11150 ppm Na, 1300-3600 ppm Li, 415-2200 ppm Fe, and 340-4600 Cs ppm in pegmatite 2. Values tend to be higher in pegmatite 1 when compared with pegmatite 2 (Figure 5.4).

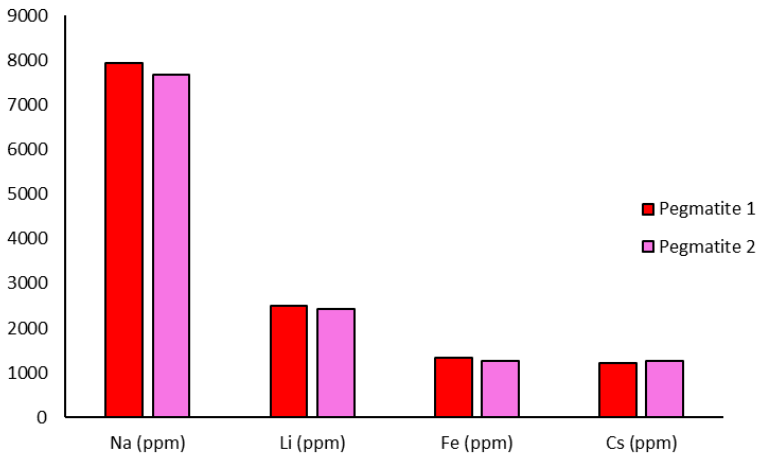

Figure 5.4 Average values in ppm for selected elements in beryl from the different pegmatitic bodies

Beryl analyses from both pegmatites reveal a slight positive correlation (0.4) between Cs and Na, as seen in figure 5.5.

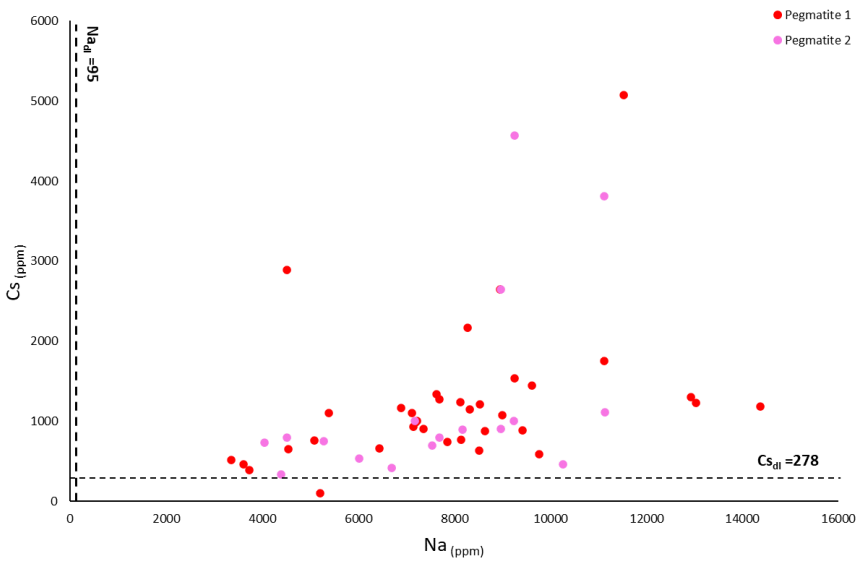

Figure 5.5 Relation between Cs (ppm) and Na (ppm), showing a positive correlation between elements. Dotted lines representing detection limits for both Cs and Na. Analyses grouped by zone.

5.1.3. Feldspars

Feldspars are aluminium tectosilicates commonly represented in terms of the three endmembers potassium-feldspar ($KAlSi_3O_8$), albite ($NaAlSi_3O_8$), and anorthite ($CaAl_2Si_2O_8$) (Deer *et al.*, 1992). Both albite and K-feldspar are major minerals in Aldeia pegmatites. A total of 101 albites and 40 K-feldspars were analysed, reflecting their relative abundance in the studied samples, and results are presented in appendixes II.II.III and II.II.IV, respectively, and summarized in Table 5.3.

Table 5.3 Representative samples of microcline and albite, and average values per zone. Full tables, with stoichiometric distributions in appendix II.II.III and II.II.IV, respectively.

Sample	#2cB9	#4B2	#13B4	#2cB7	#9cB2	#13B3	#14B1	Average											
Mineral	Microcline			Albite				Microcline			Albite			Microcline			Albite		
Zone	Pegmatite 1		Pegmatite 2	Pegmatite 1		Pegmatite 2		Pegmatite 1			Pegmatite 1			Pegmatite 2			Pegmatite 2		
wt%	2	18	1	3	3	2	3	Min.	Max.	Avg.	Min.	Max.	Avg.	Min.	Max.	Avg.	Min.	Max.	Avg.
SiO_2	64.15	63.44	64.44	67.36	67.55	66.13	68.17	62.31	65.37	63.64	65.67	68.73	67.42	64.10	64.44	64.31	66.13	68.94	67.45
Al_2O_3	17.94	17.47	18.55	19.34	19.43	18.99	19.26	16.89	18.55	17.77	17.53	19.50	18.92	18.35	18.77	18.56	18.42	19.72	18.92
P_2O_5	0.15	0.04	0.31	0.14	0.58	0.32	0.20	0.00	0.45	0.20	0.00	0.58	0.15	0.26	0.34	0.30	0.00	0.32	0.14
Fe_2O_3	0.00	0.00	0.00	0.03	0.02	0.00	0.02	0.00	0.01	0.00	0.00	0.08	0.02	0.00	0.00	0.00	0.00	0.08	0.02
K_2O	15.68	14.79	15.08	0.19	0.09	0.08	0.11	14.64	15.88	15.41	0.05	0.28	0.10	15.08	15.52	15.23	0.05	0.54	0.11
Na_2O	0.29	0.86	0.92	11.71	11.60	11.20	11.59	0.19	0.95	0.42	10.96	11.71	11.28	0.51	0.92	0.71	10.86	11.88	11.23
CaO	0.16	0.01	0.00	0.06	0.56	0.27	0.09	0.00	0.16	0.01	0.00	0.56	0.08	0.00	0.00	0.00	0.00	0.33	0.09
BaO	0.00	0.00	0.00	0.00	0.04	0.00	0.00	0.00	0.09	0.01	0.00	0.10	0.02	0.00	0.04	0.02	0.00	0.08	0.02
SrO	0.12	0.11	0.00	0.04	0.00	0.02	0.05	0.00	0.15	0.04	0.00	0.20	0.05	0.00	0.00	0.00	0.00	0.20	0.05
Cs_2O	0.00	0.00	0.00	0.00	0.00	0.00	0.00	0.00	0.08	0.02	0.00	0.09	0.01	0.00	0.00	0.00	0.00	0.04	0.00
ZnO	0.08	0.00	0.07	0.06	0.06	0.01	0.00	0.00	0.16	0.03	0.00	0.17	0.04	0.07	0.19	0.12	0.00	0.14	0.04
MnO	0.00	0.00	0.00	0.00	0.00	0.00	0.03	0.00	0.06	0.01	0.00	0.11	0.01	0.00	0.05	0.02	0.00	0.08	0.01
Total	98.58	96.71	99.38	98.93	99.91	97.03	99.52	95.99	99.69	97.56	96.15	99.91	98.10	98.68	99.74	99.27	96.82	100.18	98.08
% An	0.8	0.1	0.0	0.3	2.6	1.2	0.4	0.0	0.8	0.1	0.0	2.6	0.4	0.0	0.0	0.0	0.0	1.6	0.5
% Ab	2.7	8.1	8.5	98.7	96.9	98.2	99.0	1.8	9.0	4.0	96.9	99.6	99.0	4.8	8.5	6.6	96.9	99.5	98.9
% Or	96.4	91.8	91.5	1.1	0.5	0.7	0.6	91.0	98.2	95.9	0.3	1.6	0.6	91.5	95.2	93.4	0.3	3.1	0.7

K-feldspar and albite are extremely pure, plotting very close to the endmembers in the ternary diagram An-Ab-Or (Figure 5.6)

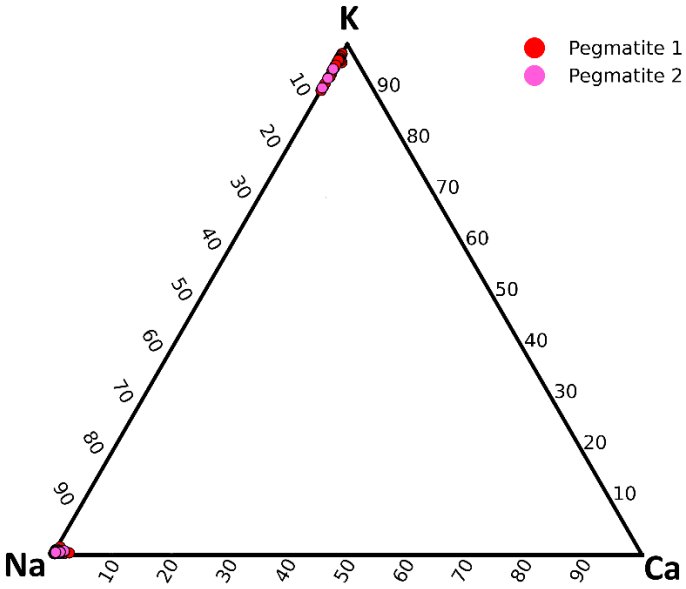

Figure 5.6 Analysed microclines and albites in a ternary diagram, K(Orthoclase/Microcline/Sanidine,) Na (Albite), Ca (Anorthite).

Comparison between both pegmatite's K-feldspar is hard due to the restricted number of analyses in pegmatite 2. Nonetheless, it is possible to see a higher Na content of K-feldspar on pegmatite 2 (average composition of $Or_{93.4}Ab_{6.6}$) relative to pegmatite 1 (average composition of $Or_{95.9}Ab_{4.0}An_{0.1}$), with both displaying extremely low Ca content. Although with variable contents, P is the main trace element present, averaging 0.21 wt. % P_2O_5 but reaching up to 0.45 wt. % of P_2O_5. The correlation between Al_2O_3 and P_2O_5 (Figure 5.7) reflects in part a berlinitic substitution mechanism (Al+P = 2Si) for the incorporation of P into the feldspar structure. With a few exceptions, Na seems to increase with P content (Figure 5.7).

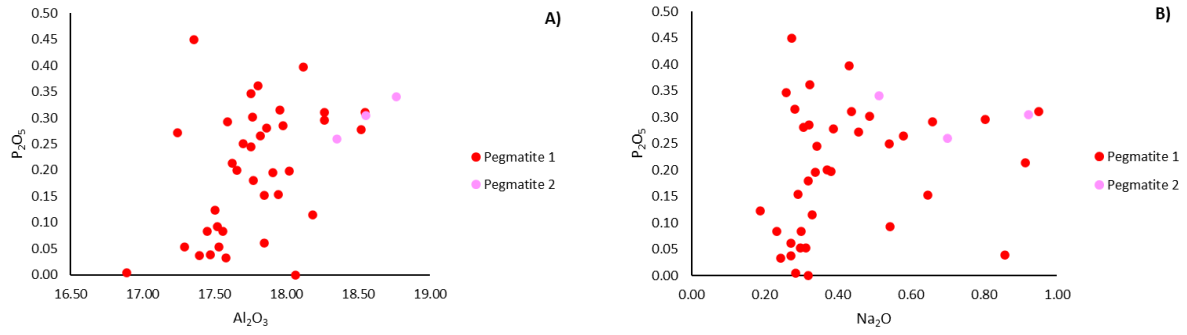

Figure 5.7 ***A)*** *Correlation between Al_2O_3 and P_2O_5 reflecting a berlinitic substitution mechanism* ***B)*** *Correlation between Na_2O and P_2O_5 revealing a slight increase of Na with P.*

Albite is almost pure (An>98) and, on average, compositionally identical for both pegmatites, $An_{0.4}Ab_{99}Or_{0.6}$ in pegmatite 1 and of $An_{0.5}Ab_{98.9}Or_{0.7}$ in pegmatite 2. Identical trace element composition is also seen for both pegmatites, with P being again the most abundant, with an average P content slightly lower than K-feldspar (0.15 wt. % P_2O_5) but reaching up to 0.58 wt. % of P_2O_5 in pegmatite 1 and 0.32 wt.% in pegmatite 2.

5.1.4. Muscovite

Muscovite is a dioctahedral mica which can be represented by the general formula $KAl_2[Si_3AlO_{10}](OH,F)_2$ (Deer *et al.*, 1992). This structure allows for various isomorphic substitution in

both the dodecahedral, octahedral, and tetrahedral positions. On the dodecahedral position substitutions occur when K is replaced by Ba, Ca, Cs, Na and Rb. Octahedral position substitutions occur when Al is replaced by Cr, Fe^{2+}, Fe^{3+}, Li, Sn, Zn, Nb, Ta, Mg, Mn, and Ti. Tetrahedral position substitutions can be summarized as different ratios between Si and Al. Muscovite is a highly abundant mineral in pegmatitic systems, and due to its ability to incorporate Li in its structure it is sometimes considered economically relevant (Linnen *et al.*, 2012). Muscovite was analysed in both pegmatite 1 and 2 as well as in host rock samples including metasomatic alteration halos close to pegmatites. The widespread abundance of this mineral resulted in 222 analyses. Composition of representative samples is compiled in Table 5.4, (extracted from appendix II.II.V).

Table 5.4 Representative samples of muscovite. Full tables, with stoichiometric distributions in appendix II.II.V.

Sample	#2cB5	#5B2	#13B1	#17B2	#11cB8	#12B1	#18aB1	#19B5
Zone	Pegmatite 1		Pegmatite 2		MAZ		Host Rock	
wt%	1	1	1	3	2	3	1	2
SiO_2	46.32	46.90	47.04	46.55	46.92	46.14	47.50	46.80
Al_2O_3	38.57	38.95	38.34	37.15	35.26	33.50	37.73	37.98
K_2O	10.07	10.04	8.70	10.42	9.78	9.97	9.06	8.63
Fe_2O_3	0.00	0.00	0.00	0.00	0.00	0.43	0.00	0.00
FeO	0.90	0.73	1.27	1.02	1.52	2.03	1.02	1.14
MgO	0.01	0.04	0.01	0.02	0.75	1.40	0.46	0.47
Mn_2O_3	0.00	0.00	0.00	0.00	0.00	0.00	0.00	0.00
MnO	0.02	0.02	0.13	0.05	0.05	0.05	0.04	0.00
CaO	0.01	0.01	0.07	0.00	0.02	0.00	0.01	0.00
Na_2O	0.41	0.23	0.25	0.57	0.87	0.66	0.46	0.38
BaO	0.00	0.00	0.00	0.00	0.11	0.11	0.23	0.27
SnO_2	0.04	0.00	0.06	0.04	0.06	0.04	0.01	0.00
TiO_2	0.01	0.00	0.02	0.02	0.27	0.19	0.44	0.40
Cr_2O_3	0.03	0.07	0.02	0.02	0.03	0.06	0.06	0.06
V_2O_3	0.00	0.00	0.00	0.00	0.00	0.00	0.00	0.00
ZnO	0.01	0.08	0.06	0.09	0.00	0.02	0.09	0.00
Li_2O*	0.00	0.00	0.00	0.00	0.00	0.83	0.00	0.00
Ta_2O_5	0.15	0.00	0.15	0.00	0.09	0.02	0.01	0.00
Nb_2O_5	0.10	0.05	0.02	0.07	0.08	0.04	0.05	0.06
PbO	0.00	0.07	0.00	0.01	0.02	0.00	0.06	0.00
SrO	0.00	0.00	0.09	0.00	0.02	0.00	0.00	0.01
CoO	0.00	0.02	0.00	0.00	0.03	0.00	0.01	0.01
Cl	0.02	0.01	0.02	0.00	0.03	0.00	0.01	0.01
F	0.02	0.19	0.20	0.23	0.12	0.47	0.00	0.01
Total	96.68	97.40	96.44	96.26	96.01	95.96	97.24	96.22

Following the classification diagram of Tschindorff *et al.* (1997) muscovite from Aldeia aplite-pegmatite bodies have compositions varying between pure muscovite and Li muscovite (Figure 5.8), with estimated average Li content of 0.21 and 0.42 wt.% Li_2O, for pegmatite 1 and 2 respectively. Muscovite from the host rock deviates towards a more phengitic composition (Figure 5.8), however maintaining considerable average Li contents (0.19 wt.% Li_2O). Lastly, muscovite from MAZ also deviates towards a more phengitic component however in a significant number of samples towards the Li-Phengite component (0.32 wt.% Li_2O).

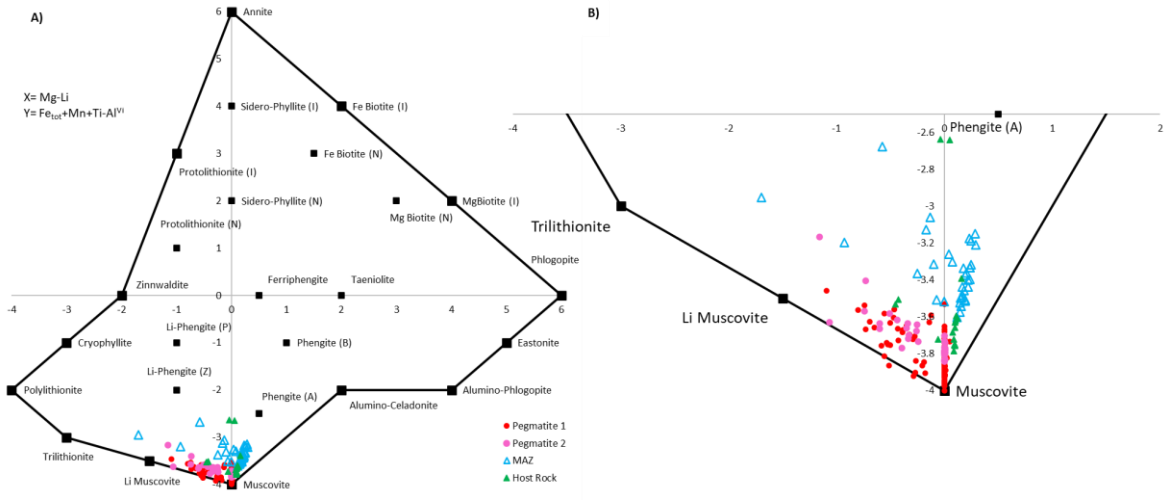

Figure 5.8 ***A)****Analysed muscovite plotted on mica classification diagram (after Tischendorf et al., 1997). Squares representing ideal mica endmembers. Analyses were plotted on the basis of 22 oxygens and grouped by zone.* ***B)*** *Zoom in the compositional field of interest.*

Muscovite analyses reveal an overall excess of Si (Si^{iv} = 3.054 *a.p.f.u* on average), deficit of Al in the tetrahedral position (Al^{iv} = 0.946 *a.p.f.u* on average) and deficit of K in the octahedral position ($\bar{x}$ = 0.828 *a.p.f.u*), it is important however to refer that host rock show a considerably bigger deficit in K in this position ($\bar{x}$ = 0.780 *a.p.f.u*). The excess of atoms in the octahedral position indicates a trioctahedral deviation in Aldeia's muscovite. Data shows that the replacement of Al^{3+} in the octahedral position is done via incorporation of several elements (Figure 5.9) with particular emphasis on Mg, Fe, and Li (Table 5.4).

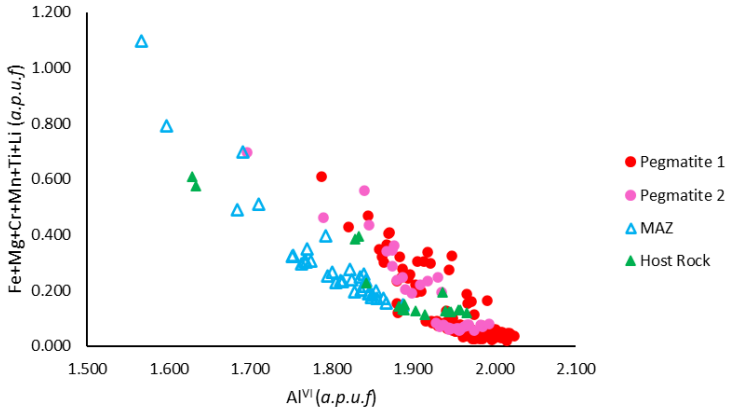

Figure 5.9 Relation between Al in octahedral position vs sum of other relevant elements in that same position, in analysed muscovite. Analyses grouped by zone.

Data show high Li, Sn, Ta, Nb, Mn, and Zn contents and low Ti and Ba in muscovite from both pegmatites when compared to host-rock muscovite (Table 5.5). MAZ samples show significant enrichments in Na and Sn when compared to the remaining samples. Fluorine content also allows for a distinction between zones, with MAZ muscovite presenting the highest average value (0.31 wt.% F) contrasting with the low host rock muscovite (0.07 wt.% F). Muscovite from pegmatites present intermediate values (0.12 and 0.15 wt.% F for pegmatite 1 and 2 respectively).

.

Table 5.5 Average trace element values (in ppm) for muscovite from different zones

	Li	Sn	Ta	Nb	Mn	Zn	Ba	Ti	Na	F
Pegmatite 1	970	227	346	359	273	450	161	86	3251	1362
Pegmatite 2	1937	209	477	401	335	400	134	102	3114	1499
MAZ	1474	442	226	283	221	182	1683	2095	5310	3613
Host Rock	863	14	114	287	106	335	1888	2014	3121	723

5.1.5. Biotite

Biotite is a trioctahedral mica represented by the general formula $K(Mg,Fe^{2+})_3[Si_3AlO_{10}](OH,F)_2$ (Deer *et al.*, 1992). Just like muscovite, biotite's structure allows for various isomorphic substitution in both the dodecahedral, octahedral, and tetrahedral positions. Dodecahedral and tetrahedral position substitutions occur just like in muscovite. While octahedral position substitutions occur when Mg and Fe^{2+} are replaced by Al, Fe^{3+}, Li, Mn, and Ti. Biotite is only present in host rocks, including the metasomatic alteration zone, and 36 EMPA analyses were performed (Appendix II.II.VI) from which representative analyses were chosen to document compositional variation (Table 5.6)

Table 5.6 Representative samples of biotite. Full tables, with stoichiometric distributions in appendix II.II.VI

Sample	**#12B2**	**#12B2.2**	**#18aB3**	**#18aB5**	**#19B1**	**#19B4**
Zone	**MAZ**		**Host Rock**			
wt%	6	3	1	1	1	3
SiO_2	37.46	37.44	35.35	34.66	35.35	35.08
Al_2O_3	20.12	20.40	21.68	21.41	20.70	20.40
MgO	5.46	5.42	7.36	5.66	5.48	5.72
K_2O	8.25	8.15	6.35	7.94	8.21	7.81
FeO	9.03	11.32	11.86	13.60	12.86	13.18
Fe_2O_3	12.77	10.60	11.83	10.99	11.90	11.28
Mn_2O_3	0.00	0.00	0.00	0.00	0.00	0.00
MnO	0.28	0.27	0.27	0.23	0.20	0.15
CaO	0.02	0.03	0.31	0.01	0.00	0.01
Na_2O	0.10	0.12	0.08	0.11	0.07	0.05
BaO	0.01	0.07	0.05	0.04	0.11	0.05
Cs_2O	0.12	0.00	0.00	0.00	0.00	0.00
TiO_2	1.42	1.78	0.07	0.62	1.50	1.57
Cr_2O_3	0.09	0.05	0.06	0.08	0.07	0.09
ZnO	0.10	0.07	0.29	0.13	0.07	0.08
Li_2O	1.89	0.15	1.12	1.00	0.24	1.64
Ta_2O_5	0.00	0.05	0.01	0.00	0.16	0.18
Nb_2O_5	0.08	0.19	0.05	0.04	0.09	0.01
Ga_2O_3	0.00	0.00	0.00	0.04	0.00	0.00
PbO	0.00	0.00	0.06	0.02	0.02	0.07
SrO	0.06	0.01	0.00	0.01	0.03	0.01
CoO	0.04	0.02	0.03	0.04	0.06	0.05
Cl	0.01	0.00	0.03	0.01	0.01	0.01
F	1.69	1.39	0.54	0.53	0.11	0.19
Total	99.02	97.53	97.39	97.17	97.23	97.61

According to the Tschindorff *et al.* (1997) classification diagram, Aldeia biotite falls in a compositional trend between Fe-biotite and siderophyllite (Figure 5.10). Despite this trend, it is important to refer that host rock biotite tends to approach the Fe-biotite endmember whereas MAZ biotite fall closer to siderophyllite but with some deviation towards a tainiolitic composition.

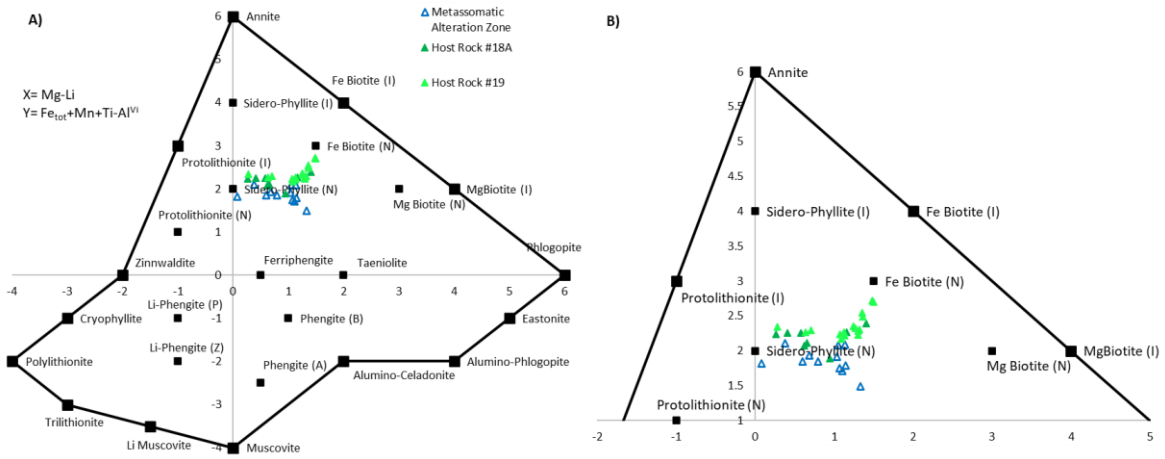

Figure 5.10 ***A)*** *Analysed biotite plotted on mica classification diagram (after Tischendorf et al., 1997). Squares representing ideal mica endmembers. Analyses were plotted on the basis of 22 oxygens and grouped by zone.* ***B)*** *Zoom in the compositional field of interest.*

Biotite analyses reveal, when compared to ideal compositions, a dearth of Si (2.652 *a.p.f.u* on average) in the tetrahedral position compensated by and excess of Al (1.348 *a.p.f.u* on average). The octahedral position is dominated by both Fe^{2+}, Fe^{3+} and Mg (0.857 *a.p.f.u*, 0.584 *a.p.f.u*, 0.630 *a.p.f.u* on average respectively). This position is also occupied to a lesser extent by Al (on average 0.46 *a.p.f.u*), indicating a moderate tschermark or phengitic substitution. In this position is also worth mentioning a significant Li contribution (0.149 *a.p.f.u* on average). Nonetheless the octahedral position is not fully occupied (2.793 *a.p.f.u* on average), which indicates a clear dioctahedral deviation.

Biotite trace element content variability allows for a clear distinction among samples (Table 5.7). Biotite from MAZ samples is enriched in Li, Na, Nb, Mn, Zn and particularly F when compared to biotite from host rock sample #19. Surprisingly, host rock sample #18A shows biotite trace element enrichments similar to MAZ, even with higher Li, Na, Mn, and Zn contents, suggesting an interaction with a similar metasomatic fluid but further away from the aplite-pegmatite contact. The compositional similarity of biotite from MAZ and sample #18A is not observed in any other mineral present in those samples. Therefore, biotite trace element composition can be extremely useful in recognizing metasomatism at distal zones of the system.

Table 5.7 Average trace element values (in ppm) for biotite from different zones

	Li	Nb	Na	Mn	Zn	F
MAZ	2574	524	728	1834	704	13229
#18A	3986	434	1393	1958	783	3729
#19	1293	376	434	1175	332	1849

5.1.6. Garnet

Garnet supergroup is defined, according to Grew *et al.* (2013) by a set of isomorphic and isostructural species following the general formula $X_6Y_4Z_6O_{24}$, where X can be occupied by Ca, Fe^{2+}, Mg, Y and Zn; Y can be occupied by Al, Fe^{3+}, Cr, Sn, Ti, V, and Zr; and Z can be occupied Si, Al, Fe^{3+}.

The compositional variation derived from the garnet structure results in the division of the garnet supergroup into two series: the pyralspite and the ugrandite series. In the pyralspite series the X position does not contain Ca and the Y position is mostly filled by Al. This series is defined by the three endmembers pyrope (X=Mg), almandine (X=Fe^{2+}), and spessartine (X=Mn). The ugrandite series has the X position filled with Ca, whereas the Y position can be filled with Cr (uvarovite), Al (grossular) or Fe^{3+} (andradite). Garnet was only found in Aldeia host rocks, being isotropic and not showing any kind

of optical chemical zonation (Figure 5.11). Core to rim profiles were performed in five different garnet grains, resulting in 16 analyses (Appendix II.II.VII). A representative summary is presented in Table 5.8.

Table 5.8 Representative samples of garnet. Full table, with stoichiometric distributions in appendix II.II.VII

Sample	#19B1					
Position	Core	Mid	Rim	Core	Mid	Rim
wt%	1	2	3	4	5	6
SiO_2	36.34	36.19	36.26	36.49	36.24	36.60
TiO_2	0.13	0.02	0.02	0.01	0.03	0.01
Al_2O_3	20.71	20.94	20.84	20.76	20.92	20.84
Cr_2O_3	0.10	0.07	0.09	0.05	0.04	0.08
Fe_2O_3	0.04	0.00	0.00	0.00	0.00	0.00
FeO	29.75	29.10	29.85	31.08	31.12	31.02
MnO	9.52	10.24	9.26	7.75	7.89	7.90
MgO	1.18	1.15	1.18	1.27	1.37	1.34
CaO	1.94	1.90	1.95	1.88	1.93	1.92
Y_2O_3	0.00	0.00	0.00	0.00	0.00	0.00
Total	99.71	99.61	99.44	99.28	99.53	99.70

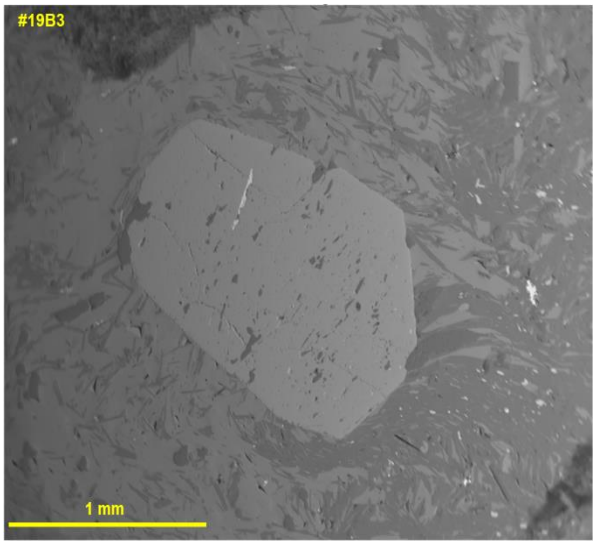

Figure 5.11 Backscatter image of garnet crystal. Noteworthy the absence of chemical zoning.

Based on the microprobe data, Aldeia garnets are classified as almandine, averaging 66% Alm component, with a significant spessartine component (averaging 22%), as shown in Figure 5.12

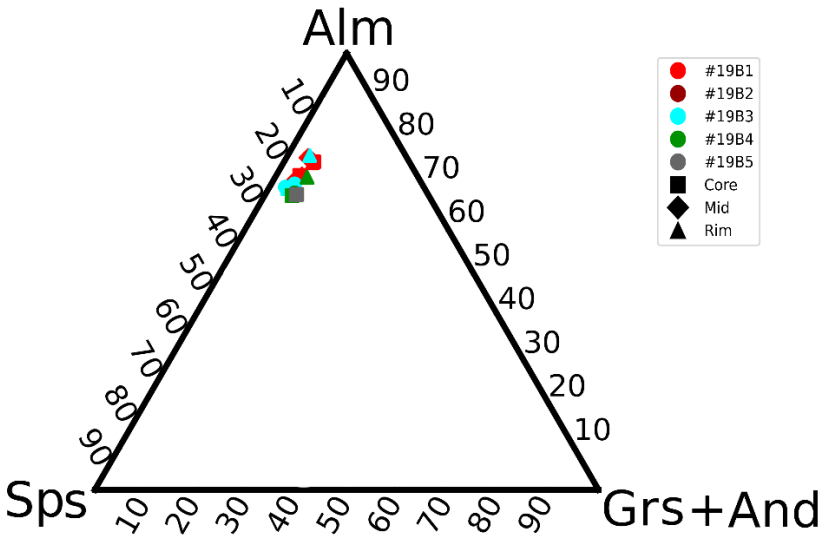

Figure 5.12 Analysed garnets in a ternary diagram: Alm (Almandine), Sps (Spessartine), And+Grs (Andradite+Grossular)

Although garnets are compositionally homogeneous, a slight increase in the almandine component, and consequently a decrease in the spessartine component, can be seen from core to rim, which is also accompanied by an increase in Cr (Figure 5.13)

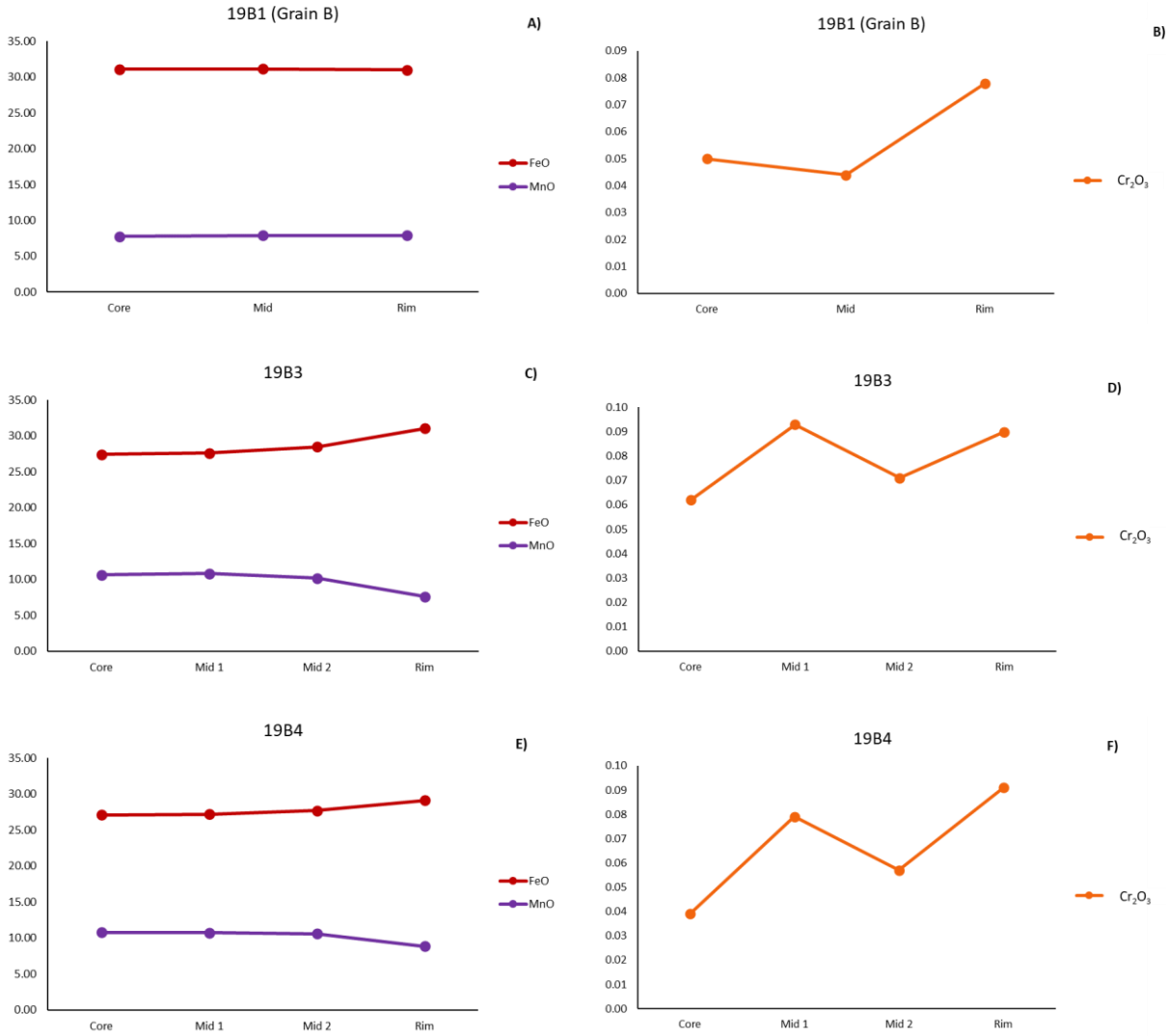

Figure 5.13 Intra grain composition variation for selected garnet grains. Red lines representing FeO values, purple lines representing MnO values and orange lines representing Cr_2O_3. ***A-B*** *representing 19B1 (Grain B),* ***C-D*** *representing 19B3 (Grain A),* ***E-F*** *representing 19B4 (Grain A).*

5.1.7. Tourmaline

Tourmaline is a borosilicate mineral group with the general chemical formula of $XY_3Z_6(T_6O_{18})(BO_3)_3(O,OH)_3(W)$, where X is typically occupied by Ca^{2+}, Na^{+}, K^{+} or vacancies ($X_{\square}$), Y is generally occupied by Mg, Fe^{2+}, Mn^{2+}, AI, Li, Cr^{3+}, V^{3+}, Fe^{3+}, Ti^{4+}, Z is occupied by Mg, AI, Fe^{3+}, V^{3+}, Cr^{3+}, T is typically occupied by Si, AI or even excess B; and W can be filled by F, O and/or OH (Hawthorne and Henry, 1999). Tourmaline in Aldeia was only recognized in the host rocks (HR), including the metasomatic alteration zone (MAZ), and shows a chromatic zonation that should reflect a chemical variation. EMPA and structural formula calculation are tabulated in Appendix II.II.VIII and summarized in Table 5.9.

Table 5.9 Representative samples of tourmaline. Full table, with stoichiometric distributions in appendix II.II.VIII. Lithium values are estimated.

Sample	#11bB1		#11cR		#18aB7	
Zone	MAZ				Host Rock	
Position	Core	Rim	Core	Rim	Core	Rim
Wt%	1	2	1	4	1	2
SiO_2	35.33	35.37	35.59	34.78	35.23	35.54
Al_2O_3	33.42	33.13	34.55	32.79	34.32	34.30
Fe_2O_3	0.00	0.00	0.00	0.00	0.00	0.00
FeO	10.48	10.39	9.53	10.24	8.31	8.23
MgO	3.36	3.37	3.11	3.36	4.24	4.25
B_2O_3	10.40	10.38	10.47	10.28	10.48	10.50
MnO	0.08	0.10	0.02	0.09	0.09	0.05
K_2O	0.01	0.03	0.01	0.03	0.03	0.03
Na_2O	1.68	1.67	1.52	1.78	1.15	1.05
CaO	0.07	0.07	0.02	0.11	0.46	0.49
Cr_2O_3	0.06	0.11	0.06	0.05	0.10	0.05
TiO_2	0.47	0.55	0.19	0.79	0.61	0.60
ZnO	0.06	0.00	0.07	0.02	0.06	0.00
CoO	0.03	0.02	0.00	0.03	0.00	0.02
WO_3	0.00	0.00	0.06	0.02	0.09	0.00
Nb_2O_5	0.01	0.10	0.09	0.00	0.10	0.05
SnO_2	0.01	0.03	0.07	0.03	0.00	0.00
V_2O_3	0.02	0.01	0.00	0.02	0.00	0.00
SrO	0.05	0.00	0.07	0.00	0.00	0.01
Li_2O*	0.12	0.14	0.22	0.15	0.12	0.15
F	0.40	0.20	0.05	0.27	0.07	0.04
Total	96.04	95.66	95.69	94.85	95.44	95.36

According to the tourmaline classification of Henry *et al.* (2011) HR tourmaline fall mostly into the X-vacant group and MAZ tourmaline fall into the alkali group (Figure 5.14), reflecting the higher Na content of the X position in MAZ tourmaline relative to those in HR (average Na *a.p.f.u* of 0.552 in MAZ contrasting with 0.4 *a.p.f.u* in HR).

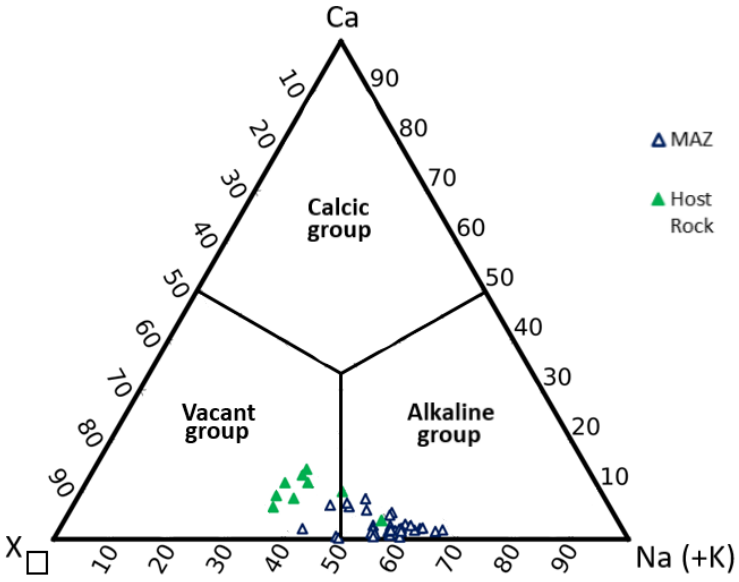

Figure 5.14 Ternary system for the primary tourmaline groups based on the dominant occupancy of the X site. Values normalized to 100%. Analyses were grouped by zone.

The Z position is fulfilled almost exclusively by Al in all samples, averaging 5.99 *a.p.f.u*, confirming they belong to the Al-rich subgroup. The Y position is mostly occupied by Mg, Fe^{2+} and Al, with calculated Li representing only residual sums (Figure 5.15). The relative abundance of Mg and Fe varies, but most MAZ tourmaline have schorl compositions whereas those from HR are mostly foitite. Only a few MAZ tourmaline fall into the dravite field, yet very close to the boundary (Figure 5.15).

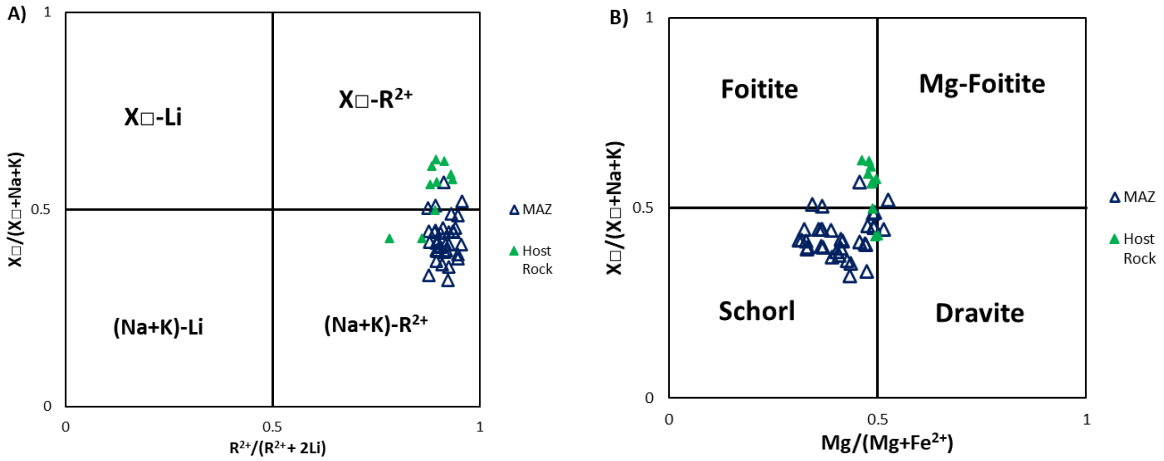

Figure 5.15 ***A)*** *Binary diagram to determine tourmaline subgroups, using to the ratio $R^{2+}/(R^{2+}+2Li)$ vs. X□/(X□+Na+K);* ***B)*** *Binary diagram to determine tourmaline variety using to the ratio Mg/(Mg+Fe) vs. X□/(X □+Na+K); (Henry et al., 2011). Analyses were grouped by zone.*

Fluorine can reach up to 23% of the W position and shows a general positive correlation with Na (Figure 5.16).

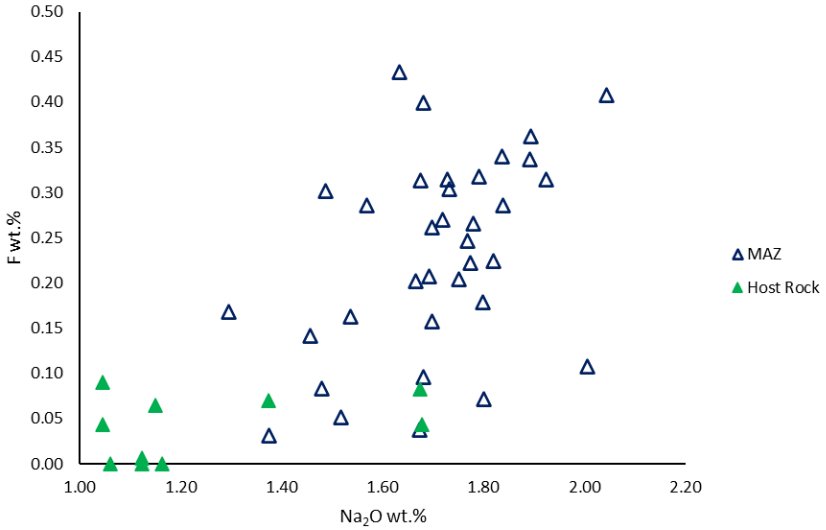

Figure 5.16 Projection of Na_2O vs. F (in atomic percentage) of analysed tourmalines. Analyses were grouped by zone.

The general compositional variations observed between MAZ and HR samples are also recorded at the intergranular as revealed by BSE (backscattering electron) images and X-Ray maps (Figure 5.17). There is a general tendency for Mg-enriched cores and Na- and Fe-enriched rims. However, some tourmaline grains have a complex history sometimes showing inherited nuclei with zoned overgrowths.

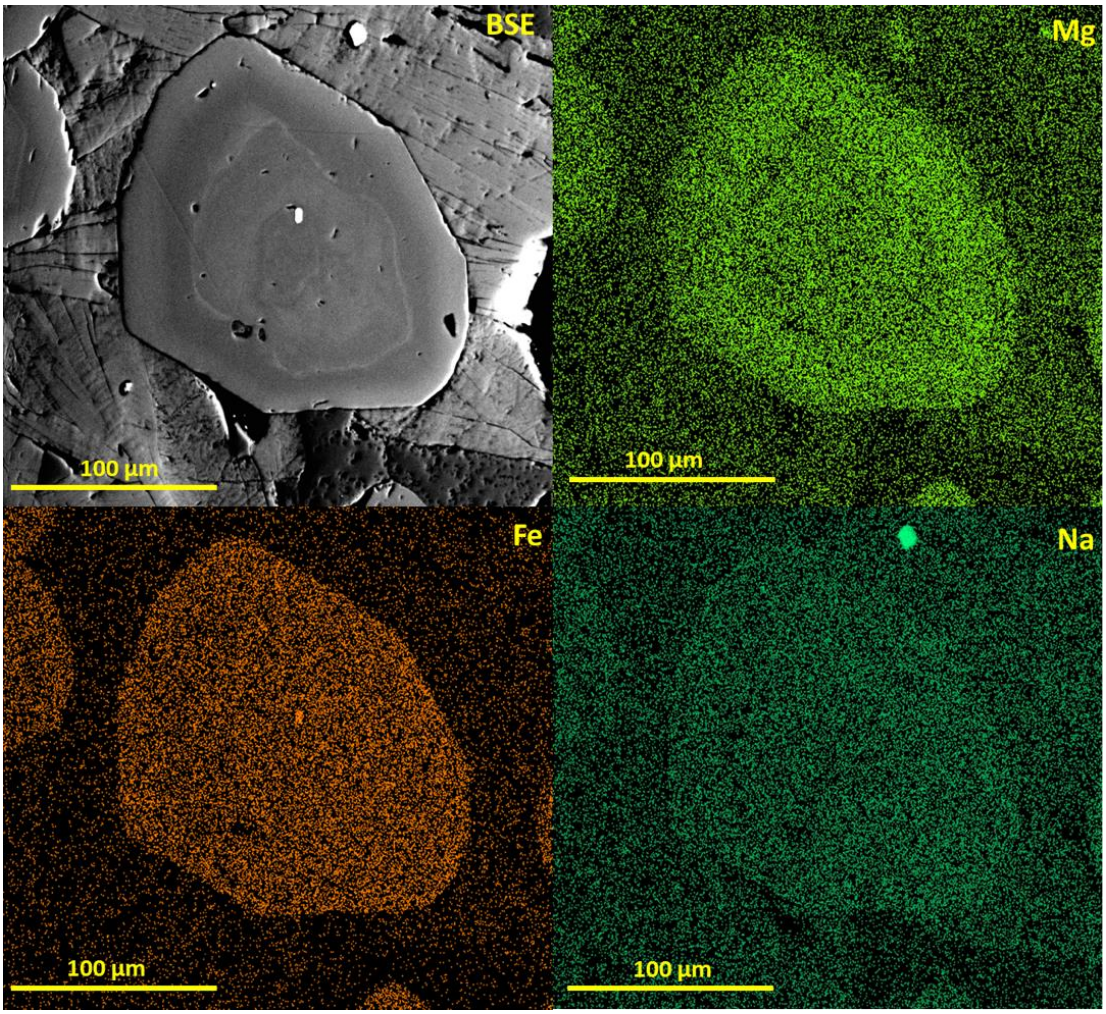

Figure 5.17 Backscattered electron (BSE) images and selected compositional X-ray maps (EPMA) of a tourmaline grain showing compositional zoning.

Lithium, indicated to be present by the need of charge balance, has an average of 0.17 wt.% Li_2O in both MAZ and HR, showing no apparent preference for either of the populations and a highly variable intragranular distribution.

5.2. PHOSPHATES

5.2.1. Apatite

Apatite is a calcium phosphate with general formula $M_5(ZO_4)_3X$, where, according to Pan and Fleet (2002), M = Ca^{2+}, Mn^{2+}, Na^{+}, Pb^{2+}, REE^{3+}, Sr^{2+} amongst others; Z = Cr^{3+}, Mn^{5+}, P^{5+}; X= F^{-}, OH^{-}, Cl^{-}. Apatite in aldeia's prospect appears in both pegmatite 1 and pegmatite 2, metasomatic alteration zone and host rocks samples, therefore being present in all analysed segments. This widespread distribution resulted in 29 acceptable analyses (11, 2 ,13 and 3 analyses respectively). Representative samples of apatite are presented on table 5.10 (complete version on appendix II.II.IX).

Table 5.10 Representative samples of apatite. Full table, with stoichiometric distributions in appendix II.II.IX.

Sample	#5B1		#11bB2		#18aB4	#18aB7	#14B5	
Zone	Pegmatite 1		MAZ		Host Rock		Pegmatite 2	
Species	Fluorapatite						Hydroxylapatite	
wt%	1	2	2	3	1	3	1	2
CaO	55.09	54.72	53.64	54.74	53.29	52.95	55.07	54.25
P_2O_5	43.40	43.33	39.48	39.31	40.37	40.82	41.95	42.83
FeO	0.07	0.06	0.00	0.00	0.00	0.17	0.21	0.00
Fe_2O_3	0.00	0.00	0.38	0.23	0.15	0.00	0.00	0.00
SrO	0.00	0.00	0.24	0.09	0.29	0.19	0.00	0.22
SiO_2	0.00	0.00	0.05	0.05	0.05	0.08	0.00	0.00
MnO	1.02	1.15	0.00	0.00	0.00	0.00	0.00	0.00
Mn_2O_5	0.00	0.00	1.71	0.81	0.18	0.41	0.00	0.00
Mn_2O_3	0.00	0.00	0.00	0.00	0.00	0.00	0.00	0.00
Na_2O	0.03	0.03	0.05	0.06	0.02	0.00	0.00	0.16
MgO	0.00	0.00	0.00	0.00	0.04	0.08	0.00	0.02
K_2O	0.00	0.00	0.01	0.02	0.06	0.00	0.00	0.00
PbO	0.00	0.00	0.00	0.00	0.31	0.13	0.00	0.00
BaO	0.07	0.12	0.00	0.04	0.05	0.30	0.00	0.00
Al_2O_3	0.00	0.01	0.01	0.01	0.00	0.08	0.00	0.02
Nb_2O_5	0.00	0.00	0.00	0.00	0.00	0.00	0.00	0.00
SO_3	0.00	0.00	0.00	0.03	0.20	0.13	0.00	0.00
Cl	0.00	0.01	0.00	0.02	0.00	0.00	0.03	0.01
F	2.74	2.97	2.31	2.02	3.10	3.06	1.46	1.07
Total	102.42	102.40	97.88	97.41	98.08	98.38	98.72	98.58

Apatite have an average composition of $Ca_{4.85}(PO4)_{2.97}(F_{0.79}OH_{0.21})$ in pegmatite 1, of $Ca_{4.92}(PO4)_{3.02}(F_{0.34}OH_{0.66})$ in pegmatite 2, of $Ca_{4.85}(PO4)_{2.90}(F_{0.62}OH_{0.38})$ in host rock, and finally an average a composition of $Ca_{4.92}(PO4)_{2.96}$ $(F_{0.69}OH_{0.31})$ in MAZ, showing a clear predominance of fluorapatite over hydroxyapatite. It is also important to mention the presence of considerable contents of trace elements such as Fe, Mn, Sr, and Na as summarized on table 5.11.

Table 5.11 Average composition of apatite in different zones. Values in atoms per formula unit.

Average	Pegmatite 1	Pegmatite 2	MAZ	Host Rock
Ca	4.85	4.92	4.92	4.85
P	2.97	3.02	2.96	2.90
OH	0.21	0.66	0.31	0.38
F	0.79	0.34	0.68	0.62
Sr	0.01	0.01	0.01	0.01
Na	0.01	0.01	0.01	0.01
Fe	0.07	0.01	0.02	0.01
Mn	0.03	0.00	0.05	0.02
Z Pos	2.98	3.02	3.00	2.94
M Pos	4.98	4.95	4.98	4.90

Trace element contents do not seem to vary between hydroxyapatite and fluorapatite (Figure 5.18). However, it seems that the incorporation of Mn is much more prevalent in apatite from MAZ (Figure 5.18).

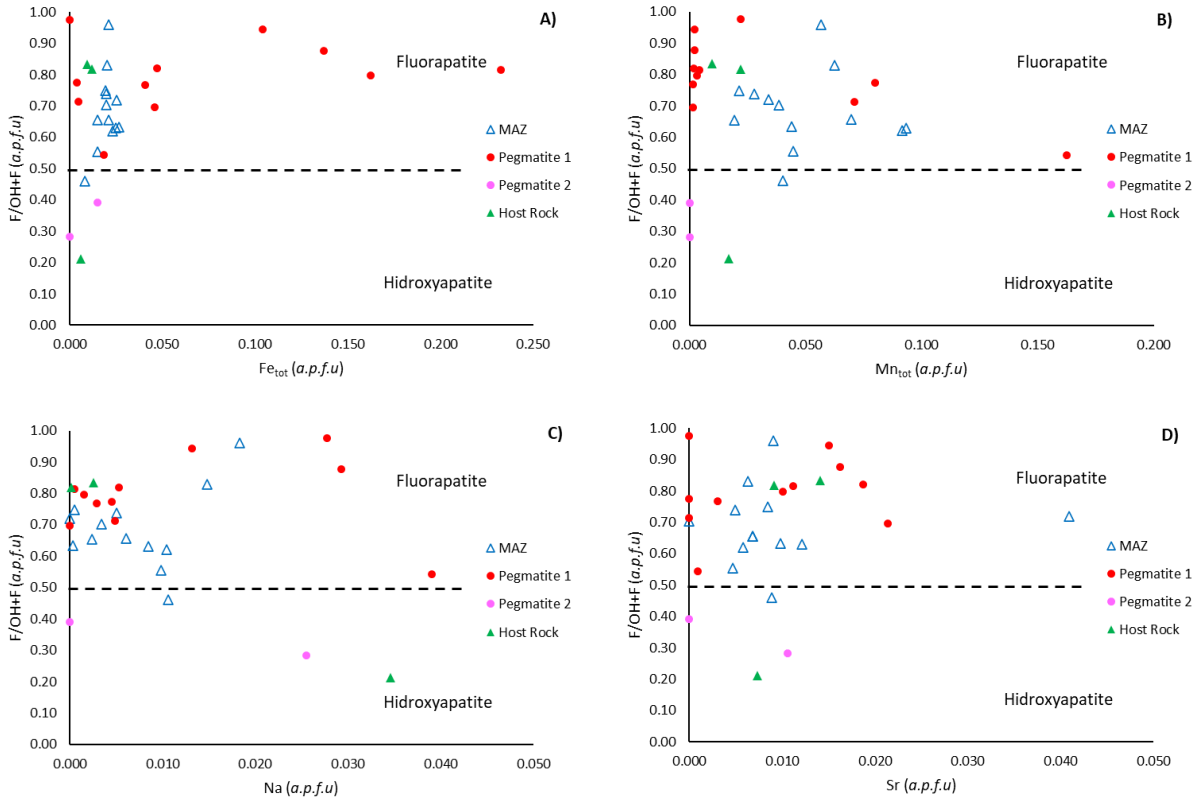

Figure 5.18 Diagrams of F/(F+OH) (a.p.f.u) vs. ***A)*** *Fe_{Tot} (a.p.f.u)* ***B)*** *Mn_{Tot} (a.p.f.u)* ***C)****Na (a.p.f.u)* ***D)*** *Sr (a.p.f.u). Dashed line represents the division between fluorapatite and hydroxyapatite fields.*

Figure 5.19 shows that the substitution of Ca^{2+} by similar sized divalent cations, is the most prevalent substitution mechanism with R^{2+} (Mg^{2+}, Mn^{2+}, Fe^{2+} and Sr^{2+}) showing an almost ideal substitution.

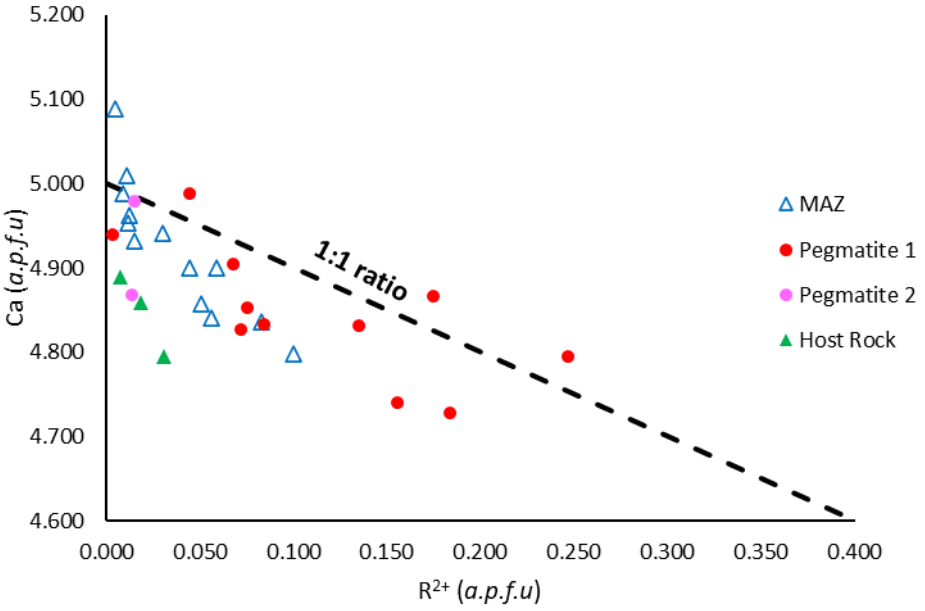

Figure 5.19 Distribution of the atomic ratio of Ca vs. divalent cations (R^{2+}), in a.p.f.u., where R^{2+} = Sr + Mn + Fe + Mg.

5.2.2. Other Phosphates

Besides apatite, several other accessory phosphates were identified and classified using quantitative EMPA, including phosphate minerals from the amblygonite-montebrasite series, the lithiophilite-triphylite series, the heterosite-purpurite series, the fairfieldite-messelite series, and ludlamite. Because a detailed and proper study of these phosphates requires the development of special analytical routines, which was out of the scope and goals of this work, they were lumped together in this section and presented briefly without considering individual chapters for each species.

Lithiophilite ($LiMn^{2+}PO_4$) and triphylite ($LiFe^{2+}PO_4$) are the endmembers of a complete solid solution series. Both lithiophilite and triphylite are present in pegmatite, whereas in MAZ only the latter is present. In 69 of the total 72 analyses Fe^{2+} is greater than Mn^{2+}, which justifies the predominance of triphylite. Representative analyses for these phosphates are presented in table 5.12 whereas the full analyses catalogue is present in appendix II.II.X. Lithium values for lithiophilite-triphylite are extremely consistent varying from 3.49 to 4.54 wt.% Li. Besides the principal elements, Ca (reaching up to 2.69 wt.% CaO), Eu (reaching up to 0.42 wt.% Eu_2O_3) and Si (reaching up to 0.98 wt.% SiO_2) stand out as the main trace elements in triphylite and lithiophilite.

Heterosite ($Fe^{3+}PO_4$) and Purpurite ($Mn^{3+}PO_4$) are endmembers of a solid solution series and are typically considered to result from the oxidation of triphylite and lithiophilite (Lyalina et al., 2023). It is believed that ferrisicklerite ($Li_{1-x}(Fe^{3+},Mn^{2+})(PO_4)$) and sicklerite ($LiMn^{2+}(PO_4)$) represent the intermediate stage of this oxidation, however Lyalina et al. (2023) discredits these two endmembers in this transition. From the 21 analyses, 5 of them represent purpurite, that was only identified in pegmatite 1, whereas heterosite occurs in both pegmatites. Representative analyses for these phosphates are listed in table 5.12 whereas the total amount of samples is presented in appendix II.II.XI (qual). Adding to the typical elements both heterosite and purpurite show considerable values for Ce (up to 2.44 and 2.18 wt.% Ce_2O_3 respectively). In heterosite is also worth mentioning relevant values of both CaO and Na_2O reaching up to 1.42 wt.% and 8.41 wt.% respectively.

Fairfieldite and messelite are (Fe,Mn) endmembers of Ca-phosphate series with compositions $Ca_2Mn^{2+}(PO_4)_2 \cdot 2H_2O$ and $Ca_2Fe^{2+}(PO_4)_2 \cdot 2H_2O$, respectively. Phosphates from this series were found in both pegmatites, with fairfieldite being especially abundant in pegmatite 1 whereas messelite is more common in pegmatite 2. Representative samples for these phosphates are presented in table 5.12 whereas the full table containing all the analyses is found in appendix II.II.XII. Besides major elements, values of Sr stand out in messelite reaching up to 0.84 wt.% SrO. Fairfieldite shows considerable values for PbO reaching up to 0.45 wt.%. Common to both mineral phases are values of Nd, Er and Dy. In messelite these elements can reach up to 0.90, 0.71 and 2.66 wt.% in their oxide form respectively. Whereas in fairfieldite the same elements can get to 1.37, 0.33 and 1.91 in their oxide form respectively.

Ludlamite is an iron phosphate of composition $Fe^{2+}{}_3(PO_4)_2 \cdot 4H_2O$. Ludlamite was only found in pegmatite 2 and has appreciable Mn contents (ranging from 3.02 to 11.17 MnO wt.%). Representative samples for ludlamite are represented in table 5.12 whereas the total amount of samples is presented in appendix II.II.XIII. Ludlamite analyses reveal, besides the typical elements, relevant contents of trace elements Mg, Ca, Na. Values for these elements reach up to 0.95, 5.54 and 0.31 wt.% in their oxide form respectively.

Montebrasite ($LiAl(PO_4)(OH)$) - amblygonite ($LiAl(PO_4)F$) represent a lithium-aluminium phosphate solid solution basically defined by the OH/(OH+F) ratio. Aldeia Li-Aluminium phosphates fall into montebrasite classification, *i.e.,* when OH/(OH+F) >0.5. This phosphate was only found in pegmatite 1 and the resulting 16 analyses are presented in appendix II.II.XIV. Representative samples for these phosphates are represented in table 5.12. Lithium values in montebrasite are very consistent varying from 4.3 up to 4.7 wt.% Li. Montebrasite analyses reveal, besides the typical elements,

important contents of Ta, Nb, Nd, Dy and Ce. These elements reach in their oxide form values up to 1.38, 1.11, 1.58, 1.21 and 2.82 wt.% respectively.

It is nonetheless important to mention that rare earth elements values should be taken with some precaution due to the high detection limits for these elements in the phosphate group.

Ternary diagrams were built taking into consideration the 4 most recurring elements in these minerals: Fe, Ca, Li, Mn (Figure 5.20 A) to show and compare their compositional variation (Figure 5.20 B).

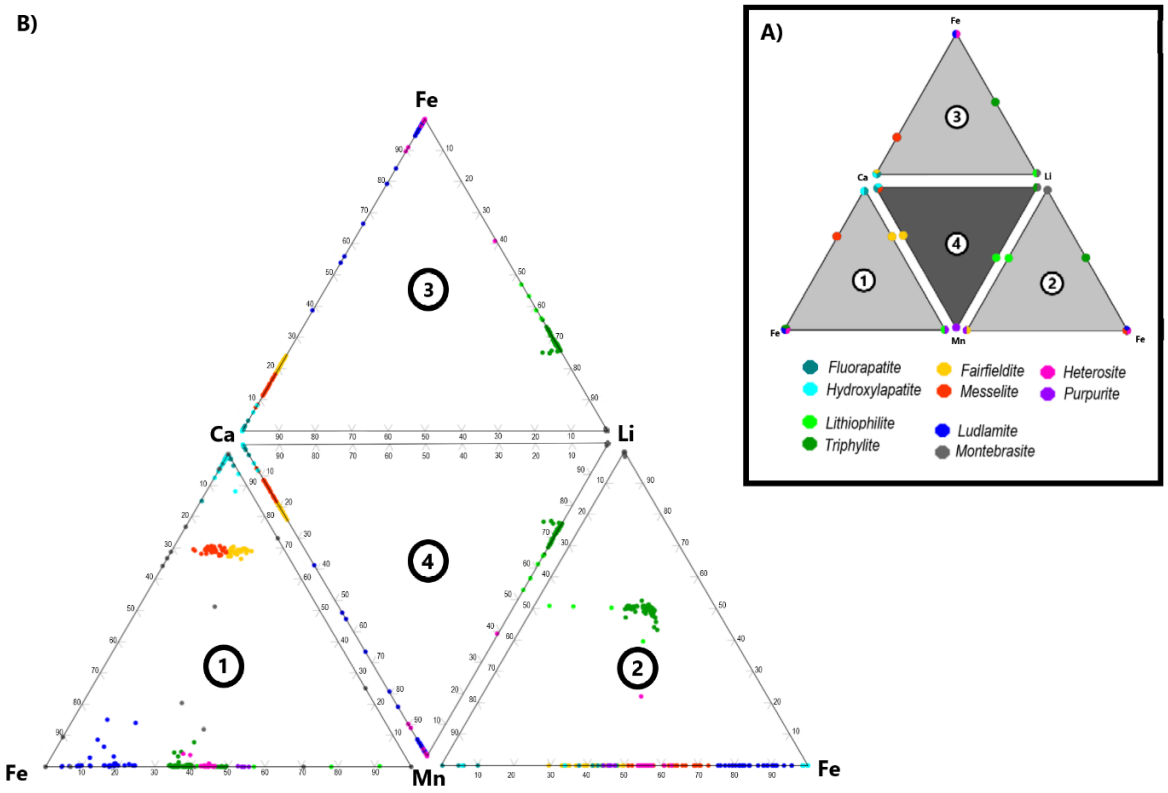

Figure 5.20 ***A)*** *Phosphate endmember composition* ***B)*** *compositional variation of accessory phosphate minerals from Aldeia aplite-pegmatites.*

Phosphates from aldeia's prospect follow the expected trends with some variations. These variations, reflected by the slight offset from the ideal solid solution lines, result from the incorporation of additional elements other than the characteristic for each series.

Table 5.12 Representative samples of phosphate minerals. Dashes represent elements which were either consistently under the detection limit or do not incorporate the mineral structure. Li values are calculated. Full table, with stoichiometric distributions in appendix II.II.X – II.II.XIV

Sample	#4B2	#4B3	#13B5	#9bB2	#11bB7	#9bB2	#5B2		#9bB1		#13B1	#13B2	#13B6	#17B5		#4B7	#7aB4	
Mineral	Lithiophilite		Triphylite		Heterosite		Purpurite		Fairfieldite		Messelite			Ludlamite		Montebrasite		
wt%	9	4	2	13	2	8	1	3	2	6	7	2	2	1	8	5	3	
P_2O_5	42.37	43.18	44.15	43.22	41.49	46.84	45.93	46.54	38.02	37.21	36.43	37.21	31.45	32.21	31.88	48.21	46.40	
Al_2O_3	-	-	-	-	-	-	-	-	0.00	0.02	0.03	0.00	0.07	0.07	0.02	35.62	35.87	
Li_2O*	9.40	9.54	8.58	9.36	0.00	0.00	-	-	-	-	-	-	-	-	-	9.88	9.24	
FeO	3.77	9.77	28.11	24.49	-	-	-	-	8.34	7.82	9.89	10.10	40.59	30.93	34.94	0.00	0.03	
Fe_2O_3	0.00	0.00	0.00	0.00	29.39	28.40	24.51	25.59	-	-	-	-	3.61	4.01	0	0.00	0.00	
MnO	39.50	34.39	14.12	16.04	13.50	0.00	-	-	8.85	9.29	7.98	6.08	3.02	8.87	11.17	-	-	
Mn_2O_3	-	-	-	-	2.20	24.27	30.38	29.56	-	-	-	-	-	-	-	-	-	
CaO	0.07	0.00	0.15	2.69	1.42	0.07	0.00	0.03	30.54	29.79	31.38	29.33	0.08	5.54	0.12	0.09	0.00	
MgO	0.00	0.04	0.00	0.06	0.36	0.09	0.03	0.12	0.01	0.00	0.21	0.50	0.95	0.27	0.45	0.00	0.03	
K_2O	0.01	0.02	0.00	0.00	-	-	-	-	0.05	0.00	0.03	0.00	0.13	0.03	0.01	0.00	0.00	
Na_2O	0.03	0.05	0.00	0.09	8.41	0.00	0.04	0.10	0.16	0.10	0.00	0.21	0.31	0.18	0.21	0.00	0.06	
Ta_2O_5	-	-	-	-	-	-	-	-	-	-	-	-	-	-	-	0.00	1.00	
Nb_2O_5	-	-	-	-	-	-	-	-	-	-	-	-	-	-	-	0.19	1.11	
PbO	0.03	0.00	0.00	0.07	-	-	-	-	0.45	0.25	0.00	0.17	0.12	0.01	0.01	-	-	
SrO	-	-	-	-	-	-	-	-	0.02	0.00	0.18	0.80	-	-	-	-	-	
UO_3	0.04	0.00	0.00	0.04	-	-	-	-	-	-	-	-	0.07	0	0	-	-	
SiO_2	0.83	0.20	0.37	0.15	-	-	-	-	0.07	0.70	0.00	0.11	0	0.13	0.43	0.00	0.02	
Lu_2O_3	-	-	-	-	-	-	-	-	-	-	-	-	-	-	-	0.00	0.85	
Dy_2O_3	-	-	-	-	-	-	-	-	1.06	0.61	0.00	2.66	-	-	-	0.96	0.00	
Nd_2O_3	-	-	-	-	-	-	-	-	0.19	1.37	0.90	0.00	0.46	0.14	0.02	0.48	0.00	
Ce_2O_3	-	-	-	-	1.74	2.44	2.00	2.18	-	-	-	-	-	-	-	1.16	2.82	
La_2O_3	-	-	-	-	-	-	-	-	-	-	-	-	-	-	-	0.22	0.00	
Er_2O_3	0.00	0.00	0.38	0.00	-	-	-	-	0.33	0.00	0.04	0.33	0.14	0.01	0	-	-	
Eu_2O_3	0.30	0.34	0.18	0.07	-	-	-	-	-	-	-	-	-	-	-	-	-	
Cl	-	-	-	-	-	-	-	-	-	-	-	-	-	-	-	0.00	0.00	
F	-	-	-	-	-	-	-	-	-	-	-	-	-	-	-	0.72	0.00	
Total	96.34	97.53	96.04	96.28	98.52	102.11	102.88	104.14	88.08	87.16	87.07	87.50	81	82.4	79.26	97.53	97.44	
Li wt.%	4.37	4.43	3.99	4.35	-	-	-	-	-	-	-	-	-	-	-	4.59	4.30	

5.3. OXIDES

5.3.1. Ilmenite

Ilmenite is an oxide with an ideal chemical formula of $Fe^{2+}Ti^{4+}O_3$, where Mn, Mg and Cr can typically substitute for both Fe and Ti in its crystalline structure. Other elements such as Al, Si, Th, P, and V can be incorporated into ilmenite during weathering processes (Mehdilo *et al.* 2015). Ilmenite is relatively rare in Aldeia, and it was exclusively identified in host rock samples. EMPA data results are presented in appendix II.II.XV and summarized in Table 5.13.

Table 5.13 Representative samples of Ilmenite. Full table with stoichiometric distributions in appendix II.II.XV

Sample	#18aB1		#18aB2		#19B2	#19B3	
wt%	1	2	1	3	1	1	2
TiO_2	52.69	52.89	51.64	52.28	52.32	51.58	51.52
FeO	42.75	42.68	41.49	42.54	42.89	42.65	42.83
MnO	3.31	3.49	3.30	3.18	2.50	2.46	2.36
MgO	0.00	0.01	0.03	0.00	0.00	0.00	0.02
ZnO	0.04	0.02	0.00	0.02	0.04	0.06	0.01
Nb_2O_5	0.14	0.11	0.05	0.13	0.15	0.19	0.17
WO_3	0.10	0.00	0.18	0.03	0.17	0.00	0.15
BaO	0.02	0.04	0.10	0.10	0.06	0.09	0.08
Al_2O_3	0.00	0.00	0.20	0.01	0.00	0.02	0.03
Na_2O	0.02	0.03	0.02	0.00	0.01	0.03	0.00
SiO_2	0.04	0.04	0.11	0.07	0.04	0.04	0.02
ZrO_2	0.00	0.00	0.00	0.03	0.05	0.03	0.03
CoO	0.06	0.04	0.04	0.10	0.03	0.09	0.03
PbO	0.12	0.04	0.00	0.03	0.04	0.01	0.04
Ta_2O_5	0.01	0.00	0.00	0.10	0.20	0.15	0.01
UO_2	0.00	0.02	0.09	0.00	0.13	0.08	0.04
HfO_2	0.16	0.00	0.00	0.22	0.00	0.00	0.00
Total	99.45	99.40	97.24	98.82	98.62	97.47	97.35

Data show a clear deviation from the ideal composition with an overall excess of Ti relative to Fe (Figure 5.21). The incorporation of Mn (pyrophanitic component) is the most significant (Figure 5.22 A), averaging 3.01 wt.% MnO and reaching up to 3.49 wt.%. Several traces are present including Nb, Ta, W, Ba, Co, Zn and even Si.

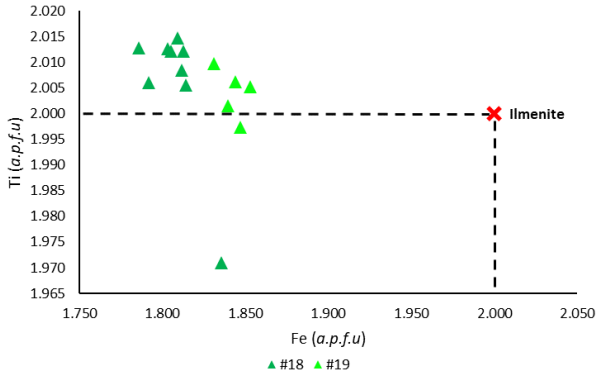

Figure 5.21 Distribution of atomic proportions, Fe vs. Ti, in a.p.f.u, of all ilmenite analyses. Red cross representing ideal composition of Ilmenite. Analyses were grouped by sample.

Noteworthy is the spatial compositional variation of ilmenite relative to the distance of the pegmatitic-aplitic bodies, particularly the more Mn-enriched and HFSE-depleted proximal compositions when compared to the distal compositions (Figure 5.22).

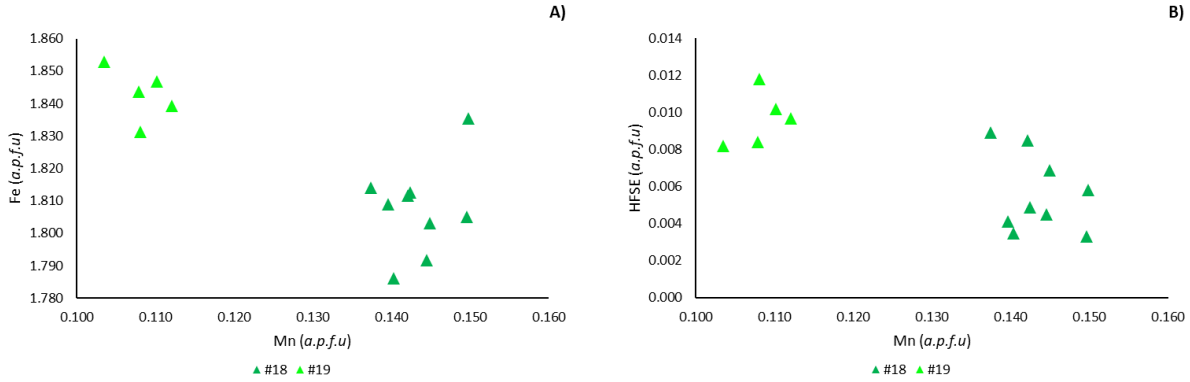

*Figure 5.22 Distribution of atomic proportions **A)** Mn vs Fe **B)** Mn vs HFSE, in a.p.f.u. Analyses were grouped by sample.*

5.3.2. Columbite-Tantalite

Minerals from the columbite-tantalite group have a general formula of AB_2O_6. in which the A position is typically occupied by Fe^{2+} and Mn^{2+} with minor incorporation of Mg^{2+} and trivalent cations. B position is occupied primarily by Nb^{5+} and Ta^{5+} and in minor quantities Ti^{4+} and Sn^{4+}. Columbo-Tantalite is relatively rare in Aldeia, and it was exclusively identified in pegmatite samples. EMPA data results are presented in appendix II.II.XVI and summarized in Table 5.14.

Table 5.14 Representative samples of Columbite-Tantalite. Full table with stoichiometric distributions in appendix II.II.XVI

Sample	#7aB5	#7bB7		#13B1	
Zone	Pegmatite 1			Pegmatite 2	
wt%	4	1	2	1	2
Ta_2O_5	19.71	42.75	42.23	45.65	41.15
Nb_2O_5	59.41	40.22	40.15	29.95	37.21
Fe_2O_3	0.00	0.00	0.00	4.99	3.04
FeO	11.84	10.74	10.79	6.68	8.48
MnO	6.75	5.99	6.09	6.13	5.82
TiO_2	0.41	0.33	0.51	0.56	0.29
SiO_2	0.11	0.25	0.24	0.41	1.47
Tm_2O_3	0.42	0.77	0.31	0.70	0.66
Ce_2O_3	0.48	0.30	0.00	0.70	0.55
UO_2	0.01	0.14	0.01	0.10	0.10
PbO_2	0.11	0.10	0.02	0.13	0.07
ZrO_2	0.08	0.14	0.13	0.05	0.02
Y_2O_3	0.18	0.12	0.15	0.06	0.15
Total	99.51	101.84	100.62	96.10	99.01

EMPA data allows to classify four of the sample as tantalite-(Fe), Ta>Nb and Fe>Mn, and one samples as columbite-(Fe), Nb>Ta and Fe>Mn. Several traces are present including Ti, Si, Ce and Tm on average 2500, 2300, 3400 and 5000 ppm respectively.

5.4. SULFIDES

Sulfides are scarce and include pyrite, arsenopyrite, and sphalerite. Sphalerite was the only sulfide found within aplite-pegmatites, whereas pyrite and arsenopyrite are restricted to the host metasediments, including the metasomatic alteration zone (MAZ). Because of their small grain size, sulfide analysis from the host metasediments do not fulfil the criteria to be considered acceptable, due to contamination from surrounding crystals. Therefore only 11 pyrite and 8 arsenopyrite from the MAZ and 10 sphalerite

analysis from the pegmatites were considered for this study (Appendix II.II.XVII, II.II.XVIII, II.II.XIX, respectively). A selection of representative analyses is presented in Table 5.15.

Table 5.15 Representative samples of sulfides. Full table with stoichiometric distributions in appendix II.II.XVII-II.II.IX. bdl-below the detection limit

Mineral	Pyrite				Arsenopyrite				Sphalerite			
Sample	#11bB5		#12B6		#11bB2		#12B3		#8bB7	#9bB9	#13B3	
Zone	Proximal MAZ		Distal MAZ		Proximal MAZ		Distal MAZ		Pegmatite 1		Pegmatite 2	
wt%	2	5	1	2	1	2	2	3	1	1	1	2
Fe	45.10	44.97	45.24	46.17	26.43	30.41	27.90	27.66	0.60	0.98	5.48	5.46
Zn	0.00	0.09	0.00	0.00	bdl	bdl	bdl	bdl	62.88	62.68	60.39	60.78
As	0.05	0.07	0.10	0.10	50.00	49.32	47.89	48.73	0.02	0.00	0.01	0.04
S	51.74	50.99	52.14	52.73	15.53	16.11	17.16	17.19	32.83	33.31	33.57	33.57
Ni	0.03	0.30	0.64	0.05	4.61	1.13	5.09	3.62	bdl	bdl	bdl	bdl
Co	0.00	0.02	0.05	0.00	2.34	1.62	0.97	2.77	0.00	0.00	0.01	0.01
Pb	0.00	0.10	0.03	0.00	0.00	0.04	0.02	0.01	0.00	0.02	0.00	0.05
Mo	0.04	0.05	0.04	0.08	0.00	0.02	0.05	0.02	0.13	0.08	0.13	0.14
Cu	0.08	0.03	0.02	0.00	0.00	0.00	0.02	0.00	0.12	0.18	0.00	0.00
Mn	0.00	0.00	0.00	0.02	0.04	0.00	0.04	0.00	0.00	0.36	0.05	0.02
W	0.13	0.12	0.00	0.00	bdl	bdl	bdl	bdl	bdl	bdl	bdl	bdl
In	bdl	bdl	bdl	bdl	0.00	0.00	0.05	0.00	0.00	0.07	0.00	0.00
Sb	bdl	bdl	bdl	bdl	0.00	0.06	0.05	0.04	0.00	0.00	0.07	0.01
Au	bdl	bdl	bdl	bdl	0.00	0.00	0.00	0.02	0.03	0.00	0.00	0.00
Ag	bdl	bdl	bdl	bdl	0.00	0.04	0.05	0.02	0.06	0.01	0.00	0.02
Cd	bdl	bdl	bdl	bdl	bdl	bdl	bdl	bdl	0.10	0.02	0.22	0.22
Total	97.18	101.74	99.27	101.14	99.94	100.76	101.26	103.07	97.78	98.70	100.93	102.32

5.4.1. Pyrite

Pyrite (FeS2) can incorporate Co, Ni, Mo, and many other trace elements replacing Fe in the structure, whereas S can be typically replaced by As, Sb, Se, or Te. Pyrite from Aldeia MAZ samples show an almost ideal and homogenous composition (Fe1.00S1.99), with As, Ni, and Mo being the most relevant trace elements present (Appendix II.II.XVII; Table 5.15).

5.4.2. Arsenopyrite

Arsenopyrite (FeAsS) can incorporate several different elements depending on its structural position. It is common to find As and Te replacing S; S, Sb, Bi, Cd, and In replacing As; Co, Ni, Cu, Zn, Pb, amongst others, replacing Fe. Arsenopyrites from Aldeia MAZ samples slightly deviate from the ideal arsenopyrite composition (Appendix II.II.XVIII; Table 5.15). They show an excess of As (> 33.33 at. %) and a deficit in S (< 33.33 at.%) representing a deviation towards loellingite (FeAs2), with a loellingitic component slightly higher in metasediments closer to the pegmatite (Figure 5.23).

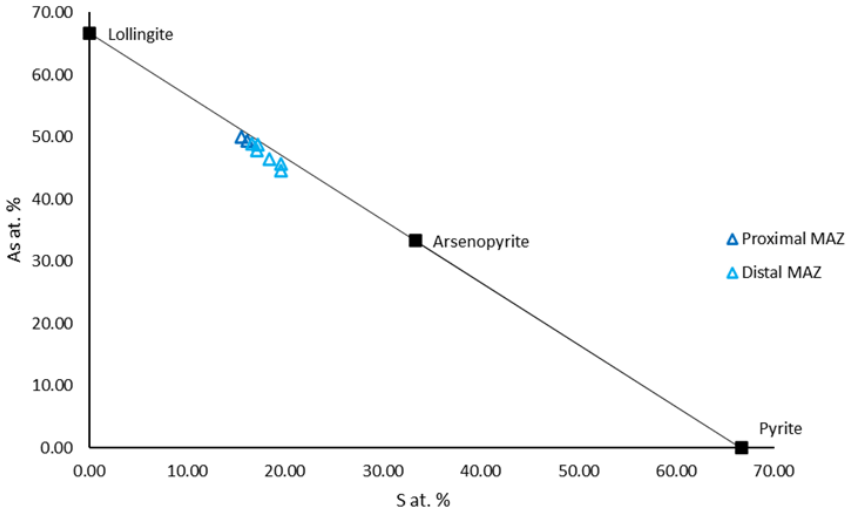

Figure 5.23 Projection of As vs. S (in atomic percentage) of analysed arsenopyrites, with emphasis in pyrite and lollingitic components. Analyses divided by zone, proximal and distal MAZ.

Yet variable, high Co and Ni contents are registered, reaching up to 2.8 and 4.8 wt.% respectively. Other than Co and Ni (Figure 5.24), incorporation of other elements replacing Fe is very limited, with values typically below the detection limit.

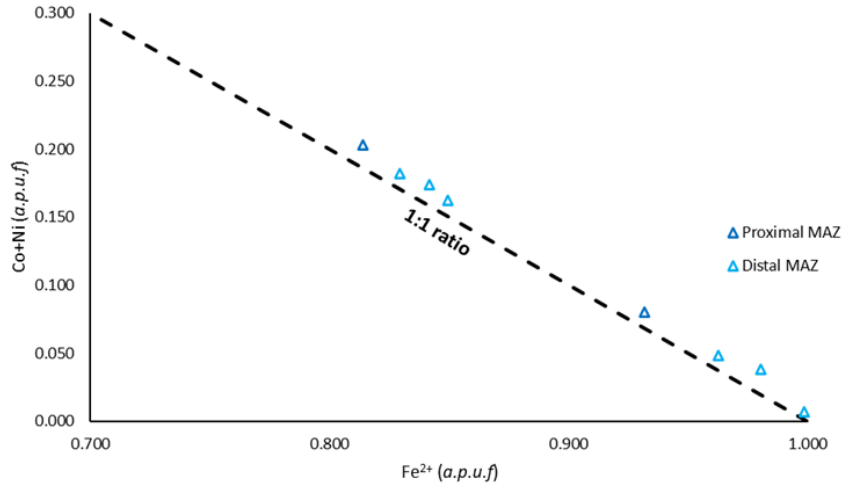

Figure 5.24 Distribution of atomic proportions Fe vs. Co+ Ni, in a.p.f.u of analysed arsenopyrites,. Analyses were grouped by zone, proximal and distal MAZ.

5.4.3. Sphalerite

Sphalerite (ZnS) can incorporate significant amounts of Fe (up to 15 wt.%), as well as considerable trace amounts of Cd, Cu, Co, Mn, Mo, Ga, Ge, Sn, or W (Cook *et al.*, 2009). Sphalerite from Aldeia pegmatites shows a clear deviation from its ideal composition (Appendix II.II.XIX; Table 5.15), essentially due to the incorporation of Fe and trace amounts of Cd, Mo, and Cu (Figure 5.25). Despite the limited dataset it is possible to distinguish sphalerite from pegmatite 1 and pegmatite 2. Whereas sphalerite from pegmatite 1 has Fe < 1 wt.% and Cd ranging from 170 to 1040 ppm, sphalerite from pegmatite 2 has Fe ranging from 3.1 to 5-5 wt.% and Cd ranging from 2100 to 3350 ppm. Note that Mo content is very similar – 800-1320 ppm and 850-1440 in pegmatite 1 and 2 respectively.

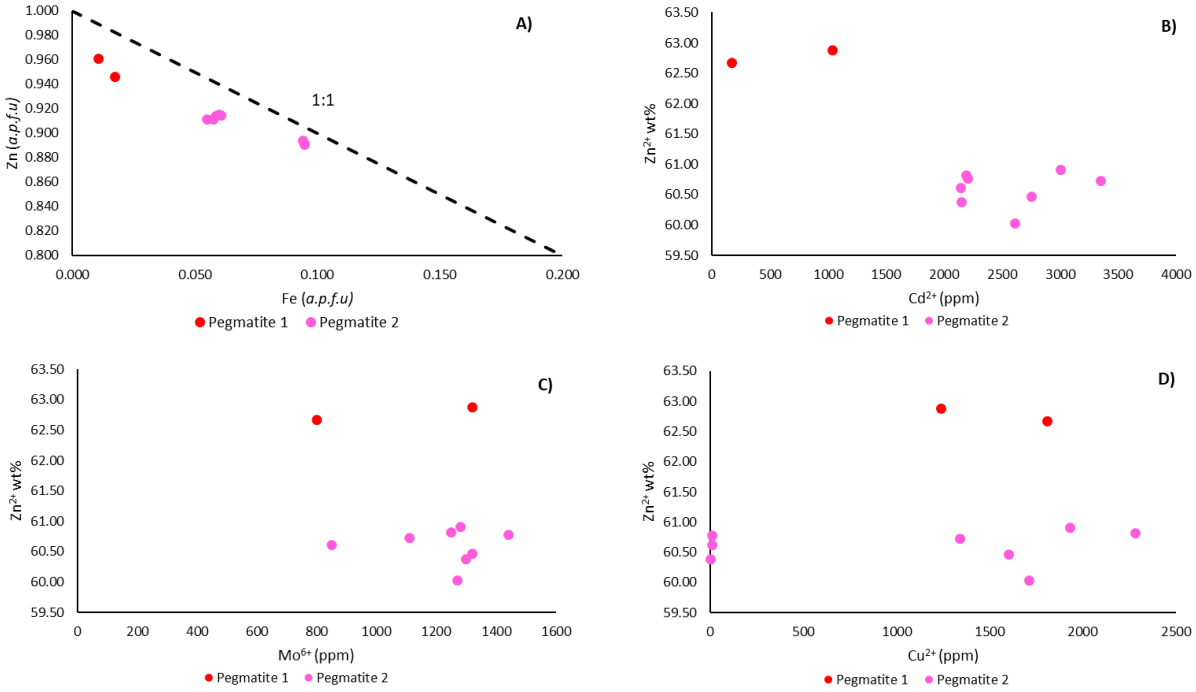

Figure 5.25 ***A)*** *Distribution of atomic proportions Zn vs. Fe , in a.p.f.u.* ***B)*** *projection of Zn in atomic percentage vs. Cd in ppm* ***C)*** *projection of Zn in atomic percentage vs. Mo in ppm* ***D)*** *projection of Zn in atomic percentage vs. Cu in ppm of analysed sphalerites.*

5.5. OTHER MINERALS

During the EMPA analysis, other mineral phases were identified however for distinct reasons not considered for a further detailed study. These minerals include rutile, monazite, chlorite, Na-rich and Sr-rich phosphates. Both rutile and monazite were not considered due to the scarce number of samples. Chlorite was identified petrographically, but analysis conducted on this mineral revealed problematic not meeting the necessary consistency to be considered relevant, with analytical errors greater than 4-5%. Na-rich and Sr-rich phosphates were identified but due to their small size and/or analytical limitations, errors are greater than 4% and could not be classified precisely. Nevertheless, their compositions approach those of natrophylite and crandalite-goyazite series, respectively.

6. DISCUSSION

This chapter aims to synthesize and integrate data and findings attained throughout this dissertation, with the overall goal of advancing in the understanding of the mineralogical and geochemical aspects of the Aldeia's aplite-pegmatite swarm and, consequently, the broader Barroso-Alvão aplite-pegmatite field. To this end, the following objectives are pursued:

i. Establish broad emplacement conditions for Aldeia aplite-pegmatite bodies.
ii. Develop a coherent paragenetic sequence outlining the chronological sequence of mineral phases inside the aplite-pegmatite body.
iii. Characterize the main geochemical features of the aplite-pegmatite bodies and how they influence the surrounding host rocks.
iv. Attempt to discern the underlying genetic factors responsible for the distinct stages identified through petrographic analysis.
v. Conduct a comparative assessment of various genetic models, aiming to identify the most fitting model for this specific case study.

6.1. EMPLACEMENT CONDITIONS

As previously mentioned, Aldeia aplite-pegmatite is categorized under the spodumene-albite subtype. The absence of spodumene-quartz intergrowth textures suggests that spodumene did not originate from the decomposition of petalite (Spd + 2 Qz = Pet). Furthermore, the spodumene within the aplite-pegmatite exhibits no evident signs of weathering or alteration to either eucryptite or petalite, strongly suggesting its primary nature and concurrent formation with the aplite-pegmatite body that contains it, constraining the emplacement even more. The relations between the three main Li-aluminosilicates are given by three main reactions represented by the following expressions: i) Spd + 2 Qz = Pet; ii) Ecp + 3 Qz = Pet iii) Ecp + Qz = Spd.

Modeling these reactions using the variables reported in Wood and William-Jones (1993), it is possible to outline the stability field domains for the various Li-aluminosilicates. Considering the abundance of andalusite in the region, even though it is not present in the examined thin sections, and the absence of both kyanite and sillimanite (with some exceptions where relics of sillimanite exist in some granite facies of the Barroso pluton), is possible to further constrain the emplacement conditions of these aplite-pegmatite bodies. This can be achieved by combining the aluminosilicate stability fields proposed by Richardson *et al.* (1968) with those proposed by Wood and William-Jones (1993), as illustrated in Figure 6.1. Therefore, the emplacement and crystallization of the spodumene aplite-pegmatite melt likely occurred between 235-665ºC and 1.3-5.5 kbar.

In terms of chronology, absolute ages from the pegmatite bodies are not readily available at the time. The same is the case for some of the surrounding granites as described in the respective chapter. However, it is possible to establish age relations by scrutinizing deformation patterns observed in the field. The aplite-pegmatite bodies exhibit deformation characteristics at both micro and macro scales that align with the late stage D2 deformation. According to the age estimations proposed by Dallmeyer (1997), the D2 deformation phase occurred approximately 337-316 million years ago. Therefore, the emplacement of the aplite-pegmatites likely occurred toward the later part of this interval, in order to be compatible with the observed deformation patterns.

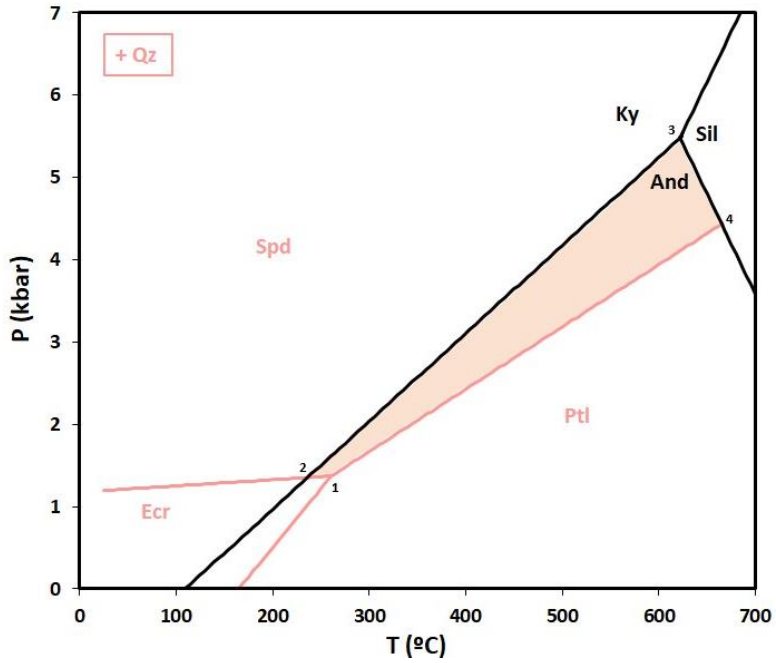

Figure 6.1 Stability fields for aluminossilicates (black lines; Ky-Kyanite, And-Andalusite and Sil-Sillianite) from Richardson et al. (1968) and Li-aluminossilicates (salmon lines; Ecr-Eucryptite, Ptl-Petalite and Spd- Spodumene)from Wood and William-Jones (1993). Salmon area represents possible emplacement conditions for the pegmatitic bodies. Numbers 1-4 represent limit vertices for the emplacement area. ***1)****261ºC and 1.4 kbar;* ***2)****235ºC and 1.3 kbar;* ***3)*** *621ºC and 5.5 kbar* ***4)*** *665ºC and 4.4 kbar*

6.2. PARAGENETIC SEQUENCE

As previously discussed in the petrography chapter, we have identified two distinct evolutionary stages within the aplite-pegmatite body, each characterized by a unique mineral assemblage. The first stage boasts a mineral composition comprising quartz, albite, microcline, and muscovite. Additionally, it includes accessory quantities of beryl, apatite, and Fe-Mn (Li) phosphates, with very minor traces of U-REE phosphates and sulfides (pyrite ± sphalerite). In contrast, the second stage presents an assemblage of spodumene, albite, quartz, and muscovite, accompanied by accessory montebrasite and a few minor columbite-tantalite series minerals. The transition between these stages is often marked by muscovite recrystallization. Consequently, these stages are designated as Stage I and Stage II, respectively. Furthermore, an additional metasomatic alteration stage superimposed on these two primary stages was identified. This stage is predominantly characterized by various phosphate phases, including Fairfieldite, Messelite, and Ludlamite.

Within Stage I, the major mineral assemblage reveals some noteworthy characteristics. Microcline is observed as a single generation, showing no evidence for multiple generations. Quartz, on the other hand, displays two distinct occurrences: one along the pegmatitic assemblage (Qz I) and another within the aplite groundmass that mingles with the pegmatitic texture (Qz II). Albite is a prominent presence throughout Stage I, with three different generations identified in this early stage. The first generation is marked by large, highly deformed crystals exhibiting myrmekitic textures, and it appears concurrently with microcline (Ab I). Following closely is a less developed non-myrmekitic albite, which serves as the primary constituent, along with quartz, in the aplite groundmass that intertwines with the pegmatitic texture (Ab II). The third generation comprises albite inclusions within microcline, often in the form of sub-euhedral crystals (sometimes recrystallized). These inclusions likely result from an exsolution process driven by decreasing temperatures within the system (Ab III). Muscovite, similar to albite, is present alongside quartz, microcline, and albite I in large-sized crystals, often exhibiting deformation

features (Ms I). Subsequently, muscovite delineates the contact between Stage I and Stage II (Ms II). This later-stage muscovite likely forms as the result of the interactions between well-developed crystals in Stage I and the fluids that give rise to Stage II. Following the primary mineral assemblage, beryl (Brl) is found along the boundaries of minerals from the main stage but is rarely mixed with that assemblage. This suggests that, despite some overlap between the main stage and beryl, beryl likely forms slightly later than the main mineral assemblage. Fe-Mn (Li) phosphates, including phosphates from the lithiophilite (Lhp) - triphylite (Trp) series, as well as minerals from the heterosite (Het) -purpurite (Pur) (resultant from the late stage alteration of Lhp-Trp) series along with apatite (Ap I), tend to appear mainly as inclusions within microcline crystals. It is reasonable to assume that these minerals, similar to Ab II, result from microcline exsolution. The presence of significant phosphorus content (average 0.15 wt% P_2O_5) in microcline crystals supports this hypothesis. Regarding the reduced quantities of both U-REE phosphates (UREE) and sulfides (Pyr + Sph), determining their place in the crystallization sequence is quite complex and would require further detailed study. Nevertheless, it is plausible to assume that U-REE phosphates share genetic relationships with other phosphate minerals, whereas sulfides likely form during a later stage of Stage I, given their intrusion into Ab I crystals.

In Stage II, we have identified only one generation of albite, represented by large-sized, frequently twinned sub-euhedral to euhedral crystals (Ab IV). These albites exhibit less pronounced deformation compared to those in Stage I. Muscovite is consistently present throughout this stage, appearing in large-sized crystals with deformation features, although less deformed than the muscovite in Stage I (Ms III). The existence of a fourth generation of muscovite is debatable due to the presence of extremely small crystals along the borders of albite (Ab IV) crystals. The relationship between these muscovites and Ms III cannot be definitively determined from the analysed thin sections. Quartz is also highly abundant in Stage II, and like in Stage I, it appears to crystallize continuously throughout the stage (Qz III). Spodumene exhibits three distinct morphologies in Stage II: i) sub-euhedral to euhedral crystals of larger dimensions displaying typical spodumene twinning; ii) anhedral and irregular crystals that typically do not exhibit twinning; iii) small needle-like crystals occurring in close proximity to muscovite at the stage transition (Ms II). These distinct morphologies have been identified as different generations of spodumene. The fact that the small anhedral needle-like crystals occur in association with transition muscovite suggests that they are the earliest in the crystallization sequence (Spd I). The anhedral/irregular crystals are often crosscut by the longer euhedral twinned crystals, suggesting that these anhedral crystals likely formed earlier in the sequence (Spd II) than the euhedral twinned crystals (Spd III). Montebrasite (Mbs I), is typically associated with the second generation of spodumene in this stage. However, the limited amount of montebrasite in the samples raises the possibility of sampling bias influencing this conclusion similar to the situation with U-REE and sulfides in Stage I. Columbite (Cbl)-Tantalite (Ttl) series minerals in Stage II are present in very few quantities and are highly dispersed. Determining their place in the crystallization sequence requires further detailed study. Nevertheless, it appears evident that these minerals often crystallize in close proximity to Spd III crystals, suggesting a potentially similar timing in their genetic formation.

In the metasomatic alteration stage, a common observation is the alteration of grain cores into ludlamite, while the borders are typically composed of members of the fairfieldite-messelite series. It's important to note that this stage exclusively manifests in the form of phosphate minerals.

This polyphasic nature of the aplite-pegmatite system and the intricate relationships between various phases are succinctly summarized in Figure 6.2. From a general standpoint the paragenetic sequence presented in this dissertation is similar to the one proposed by Charoy *et al.* (2001), with the exception of containing neither petalite or eucryptite as well as individualizing evolutionary stages in the pegmatite body.

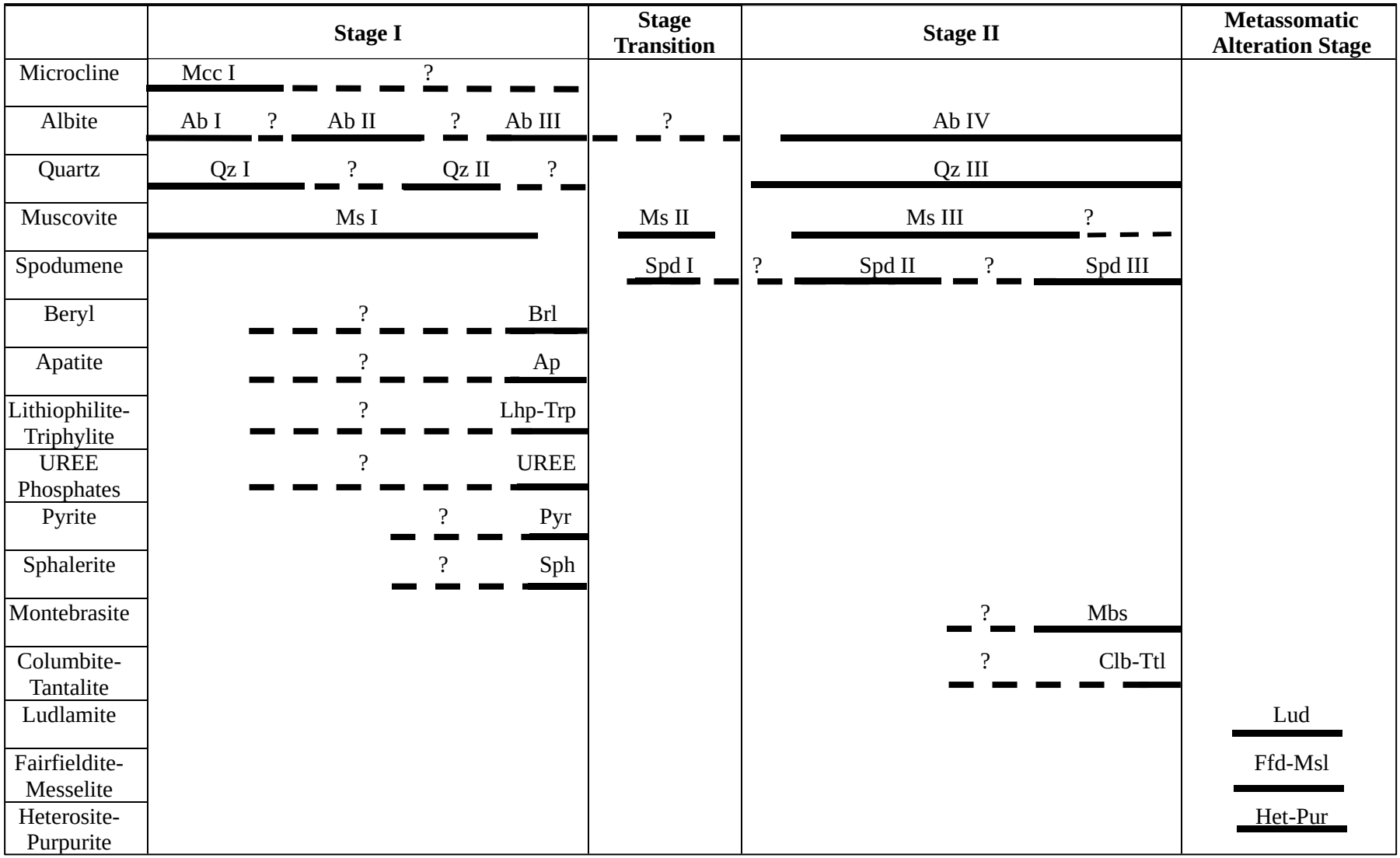

Figure 6.2 Paragenetic table illustrating the characteristic mineral deposition sequence for aldeia's pegmatite. Dotted lines indicate the possibility of deposition, although not confirmed, in that temporal interval.

6.3. MINERAL COMPOSITIONAL FEATURES

The EMPA data collected throughout this dissertation highlights several mineral chemistry features of both the pegmatite and host rock samples, including those within the metasomatic alteration zone. Mineral phases within the pegmatite body generally obey to their established chemical compositions. It is nonetheless worth mentioning the constant presence of some elements in the system.

In general, the system exhibits a substantial enrichment in sodium (Na), as indicated by the predominance of albite accompanying Li-Bearing minerals. Adding to that the reoccurring presence of Na as a main trace element in most of the analysed minerals (*e.g.*, spodumene, microcline, beryl, tourmaline), and even Na dominated phosphates.

The system also shows consistent values for elements such as F, Fe, Mn, P, Zn and to a lesser extent Sn, Nb and Ta. The significant enrichments in Na, F, Sn, Ta, and Mn in muscovite from MAZ relative to the host rock muscovite compositions most certainly reflect the contribution of the pegmatite(magmatic) component of the metasomatic fluid. Furthermore, the Na, F and Fe enrichments recorded in tourmaline from MAZ are compatible with the presence of a magmatic-hydrothermal fluid component during mineral growth. In fact, in a Mg/(Mg+Fe) versus Ca/(Ca+Na+K) diagram (Figure 6.3), data fits a mixing line identical to those suggested by Gaspar *et al.* (2022) for tourmaline formed in metasedimentary rocks associated with magmatic-hydrothermal systems. Additionally, arsenopyrite data might also suggest the presence of pegmatite emplacement derived geochemical variation seeing that proximal samples present a stronger lollingitic component than distal samples.

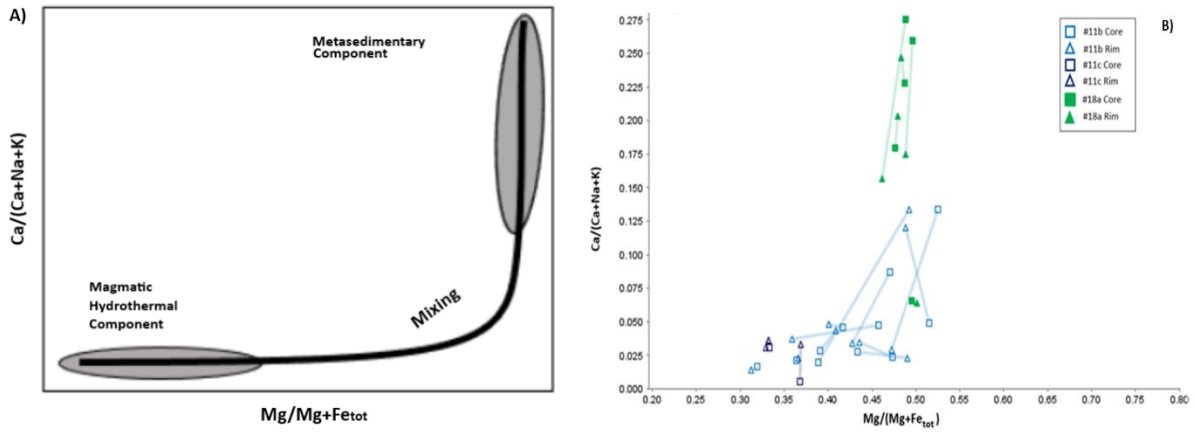

Figure 6.3 ***A)*** *Ca/(Ca+Na+K) vs Mg/(Mg + Fe) diagram showing a theoretical mixing line between a possible magmatic-hydrothermal component and a metamorphic component controlling tourmaline compositions* ***B)*** *Tourmaline from aldeia's MAZ and Host rock. Lines representing Core-rim connections.*

The trace element contents of biotite can be valuable on the identification of metasomatic processes in the more distal areas of the system, as previously discussed. However, it's worth noting that, albeit the limited sampling, ilmenite from the host rock also points in this direction. Its composition exhibits significant enrichment Mn and a depletion in high-field-strength elements (HFSE) in close proximity to pegmatites. This suggests a recrystallization process induced by the intrusion of the pegmatitic body, resulting in the incorporation of Mn (pyrophanitic component) at the expense of HFSE elements being released.

The presence of Zn is noteworthy and can't be ignored, as concentrations in the system are sufficient to form Zn-dominated phases, as is the case of sphalerite.

Fluorine also shows a curious trend, being particular enriched in phosphate minerals typically associated with the first stage (*e.g.*, apatite and triphylite-lithiophilite), but extremely scarce in phosphate minerals from the second stage, fact evidenced by the presence of montebrasite - $LiAl(PO_4)OH$- instead of amblygonite- $LiAl(PO_4)F$.

Phosphorous behaviour needs further study although chemical data seems to support the petrographic analyses that this element is crucial in the geochemical processes associated with the first stage melt.

The main Li carrier minerals found in aldeia's pegmatite are spodumene and montebrasite, both relatively pure in composition with average Li contents of 3.67 and 4.48 wt% respectively. Fe-Mn (Li) phosphates were also found and must be taken into consideration when evaluating total Li contents.

It is also noteworthy the absence of Rb and Cs, with this latter one only showing relevant values in beryl. This is also confirmed by the whole-rock geochemical database present in Mateus *et al.* (2023)

Despite the data collected some questions still linger regarding the geochemical signature of aldeia's pegmatitic swarm. Firstly, the origin of all the Na in the system? Is it of primary (magmatic) origin, or does it result from interaction between the melt and the host rocks? This question persists without a definitive answer and warrants further in-depth research.

Another puzzling aspect is the absence of Rb and Cs which is atypical for LCT (Lithium-Cesium-Tantalum) type pegmatites. This anomaly raises the question if these pegmatites are true LCT pegmatites? Once again, this question remains unanswered and calls for a more comprehensive investigation.

6.4. MULTIPLE STAGE ORIGIN: POSSIBLE CAUSES

This subchapter aims to formulate hypotheses regarding the origin of the two stages that have been discerned through petrographic analysis. These stages exhibit disparate mineral assemblages and a discernible distinction between them, strongly suggesting the involvement of distinct melts in their genesis. Observing mineral assemblages, textural arrangements and correlation between stages four plausible hypotheses that could account for the occurrence of these distinct stages can be considered.

One of the hypotheses, perhaps the most straightforward, speculates that the discrepant stages result from separate injections of molten material, each establishing itself adjacent to the other. However, this hypothesis prompts a geometrical conundrum: why do distinct injections converge consistently at the same location and always exhibit identical textural relationships (*i.e.*, Stage II intersecting Stage I)?

Another conceivable scenario is the process of fractional crystallization within the pegmatitic melt, leading to the formation of two distinct stages. In this scenario, early formed crystals along the pegmatite bodies fail to reequilibrate with the remaining melt, thereby retaining fluxing/incompatible elements for incorporation into subsequent mineral phases. In the context of Aldeia's swarm, this could account for the presence of Li-bearing minerals exclusively in Stage II. This process bears resemblance to the one described by London and Morgan (2012).

A third possibility centers on the notion that the distinct stages stem from an autometasomatic alteration affecting the initial Stage I. This alteration process would entail the reabsorption of primary albite and the leaching of Li from Li-bearing phases present in Stage I (*e.g.*, Muscovite). Subsequently, this Li- and Na-rich fluid could give rise to Stage II. This process shares some similarities with the one described in Barros *et al.* (2022). It is also conceivable that the second melt arises from metasomatic

alterations within the host rock, driven by the heat generated by the emplacement of the parental melt of Stage I. This process bears a resemblance to the one presented by Errandonea-Martin *et al.* (2022).

The final hypothesis revolves around melt-melt immiscibility, drawing inspiration from the studies conducted by Thomas and Davidson (2013, 2014, 2016) and Thomas *et al.* (2012). This hypothesis proposes that, due to a pronounced enrichment in melt structure modifiers (*e.g.*, Li, Na) two distinct melts form. According to Thomas *et al.* (2012), these two melts constitute conjugate melt fractions that subsequently segregate into separate melts. The extraordinary mobility of rare metals within these conjugate melt fractions facilitates this interpretation. Nevertheless, this hypothesis necessitates further investigation into the behavior of various elements, including both fluxing and rare metals, under the conditions conducive to pegmatite formation.

It is imperative to highlight two key points when discussing this matter. Firstly, regardless of the process or processes at play in the formation of these distinct stages, it is essential to acknowledge that the melts involved are inherently rich in fluxing elements and possess high water content, consistent with the characteristics of all fluids associated with pegmatite formation. These attributes confer a low density and high volatility to the melt, resulting in the requisite low viscosity for the separation of the pegmatite-forming fluid(s) from their parental source (Thomas and Davidson 2014). This low viscosity allows the ascension of the pegmatitic fluid in the crust until it reaches a viscosity equilibrium with the surrounding rocks. This is valid whether the melt source is granitic or anatectic. Secondly, it is crucial to note that the data amassed during this dissertation, while valuable, remains insufficient to conclusively favor any single hypothesis or even a combination of hypothesis. Importantly, the data collected does not directly contradict nor support any of the hypotheses presented. Thus, a comprehensive study of this matter is warranted, as outlined in the following "Study Limitations and Future Work" subchapter.

6.5. GENETIC MODELS: MAGMATIC, ANATECTIC OR SOMETHING IN BETWEEN

The Barroso-Alvão aplitic-pegmatitic field has conventionally been associated with the established genetic model for LCT-type pegmatites, which suggests their formation through classic magmatic processes linked to granitic bodies. At first glance, regional geology seems to support this notion, given the abundant exposure of granites in the area. However, establishing a direct connection between these granites and the pegmatites has proven to be a challenging task, as noted by Martins (2011). This traditional model suggests that pegmatitic bodies are the result of fractional crystallization, melt immiscibility, and the enrichment of volatiles within an originally fertile parental granitic melt, as proposed by Cerny *et al.* (2012). According to this model, pegmatites represent the later stages of silicate melt evolution, with fractional crystallization leading to an enrichment in incompatible, fluxing and rare elements, subsequently reflected in their mineralogy (Cerny, 1991a). However, a significant point of contention exists for the applicability of this hypothesis to Aldeia's swarm. The deformation patterns observed in the aplite-pegmatite bodies is not consistent with those exhibited by the exposed potential parental granites. Indeed, the pegmatite bodies display deformation patterns consistent with late-stage D2 deformation, whereas the surrounding granites only show D3 type deformation patterns. Given these observations, it is reasonable to assume that the enveloping granites are younger, even if only slightly, than the pegmatites. This raises a perplexing question: how can a granitic body give rise to something older than itself? One conceivable hypothesis is that the parental granite responsible for the pegmatites exists at greater depths and is not exposed at the surface nor intersected in drill-hole campaigns.

This classical genetic model has faced opposition from an alternative model that places anatexis as a primary melt source. This model suggests that the partial melting of Li-rich metasediments can yield Li-rich melts, as depicted in Figure 6.4. Importantly, this model has the potential to account for pegmatite bodies that are not contemporaneous or genetically related to neighboring granites. Anatectic

origins have been proposed for various LCT-type pegmatite bodies, fields, and regions worldwide, as evidenced by studies conducted by Simmons *et al.* (2016), Shaw *et al.* (2016), and Lv *et al.* (2021). Typically, this anatectic model is linked to orogenic regions where crustal thickening occurs during the convergence process, leading to nappe formation. The extensional collapse within orogenic settings creates conditions conducive to the partial melting of metasedimentary rocks, resulting in Li-rich, low viscosity melts. These melts capitalize on physical discontinuities as conduits for upward migration until they reach a viscosity equilibrium with the surrounding rocks, allowing for crystallization (Muller, 2015a,b; Muller, 2017; Knoll, 2023). Knoll (2023) suggests that the melting processes for the metasedimentary Li source occur below the biotite dehydration melting point and the breakdown of oxide and phosphate minerals. This could explain why these pegmatites, despite belonging to the LCT family, are predominantly enriched in Li, as Li mobility under these conditions surpasses that of Cs and Ta (Knoll, 2023). Altough this anatectic model has been proposed for the Barroso-Alvão aplite-pegmatite field (Deveaud *et al.*, 2014), no comprehensive studies have yet been undertaken to conclusively validate its applicability.

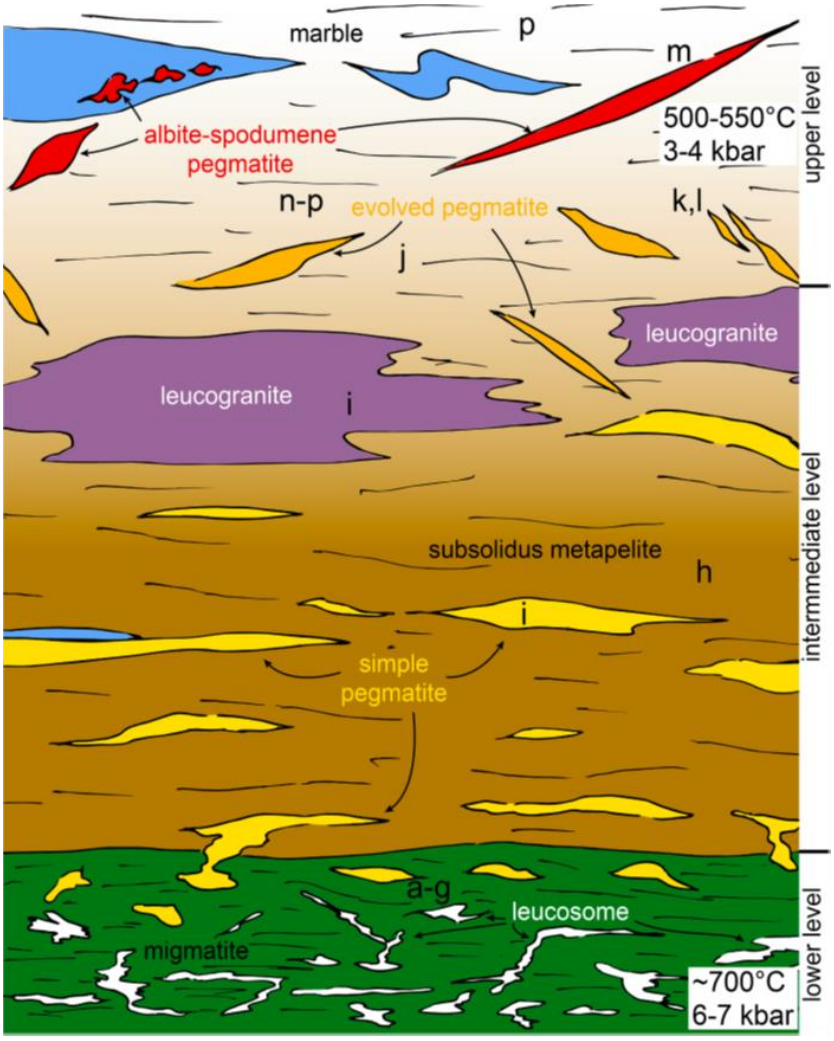

Figure 6.4 Illustration depicting the interconnections among subsolidus metapelite, migmatite, various pegmatite variants, and leucogranite within the three structural levels. Sizes of individual bodies are not depicted to scale. Adapted from Knoll et al. (2023)

A third hypothesis introduces the concept of a hybrid process involving a combination of magmatic and anatectic mechanisms. In this scenario, the anatectic fluid ,resultant from the partial melting of the sedimentary sequence, could interact with a contemporaneous magmatic melt responsible for generating

the surrounding granitic bodies. It is worth noting that as of now, there is no existing scientific literature that explicitly discusses or describes this amalgamation of processes. Consequently, this hypothesis remains speculative and warrants further in-depth investigation, beyond the scope of this dissertation.

The geological features of the Barroso-Alvão region, and consequently Aldeia's Swarm, appear to align with the plausibility of these hypotheses. During the course of this dissertation, no evidence was uncovered that could definitively substantiate or refute any one of these hypotheses. However, several factors point to the anatectic origin and/or mixed processes hypotheses when considered in conjunction. These factors include the absence of a parental granite exhibiting deformation patterns congruent with those observed in the mineralized bodies and the geological context of an orogenic belt featuring the overthrust of crustal nappes over pelitic metasedimentary sequences, and the significant enrichment in Li (not replicated in Cs, Ta or Rb). It is nonetheless essential to emphasize that, at the time of writing, academic literature lacks a definitive geochemical signature capable of clearly distinguishing between models.

7. STUDY LIMITATIONS

Considering the data presented in the preceding chapters, it is imperative to acknowledge several limitations inherent to this study, which underscore the need for caution and further investigation in this subject matter:

i. For some minerals it was not possible to discuss in detail some elemental substituition vectors due to technical limitations mainly attributed to suboptimal calibration of the Electron Microprobe system (EMPA). Future calibration refinements are needed.
ii. While the phosphate data consistently provides relevant values, it remains limited in its capacity to deliver a comprehensive analysis of these minerals. This limitation results from the relatively high detection limits for the counting times employed, warranting future investigation with extended counting intervals.
iii. The analysis of some minerals encounters constraints stemming from the diminutive dimensions of the crystals. This constraint introduces the potential for contamination from adjacent minerals, thereby tempering with the accuracy of the results and consequently reducing the number of accepted analyses.
iv. Sampling of Nb-Ta Oxides was notably constrained, primarily due to the scarcity of grains and the restricted size of the available ones.
v. The numerical estimation of lithium (Li) and beryllium (Be) values, as opposed to direct measurement, introduces an inherent degree of imprecision into the results.
vi. The detection limits for crucial elements in aplite-pegmatite systems, namely Rb and Cs, are excessively high in relevant mineral phases like muscovite and feldspars. It is imperative to significantly reduce these detection limits for a more precise characterization of these elements within these minerals.
vii. It is crucial to emphasize that the data presented herein results exclusively to one specific drill hole within a singular pegmatitic swarm. Extrapolating these findings to a broader scale, such as the entirety of the Barroso-Alvão pegmatitic field, necessitates caution and emphasizes the potential for unanticipated challenges in future investigations. Comprehensive field-wide studies will be indispensable for robust and reliable conclusions, especially in an exploration context.

8. FINAL REMARKS & FUTURE WORK

Lithium mineralization in the Barroso-Alvão region has the potential to become an asset for Europe's quest for self-sufficiency in lithium production and supply. While this region is often associated with the conventional pegmatite-forming process linked to granitic intrusions, it is not uncommon for these formations to display structural, textural, and mineralogical features that cast doubt on a purely magmatic origin. Various criteria, including field data and deviations from the typical geochemical patterns found in granitic LCT pegmatites, open the door to a fresh interpretation of these geological structures.

The petrographic analysis revealed that spodumene- bearing aplite-pegmatites are poorly zoned, and show a complex mineral assemblage developed along two main crystallization stages, with a superimposed later metasomatic event. These two stages present different mineralogical assemblages and find themselves often in contact. The absence of SQI textures indicates spodumene in aldeia's pegmatite is primary and not resultant from the decomposition of petalite to which is important to add the absence of weathering of that same mineral. Furthermore, petrographic analysis is consistent with field data seeing that all the main mineral phases from both stages exhibit micro-textures and intra-crystalline high-T deformation features, suggesting deformation under crystallization and cooling conditions, compatible with the regional Variscan deformation patterns observed in the metasedimentary host-rocks.

Geochemical data allow to classify aldeia's pegmatite as Complex Spodumene Rare Element-Li pegmatites. Furthermore, reveals a pegmatitic system mainly enriched Li and Na, highly deficient in Rb and Cs with remarkable values for atypical elements such as F, Fe, Mn, Nb, P, Sn, Ta, and Zn. Moreover, geochemical data seems to indicate that pegmatite emplacement caused a substantial modification in the composition of host rock minerals such as muscovite, tourmaline, biotite and ilmenite.

From and economic standpoint geochemical data reveals that lithium is carried in a very pure spodumene with typical lithium values (average 3.6 wt.%) as well as by phosphates from the montebrasite-amblygonite series and lithiophilite-triphylite group. Also relevant is the absence of iron/arsenic sulfides in the pegmatitic system, relevant from an ecological standpoint.

Nonetheless, key questions remain open at the end of this dissertation:

(1) What's the source of the overabundant Na?
(2) Why are Rb and Cs values so low in an LCT type pegmatite? Are the pegmatite bodies of Aldeia typical LCT systems?
(3) Which mechanism(s) originate the two petrographically distinct stages?
(4) Is Aldeia's aplite-pegmatite a magmatic anatectic or mixed type mineralized body?

In order to solve these problems and in addition to the aforementioned research directives conducted during this dissertation, there are several other avenues for future work that can provide deeper insights into the geological evolution of the Barroso-Alvão field and the processes controlling the formation of aplite-pegmatite bodies. Future work, from the author perspective, should consist in:

(1) Expanding the sample size, over a broader array of drill-holes and diverse aplite-pegmatite bodies within the Barroso-Alvão field.
(2) Absolute dating of both the pegmatitic swarm and the surrounding granites, with the aim of establishing a precise temporal relationship between these two geological groups;

(3) Fluid/melt inclusion studies in minerals from both stages, in order to characterize original fluid composition for both stages potentially revealing which mechanisms were at play during their formation;
(4) Implementing laser ablation inductively coupled plasma mass spectrometry (LA-ICP-MS) to rectify potential inaccuracies in lithium (Li) and beryllium (Be) estimations, while simultaneously obtaining more intricate geochemical data pertaining to trace elements within the examined mineral phases.
(5) Performing isotope studies including not only the granites but also the host rocks and aplite-pegmatite bodies, in order to discern provenance relationships among these rock formations.
(6) Establishing a comprehensive geochemical database of different mineral phases from various worldwide aplite-pegmatite deposits. This database would facilitate comparative analysis of geochemical features among various pegmatite generation mechanisms, providing valuable insights into the global context of pegmatite formation processes.

These future research directions are key for a more comprehensive understanding of the geological processes within the Barroso-Alvão field and its associated mineralization processes, being fundamental to an educated and responsible future exploration of Lithium in Portugal.

9. REFERENCES

Almeida, A. (1998). Especialização metalogénica dos granitos peraluminosos de duas micas do complexo de Cabeceiras de Basto. In Actas do V Congresso Nacional de Geologia. Comunicações do Instituto Geológico e Mineiro (Vol. 84, No. 1, pp. B79-B82).

Almeida, A., Martins, H. C., & Noronha, F. (2002). Hercynian acid magmatism and related mineralizations in northern Portugal. Gondwana Research, 5(2), pp. 423-434.

Almeida, M. Â. D. C. F. (1994). Geoquímica, petrogénese e potencialidades metalogénicas dos granitos peraluminosos de duas micas do complexo de Cabeceiras de Basto.

Andersen, T., Erambert, M., Larsen, A. O., & Selbekk, R. S. (2010). Petrology of nepheline syenite pegmatites in the Oslo Rift, Norway: Zirconium silicate mineral assemblages as indicators of alkalinity and volatile fugacity in mildly agpaitic magma. Journal of Petrology, 51(11), pp. 2303-2325.

Barros, R., Kaeter, D., Menuge, J. F., Fegan, T., & Harrop, J. (2022). Rare element enrichment in lithium pegmatite exomorphic halos and implications for exploration: Evidence from the Leinster Albite-Spodumene Pegmatite Belt, Southeast Ireland. Minerals, 12(8), 981

Beard, J. S., Fullagar, P. D., & Krisha Sinha, A. (2002). Gabbroic pegmatite intrusions, Iberia Abyssal Plain, ODP Leg 173, Site 1070: Magmatism during a transition from non-volcanic rifting to sea-floor spreading. Journal of Petrology, 43(5), pp. 885-905.

Cameron, E. N., Jahns, R. H., McNair, A. H., & Page, L. R. (1949). Internal structure of granitic pegmatites.

Černý, P & Ercit, T. S. (2005). The Classification Of Granitic Pegmatites Revisited. The Canadian Mineralogist, 43, pp. 2005-2026

Černý, P. (1991a). Rare-element granitic pegmatites. Part I: Anatomy and internal evolution of pegmatite deposits. Geoscience Canada, 18, pp. 49-67.

Černý, P. (1991b) Rare-element granitic pegmatites. Part II: regional and global environments and petrogenesis. Geoscience Canada, 18, pp. 68-81

Černý, P. (2002). Mineralogy of beryllium in granitic pegmatites. Reviews in Mineralogy and Geochemistry, 50, pp. 405-444.

Černý, P., London, D., & Novák, M. (2012). Granitic pegmatites as reflections of their sources. Elements, 8, pp. 289-294

Charoy B., Noronha F., & Lima A.M.C (2001) Spodumene-Petalite-Eucryptite: mutual relationships and alteration stylein pegmatite-aplite dykes from Northern Portugal. The Canadian Mineralogist, 39; pp. 729-746.

Charoy, B., Lhote, F., Dusausoy, Y., & Noronha, F. (1992). The crystal chemistry of spodumene in some granitic aplite-pegmatite bodies of northern Portugal; a comparative review. The Canadian Mineralogist, 30, pp. 639-651

COCHILCO (Comisión Chilena del Cobre) (2021). El mercado de lítio Desarrollo reciente y proyecciones al 2030.

Cook, N. J., Ciobanu, C. L., Pring, A., Skinner, W., Shimizu, M., Danyushevsky, L., Saini-Eidukat, B. & Melcher, F. (2009). Trace and minor elements in sphalerite: A LA-ICPMS study. Geochimica et Cosmochimica Acta, 73, pp. 4761-4791.

Dallmeyer, R.D.; Martínez-Catalán, J.R.; Arenas, R.; Gil-Ibarguchi, J.I.; Gutiérrez-Alonso, G.; Farias, P.; Bastida, F. (1997) Diachronous Variscan tectonothermal activity in the NW Iberian Massif: evidence from 40Ar/39Ar dating of regional fabrics. Tectonophysics, 277, pp. 307-337.

Deer, W.A., Howie, R.A., & Zussman, J. (1992). Minerais constituintes das rochas – uma introdução. Tradução de C. A. R. Macedo. Fundação Calouste Gulbenkian

Deveaud, S., Silva, D., Gumiaux, C., Gloaguen, E., Branquet, Y., Lima, A., Villaros, A., Guillou-Frottier, L. and Melleton J. (2014). Which parameters control the Variscan pegmatite field-scale organization?

Dias da Silva Í, Díez Fernández R, Díez-Montes A, González Clavijo E, Foster DA (2016) Magmatic evolution in the N-Gondwana margin related to the opening of the Rheic Ocean— evidence from the Upper Parautochthon of the Galicia-Trás-os-Montes Zone and from the Central Iberian Zone (NW Iberian Massif). International Journal of Earth Sciences, 105, pp. 1127-1151.

Dias, R & Ribeiro, A., (1995). Dias, R., & Ribeiro, A. (1995). The Ibero-Armorican Arc: a collision effect against an irregular continent? Tectonophysics, 246, pp. 113-128.

Dias, F. C. L. (2016). Lithium mineralizations of Barroso-Alvão aplite-pegmatite field (Doctoral dissertation, Universidade do Porto (Portugal)

Díez Fernández, R., Arenas, R., Pereira, M.F., Sánchez-Martínez, S., Albert, R., Martin Parra, L.M.,932 Rubio Pascual, F.J., and Matas, J., (2016 Tectonic evolution of Variscan Iberia: Gondwana–933 Laurussia collision revisited: Earth-Science Reviews, v. 162, p. 269-292.

Direção Geral de Energia e Geologia (DGEG),https://portalgeo.dgeg.gov.pt /arcgis /apps/ webappviewer/index.html?id=de764a4a5ccd446292cb26a7e5c2e725&extent=-1301451.0276%2C4739395.255%2C-400105.59%2C5198628.921%2C102100

Dunlap, A., & Riquito, M. (2023). Social warfare for lithium extraction? Open-pit lithium mining, counterinsurgency tactics and enforcing green extractivism in northern Portugal. Energy Research & Social Science, 95, 102912.

Dwyer, S., & Teske, S. (2018). Renewables 2018 Global Status Report. Renewables 2018 Global Status Report.

Eby, G. (1990). The A-type granitoids: A review of their occurrence and chemical characteristics and speculations on their petrogenesis. Lithos, 26, pp. 115-134

Errandonea-Martin, J., Garate-Olave, I., Roda-Robles, E., Cardoso-Fernandes, J., Lima, A., dos Anjos Ribeiro, M., & Teodoro, A. C. (2022). Metasomatic effect of Li-bearing aplite-pegmatites on psammitic and pelitic metasediments: Geochemical constraints on critical raw material exploration at the Fregeneda–Almendra Pegmatite Field (Spain and Portugal). Ore Geology Reviews, 105155.

European Commission. (2020). Communication from the Commission to the European Parliament, the Council, the European Economic and Social Committee, and the Committee of the Regions - Critical Raw Materials Resilience: Charting a Path towards Greater Security and Sustainability.

Farinha, J. & Lima, A. (2000) Estudo dos filões aplitopegmatíticos litiníferos da Região do Barroso-Alvão (Norte de Portugal). Estudos, Notas e Trabalhos, Tomo 42, pp. 3-50. IGM, Lisboa

Ferreira, N., Iglesias, M., Noronha, F., Pereira, E., Ribeiro, A., Ribeiro, M. (1987). Granitóides da Zona Centro Ibérica e seu enquadramento geodinâmico. In: Geologia de los granitoides y rocas associadas del Macizo Hespérico, (F. Bea, E. Carnicero, J. C. Gonzalo, M. López Plaza, M. D. Rodríguez, Eds.), Libro homenaje a L. C. Garcia de Figuerola, Rueda, Madrid, pp. 37-51

Gaspar M., Ribeiro da Costa I., Mateus A., Martins I., Rodrigues P., 2022, Assessment of tourmaline composition as a vectoring tool for Sn-W deposits – the Góis-Panasqueira-Segura Belt (Central Portugal). SEG 2022 Conference: Minerals for Our Future, ID4317, 27-30 Aug, Denver, CO.

Giurco, D., Dominish, E., Florin, N., Watari, T., McLellan, B. (2019). Requirements for Minerals and Metals for 100% Renewable Scenarios. In: Teske, S. (eds) Achieving the Paris Climate Agreement Goals. Springer, Cham, pp. 437-457

Glover, A. S., Rogers, W. Z., & Barton, J. E. (2012). Granitic pegmatites: Storehouses of industrial minerals. Elements, 8, pp. 269-273

Goonan, T. G. (2012). Lithium Use in Bateries, US Geological Survey Circular 1371

Grew, E. S., Locock, A. J., Mills, S. J., Galuskina, I. O., Galuskin, E. V., & Hålenius, U. (2013). Nomenclature of the garnet supergroup. American Mineralogist, 98, pp. 785-811

Gruber, P. W., Medina, P. A., Keoleian, G. A., Kesler, S. E., Everson, M. P., & Wallington, T. J. (2011). Global lithium availability: A constraint for electric vehicles?. Journal of Industrial Ecology, 15, pp. 760-775.

Hawthorne, F. C., & Černý, P. (1977). The alkali-metal positions in Cs-Li beryl. The Canadian Mineralogist, 15, pp. 414-421

Hawthorne, F. C., & Henry, D. J. (1999). Classification of the minerals of the tourmaline group;

Henry, D. J., Novák, M., Hawthorne, F. C., Ertl, A., Dutrow, B. L., Uher, P., & Pezzotta, F. (2011). Nomenclature of the tourmaline-supergroup minerals. American Mineralogist, 96, pp. 895-913

Jaskula, B.W. (2013) Lithium: U.S. Geological Survey Mineral Commodity Summaries. USGS National Minerals Information Center, Virginia, pp. 94-95.

Jaskula, B.W. (2023) Lithium: U.S. Geological Survey Mineral Commodity Summaries. USGS National Minerals Information Center, Virginia, pp. 108-109.

Kesler, S. E., Gruber, P. W., Medina, P. A., Keoleian, G. A., Everson, M. P., & Wallington, T. J. (2012). Global lithium resources: Relative importance of pegmatite, brine and other deposits. Ore geology reviews, 48, pp. 55-69

Knoll, T., Huet, B., Schuster, R., Mali, H., Ntaflos, T., & Hauzenberger, C. (2023). Lithium pegmatite of anatectic origin-A case study from the Austroalpine Unit Pegmatite Province (Eastern European Alps): geological data and geochemical model. Ore geology reviews, 105298.

Lima, A., Vieira, R. C., Martins, T., & Noronha, F. (2010). Minerais de Lítio. Exemplos dos Campos Aplitopegmatíticos de Barroso-Alvão e Almendra-Barca D'Alva. João M. Cotelo Neiva, António Ribeiro, Luís Mendes Victor, Fernando Noronha, & Miguel Magalhães Ramalho, Ciências Geológicas-Ensino e Investigação e sua história, 1, pp. 89-98.

Lima, A.M.C. (2000) Estrutura, mineralogia e génese dos filões aplitopegmatíticos com espodumena da região do Barroso-Alvão (Norte de Portugal). Tese de Doutoramento, Universidade do Porto, Portugal, e INPL, Nancy, França

Linnen, R. L., Van Lichtervelde, M., & Černý, P. (2012). Granitic pegmatites as sources of strategic metals. Elements, 8(4), 275-280.

London, D. (2008) Pegmatites. Canadian Mineralogist Special Publication 10.

London, D. (2014) A petrologic assessment of internal zonation in granitic pegmatites. Lithos, pp. 184-187

London, D. and Kontak, D. (2012) Granitic Pegmatites: Scientific Wonders and Economic Bonanzas. Elements 8, pp. 257-261

London, D., & Morgan, G. B. (2012). The pegmatite puzzle. Elements, 8(4), 263-268.

London, D., Wolf, M. B., Morgan, G. B., & Garrido, M. G. (1999). Experimental silicate–phosphate equilibria in peraluminous granitic magmas, with a case study of the Alburquerque batholith at Tres Arroyos, Badajoz, Spain. Journal of Petrology, 40, pp. 215-240

Lv, Z. H., Zhang, H., & Tang, Y. (2021). Anatexis origin of rare metal/earth pegmatites: Evidences from the Permian pegmatites in the Chinese Altai. Lithos, 380, 105865

Lyalina, L. M., Selivanova, E. A., & Hatert, F. (2023). Nomenclature of the triphylite group of minerals. European Journal of Mineralogy, 35, pp. 427-437.

Martin, R. F., De Vito, C., & Pezzotta, F. (2008). Why is amazonitic K-feldspar an earmark of NYF-type granitic pegmatites? Clues from hybrid pegmatites in Madagascar. American Mineralogist, 93, pp. 263-269.

Martin, R.F. and De Vito, C. (2005) The patterns of enrichment in felsic pegmatites ultimately depend on tectonic setting. Canadian Mineralogist, 43, pp. 2027-2048

Martinez F.J., Corretge L.G. & Suarez O. (1990). Distribution, Characteristics and Evolution of Metamorphism. In: Pre-Mesozoic Geology of Iberia (R.D. Dallmeyer & E. Martínez Garcia eds.)

Martins H. C. B. & Sant'Ovaia H. M. (1998). Zonalidade e processo de instalação dosgranitóides biotíticos do maciço de Vila Pouca de Aguiar. Abordagem Multidisciplinar. Actas do V Congresso Nacional de Geologia. Comunicações do Instituto Geológico Mineiro, Lisboa,84, pp.B31-B34

Martins, T.C & Lima, A. (2011) Pegmatites from Barroso-Alvão, Northern Portugal: anatomy, mineralogy and mineral geochemistry. Cadernos do Laboratorio Xeolóxico de Laxe, 36, pp. 177-206.

Martins, T.C. (2009) Multidisciplinary study of pegmatites and associated Li and Sn-Nb-Ta mineralizations from the Barroso-Alvão region. Tese de Doutoramento, Universidade do Porto, Portugal, e INPL, Nancy, França.

Mateus, A., Gaspar, L.M., Dias da Silva, Í. (2022). Main features of the Aldeia spodumene-bearing pegmatites and their metasedimentary hosts based on field observations. Internal Report #2/A7, Project INOVMINERAL4.0, 18 pp and geological maps.

Mateus, A., Gaspar, L.M., Rodrigues, P.C.R., Figueiras, J. (2023). Whole-rock geochemical features displayed by aplite-pegmatite bodies and country rocks (granites and metasediments) from Ribeira de

Pena – Boticas area (lithium-rich pegmatite field of Alvão-Barroso, North Portugal). Internal Report #4/A7, Project INOVMINERAL4.0, 23 pp.

Mateus, A.; Noronha, F. (2010) Sistemas mineralizantes epigenéticos na Zona Centro-Ibérica; expressão da estruturação orogénica Meso-a Tardi-Varisca. In Ciências Geológicas: Ensino e Investigação e sua História; Cotelo Neiva, J.M., Ribeiro, A., Mendes Victor, L., Noronha, F., Ramalho, M., Eds.; Associação Portuguesa de Geólogos e Sociedade Geológica de Portugal, Lisboa, Portugal, Volume II.

Mehdilo, A., Irannajad, M., & Rezai, B. (2015). Chemical and mineralogical composition of ilmenite: Effects on physical and surface properties. Minerals Engineering, 70, pp. 64-76

Miyashiro, A., (1961). Evolution of metamorphic belts. Journal of Petrology, 2, pp. 277-311.

Morimoto, N. (1989). Nomenclature of pyroxenes. Mineralogical Journal, 14(5), 198-221.

Müller, A., Ihlen, P.M., Bingen, B., Snook, B., Romer, R., (2015a). The Sveconorwegian Pegmatite Province: 5000 pegmatite and no parental granites? 7th International Symposium on Granitic Pegmatites, PEG 2015 Ksiqź, Poland, Book of Abstracts, pp. 58–59

Müller, A., Ihlen, P.M., Snook, B., Larsen, R.B., Flem, B., Bingen, B., Williamson, B.J., (2015b). The chemistry of quartz in granitic pegmatites of southern Norway: petrogenetic and economic implications. Economic Geology 110, pp. 1737–1757.

Müller, A., Romer, R. L., & Pedersen, R. B. (2017). The Sveconorwegian Pegmatite Province–Thousands of pegmatites without parental granites. The Canadian Mineralogist, 55, pp. 283-315

Müller, A.; Simmons, W.; Beurlen, H.; Thomas, R.; Ihlen, P.M.; Wise, M.; Roda-Robles, E.; Neiva, A.M.R.; Zagorsky, V (2022). A proposed new mineralogical classification system for granitic pegmatites; Part I, History and the need for a new classification. The Canadian Mineralogist, 60, pp. 203-227.

Neiva, A. M. R., Silva, M. M. V. G., Antunes, I. M. H. R., & Ramos, J. M. F. (2000). Phosphate minerals of some granitic rocks associated quartz veins from northern and central Portugal. Journal of the Czech Geological Society, pp. 1-9

Niggli, P. (1920) The volatile components in the magma. Preisschriften der F¨urstlich Jablonowskischen Gesell-schaft, B.G. Teubner, Leipzig, p. 272

Nizamoff, J.W., Falster, A.U., Simmons, W.B. & Webber, K.L. (1999): Phosphate mineralogy of NYF-LCT- andmixed-type granitic pegmatites. Canadian Mineralogist, 37, pp. 853-854

Noronha, F. & Ribeiro, M. L. (1983) – Carta Geológica de Portugal na Escala 1/50 000. Notícia Explicativa da Folha 6-A, Montalegre. Serviços Geológicos de Portugal

Noronha, F., Ramos, J. M. F., Rebelo, J. A., Ribeiro, A., & Ribeiro, L. (1981). Essai de corrélation des phases de déformation hercyniennes dans le nord-ouest Péninsulaire. Leidse Geologische Mededelingen, 52, pp. 87-91.

Noronha, F., Ribeiro, M., Almeida, A., Dória, A., Guedes, A., Lima, A., Martins, H., Sant'Ovaia, H., Nogueira, P., Martins, T., Ramos, R. & Vieira, R. (2013). Jazigos filonianos hidrotermais e aplitopegmatíticos espacialmente associados a granitos (Norte de Portugal). In: Geologia de Portugal: Geologia Pré-Mesozoica de Portugal. Escolar Editora.

Oliveira, D.P., Lisboa, J.V., Carvalho, J.M., Salgueiro, R.M., Inverno, C.M., Leite, M.M., (2018). Lítio em Portugal: enquadramento, geologia e mineralogia. Boletim. De Minas, 52 - Edição Especial - Lítio - 2017-2018.

Oliveira, A., Martins, H., & Sant'Ovaia, H. (2020). Insights into the felsic vein magmatism in northern Portugal (Central Iberian Zone): an integrated geochemical and petrophysical study. International Multidisciplinary Scientific GeoConference: SGEM, 20(1.1), 139-146.

Pan, Y. and Fleet, M.E. (2002) Compositions of the Apatite-Group Minerals: Substitution Mechanisms and Controlling Factors. Reviews in Mineralogy and Geochemistry, 48, pp. 13-49

Pap, M. S. A. S. (1969). Crystal-chemical characterization of clinopyroxenes based on eight new structure refinements'.

República Portuguesa. 2017. Relatório do grupo de trabalho "lítio". despacho nº 15040/2016 de Secretaria de Estado da Energia. Lisboa: Março 2017.

Ribeiro, A. (1974). Contribuition à l'étude tectonique de Trás-os-Montes Oriental. Comunicações dos Serviços Geológicos de Portugal, 24,pp. 1-168p

Ribeiro, M.A.; Martins, H.C.; Almeida, A.; Noronha, F.(2000) Carta Geológica de Portugal, escala 1:50.000 (Cabeceiras de Basto), Notícia Explicativa. Serviços Geológicos de Portugal

Ribeiro, M.A.; Ramos, R.; Noronha, F. (2007) Pegmatite-aplite veins of Barroso-Alvão field. Lithostratigraphy and metamorphism of host rocks. In: Graniic Pegmatites: the State of the Art (A. Lima and E. Roda-Robles eds.), Fieldtrip Guidebook, Memórias 9, Faculdade de Ciências da Universidade do Porto, pp. 39-45.

Richardson, S. W., Bell, P. M., & Gilbert, M. C. (1968). Kyanite-sillimanite equilibrium between 700 degrees and 1500 degrees C. American Journal of Science, 266(7), 515-541.

Schneiderhöhn, H. (1961) Ore deposits of the world. Volume II. Pegmatites. Gustav Fischer Verlag, Stuttgart

Shaw, R.A., Goodenough, K.M., Roberts, N.M.W., Horstwood, M.S.A., Chenery, S.R., Gunn, A.G., (2016). Petrogenesis of rare-metal pegmatites in high-grade metamorphic terranes: A case study from the Lewisian Gneiss Complex of northwest Scotland. Precambrian Research 281, pp. 338–362

Silva, D. (2014) Spatial analysis applied to the Barroso-Alvão rare-elements pegmatite field (Northern Portugal). Tese de Mestrado em Geomateriais e Recursos Geológicos, Faculdade de Ciências da Universidade do Porto

Simmons, W. and Webber, K. (2008) Pegmatite genesis: State of the art. European Journal of Mineralogy, 20(4), pp. 421-438

Simmons, W. *et al.*, (2012) Granitic Pegmatites as Sources of Colored Gemstones. Elements, 8, pp. 281-287

Simmons, W.B., Falster, A.U., Webber, K.L., Roda-Robles, E., Boudreaux, A.P., Grassi, L.R., Freeman, G., (2016). Bulk composition of Mt. Mica Pegmatite, Maine, USA: Implications for the origin of an LCT type pegmatite by anatexis. Canadian Mineralogist. 54, pp. 1053–1070

Sterba, J., Krzemień, A., Fernández, P. R., García-Miranda, C. E., & Valverde, G. F. (2019). Lithium mining: Accelerating the transition to sustainable energy. Resources Policy, 62, 416-426.

Thomas, R., & Davidson, P. (2013). The missing link between granites and granitic pegmatites. Journal of Geosciences, 58, pp. 183-200.

Thomas, R., & Davidson, P. (2014). Liquid immiscibility—important processes during pegmatite formation. In Pan-American Current Research on Fluid Inclusions (PACROFI-XII), p. 52.

Thomas, R., & Davidson, P. (2016). Revisiting complete miscibility between silicate melts and hydrous fluids, and the extreme enrichment of some elements in the supercritical state—Consequences for the formation of pegmatites and ore deposits. Ore Geology Reviews, 72, pp. 1088-1101.

Thomas, R., Davidson, P., & Beurlen, H. (2012). The competing models for the origin and internal evolution of granitic pegmatites in the light of melt and fluid inclusion research. Mineralogy and Petrology, 106, pp. 55-73.

Tischendorf G (1977) Geochemical and petrographic characteristics of silicic magmatic rocks associated with rare-element mineralization. In Stemprok M, Burnol L, Tischendorf G (eds) Metallization associated with acid magmatism, 2. Geol Surv Prague, Prague, p 41-96

Tischendorf, G., Gottesmann, B., Förster, H. J., & Trumbull, R. B. (1997). On Li-bearing micas: estimating Li from electron microprobe analyses and an improved diagram for graphical representation. Mineralogical Magazine, 61(409), 809-834.

Warr, L. N. (2021). IMA–CNMNC approved mineral symbols. Mineralogical Magazine, 85(3), 291-320.

Wise, M. A., Müller, A., & Simmons, W. B. (2022). A proposed new mineralogical classification system for granitic pegmatites. The Canadian Mineralogist, 60, pp. 229-248.

Wood, S. A., & Williams-Jones, A. E. (1993). Theoretical studies of the alteration of spodumene, petalite, eucryptite and pollucite in granitic pegmatites: exchange reactions with alkali feldspars. Contributions to Mineralogy and Petrology, 114(2), 255-263.

Appendix

I. MACROSCOPIC DESCRIPTION

I.I Alarc #1

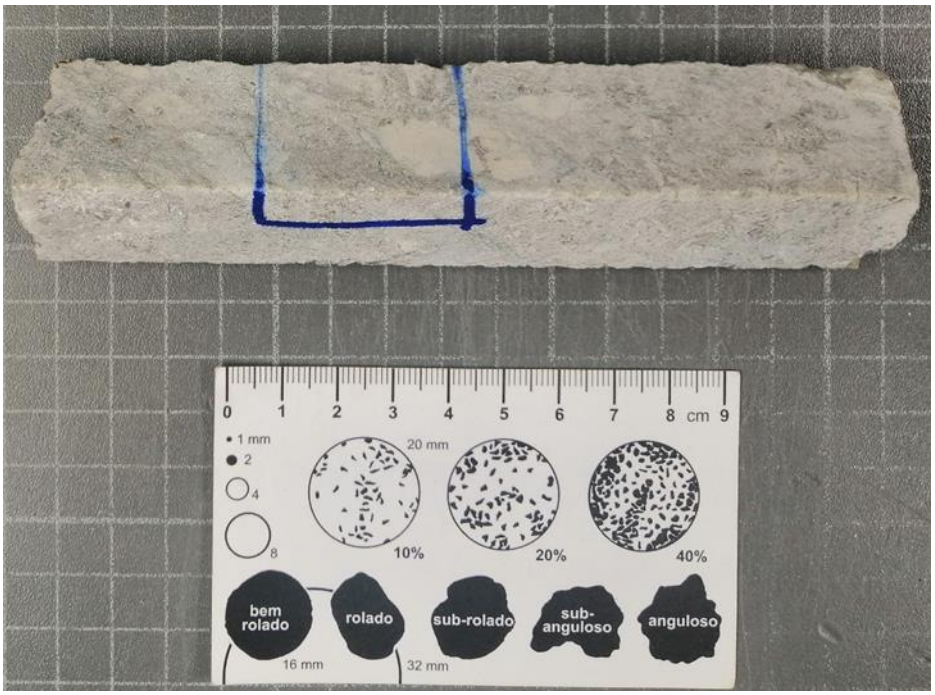

Grey coloured pegmatitic sample, presenting 3 distinct grain sizes (thin, medium, and coarse) as well as greenish alteration patches. Sample's main mineralogy is mica, quartz, feldspar, an unidentified black mineral which appears in small crystals and some spodumene. Feldspar presents a blocky texture and appears to be altered by a greyish mass, especially evident on the grain borders. Mica appears in 2 colours, green and white, and in 2 different morphologies with both massive blocky crystals and elongated needle like crystals. Also is remarkable the presence of ferruginous dots most likely representative of late-stage iron oxides or even consequence of the drilling process. The fractures in the samples seem to be filled with both white and green mica.

I.II Alarc #2

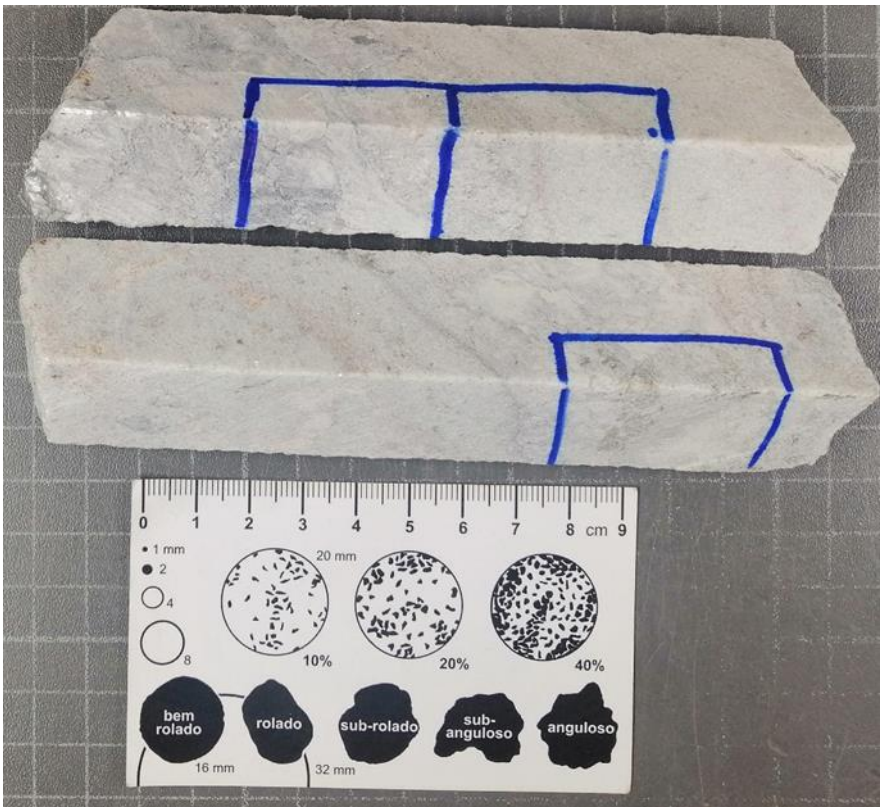

This sample is split in two blocks, one of the sectors presents a layering with a quartz mass at top followed by a mica layer another quartz layer and the typical pegmatitic mass. This first sector is characterized by what appears to be some reaction halos between each layer. Some breccification processes are evident, with the veinlets resulting from this process being filled with quartz. From a mineralogical standpoint it's remarkable the presence of blocky feldspar, as well as the absence of recognizable spodumene. The second sector presents a mineralogy composed of feldspar, quartz, and mica. The former appears in a blocky texture with a pinkish colour and in some cases greyish colour. The feldspar also seems to be crossed by dark veinlets of unknown composition. The mica in this sector presents a greenish tint more evident than in any other sample. As in the previous samples the ferruginous dots most likely represent late-stage iron oxides or might even be consequence of the drilling process.

I.III Alarc #3

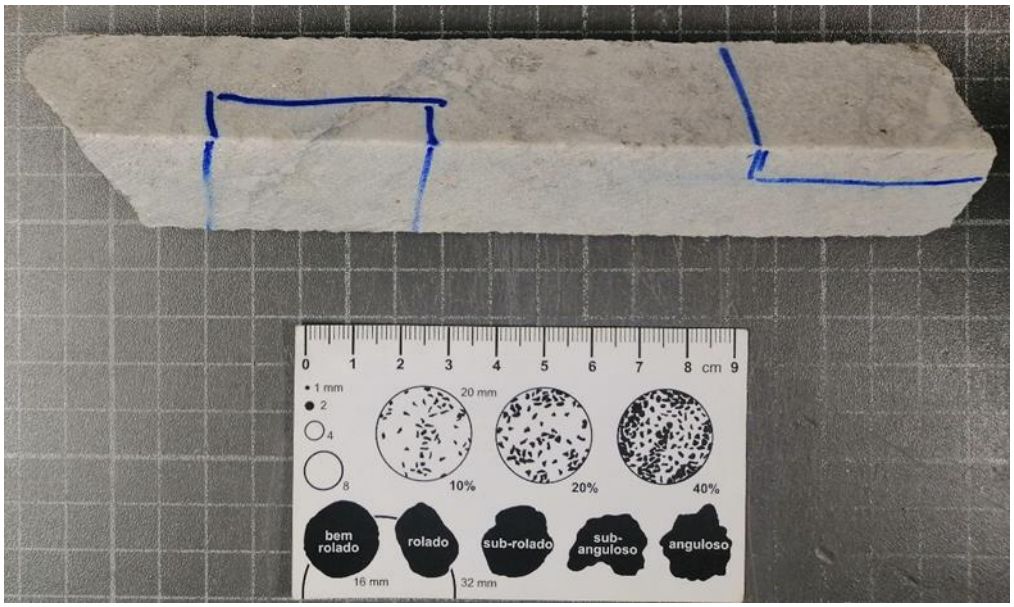

Greyish coloured sample showing a quasi-aplitic matrix with occasionally blocky feldspar, although smaller than usual, when compared with the other samples. The mineral assemblage is dominated by quartz, mica, and feldspar with small crystals of an unidentified black mineral. This sample shows no presence of alteration whatsoever. It is important to emphasize the presence of small "pockets" filled with a material similar to the matrix, as well document the existence brown layers.

I.IV Alarc #4

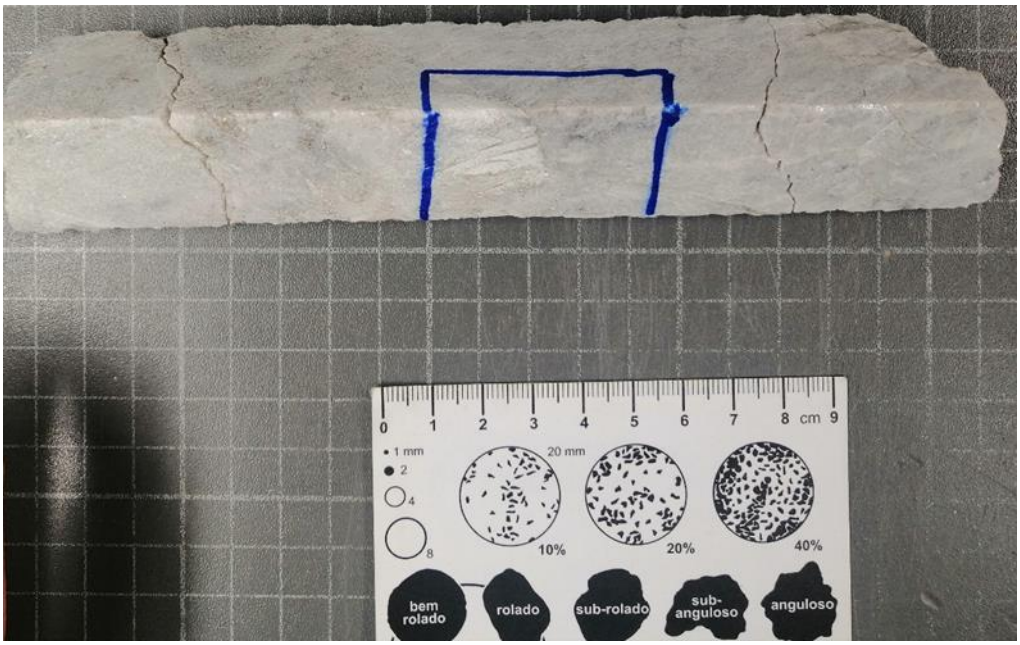

Grey colored sample with pegmatitic texture. The mineral assemblage is dominated by quartz, mica, feldspar and some spodumene. The contact between spodumene and feldspar grains seems to be marked by a greyish mass, possibly micaceous in nature, a similar effect appears to occur in the contact between quartz and mica grains, however it is less evident than in the former pair of minerals. Part of the sample seems to preserve some evidence for breccification processes, marked by anastomosed quartz

rich veins. Throughout the sample is evident the presence of thin veinlets composed by an unidentified dark mineral as well as the presence of a pervasive greenish alteration.

I.V Alarc #5

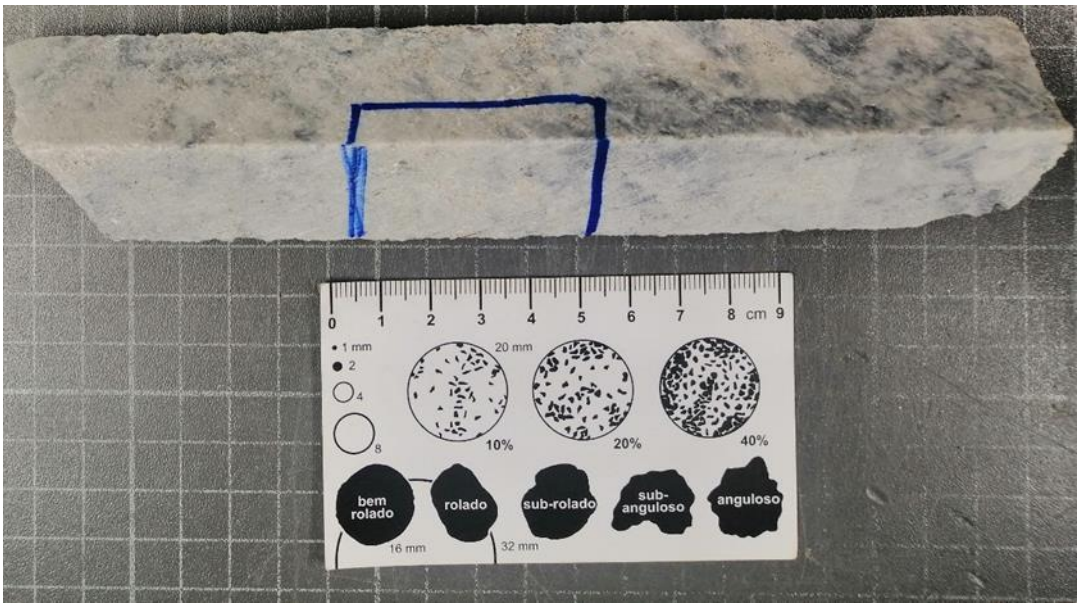

Grey and black sample with pegmatitic texture. Mineralogic assemblage is dominated by quartz, white-mica, dark-mica, feldspar and abundant spodumene. Feldspar appears in both a blocky texture, with these crystals being often intruded by brownish veinlets very contrasting with its white color, and as thin crystals this mineral is also affected by a greenish alteration.

I.VI Alarc #6

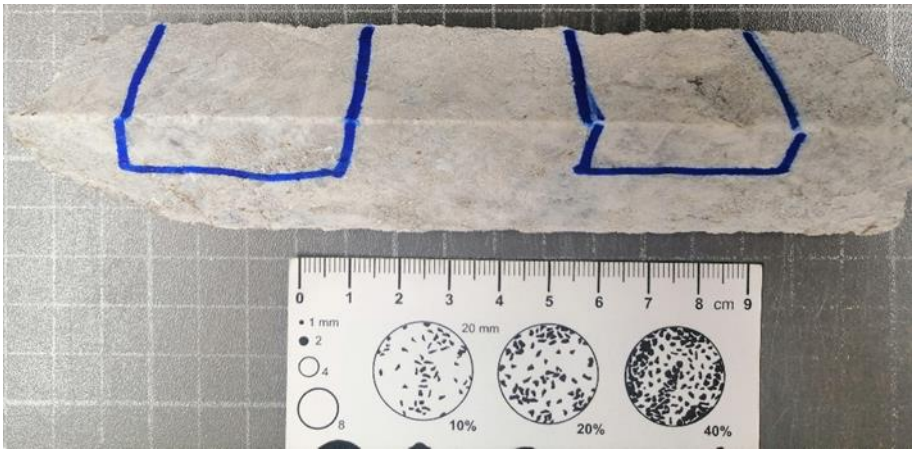

Grey and white sample with pegmatitic texture. The mineralogic assemblage is dominated by quartz, white-mica, feldspar and abundant spodumene. Feldspar appears both in a blocky feldspar texture mostly white in color and as a thin crystal. The sample shows evidence of breccification processes. There are some dispersed veinlets filled with small sized mica. The sample also shows masses comprised of mica with variable sizes. The latter ones contact directly with the pegmatitic matrix, but the contact does not appear reactive.

I.VII Alarc #7

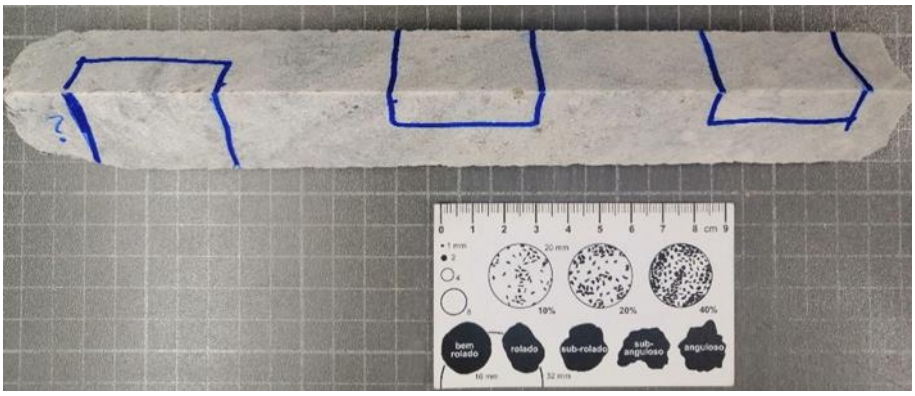

Greyish sample with pegmatitic texture. The mineralogical assemblage is dominated by quartz, white-mica, feldspar, spodumene and unidentified black crystals. The matrix in this sample presents two different colors, this contrast is more evident with a wet sample, the contacts between the different colored zones are reasonably thought of as possible metasomatic fronts. Feldspar appears once again in a blocky texture as well as thin crystals, with the former crystals being somewhat weathered. Spodumene appears as long, thin crystals usually disperse, with the occasional presence of some clusters. The central thin section position contains in itself what appears to be a full reaction zone.

I.VIII Alarc #8

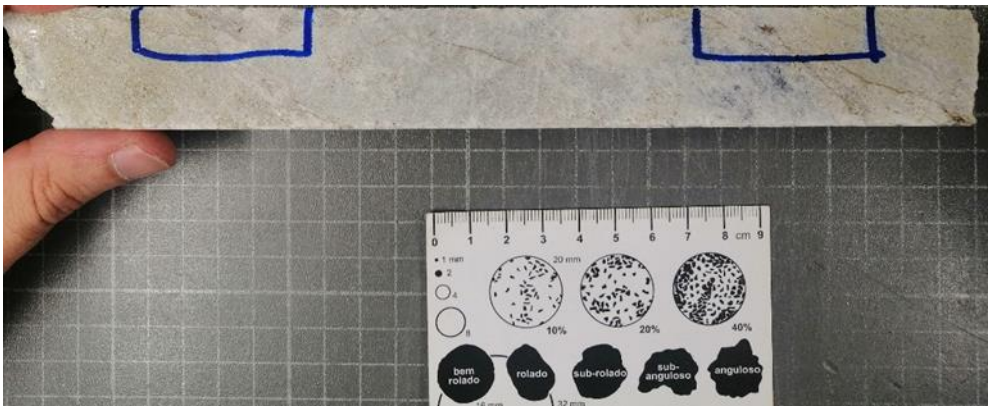

Grey sample of aplitic texture. The mineralogic assemblage is dominated by quartz, white-mica, feldspar, an unknown dark colored mineral as well as spodumene. The feldspar appears once again in rare blocky texture as well as in thin crystals included in the sample matrix. The blocky feldspar presents visible fractures filled with quartz and a brownish mass of unknown composition. The largest crystals of spodumene are found in this sample reaching sizes of up to 6 cm in length. In this sample mica aggregates of considerable size are fairly abundant and seem to be associated with alteration processes. Sample presents possible reaction boundaries specially in contacts between quartz and dark aggregates. On the reference side of the sample there's a visible mica-band which seems to react with the matrix.

I.IX Alarc #9

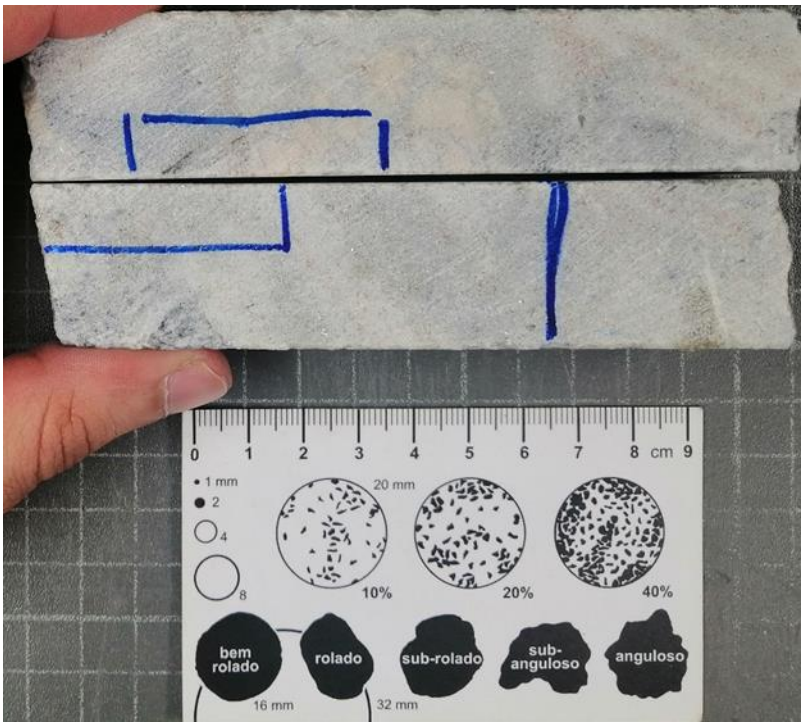

Grey and black sample of pegmatite-aplite texture, divided in two sectors. The first sector presents a quasi-aplitic texture and the mineralogic assemblage is dominated by quartz, feldspar, black crystals of unknown composition and white mica. This sector presents mica masses which seem to react with the matrix turning it into a yellowish matrix. The sample seems to be layered with orange and white bands visible in a wet sample. It is also important to mention the widespread ferruginous dots present in this sector, possibly iron oxides, or result of the drilling process. The second sector presents a pegmatitic texture with the mineralogic assemblage being dominated by quartz, feldspar, dark and white mica, spodumene and what appears to be iron oxide minerals. The feldspar appears in a blocky texture pink in color and seems to react with quartz resulting in a greenish mass. The iron oxide minerals seem to be associated with blocky feldspar appearing in the boundaries of feldspar crystals.

I.X Alarc #10

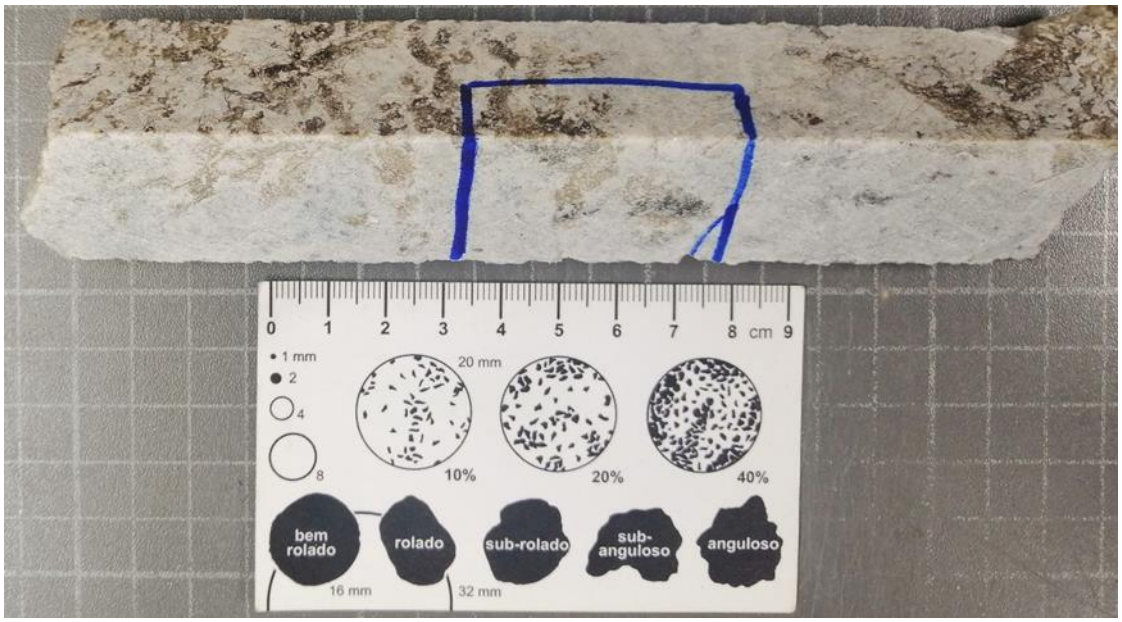

Grey sample with aplitic texture, with one of the sides covered in deep brown alteration. The mineralogy of this sample is dominated by quartz, feldspar, mica, and a dark mineral of unknown composition. The feldspar presents itself as thin crystals. Quartz is plenty abundant in this sample. The brown alteration seems to fill veinlets and seem to react with quartz.

I.XI Alarc #11

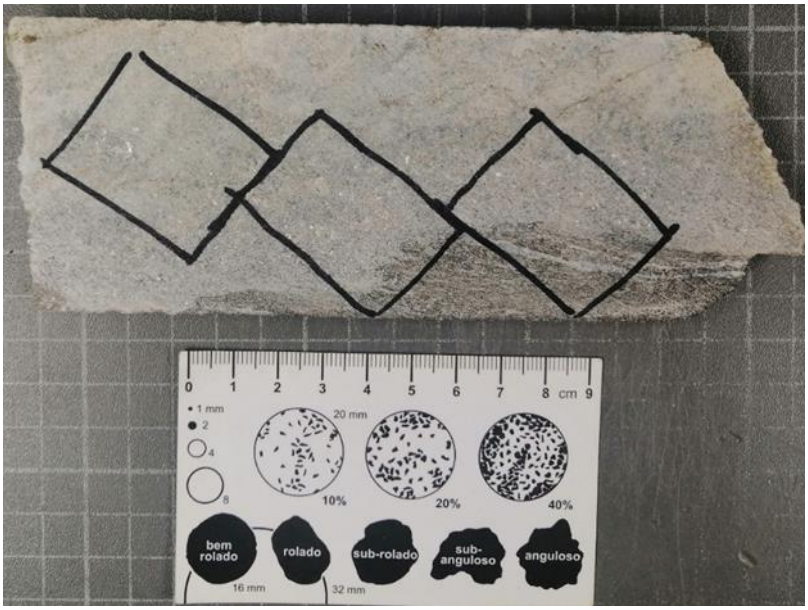

Grey and Black sample with aplitic texture. This sample seems to be comprised by 3 different layers. One layer, black in color presenting some sort of foliation resembling a schist with a recognizable mineralogy of only dark mica. The second layer in the center comprised mostly of homogenous mica. Finally, the third layer is comprised of the normal matrix (feldspar, quartz, and mica). The boundaries between these layers seem sharp and reactive. The position of this sample in the drilling hole, as well as the features it presents, point towards a contact sample between pegmatite and host rock, with presence of metasomatic alteration resulting of that contact.

I.XII Alarc #12

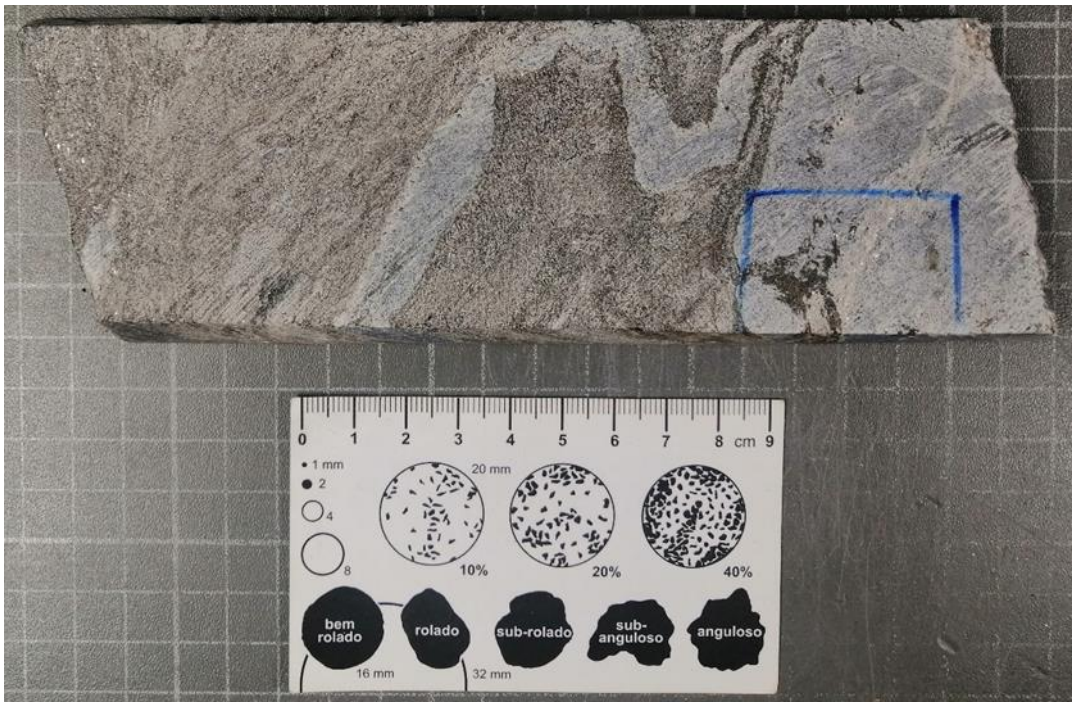

Dark colored sample resembling a mica schist, it's a fine-grained sample loaded with what seems to be either metasomatic haloes or anatectic haloes seeing that the texture suggests the presence of neosomes. The mineral assemblage is dominated by mica both dark and white in color, with the former being considerably less abundant than the latter. Besides mica there's the presence of some small greenish crystals.

I.XIII Alarc #13

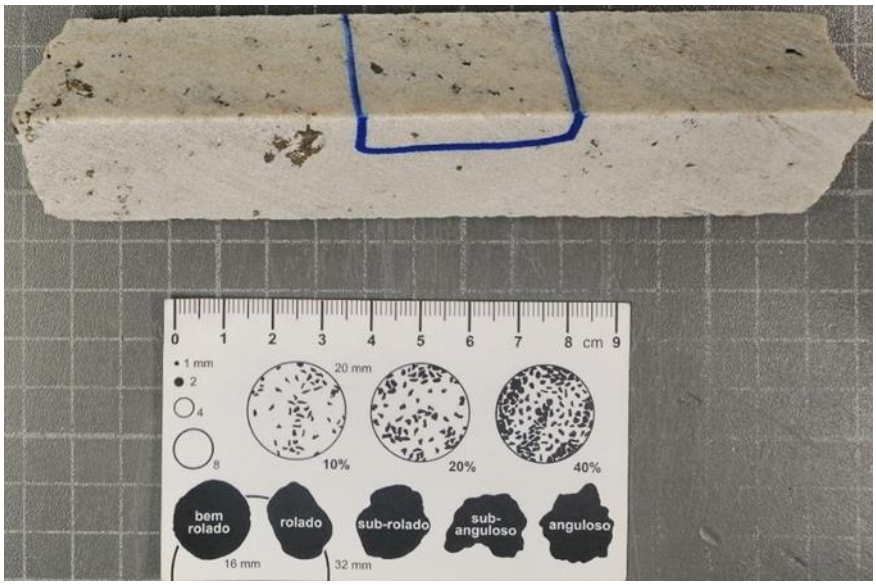

White sample presenting a quasi-aplitic texture. The sample presents some intense brown alteration although it seems superficial. The mineralogic assemblage is dominated by the typical matrix of pegmatites, that is, quartz, feldspar, mica and some rare spodumene crystals. This sample also presents the layering between orange and white bands.

I.XIV Alarc #14

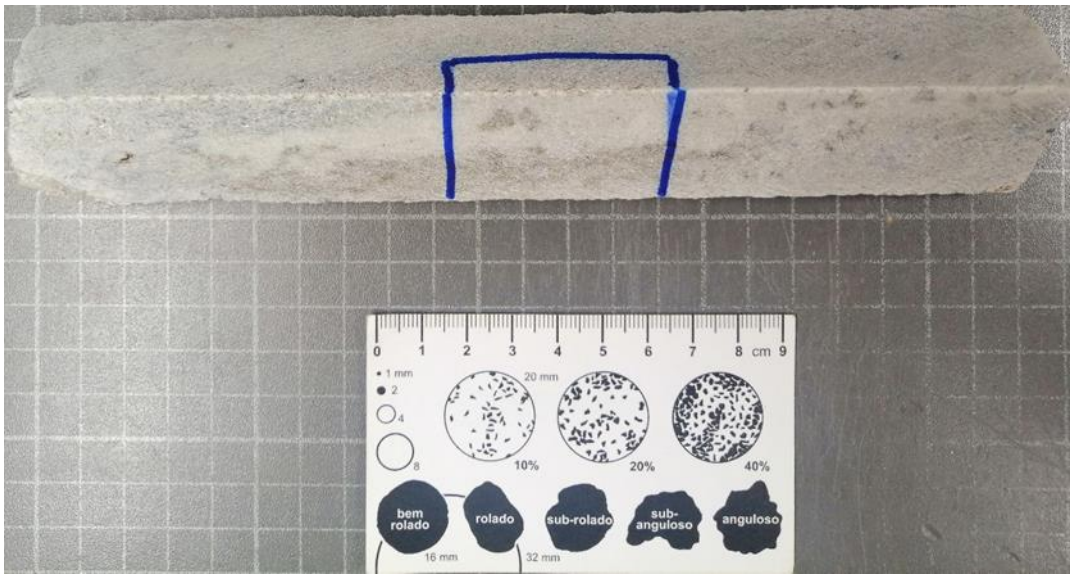

White and grey sample of mostly aplitic texture. The mineralogic assemblage is dominated by quartz, feldspar, mica, and an unknown black mineral. Despite being a unique piece, the sample can be divided in 3 sides. The first side, where we find the reference, shows a clear contact between a micaceous band and the normal matrix. The other two sides of the sample are quite distinct, one of the sides (the one with no thin section scheduled) presents a very homogenous aplitic texture with very thin mica grains, this side also seems to show some grain orientation. The second side shows the same aplitic texture, however more heterogenous with mica varying in size, adding to that this side seems to have reaction zones as well as some alteration.

I.XV Alarc #15

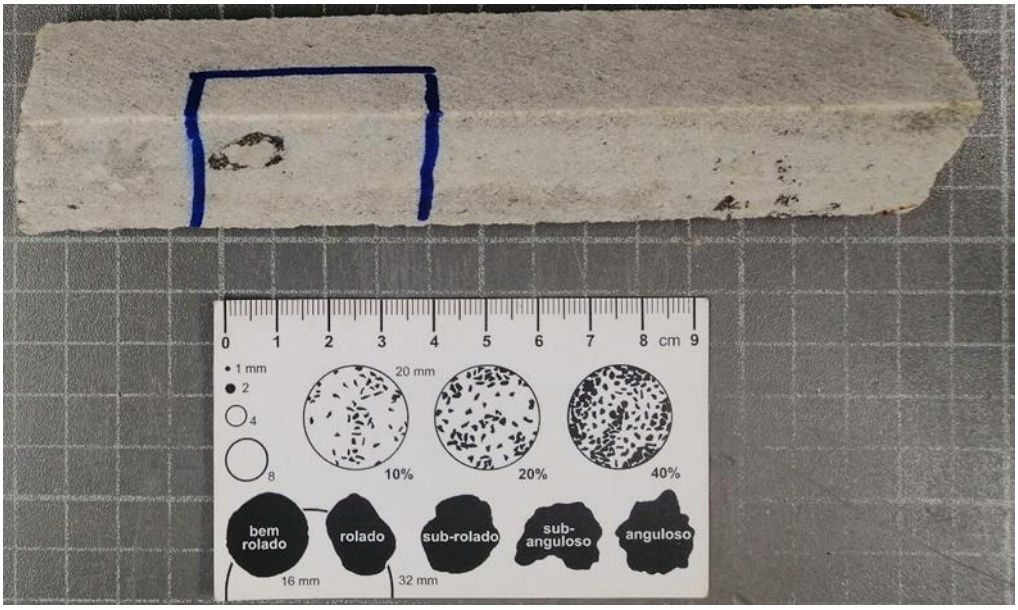

White sample of variable texture although some patches seem to escape this definition. The mineralogic assemblage of this sample is dominated by quartz, feldspar, and mica. The feldspar presents itself in both blocky texture as well as in thin crystals in the matrix. There seems to be a clear boundary between a homogenous vein and another vein of unknown nature.

I.XVI Alarc #16

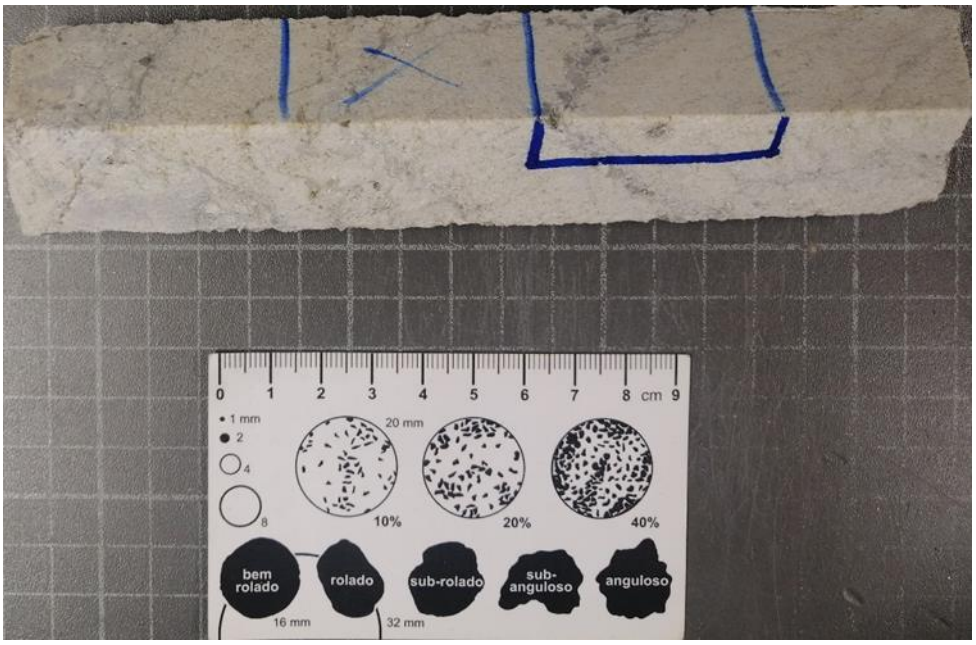

White and black sample with aplitic texture. The main mineralogy of this sample is quartz, feldspar mica, spodumene and an unknown black mineral. The sample seems to present slight breccification with the opening of some veins. Associated to those veins there's the formation of mica and of some blackish alteration. The veins are filled with quartz and mica. Above the written reference there seems to exist a "honeycomb" pattern. In this sample is once again possible to observe the presence of white and orange bands alternating between themselves.

I.XVII Alarc #17

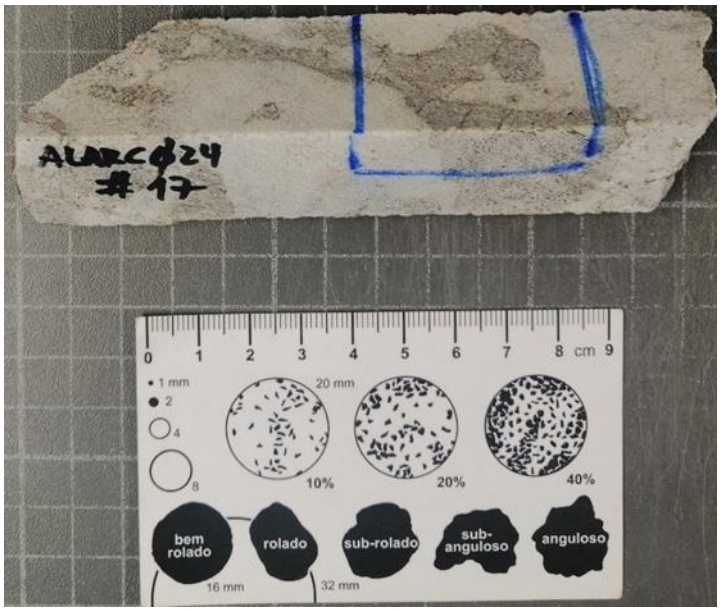

White and black colored sample of pegmatitic texture. The main mineralogy of this sample is quartz, feldspar (both in blocky and matrix textures), mica and the only spodumene found is of little dimension and/or cannot be confirmed as spodumene. The main characteristic of this sample is the

brownish/blackish alteration patches present. The alteration patches seem to be filled with late-stage mica and quartz and seem to be limited by small irradiating fractures.

I.XVIII Alarc #18

Grey and Brown sample, resembling a mica schist. It's a fine-grained sample loaded with what seems to be either metasomatic haloes or anatexis haloes seeing that the texture suggests the presence of neosomes. The sample's mineralogy is dominated by quartz and mica, with the latter appearing both as white mica and dark mica. The sample's main characteristic is the sigmoidal openings filled with a mixture of mica quartz and an unidentified green mineral. The sample also presents multiple micaceous bands.

I.XIX Alarc #19

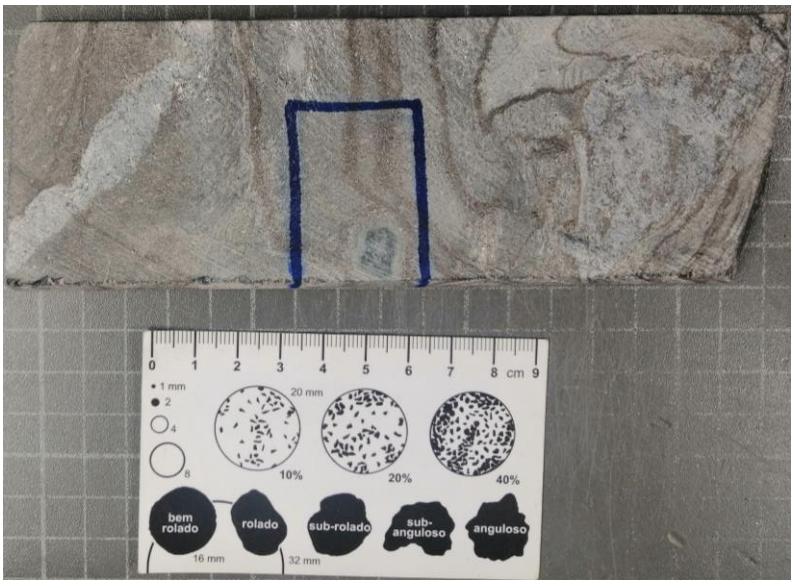

Grey and Brown sample, resembling a mica schist. It's a fine-grained sample loaded with what seems to be either metasomatic haloes or anatexis haloes seeing that the texture suggests the presence of neosomes. The sample's mineralogy is dominated by quartz and mica with the latter appearing both as white mica and dark mica. It is also important to denote the presence of dark red spots, perhaps garnet. The sample's main characteristic is the presence of fluence folding filled with mica. Also, in this sample it's possible to observe the presence of quartz rich veinlets as well as a green unidentified mineral, most likely chlorite.

II. MINERAL CHEMISTRY

II.I Analytical Conditions and detection limits

In order to characterize the different mineral phases twelve analytical profiles were used in the EMPA analyses.

Analytical Profile 1				Detection limits (ppm)
Element	**Emission Line**	**Detector Crystal**	**Standard name**	**Spodumene**
Al	Ka	TAP	Spodumene	100
Ba	La	PETJ	Benitoite	334
Ca	Ka	PETJ	Diopside	111
Cr	Ka	PETJ	Chromium Oxide	160
F	Ka	TAP	Fluorite	572
Fe	Ka	LIFH	Almandine	154
K	Ka	PETH	Sanidine	51
Mg	Ka	TAP	Diopside	97
Mn	Ka	PETJ	Bustamite	202
Na	Ka	TAP	Jadeite	93
Ni	Ka	LIF	Nickel Silicide	281
P	Ka	TAP	Apatite	119
Rb	La	PETH	Cal-STD	446
Si	Ka	PETH	Diopside	101
Sr	La	PETJ	Celestite	392
Ti	Ka	PETJ	Rutile	174
V	Ka	LIFH	V	135
Zn	Ka	LIF	Sphalerite	479

Analytical profile 2				Detection limits (ppm)	
Element	**Emission Line**	**Detector Crystal**	**Standard name**	**Plagioclase**	**K-feldspar**
Al	Ka	TAP	Sanidine	157	163
Ba	La	PETJ	Benitoite	548	578
Ca	Ka	PETJ	Diopside	185	203
Cs	La	PETJ	Pollucite	460	411
Fe	Ka	LIFH	Almandine	252	256
K	Ka	PETH	Sanidine	82	92
Mg	Ka	TAP	Olivine	144	152
Mn	Ka	PETJ	Bustamite	331	349
Na	Ka	TAP	Tugtupite	249	179
P	Ka	TAP	Apatite	194	200
Rb	La	PETH	Cal-STD	739	762
Si	Ka	PETH	Sanidine	176	195
Sr	La	PETJ	Celestite	737	776
Ti	Ka	PETJ	Rutile	292	297
Zn	Ka	LIF	Willemite	723	757

Analytical Profile 3				Detection limits (ppm)		
Element	**Emission Line**	**Detector Crystal**	**Standard name**	**Muscovite**	**Biotite**	**Beryl**
Al	Ka	TAP	Almandine	119	115	115
Ba	La	LIFH	Barite	301	326	286
Ca	Ka	PETJ	Diopside	118	133	112
Cl	Ka	PETJ	Tugtupite	85	91	79
Co	Ka	LIFH	Skutterudite	149	162	142
Cr	Ka	PETJ	Chromium Oxide	167	179	158
Cs	La	PETJ	Pollucite	298	399	278
F	Ka	TAP	Fluorite	565	700	532
Fe	Ka	LIFH	Kaersutite	168	190	162
Ga	La	TAP	Ga	185	176	184
Ge	La	TAP	Ge	234	994	160
K	Ka	PETH	Sanidine	55	59	50
Mg	Ka	TAP	Chlorite	103	96	96
Mn	Ka	PETJ	Bustamite	211	230	199
Na	Ka	TAP	Jadeite	98	93	95
Nb	La	TAP	Nb	217	233	208
Ni	Ka	LIF	Nickel Silicide	327	363	307
Pb	Ma	PETJ	Galena	330	371	310
Rb	La	PETH	Cal-STD	407	372	453
Sc	Ka	PETH	Cal-STD	290	313	93
Si	Ka	PETJ	Almandine	236	219	232
Sn	La	PETH	Cassiterite	158	177	142
Sr	La	PETJ	Celestite	383	391	408
Ta	La	LIF	LiTa03	871	946	820
Ti	Ka	PETJ	Rutile	185	199	178
Zn	Ka	LIF	Willemite	460	502	432

Analytical profile 4				Detection limits (ppm)
Element	**Emission Line**	**Detector Crystal**	**Standard name**	**Garnet**
Al	Ka	TAP	Pyrope	118
Ca	Ka	PETJ	Bustamite	142
Cr	Ka	PETJ	Chromium Oxide	197
F	Ka	TAP	Apatite	787
Fe	Ka	LIFH	Almandine	202
Mg	Ka	TAP	Pyrope	112
Mn	Ka	PETJ	Bustamite	322
Si	Ka	PETH	Almandine	114
Sn	La	PETJ	Cassiterite	316
Ti	Ka	PETJ	Rutile	213
Y	La	PETH	Yttrium phosphate	223
Zr	La	PETJ	Zirconia	372

Analytical Profile 5				Detection limits (ppm)
Element	**Emission Line**	**Detector Crystal**	**Standard name**	**Tourmaline**
Ag	La	PETH	Ag	104
Al	Ka	TAP	Pyrope	112
Ba	La	PETJ	Benitoite	349
Ca	Ka	PETJ	Diopside	117
Ce	La	LIFH	CeP5O14	270
Cl	Ka	PETJ	Tugtupite	87
Co	Ka	LIFH	Skutterudite	154
Cr	Ka	PETJ	Chromium Oxide	168
Cs	La	PETJ	Pollucite	323
Cu	Ka	PETH	Cuprite	0
Eu	La	PETJ	EuP5O14	850
F	Ka	TAP	Apatite	678
Fe	Ka	LIFH	Almandine	163
Ga	La	TAP	Ga	218
Gd	La	LIF	GdP5O14	674
K	Ka	PETJ	Sanidine	107
La	La	PETJ	Mcnazite	315
Mg	Ka	TAP	Olivine	93
Mn	Ka	PETJ	Bustamite	214
Na	Ka	TAP	Jadeite	101
Nb	La	TAP	Nb	216
Nd	La	LIFH	NdP5O14	295
Ni	Ka	LIFH	Nickel Silicide	185
Pb	Ma	PETJ	Galena	346
Pr	La	PETJ	PrP5O14	327
Rb	Rb	TAP	Cal-STD	151
S	Ka	PETJ	Stibnite	175
Sc	Ka	PETJ	Sc	138
Si	Ka	TAP	Diopside	106
Sm	La	LIFH	GdP5O14	351
Sn	La	PETJ	Cassiterite	264
Sr	La	PETJ	Celestite	352
Ta	La	LIFH	LiTa03	566
Ti	Ka	PETJ	Rutile	186
U	Ma	PETJ	UO2	333
V	Ka	LIF	V	338
W	La	LIFH	W	532
Y	La	PETJ	Yttrium phosphate	411
Zn	Ka	LIFH	Willemite	303
Zr	La	PETJ	Zr	406

Analytical Profile 6 - Phosphates short				Detection limits (ppm)	
Element	**Emission Line**	**Detector Crystal**	**Standard Name**	**Apatite**	**Heterosite-purpurite**
Al	Ka	TAP	Plagioclase	324	529
As	La	TAP	Boron Nitride	1178	1851
Ba	La	PETH	Benitoite	1326	2232
Ca	Ka	PETH	Apatite	231	368
Ce	La	LIF	Monazite	6640	8788
Cl	Ka	PETJ	Tugtupite	499	653
F	Ka	TAP	Apatite	3841	3814
Fe	Ka	LIFH	Almandine	633	977
La	La	PETJ	Monazite	1083	1998
Mg	Ka	TAP	Periclase	291	496
Mn	Ka	PETJ	Bustamite	742	1966
Na	Ka	TAP	Jadeite	409	716
Nd	La	PETJ	NdP5O14	1194	2063
P	Ka	PETH	Apatite	495	891
Sr	La	PETJ	Celestite	2513	4592
Zr	La	PETH	Zirconia	1134	1476

Analytical Profile 7 - Phosphates long + Columbite-Tantalite				Detection limits (ppm)						
Element	**Emission Line**	**Detector Crystal**	**Standard Name**	**Apatite**	**Ambligonite-Montebrasite**	**Lithiophilite-Triphylite**	**Heterosite-purpurite**	**Fairfieldite-Messelite**	**Ludlamite**	**Columbite-Tantalite**
Al	Ka	TAP	Almandine	387	587	358	526	560	275	232
As	La	TAP	Galium Arsenide	1204	1880	963	1942	1869	833	760
Ba	La	PETJ	Benitoite	1357	1933	1330	2373	2122	1127	914
Ca	Ka	PETJ	Diopside	463	742	430	432	795	359	288
Ce	La	LIF	Monazite	7503	13697	6624	9981	12125	3324	2424
Cl	Ka	PETJ	Tugtupite	471	738	390	673	729	331	210
Dy	Lb	LIF	DyP5O14	6095	8574	6297	14484	8610	4993	4065
Er	La	LIFH	ErP5O14	1775	2072	1608	2514	2410	1386	1268
Eu	La	LIFH	EuP5O14	1350	2434	1464	1578	2016	1084	977
F	Ka	TAP	Apatite	4292	7783	3848	6088	6990	3552	1966
Fe	Ka	LIFH	Almandine	643	975	625	993	968	522	455
Gd	La	LIF	GdP5O14	3345	6325	3331	8250	5850	2290	1991
Hf	La	LIF	Hf	2788	4306	2756	5821	4600	2102	1949
Ho	La	LIF	HoP5O14	3326	5740	3537	6202	5654	2704	2026
K	Ka	PETH	Sanidine	216	308	212	369	296	168	135
La	La	PETJ	Monazite	1186	1859	1265	1943	1913	1047	853
Lu	La	LIF	LuP5O14	4188	5219	3587	6857	5887	3085	2691
Mg	Ka	TAP	Pyrope	354	531	349	494	587	244	222
Mn	Ka	PETJ	Bustamite	790	1049	882	1813	1123	673	657
Na	Ka	TAP	Jadeite	444	688	398	804	551	275	225
Nb	La	PETJ	LiNbO3	2257	3727	2078	3273	3541	1437	1056
Nd	La	LIF	REE 6	3441	6308	3522	3223	5813	1688	1822
P	Ka	TAP	Apatite	597	880	538	922	848	437	582
Pa	Ma	PETJ	Cal-STD	1705	2199	2821	4726	3492	2710	1222
Pb	Ma	PETH	Galena	811	1217	711	884	1174	588	494
Pr	Lb	LIFH	Monazite	2179	3065	2175	4219	3685	1971	1617
S	Ka	PETJ	Stibnite	928	1733	963	1621	1682	668	459
Si	Ka	TAP	Diopside	407	590	390	628	572	292	287
Sm	La	LIFH	SmP5O14	1369	1952	1364	2087	2093	1048	1015
Sr	La	TAP	Celestite	1024	959	602	3674	939	479	499
Ta	La	LIF	LiTa03	3928	4900	3578	4634	5592	2722	2585
Tb	La	LIF	TbP5O14	3840	5522	3805	6585	6080	2376	19721
Th	Ma	PETH	Monazite	854	1070	775	1534	1197	650	507
Ti	Ka	PETJ	Benitoite	679	1084	670	1213	1077	548	510
Tm	La	LIF	TmP5O14	3599	5464	3426	4619	5212	2304	2299
U	Ma	PETH	UO2	639	860	586	919	938	495	393
V	Ka	LIFH	V	612	983	566	675	744	451	403
Y	La	TAP	Y3Al5O12	748	1073	609	1220	1051	513	423
Yb	La	LIF	YbP5O14	3680	6151	3549	7844	6237	3074	2539
Zr	La	TAP	Zirconia	962	1177	842	1425	1322	684	524

Analytical profile 8				Detection limits (ppm)
Element	**Risca**	**Detector Crystal**	**Standard name**	**Ilmenite**
Ag	La	PETJ	Ag Metal	261
Al	Ka	TAP	Plagioclase	95
As	La	TAP	Galium Arsenide	336
Au	Ma	PETH	Au Metal	233
Ba	La	LIFH	Benitoite	443
Bi	Ma	PETJ	Bismuth Selenide	616
Ca	Ka	PETJ	Diopside	156
Co	Ka	LIF	Skutterudite	309
Cr	Ka	LIFH	Chromium Oxide	192
Cu	Ka	LIFH	Cuprite	306
Fe	Ka	LIFH	Haematite	207
Ga	La	TAP	Ga Metal	183
Hf	La	LIF	Hf Metal	897
K	Ka	PETJ	Sanidine	141
Mg	Ka	TAP	Periclase	83
Mn	Ka	PETJ	Rhodonite	279
Na	Ka	TAP	Jadeite	97
Nb	La	TAP	Nb	290
Ni	Ka	LIFH	Nickel Silicide	250
P	Ka	PETJ	Apatite	261
Pb	Ma	PETJ	Galena	431
S	Ka	PETJ	Stibnite	229
Sb	La	PETH	Stibnite	210
Sc	Ka	PETH	Sc	100
Si	Ka	TAP	Diopside	125
Sn	La	PETJ	Cassiterite	336
Sr	La	PETJ	Celestite	420
Ta	La	LIF	LiTa03	1164
Ti	Ka	PETJ	Rutile	250
U	Ma	PETJ	UO2	404
V	Ka	LIFH	V metal	193
W	La	LIF	W	1147
Y	La	PETJ	Yttrium phosphate	409
Zn	Ka	LIF	Willemite	640
Zr	La	TAP	Zirconia	261

Analytical profile 9				Detection limits (ppm)		
Element	**Risca**	**Detector Crystal**	**Standard name**	**Pyrite**	**Arsenopyrite**	**Sphalerite**
Ag	La	PETJ	Ag	243	286	266
As	La	TAP	Galium Arsenide	253	395	213
Au	Ma	PETH	Au	242	241	246
Bi	Ma	PETJ	Bismuth Selenide	813	690	771
Cd	La	PETJ	Cd	273	298	273
Co	Ka	LIFH	Skutterudite	170	197	190
Cu	Ka	LIFH	Cuprite	253	302	293
Fe	Ka	LIFH	Pyrite	176	199	188
Ga	La	TAP	Ga	161	209	209
Ge	La	TAP	Ge	138	206	134
In	La	PETJ	In	383	432	391
Mn	Ka	PETJ	Bustamite	241	274	263
Mo	La	PETH	Molybdenite	177	172	169
Ni	Ka	LIF	Pentlandite	336	371	365
Pb	Ma	PETJ	Galena	594	509	549
S	Ka	PETH	Pyrite	55	53	55
Sb	La	PETJ	Stibnite	307	343	315
Se	La	TAP	Bismuth Selenide	167	251	153
Sn	La	PETJ	Sn	276	319	281
Te	La	PETJ	Te	270	308	300
W	La	LIF	W	960	614	915
Zn	Ka	LIF	Sphalerite	572	699	655

II.II Mineral chemistry Tables

The following tables represent the analytical data of EMPA, corresponding to each analysed mineral. The tables contain the EMPA data (in wt%) and the respective stoichiometric distributions (in *a.p.f.u*) for elements above the respective detection limit. Elements whiich are present in the analytical profiles of each mineral. that are not included in mineral chemistry tables are elements which appear consistently under the detection limit.

II.II.I SPODUMENE

Sample	#1B1				#1B2		#1B3						#1B4								#1B5		#1B6		#2cB1							#2cB2
Observations	Anhedral						Euhedral																		Anhedral							
Zone	Pegmatite 1																															
wt%	1	2	3	4	1	2	1	2	3	4	5	6	1	2	3	4	5	6	7	8	1	2	1	2	1	2	3	4	5	6	7	1
SiO_2	64.28	64.13	63.63	64.49	64.23	64.50	62.87	63.37	62.80	63.41	63.13	63.41	63.85	64.24	64.24	64.24	63.16	64.02	63.32	63.23	63.84	63.89	63.29	63.61	62.57	64.22	63.66	64.11	64.50	62.83	64.47	65.07
Al_2O_3	28.28	28.26	27.50	27.63	27.83	27.85	26.44	26.44	27.30	26.88	27.34	27.50	27.94	27.97	27.55	27.61	27.48	27.36	27.76	27.20	27.49	27.64	27.22	27.27	27.61	27.53	27.44	27.83	27.81	27.27	27.81	28.26
Fe_2O_3	0.00	0.00	0.00	0.00	0.00	0.00	0.24	0.24	0.00	0.20	0.00	0.00	0.00	0.00	0.02	0.00	0.00	0.01	0.00	0.05	0.00	0.00	0.00	0.13	0.00	0.00	0.05	0.00	0.00	0.00	0.00	0.00
Mn_2O_3	0.00	0.00	0.00	0.00	0.00	0.00	0.01	0.00	0.00	0.00	0.00	0.00	0.00	0.00	0.00	0.00	0.00	0.00	0.00	0.00	0.00	0.00	0.00	0.00	0.00	0.00	0.00	0.00	0.00	0.00	0.00	0.00
ZnO	0.04	0.00	0.11	0.00	0.01	0.00	0.00	0.00	0.10	0.08	0.00	0.05	0.01	0.00	0.00	0.10	0.00	0.00	0.00	0.00	0.06	0.00	0.00	0.04	0.05	0.09	0.05	0.06	0.01	0.05	0.09	0.00
FeO	0.19	0.19	0.39	0.18	0.25	0.25	0.00	0.00	0.19	0.02	0.19	0.29	0.29	0.29	0.29	0.20	0.21	0.21	0.20	0.18	0.31	0.31	0.39	0.29	0.09	0.14	0.36	0.28	0.21	0.15	0.17	0.18
MnO	0.02	0.07	0.01	0.02	0.01	0.03	0.00	0.00	0.04	0.03	0.01	0.07	0.00	0.04	0.02	0.05	0.00	0.00	0.01	0.01	0.00	0.00	0.00	0.02	0.03	0.03	0.03	0.00	0.06	0.05	0.05	0.00
CaO	0.01	0.01	0.00	0.00	0.00	0.01	0.02	0.03	0.02	0.00	0.01	0.01	0.02	0.00	0.00	0.01	0.02	0.00	0.02	0.18	0.01	0.00	0.00	0.02	0.01	0.01	0.01	0.01	0.02	0.03	0.00	0.01
K2O	0.00	0.01	0.01	0.01	0.01	0.02	0.00	0.01	0.01	0.02	0.02	0.01	0.01	0.01	0.00	0.00	0.01	0.01	0.03	0.00	0.01	0.01	0.01	0.01	0.02	0.05	0.03	0.04	0.01	0.09	0.01	0.01
Na_2O	0.07	0.08	0.09	0.07	0.07	0.06	0.07	0.04	0.07	0.08	0.07	0.07	0.08	0.07	0.08	0.07	0.09	0.06	0.09	0.06	0.08	0.07	0.06	0.08	0.10	0.09	0.14	0.08	0.09	0.26	0.09	0.06
Li_2O*	8.16	8.14	7.81	7.99	8.01	8.01	7.76	7.77	7.83	7.83	7.88	7.86	8.02	8.04	7.91	7.93	7.92	7.90	8.00	7.78	7.86	7.95	7.80	7.83	7.96	7.92	7.79	7.96	7.98	7.72	7.99	8.18
Total	101.06	100.87	99.56	100.38	100.42	100.72	97.41	97.92	98.35	98.55	98.64	99.27	100.22	100.64	100.11	100.19	98.89	99.57	99.43	98.68	99.65	99.86	98.75	99.31	98.44	100.06	99.57	100.37	100.69	98.45	100.68	101.76
a.p.f.u. (calculus done on the basis of 6 oxygen)																																
Si^{4+}	1.974	1.974	1.986	1.992	1.985	1.988	2.001	2.006	1.983	1.996	1.986	1.984	1.978	1.982	1.992	1.990	1.982	1.994	1.977	1.989	1.990	1.986	1.990	1.990	1.973	1.992	1.988	1.984	1.989	1.984	1.988	1.984
Al^{3+}	0.026	0.026	0.014	0.008	0.015	0.012	0.000	0.000	0.017	0.004	0.014	0.016	0.022	0.019	0.008	0.010	0.018	0.006	0.023	0.011	0.010	0.014	0.010	0.010	0.027	0.009	0.012	0.016	0.011	0.017	0.012	0.016
Total-T	2.000	2.000	2.000	2.000	2.000	2.000	2.001	2.006	2.000	2.000	2.000	2.000	2.000	2.000	2.000	2.000	2.000	2.000	2.000	2.000	2.000	2.000	2.000	2.000	2.000	2.000	2.000	2.000	2.000	2.000	2.000	2.000
Fe^{3+}	0.000	0.000	0.000	0.000	0.000	0.000	0.006	0.006	0.000	0.005	0.000	0.000	0.000	0.000	0.000	0.000	0.000	0.000	0.000	0.001	0.000	0.000	0.000	0.003	0.000	0.000	0.001	0.000	0.000	0.000	0.000	0.000
Mn^{3+}	0.000	0.000	0.000	0.000	0.000	0.000	0.000	0.000	0.000	0.000	0.000	0.000	0.000	0.000	0.000	0.000	0.000	0.000	0.000	0.000	0.000	0.000	0.000	0.000	0.000	0.000	0.000	0.000	0.000	0.000	0.000	0.000
Al^{3+}	0.998	0.999	0.998	0.999	0.999	0.999	0.992	0.986	0.999	0.994	0.999	0.998	0.999	0.998	0.999	0.998	0.999	0.998	0.999	0.997	1.000	0.999	0.998	0.995	1.000	0.998	0.998	0.999	0.999	0.998	0.999	0.999
Zn^{2+}	0.001	0.000	0.003	0.000	0.000	0.000	0.000	0.000	0.002	0.002	0.000	0.001	0.000	0.000	0.000	0.002	0.000	0.000	0.000	0.000	0.001	0.000	0.000	0.001	0.001	0.002	0.001	0.001	0.000	0.001	0.002	0.000
Fe^{2+}	0.000	0.000	0.000	0.000	0.000	0.000	0.000	0.000	0.000	0.000	0.000	0.000	0.000	0.000	0.000	0.000	0.000	0.000	0.000	0.000	0.000	0.000	0.000	0.000	0.000	0.000	0.000	0.000	0.000	0.000	0.000	0.000
M1 Total	0.998	0.999	1.000	0.999	0.999	0.999	0.998	0.992	1.001	1.000	0.999	0.999	0.999	0.998	0.999	1.000	0.999	0.999	0.999	0.998	1.001	0.999	0.998	0.999	1.001	1.000	1.000	1.000	0.999	1.000	1.001	0.999
Fe^{2+}	0.005	0.005	0.010	0.004	0.006	0.006	0.000	0.000	0.005	0.001	0.005	0.008	0.007	0.008	0.007	0.005	0.006	0.005	0.005	0.005	0.008	0.008	0.010	0.008	0.003	0.004	0.009	0.007	0.006	0.004	0.004	0.005
Mn^{2+}	0.001	0.002	0.000	0.001	0.000	0.001	0.000	0.000	0.001	0.001	0.000	0.002	0.000	0.001	0.001	0.001	0.000	0.000	0.000	0.000	0.000	0.000	0.000	0.001	0.001	0.001	0.001	0.000	0.002	0.001	0.001	0.000
Ca^{2+}	0.000	0.000	0.000	0.000	0.000	0.000	0.001	0.001	0.001	0.000	0.000	0.000	0.001	0.000	0.000	0.000	0.001	0.000	0.001	0.006	0.000	0.000	0.000	0.001	0.000	0.000	0.001	0.000	0.001	0.001	0.000	0.000
K^{+}	0.000	0.000	0.000	0.000	0.001	0.001	0.000	0.000	0.001	0.001	0.001	0.000	0.000	0.000	0.000	0.000	0.000	0.000	0.001	0.000	0.000	0.000	0.000	0.000	0.001	0.002	0.001	0.002	0.000	0.004	0.000	0.000
Na^{+}	0.004	0.005	0.006	0.004	0.004	0.003	0.004	0.003	0.004	0.005	0.004	0.005	0.005	0.004	0.005	0.004	0.005	0.004	0.005	0.004	0.005	0.004	0.004	0.005	0.006	0.005	0.008	0.005	0.005	0.016	0.005	0.003
Li^{+}	1.008	1.007	0.981	0.993	0.996	0.993	0.993	0.989	0.995	0.991	0.997	0.989	0.999	0.997	0.987	0.988	0.999	0.990	1.004	0.985	0.986	0.993	0.986	0.985	1.010	0.988	0.978	0.991	0.990	0.980	0.990	1.003
M2 Total	1.018	1.019	0.997	1.002	1.007	1.004	0.998	0.993	1.006	0.998	1.008	1.003	1.012	1.010	1.000	0.998	1.011	0.999	1.017	0.999	0.999	1.006	1.000	0.999	1.020	1.000	0.998	1.005	1.003	1.006	1.002	1.011
Li wt%	3.79	3.78	3.63	3.71	3.72	3.72	3.61	3.61	3.64	3.64	3.66	3.65	3.72	3.73	3.68	3.68	3.68	3.67	3.72	3.62	3.65	3.69	3.62	3.64	3.70	3.68	3.62	3.70	3.71	3.59	3.71	3.80

Sample	#2cB2							#2cB3			#2cB4		#4B2						#4B3										#4B5			
Observations	Anhedral																												Euhedral			
Zone	Pegmatite 1																															
wt%	2	3	4	5	6	7	8	1	2	3	1	2	1	2	3	4	8	9	1	2	3	4	5	6	8	9	10	11	1	2	3	4
SiO_2	63.25	64.04	64.98	64.48	64.09	64.68	64.02	64.14	64.24	64.36	63.86	62.96	63.50	63.87	63.94	63.49	63.76	63.98	61.89	63.59	63.56	63.25	63.62	62.65	62.98	63.36	62.88	63.20	63.41	63.06	63.30	62.99
Al_2O_3	27.59	27.54	27.77	27.89	27.64	27.96	27.71	27.82	28.32	28.23	27.66	27.36	27.14	26.73	27.10	26.96	27.36	27.44	26.34	26.66	26.49	26.49	26.53	26.31	26.35	26.77	26.47	26.46	27.33	27.29	27.32	26.98
Fe_2O_3	0.00	0.00	0.01	0.00	0.00	0.00	0.00	0.00	0.00	0.00	0.00	0.00	0.10	0.22	0.18	0.07	0.00	0.00	0.23	0.28	0.61	0.24	0.28	0.22	0.25	0.23	0.38	0.34	0.00	0.00	0.00	0.02
Mn_2O_3	0.00	0.00	0.00	0.00	0.00	0.00	0.00	0.00	0.00	0.00	0.00	0.00	0.00	0.04	0.00	0.00	0.00	0.00	0.00	0.00	0.00	0.04	0.05	0.07	0.10	0.01	0.00	0.03	0.00	0.00	0.00	0.00
ZnO	0.02	0.00	0.06	0.09	0.00	0.06	0.12	0.00	0.00	0.04	0.01	0.00	0.00	0.03	0.00	0.00	0.04	0.00	0.00	0.02	0.06	0.01	0.01	0.00	0.00	0.00	0.03	0.00	0.00	0.02	0.01	0.00
FeO	0.14	0.21	0.07	0.25	0.31	0.13	0.26	0.14	0.15	0.24	0.13	0.08	0.24	0.00	0.08	0.05	0.23	0.20	0.18	0.00	0.00	0.00	0.00	0.00	0.00	0.00	0.01	0.00	0.14	0.25	0.35	0.23
MnO	0.03	0.06	0.08	0.02	0.02	0.08	0.01	0.05	0.02	0.03	0.00	0.03	0.02	0.00	0.02	0.00	0.05	0.01	0.03	0.00	0.00	0.00	0.00	0.00	0.00	0.00	0.01	0.00	0.03	0.01	0.06	0.04
CaO	0.00	0.01	0.02	0.00	0.01	0.00	0.02	0.01	0.00	0.01	0.00	0.04	0.00	0.01	0.01	0.02	0.00	0.00	0.03	0.01	0.00	0.00	0.01	0.02	0.02	0.04	0.01	0.01	0.03	0.01	0.01	0.00
K2O	0.01	0.00	0.01	0.00	0.02	0.00	0.01	0.01	0.00	0.01	0.02	0.06	0.02	0.03	0.02	0.01	0.05	0.01	0.09	0.00	0.00	0.01	0.01	0.01	0.03	0.01	0.04	0.03	0.02	0.01	0.05	0.01
Na_2O	0.10	0.04	0.06	0.08	0.14	0.06	0.12	0.07	0.05	0.05	0.09	0.19	0.07	0.04	0.05	0.02	0.07	0.06	0.14	0.06	0.10	0.05	0.05	0.07	0.05	0.08	0.08	0.08	0.08	0.07	0.09	0.09
Li_2O*	7.96	7.94	8.02	8.00	7.89	8.06	7.90	8.04	8.21	8.12	8.01	7.85	7.83	7.84	7.91	7.87	7.85	7.93	7.57	7.84	7.81	7.80	7.81	7.73	7.76	7.83	7.76	7.79	7.89	7.85	7.77	7.76
Total	99.10	99.83	101.07	100.81	100.11	101.02	100.17	100.29	101.00	101.08	99.78	98.57	98.91	98.80	99.30	98.50	99.42	99.62	96.50	98.46	98.63	97.89	98.38	97.08	97.53	98.32	97.65	97.93	98.92	98.57	98.95	98.11
a.p.f.u. (calculus done on the basis of 6 oxygen)																																
Si^{4+}	1.981	1.991	1.994	1.986	1.988	1.987	1.985	1.984	1.973	1.977	1.985	1.983	1.993	2.004	1.997	1.998	1.991	1.992	1.993	2.002	2.001	2.003	2.005	2.001	2.003	1.998	1.998	2.002	1.989	1.986	1.987	1.993
Al^{3+}	0.019	0.010	0.006	0.014	0.012	0.013	0.015	0.016	0.027	0.023	0.015	0.017	0.007	0.000	0.003	0.003	0.009	0.008	0.007	0.000	0.000	0.000	0.000	0.000	0.000	0.002	0.002	0.000	0.011	0.014	0.013	0.007
Total-T	2.000	2.000	2.000	2.000	2.000	2.000	2.000	2.000	2.000	2.000	2.000	2.000	2.000	2.004	2.000	2.000	2.000	2.000	2.000	2.002	2.001	2.003	2.005	2.001	2.003	2.000	2.000	2.002	2.000	2.000	2.000	2.000
Fe^{3+}	0.000	0.000	0.000	0.000	0.000	0.000	0.000	0.000	0.000	0.000	0.000	0.000	0.002	0.005	0.004	0.002	0.000	0.000	0.006	0.007	0.014	0.006	0.007	0.005	0.006	0.005	0.009	0.008	0.000	0.000	0.000	0.000
Mn^{3+}	0.000	0.000	0.000	0.000	0.000	0.000	0.000	0.000	0.000	0.000	0.000	0.000	0.000	0.001	0.000	0.000	0.000	0.000	0.000	0.000	0.000	0.001	0.001	0.002	0.002	0.000	0.000	0.001	0.000	0.000	0.000	0.000
Al^{3+}	0.999	0.999	0.998	0.999	0.998	1.000	0.998	0.999	0.999	1.000	0.999	0.998	0.997	0.989	0.995	0.997	0.998	0.999	0.993	0.989	0.983	0.989	0.985	0.990	0.987	0.993	0.990	0.988	0.999	0.999	0.999	0.999
Zn^{2+}	0.000	0.000	0.001	0.002	0.000	0.001	0.003	0.000	0.000	0.001	0.000	0.000	0.000	0.001	0.000	0.000	0.001	0.000	0.000	0.000	0.001	0.000	0.000	0.000	0.000	0.000	0.001	0.000	0.000	0.000	0.000	0.000
Fe^{2+}	0.000	0.000	0.000	0.000	0.000	0.000	0.000	0.000	0.000	0.000	0.000	0.000	0.000	0.000	0.000	0.000	0.000	0.000	0.000	0.000	0.000	0.000	0.000	0.000	0.000	0.000	0.000	0.000	0.000	0.000	0.000	0.000
M1 Total	0.999	0.999	1.000	1.001	0.998	1.001	1.001	0.999	0.999	1.000	0.999	0.998	0.999	0.995	0.999	0.999	0.999	0.999	0.999	0.996	0.999	0.996	0.993	0.997	0.996	0.999	0.999	0.997	0.999	0.999	0.999	0.999
Fe^{2+}	0.004	0.005	0.002	0.006	0.008	0.003	0.007	0.004	0.004	0.006	0.003	0.002	0.006	0.000	0.002	0.001	0.006	0.005	0.005	0.000	0.000	0.000	0.000	0.000	0.000	0.000	0.000	0.000	0.004	0.007	0.009	0.006
Mn^{2+}	0.001	0.002	0.002	0.001	0.000	0.002	0.000	0.001	0.001	0.001	0.000	0.001	0.000	0.000	0.000	0.000	0.001	0.000	0.001	0.000	0.000	0.000	0.000	0.000	0.000	0.000	0.000	0.000	0.001	0.000	0.002	0.001
Ca^{2+}	0.000	0.000	0.001	0.000	0.000	0.000	0.001	0.000	0.000	0.000	0.000	0.001	0.000	0.000	0.001	0.001	0.000	0.000	0.001	0.000	0.000	0.000	0.000	0.001	0.001	0.001	0.000	0.000	0.001	0.000	0.000	0.000
K^{+}	0.001	0.000	0.000	0.000	0.001	0.000	0.001	0.001	0.000	0.000	0.001	0.003	0.001	0.001	0.001	0.000	0.002	0.001	0.004	0.000	0.000	0.000	0.000	0.001	0.001	0.000	0.002	0.001	0.001	0.000	0.002	0.000
Na^{+}	0.006	0.002	0.003	0.005	0.009	0.003	0.007	0.004	0.003	0.003	0.006	0.012	0.004	0.003	0.003	0.001	0.004	0.003	0.009	0.004	0.006	0.003	0.003	0.005	0.003	0.005	0.005	0.005	0.005	0.004	0.006	0.006
Li^{+}	1.003	0.993	0.990	0.991	0.984	0.996	0.985	1.000	1.014	1.003	1.002	0.994	0.988	0.990	0.993	0.996	0.986	0.993	0.981	0.992	0.989	0.993	0.990	0.992	0.992	0.993	0.992	0.992	0.995	0.995	0.982	0.987
M2 Total	1.014	1.002	0.998	1.003	1.002	1.005	1.000	1.010	1.022	1.014	1.011	1.013	1.000	0.993	1.000	0.999	0.999	1.002	1.000	0.997	0.996	0.997	0.994	0.998	0.997	0.999	0.999	0.998	1.006	1.006	1.000	1.000
Li wt%	3.70	3.69	3.73	3.72	3.66	3.74	3.67	3.73	3.81	3.77	3.72	3.65	3.64	3.64	3.67	3.66	3.65	3.68	3.52	3.64	3.63	3.62	3.63	3.59	3.61	3.64	3.61	3.62	3.66	3.65	3.61	3.60

Sample	#4B5					#4B7							#4B8							#4B10				#5B1							#7aB1	
Observations	Euhedral																														Anhedral	
Zone	Pegmatite 1																															
wt%	5	6	7	8	9	1	2	3	4	5	6	7	1	2	3	4	5	6	7	2	3	4	5	1	2	3	4	5	6	7	1	2
SiO_2	63.00	63.28	63.05	63.19	63.04	63.44	63.80	63.47	63.74	63.56	63.89	63.03	63.45	64.59	64.04	63.51	63.69	62.61	63.30	63.32	63.20	63.83	64.38	62.16	63.84	64.15	63.74	64.16	63.87	63.94	64.21	64.27
Al_2O_3	27.05	27.30	27.03	27.18	26.95	27.26	27.23	27.38	27.00	27.18	27.20	26.94	27.26	27.70	27.26	27.26	27.55	26.51	27.52	27.26	26.66	27.26	27.49	27.69	27.78	27.55	27.93	27.86	27.80	27.66	27.93	27.77
Fe_2O_3	0.00	0.00	0.00	0.00	0.02	0.00	0.06	0.00	0.19	0.11	0.03	0.00	0.00	0.00	0.06	0.00	0.00	0.26	0.00	0.00	0.27	0.01	0.00	0.00	0.00	0.08	0.00	0.00	0.00	0.00	0.00	0.00
Mn_2O_3	0.00	0.00	0.00	0.00	0.00	0.00	0.00	0.00	0.00	0.00	0.00	0.00	0.00	0.00	0.00	0.00	0.00	0.03	0.00	0.00	0.02	0.00	0.00	0.00	0.00	0.00	0.00	0.00	0.00	0.00	0.00	0.00
ZnO	0.00	0.00	0.05	0.00	0.00	0.00	0.09	0.00	0.00	0.08	0.01	0.02	0.03	0.00	0.01	0.00	0.00	0.07	0.01	0.00	0.05	0.00	0.07	0.06	0.00	0.00	0.00	0.03	0.04	0.08	0.04	0.04
FeO	0.16	0.12	0.15	0.20	0.22	0.24	0.09	0.15	0.08	0.15	0.14	0.17	0.23	0.22	0.10	0.15	0.23	0.00	0.18	0.15	0.00	0.20	0.07	0.35	0.26	0.38	0.18	0.42	0.19	0.24	0.08	0.11
MnO	0.04	0.02	0.03	0.00	0.00	0.05	0.04	0.05	0.02	0.06	0.00	0.00	0.00	0.03	0.02	0.00	0.03	0.02	0.02	0.00	0.00	0.03	0.03	0.02	0.02	0.00	0.06	0.04	0.06	0.00	0.04	0.00
CaO	0.00	0.01	0.02	0.00	0.00	0.00	0.02	0.00	0.00	0.01	0.00	0.00	0.02	0.00	0.00	0.00	0.01	0.00	0.02	0.01	0.01	0.00	0.00	0.03	0.03	0.00	0.02	0.03	0.00	0.00	0.03	0.02
K2O	0.02	0.01	0.02	0.01	0.01	0.02	0.02	0.01	0.04	0.01	0.01	0.02	0.02	0.02	0.00	0.02	0.02	0.03	0.02	0.02	0.06	0.01	0.01	0.02	0.02	0.03	0.01	0.01	0.01	0.01	0.01	0.01
Na_2O	0.08	0.07	0.07	0.07	0.07	0.06	0.06	0.10	0.09	0.10	0.05	0.07	0.10	0.08	0.06	0.09	0.08	0.10	0.04	0.10	0.12	0.13	0.10	0.09	0.08	0.09	0.10	0.12	0.05	0.08	0.06	0.08
Li_2O*	7.80	7.91	7.78	7.86	7.77	7.84	7.86	7.89	7.86	7.82	7.90	7.78	7.84	7.97	7.92	7.89	7.92	7.71	7.95	7.87	7.77	7.85	7.94	7.89	7.97	7.88	8.03	7.89	8.02	7.94	8.07	8.04
Total	98.14	98.72	98.19	98.51	98.08	98.90	99.28	99.05	99.01	99.08	99.23	98.03	98.94	100.60	99.48	98.91	99.52	97.34	99.04	98.73	98.16	99.32	100.08	98.29	100.01	100.15	100.06	100.55	100.02	99.95	100.48	100.34
a.p.f.u. (calculus done on the basis of 6 oxygen)																																
Si^{4+}	1.991	1.988	1.993	1.990	1.994	1.990	1.994	1.988	1.997	1.992	1.996	1.994	1.990	1.992	1.996	1.991	1.986	1.996	1.983	1.989	1.998	1.994	1.995	1.966	1.982	1.990	1.977	1.984	1.982	1.986	1.983	1.987
Al^{3+}	0.009	0.012	0.008	0.010	0.006	0.010	0.006	0.012	0.003	0.008	0.004	0.006	0.010	0.008	0.004	0.009	0.014	0.004	0.017	0.011	0.002	0.006	0.005	0.034	0.019	0.010	0.023	0.016	0.019	0.014	0.017	0.013
Total-T	2.000	2.000	2.000	2.000	2.000	2.000	2.000	2.000	2.000	2.000	2.000	2.000	2.000	2.000	2.000	2.000	2.000	2.000	2.000	2.000	2.000	2.000	2.000	2.000	2.000	2.000	2.000	2.000	2.000	2.000	2.000	2.000
Fe^{3+}	0.000	0.000	0.000	0.000	0.000	0.000	0.001	0.000	0.004	0.003	0.001	0.000	0.000	0.000	0.002	0.000	0.000	0.006	0.000	0.000	0.006	0.000	0.000	0.000	0.000	0.002	0.000	0.000	0.000	0.000	0.000	0.000
Mn^{3+}	0.000	0.000	0.000	0.000	0.000	0.000	0.000	0.000	0.000	0.000	0.000	0.000	0.000	0.000	0.000	0.000	0.000	0.001	0.000	0.000	0.000	0.000	0.000	0.000	0.000	0.000	0.000	0.000	0.000	0.000	0.000	0.000
Al^{3+}	0.999	0.999	0.999	0.999	0.999	0.998	0.997	0.998	0.994	0.996	0.998	0.999	0.998	0.998	0.998	0.998	0.999	0.992	0.999	0.999	0.992	0.997	0.999	0.998	0.998	0.997	0.998	1.000	0.998	0.999	0.999	0.998
Zn^{2+}	0.000	0.000	0.001	0.000	0.000	0.000	0.002	0.000	0.000	0.002	0.000	0.000	0.001	0.000	0.000	0.000	0.000	0.002	0.000	0.000	0.001	0.000	0.002	0.001	0.000	0.000	0.000	0.001	0.001	0.002	0.001	0.001
Fe^{2+}	0.000	0.000	0.000	0.000	0.000	0.000	0.000	0.000	0.000	0.000	0.000	0.000	0.000	0.000	0.000	0.000	0.000	0.000	0.000	0.000	0.000	0.000	0.000	0.000	0.000	0.000	0.000	0.000	0.000	0.000	0.000	0.000
M1 Total	0.999	0.999	1.000	0.999	0.999	0.999	1.000	0.998	0.998	1.001	0.999	0.999	0.998	0.999	0.999	0.998	0.999	1.001	0.999	0.999	0.999	0.998	1.001	0.999	0.998	1.000	0.998	1.000	0.999	1.001	1.000	0.999
Fe^{2+}	0.004	0.003	0.004	0.005	0.006	0.006	0.002	0.004	0.002	0.004	0.004	0.004	0.006	0.005	0.003	0.004	0.006	0.000	0.004	0.004	0.000	0.005	0.002	0.009	0.007	0.010	0.005	0.011	0.005	0.006	0.002	0.003
Mn^{2+}	0.001	0.001	0.001	0.000	0.000	0.001	0.001	0.001	0.001	0.002	0.000	0.000	0.000	0.001	0.001	0.000	0.001	0.001	0.000	0.000	0.000	0.001	0.001	0.000	0.001	0.000	0.002	0.001	0.001	0.000	0.001	0.000
Ca^{2+}	0.000	0.000	0.001	0.000	0.000	0.000	0.001	0.000	0.000	0.000	0.000	0.000	0.001	0.000	0.000	0.000	0.000	0.000	0.001	0.000	0.000	0.000	0.000	0.001	0.001	0.000	0.001	0.001	0.000	0.000	0.001	0.001
K^{+}	0.001	0.000	0.001	0.000	0.001	0.001	0.001	0.001	0.002	0.000	0.001	0.001	0.001	0.001	0.000	0.001	0.001	0.001	0.001	0.001	0.003	0.000	0.000	0.001	0.001	0.001	0.000	0.000	0.000	0.000	0.001	0.000
Na^{+}	0.005	0.004	0.004	0.004	0.005	0.003	0.004	0.006	0.005	0.006	0.003	0.004	0.006	0.005	0.004	0.005	0.005	0.006	0.003	0.006	0.008	0.008	0.006	0.006	0.005	0.005	0.006	0.007	0.003	0.005	0.004	0.005
Li^{+}	0.992	1.000	0.989	0.995	0.989	0.989	0.988	0.994	0.990	0.986	0.993	0.990	0.989	0.988	0.992	0.995	0.994	0.989	1.002	0.995	0.988	0.986	0.989	1.003	0.995	0.983	1.002	0.982	1.000	0.992	1.003	0.999
M2 Total	1.002	1.008	0.999	1.005	1.000	1.001	0.997	1.006	0.999	0.998	1.000	1.000	1.002	1.000	0.999	1.005	1.006	0.996	1.011	1.006	0.998	1.000	0.998	1.020	1.009	0.999	1.015	1.002	1.010	1.004	1.011	1.008
Li wt%	3.62	3.67	3.62	3.65	3.61	3.64	3.65	3.67	3.65	3.63	3.67	3.62	3.64	3.70	3.68	3.67	3.68	3.58	3.69	3.66	3.61	3.65	3.69	3.66	3.70	3.66	3.73	3.67	3.72	3.69	3.75	3.73

Sample	#7aB1			#7aB2						#7aB3			#7aB4					#7aB5				#7bB1										#7bB2
Observations	Anhedral			Euhedral						Anhedral			Euhedral					Anhedral														
Zone	Pegmatite 1																															
wt%	3	4	6	1	2	3	4	5	6	1	2	3	1	2	4	5	6	1	2	3	5	1	2	3	4	5	6	7	8	9	10	1
SiO_2	63.78	63.29	63.80	63.57	63.79	62.97	62.60	63.41	63.30	63.08	63.24	61.84	63.41	63.61	62.43	63.44	63.32	63.53	63.13	63.01	63.53	64.17	64.36	64.43	63.94	63.55	63.90	64.29	63.89	63.78	63.60	63.97
Al_2O_3	26.72	25.87	26.84	27.42	27.65	27.52	27.07	27.16	27.80	27.41	27.86	26.83	28.11	27.81	27.59	27.99	27.44	27.73	27.55	27.36	27.30	27.75	27.75	27.39	27.54	27.34	27.44	27.61	27.54	27.38	27.00	27.76
Fe_2O_3	0.12	0.27	0.10	0.00	0.00	0.00	0.00	0.00	0.00	0.00	0.00	0.00	0.00	0.00	0.00	0.00	0.00	0.00	0.00	0.00	0.00	0.00	0.00	0.15	0.00	0.00	0.00	0.00	0.00	0.00	0.07	0.00
Mn_2O_3	0.01	0.02	0.06	0.00	0.00	0.00	0.00	0.00	0.00	0.00	0.00	0.00	0.00	0.00	0.00	0.00	0.00	0.00	0.00	0.00	0.00	0.00	0.00	0.00	0.00	0.00	0.00	0.00	0.00	0.00	0.00	0.00
ZnO	0.05	0.04	0.00	0.08	0.02	0.01	0.06	0.07	0.00	0.00	0.00	0.07	0.00	0.09	0.03	0.04	0.01	0.05	0.00	0.09	0.09	0.00	0.00	0.13	0.00	0.00	0.01	0.01	0.00	0.00	0.05	0.00
FeO	0.00	0.00	0.00	0.24	0.08	0.04	0.26	0.09	0.07	0.11	0.05	0.14	0.07	0.08	0.10	0.12	0.09	0.15	0.12	0.19	0.18	0.14	0.13	0.06	0.14	0.12	0.12	0.13	0.17	0.13	0.03	0.19
MnO	0.00	0.00	0.00	0.01	0.03	0.06	0.05	0.01	0.00	0.01	0.01	0.03	0.03	0.02	0.03	0.01	0.03	0.00	0.05	0.02	0.00	0.00	0.01	0.00	0.03	0.05	0.02	0.07	0.00	0.03	0.00	0.00
CaO	0.01	0.00	0.03	0.02	0.00	0.02	0.03	0.00	0.00	0.03	0.02	0.09	0.00	0.01	0.03	0.02	0.00	0.00	0.00	0.02	0.00	0.00	0.00	0.00	0.00	0.00	0.00	0.00	0.03	0.01	0.00	0.00
K2O	0.01	0.00	0.01	0.00	0.01	0.01	0.03	0.01	0.01	0.01	0.01	0.10	0.00	0.00	0.02	0.01	0.00	0.00	0.01	0.00	0.01	0.00	0.00	0.00	0.01	0.00	0.01	0.01	0.01	0.01	0.01	0.00
Na_2O	0.07	0.08	0.07	0.07	0.09	0.04	0.09	0.09	0.06	0.10	0.11	0.15	0.06	0.07	0.07	0.10	0.07	0.06	0.07	0.07	0.05	0.09	0.07	0.10	0.06	0.07	0.06	0.05	0.07	0.10	0.07	0.07
Li_2O*	7.80	7.59	7.85	7.85	8.02	8.00	7.71	7.85	8.09	7.92	8.07	7.53	8.18	8.04	7.98	8.09	7.94	8.02	7.97	7.86	7.88	8.04	8.05	7.94	7.97	7.92	7.96	7.99	7.96	7.91	7.86	8.03
Total	98.58	97.17	98.75	99.28	99.68	98.68	97.91	98.70	99.33	98.67	99.38	96.78	99.85	99.72	98.27	99.81	98.90	99.55	98.90	98.61	99.03	100.19	100.38	100.19	99.70	99.06	99.51	100.16	99.66	99.34	98.70	100.02
a.p.f.u. (calculus done on the basis of 6 oxygen)																																
Si^{4+}	2.005	2.019	2.003	1.988	1.984	1.979	1.987	1.993	1.976	1.984	1.974	1.984	1.970	1.979	1.972	1.973	1.986	1.980	1.980	1.984	1.990	1.987	1.988	1.995	1.989	1.989	1.991	1.991	1.988	1.991	1.998	1.985
Al^{3+}	0.000	0.000	0.000	0.012	0.016	0.021	0.013	0.007	0.024	0.017	0.026	0.016	0.031	0.021	0.028	0.028	0.014	0.020	0.020	0.016	0.010	0.013	0.013	0.005	0.011	0.011	0.009	0.009	0.012	0.009	0.002	0.016
Total-T	2.005	2.019	2.003	2.000	2.000	2.000	2.000	2.000	2.000	2.000	2.000	2.000	2.000	2.000	2.000	2.000	2.000	2.000	2.000	2.000	2.000	2.000	2.000	2.000	2.000	2.000	2.000	2.000	2.000	2.000	2.000	2.000
Fe^{3+}	0.003	0.007	0.002	0.000	0.000	0.000	0.000	0.000	0.000	0.000	0.000	0.000	0.000	0.000	0.000	0.000	0.000	0.000	0.000	0.000	0.000	0.000	0.000	0.003	0.000	0.000	0.000	0.000	0.000	0.000	0.002	0.000
Mn^{3+}	0.000	0.001	0.001	0.000	0.000	0.000	0.000	0.000	0.000	0.000	0.000	0.000	0.000	0.000	0.000	0.000	0.000	0.000	0.000	0.000	0.000	0.000	0.000	0.000	0.000	0.000	0.000	0.000	0.000	0.000	0.000	0.000
Al^{3+}	0.990	0.972	0.993	0.999	0.998	0.998	0.999	0.999	0.999	0.999	0.999	0.998	0.998	0.999	0.999	0.998	1.000	0.999	0.999	0.999	0.998	0.999	0.998	0.995	0.998	0.998	0.999	0.999	0.998	0.999	0.997	0.999
Zn^{2+}	0.001	0.001	0.000	0.002	0.000	0.000	0.001	0.002	0.000	0.000	0.000	0.002	0.000	0.002	0.001	0.001	0.000	0.001	0.000	0.002	0.002	0.000	0.000	0.003	0.000	0.000	0.000	0.000	0.000	0.000	0.001	0.000
Fe^{2+}	0.000	0.000	0.000	0.000	0.000	0.000	0.000	0.000	0.000	0.000	0.000	0.000	0.000	0.000	0.000	0.000	0.000	0.000	0.000	0.000	0.000	0.000	0.001	0.000	0.000	0.000	0.000	0.000	0.000	0.000	0.000	0.000
M1 Total	0.994	0.980	0.996	1.001	0.998	0.998	1.000	1.001	0.999	0.999	0.999	1.000	0.999	1.001	0.999	0.999	1.000	1.000	0.999	1.001	1.000	0.999	0.998	1.001	0.999	0.998	0.999	0.999	0.998	0.999	1.000	0.999
Fe^{2+}	0.000	0.000	0.000	0.006	0.002	0.001	0.007	0.002	0.002	0.003	0.001	0.004	0.002	0.002	0.003	0.003	0.002	0.004	0.003	0.005	0.005	0.004	0.003	0.002	0.003	0.003	0.003	0.003	0.004	0.003	0.001	0.005
Mn^{2+}	0.000	0.000	0.000	0.000	0.001	0.002	0.001	0.000	0.000	0.000	0.000	0.001	0.001	0.001	0.001	0.000	0.001	0.000	0.001	0.001	0.000	0.000	0.000	0.000	0.001	0.001	0.001	0.002	0.000	0.001	0.000	0.000
Ca^{2+}	0.000	0.000	0.001	0.001	0.000	0.001	0.001	0.000	0.000	0.001	0.001	0.003	0.000	0.000	0.001	0.001	0.000	0.000	0.000	0.001	0.000	0.000	0.000	0.000	0.000	0.000	0.000	0.000	0.001	0.000	0.000	0.000
K^{+}	0.000	0.000	0.001	0.000	0.000	0.000	0.001	0.000	0.000	0.000	0.000	0.004	0.000	0.000	0.001	0.000	0.000	0.000	0.000	0.000	0.000	0.000	0.000	0.000	0.001	0.000	0.000	0.000	0.000	0.000	0.000	0.000
Na^{+}	0.004	0.005	0.004	0.004	0.006	0.003	0.006	0.006	0.004	0.006	0.007	0.009	0.003	0.004	0.004	0.006	0.005	0.004	0.004	0.004	0.003	0.005	0.004	0.006	0.003	0.005	0.004	0.003	0.004	0.006	0.004	0.004
Li^{+}	0.986	0.973	0.991	0.988	1.003	1.011	0.985	0.992	1.016	1.001	1.013	0.971	1.022	1.006	1.013	1.011	1.002	1.005	1.006	0.995	0.993	1.001	1.000	0.989	0.997	0.997	0.997	0.995	0.997	0.993	0.993	1.001
M2 Total	0.991	0.979	0.996	1.000	1.012	1.017	1.001	1.001	1.022	1.012	1.023	0.992	1.028	1.013	1.022	1.021	1.009	1.013	1.015	1.006	1.001	1.010	1.008	0.997	1.005	1.006	1.005	1.003	1.006	1.004	0.999	1.011
Li wt%	3.62	3.52	3.65	3.65	3.73	3.72	3.58	3.65	3.76	3.68	3.75	3.50	3.80	3.74	3.71	3.76	3.69	3.73	3.70	3.65	3.66	3.74	3.74	3.69	3.70	3.68	3.70	3.71	3.70	3.68	3.65	3.73

Sample	#7bB2				#7bB4				#7bB6					#8bB1						#8bB4				#8bB5			#8bB6			#9bB7		
Observations	Anhedral													Euhedral										Anhedral								
Zone	Pegmatite 1																															
wt%	2	3	4	5	1	2	3	4	1	2	3	4	5	1	2	3	4	5	6	1	2	3	4	1	2	3	1	2	3	1	2	3
SiO_2	63.95	63.73	64.25	63.62	63.23	63.37	63.28	63.59	63.20	63.53	64.00	63.74	63.91	63.84	63.56	63.61	63.75	64.15	64.31	63.22	63.77	63.47	63.05	63.70	63.84	63.99	63.83	63.31	63.77	63.01	63.18	63.95
Al_2O_3	27.86	27.39	27.49	27.58	27.50	27.57	26.72	26.81	26.83	27.21	27.42	26.78	26.93	27.27	27.55	27.55	27.36	27.47	27.34	26.98	27.20	27.04	27.05	27.15	27.40	27.40	27.47	27.52	27.65	27.40	27.48	27.70
Fe_2O_3	0.00	0.00	0.00	0.00	0.00	0.00	0.11	0.10	0.10	0.00	0.00	0.34	0.29	0.07	0.00	0.00	0.00	0.00	0.12	0.01	0.06	0.10	0.00	0.09	0.00	0.00	0.00	0.00	0.00	0.00	0.00	0.00
Mn_2O_3	0.00	0.00	0.00	0.00	0.00	0.00	0.05	0.04	0.00	0.00	0.00	0.00	0.00	0.00	0.00	0.00	0.00	0.00	0.00	0.00	0.00	0.00	0.00	0.00	0.00	0.00	0.00	0.00	0.00	0.00	0.00	0.00
ZnO	0.05	0.00	0.04	0.00	0.00	0.00	0.00	0.04	0.02	0.06	0.00	0.00	0.00	0.00	0.02	0.00	0.02	0.08	0.00	0.02	0.00	0.00	0.05	0.06	0.03	0.00	0.00	0.00	0.00	0.00	0.01	0.00
FeO	0.20	0.12	0.14	0.08	0.16	0.15	0.00	0.00	0.03	0.15	0.15	0.00	0.02	0.20	0.13	0.12	0.13	0.06	0.13	0.16	0.19	0.20	0.17	0.13	0.17	0.13	0.31	0.14	0.20	0.21	0.09	0.28
MnO	0.06	0.00	0.04	0.08	0.04	0.03	0.00	0.00	0.04	0.00	0.04	0.01	0.00	0.02	0.05	0.06	0.01	0.04	0.02	0.01	0.00	0.00	0.02	0.05	0.06	0.07	0.04	0.00	0.03	0.02	0.00	0.01
CaO	0.00	0.01	0.00	0.00	0.00	0.01	0.02	0.00	0.02	0.01	0.01	0.00	0.00	0.01	0.00	0.00	0.01	0.00	0.01	0.01	0.01	0.01	0.01	0.00	0.00	0.01	0.02	0.01	0.00	0.00	0.01	0.01
K2O	0.01	0.01	0.01	0.00	0.00	0.01	0.01	0.00	0.02	0.01	0.01	0.01	0.01	0.04	0.04	0.00	0.00	0.01	0.00	0.01	0.00	0.02	0.02	0.01	0.01	0.00	0.01	0.01	0.01	0.01	0.00	0.00
Na_2O	0.05	0.08	0.07	0.06	0.11	0.08	0.08	0.08	0.09	0.09	0.06	0.09	0.09	0.09	0.10	0.08	0.07	0.08	0.06	0.08	0.08	0.10	0.09	0.07	0.09	0.07	0.06	0.08	0.06	0.05	0.09	0.08
Li_2O*	8.03	7.93	7.94	7.99	7.93	7.97	7.82	7.84	7.79	7.85	7.93	7.88	7.89	7.85	7.93	7.96	7.93	7.95	7.95	7.80	7.87	7.82	7.78	7.86	7.87	7.92	7.87	7.96	7.98	7.91	7.97	7.96
Total	100.21	99.26	99.97	99.42	98.97	99.18	98.10	98.51	98.14	98.89	99.61	98.85	99.14	99.40	99.37	99.38	99.28	99.85	99.93	98.28	99.18	98.75	98.24	99.10	99.46	99.59	99.60	99.04	99.69	98.59	98.84	99.98
a.p.f.u. (calculus done on the basis of 6 oxygen)																																
Si^{4+}	1.981	1.991	1.993	1.985	1.983	1.982	2.000	2.001	1.997	1.993	1.993	2.000	1.999	1.993	1.985	1.985	1.991	1.993	1.996	1.995	1.995	1.994	1.992	1.994	1.992	1.992	1.990	1.983	1.985	1.983	1.982	1.985
Al^{3+}	0.019	0.009	0.007	0.016	0.018	0.018	0.000	0.000	0.003	0.008	0.007	0.000	0.001	0.007	0.015	0.015	0.009	0.007	0.004	0.005	0.005	0.006	0.008	0.006	0.008	0.008	0.010	0.017	0.016	0.017	0.018	0.015
Total-T	2.000	2.000	2.000	2.000	2.000	2.000	2.000	2.001	2.000	2.000	2.000	2.000	2.000	2.000	2.000	2.000	2.000	2.000	2.000	2.000	2.000	2.000	2.000	2.000	2.000	2.000	2.000	2.000	2.000	2.000	2.000	2.000
Fe^{3+}	0.000	0.000	0.000	0.000	0.000	0.000	0.003	0.002	0.002	0.000	0.000	0.008	0.007	0.002	0.000	0.000	0.000	0.000	0.003	0.000	0.001	0.003	0.000	0.002	0.000	0.000	0.000	0.000	0.000	0.000	0.000	0.000
Mn^{3+}	0.000	0.000	0.000	0.000	0.000	0.000	0.001	0.001	0.000	0.000	0.000	0.000	0.000	0.000	0.000	0.000	0.000	0.000	0.000	0.000	0.000	0.000	0.000	0.000	0.000	0.000	0.000	0.000	0.000	0.000	0.000	0.000
Al^{3+}	0.998	0.999	0.998	0.998	0.999	0.998	0.995	0.994	0.996	0.998	0.999	0.990	0.992	0.997	0.999	0.999	0.998	0.999	0.996	0.998	0.998	0.996	0.999	0.996	0.999	0.997	0.999	0.998	0.999	0.999	0.999	0.999
Zn^{2+}	0.001	0.000	0.001	0.000	0.000	0.000	0.000	0.001	0.001	0.001	0.000	0.000	0.000	0.000	0.001	0.000	0.001	0.002	0.000	0.001	0.000	0.000	0.001	0.001	0.001	0.000	0.000	0.000	0.000	0.000	0.000	0.000
Fe^{2+}	0.000	0.000	0.000	0.000	0.000	0.000	0.000	0.000	0.000	0.000	0.000	0.000	0.000	0.000	0.000	0.000	0.000	0.000	0.000	0.000	0.000	0.000	0.000	0.000	0.000	0.000	0.000	0.000	0.000	0.000	0.000	0.000
M1 Total	0.999	0.999	0.999	0.998	0.999	0.999	0.999	0.998	0.999	1.000	0.999	0.998	0.999	0.998	1.000	0.999	0.999	1.000	0.998	0.999	0.999	0.998	1.000	0.999	1.000	0.997	0.999	0.998	0.999	0.999	0.999	0.999
Fe^{2+}	0.005	0.003	0.004	0.002	0.004	0.004	0.000	0.000	0.001	0.004	0.004	0.000	0.001	0.005	0.003	0.003	0.003	0.002	0.003	0.004	0.005	0.005	0.004	0.003	0.004	0.003	0.008	0.004	0.005	0.005	0.002	0.007
Mn^{2+}	0.001	0.000	0.001	0.002	0.001	0.001	0.000	0.000	0.001	0.000	0.001	0.000	0.000	0.001	0.001	0.002	0.000	0.001	0.000	0.000	0.000	0.000	0.001	0.001	0.002	0.002	0.001	0.000	0.001	0.000	0.000	0.000
Ca^{2+}	0.000	0.000	0.000	0.000	0.000	0.000	0.001	0.000	0.001	0.000	0.000	0.000	0.000	0.000	0.000	0.000	0.000	0.000	0.001	0.000	0.000	0.000	0.000	0.000	0.000	0.000	0.001	0.000	0.000	0.000	0.000	0.000
K^{+}	0.000	0.000	0.000	0.000	0.000	0.000	0.000	0.000	0.001	0.000	0.000	0.000	0.001	0.002	0.002	0.000	0.000	0.001	0.000	0.000	0.000	0.001	0.001	0.000	0.001	0.000	0.000	0.000	0.000	0.000	0.000	0.000
Na^{+}	0.003	0.005	0.004	0.004	0.006	0.005	0.005	0.005	0.005	0.005	0.004	0.005	0.006	0.006	0.006	0.005	0.004	0.005	0.004	0.005	0.005	0.006	0.006	0.004	0.005	0.004	0.004	0.005	0.004	0.003	0.005	0.005
Li^{+}	1.000	0.997	0.991	1.002	1.000	1.003	0.994	0.993	0.990	0.991	0.993	0.994	0.993	0.986	0.996	1.000	0.996	0.993	0.992	0.990	0.990	0.988	0.989	0.990	0.988	0.991	0.986	1.003	0.999	1.001	1.006	0.994
M2 Total	1.010	1.005	1.000	1.010	1.011	1.013	1.000	0.997	0.999	1.000	1.002	1.000	1.000	0.999	1.008	1.009	1.004	1.001	1.000	0.999	1.000	1.000	1.000	0.999	1.000	1.001	1.000	1.012	1.009	1.009	1.014	1.006
Li wt%	3.73	3.69	3.69	3.71	3.68	3.70	3.63	3.64	3.62	3.65	3.68	3.66	3.67	3.65	3.68	3.70	3.68	3.69	3.69	3.62	3.65	3.63	3.61	3.65	3.66	3.68	3.65	3.70	3.71	3.67	3.70	3.70

Sample	#9bB7	#9cB4		#9cB4		#14B1								#14B2				#17B4								#17B5		#17B6				
Observations	Anhedral	Euhedral		Euhedral		Anhedral																						Euhedral				
Zone	Pegmatite 1					Pegmatite 2																										
wt%	4	1	2	3	4	1	2	3	4	5	6	7	8	1	2	3	4	1	2	3	4	5	6	7	8	1	2	1	2	3	4	5
SiO_2	62.05	63.17	63.65	63.35	63.14	63.73	63.79	63.69	63.46	63.73	63.51	63.55	63.65	63.48	63.46	63.55	62.99	62.81	63.21	63.09	63.25	62.91	63.16	63.26	63.17	63.26	63.78	64.21	64.13	63.91	64.23	64.18
Al_2O_3	27.52	27.24	27.46	27.58	27.47	27.68	27.56	27.66	27.49	27.60	27.22	27.17	26.55	27.27	27.07	27.10	27.08	27.33	27.53	27.37	27.55	27.46	27.53	27.96	27.66	27.11	27.05	27.73	27.50	27.42	27.54	27.68
Fe_2O_3	0.00	0.00	0.00	0.00	0.00	0.00	0.00	0.00	0.00	0.00	0.00	0.00	0.30	0.00	0.15	0.08	0.00	0.00	0.00	0.00	0.00	0.00	0.00	0.00	0.00	0.00	0.19	0.00	0.00	0.01	0.01	0.00
Mn_2O_3	0.00	0.00	0.00	0.00	0.00	0.00	0.00	0.00	0.00	0.00	0.00	0.00	0.05	0.00	0.00	0.00	0.00	0.00	0.00	0.00	0.00	0.00	0.00	0.00	0.00	0.00	0.00	0.00	0.00	0.00	0.00	0.00
ZnO	0.02	0.00	0.01	0.00	0.00	0.00	0.00	0.02	0.02	0.00	0.00	0.00	0.00	0.06	0.08	0.04	0.00	0.00	0.03	0.00	0.00	0.03	0.00	0.00	0.03	0.04	0.02	0.00	0.01	0.06	0.10	0.09
FeO	0.27	0.03	0.17	0.06	0.16	0.18	0.10	0.10	0.13	0.21	0.08	0.20	0.00	0.22	0.17	0.16	0.25	0.28	0.29	0.30	0.28	0.28	0.27	0.28	0.34	0.10	0.07	0.23	0.24	0.22	0.22	0.21
MnO	0.00	0.02	0.00	0.03	0.04	0.00	0.05	0.02	0.02	0.08	0.06	0.05	0.00	0.01	0.01	0.01	0.00	0.02	0.00	0.02	0.03	0.02	0.02	0.04	0.02	0.04	0.05	0.01	0.00	0.00	0.01	0.06
CaO	0.02	0.01	0.02	0.01	0.00	0.00	0.00	0.02	0.00	0.00	0.01	0.00	0.00	0.03	0.00	0.00	0.01	0.01	0.01	0.01	0.01	0.00	0.00	0.05	0.05	0.00	0.00	0.00	0.01	0.04	0.01	0.00
K2O	0.01	0.01	0.00	0.00	0.00	0.00	0.00	0.01	0.01	0.00	0.00	0.00	0.01	0.01	0.01	0.01	0.00	0.02	0.01	0.02	0.01	0.01	0.01	0.02	0.02	0.00	0.00	0.00	0.00	0.01	0.00	0.00
Na_2O	0.05	0.08	0.10	0.08	0.10	0.07	0.07	0.05	0.08	0.08	0.08	0.06	0.08	0.07	0.07	0.07	0.05	0.10	0.07	0.10	0.06	0.06	0.08	0.08	0.05	0.08	0.07	0.07	0.07	0.08	0.08	0.05
Li_2O*	7.92	7.91	7.93	8.00	7.93	8.01	7.99	8.03	7.96	7.94	7.88	7.85	7.80	7.84	7.82	7.85	7.80	7.84	7.91	7.83	7.92	7.89	7.91	8.02	7.90	7.84	7.88	8.00	7.92	7.87	7.91	7.96
Total	97.85	98.46	99.34	99.13	98.84	99.67	99.56	99.58	99.17	99.63	98.83	98.89	98.44	98.98	98.84	98.86	98.18	98.41	99.05	98.73	99.11	98.65	98.98	99.71	99.24	98.48	99.11	100.25	99.88	99.63	100.10	100.22
a.p.f.u. (calculus done on the basis of 6 oxygen)																																
Si^{4+}	1.969	1.989	1.987	1.981	1.982	1.984	1.987	1.984	1.985	1.985	1.993	1.993	2.004	1.991	1.993	1.995	1.990	1.981	1.982	1.985	1.981	1.980	1.981	1.971	1.977	1.992	1.997	1.987	1.992	1.992	1.992	1.987
Al^{3+}	0.031	0.011	0.013	0.019	0.018	0.017	0.013	0.017	0.015	0.015	0.008	0.007	0.000	0.010	0.007	0.006	0.010	0.019	0.018	0.015	0.019	0.020	0.019	0.029	0.023	0.008	0.004	0.013	0.008	0.009	0.009	0.013
Total-T	2.000	2.000	2.000	2.000	2.000	2.000	2.000	2.000	2.000	2.000	2.000	2.000	2.004	2.000	2.000	2.000	2.000	2.000	2.000	2.000	2.000	2.000	2.000	2.000	2.000	2.000	2.000	2.000	2.000	2.000	2.000	2.000
Fe^{3+}	0.000	0.000	0.000	0.000	0.000	0.000	0.000	0.000	0.000	0.000	0.000	0.000	0.007	0.000	0.004	0.002	0.000	0.000	0.000	0.000	0.000	0.000	0.000	0.000	0.000	0.000	0.005	0.000	0.000	0.000	0.000	0.000
Mn^{3+}	0.000	0.000	0.000	0.000	0.000	0.000	0.000	0.000	0.000	0.000	0.000	0.000	0.001	0.000	0.000	0.000	0.000	0.000	0.000	0.000	0.000	0.000	0.000	0.000	0.000	0.000	0.000	0.000	0.000	0.000	0.000	0.000
Al^{3+}	0.999	0.999	0.998	0.998	0.998	0.999	0.999	0.999	0.998	0.998	0.999	0.997	0.985	0.999	0.995	0.997	0.999	0.998	0.999	0.999	0.999	0.999	0.999	0.997	0.998	0.998	0.994	0.999	0.999	0.999	0.998	0.997
Zn^{2+}	0.001	0.000	0.000	0.000	0.000	0.000	0.000	0.000	0.001	0.000	0.000	0.000	0.000	0.001	0.002	0.001	0.000	0.000	0.001	0.000	0.000	0.001	0.000	0.000	0.001	0.001	0.000	0.000	0.000	0.001	0.002	0.002
Fe^{2+}	0.000	0.000	0.000	0.000	0.000	0.000	0.000	0.000	0.000	0.000	0.000	0.000	0.000	0.000	0.000	0.000	0.000	0.000	0.000	0.000	0.000	0.000	0.000	0.000	0.000	0.000	0.000	0.000	0.000	0.000	0.000	0.000
M1 Total	0.999	0.999	0.998	0.998	0.998	0.999	0.999	0.999	0.999	0.998	0.999	0.997	0.994	1.000	1.000	1.000	0.999	0.998	1.000	0.999	0.999	0.999	0.999	0.997	0.999	0.999	0.999	0.999	0.999	1.000	1.000	0.999
Fe^{2+}	0.007	0.001	0.004	0.002	0.004	0.005	0.003	0.003	0.004	0.006	0.002	0.005	0.000	0.006	0.005	0.004	0.007	0.007	0.008	0.008	0.007	0.007	0.007	0.007	0.009	0.003	0.002	0.006	0.006	0.006	0.006	0.005
Mn^{2+}	0.000	0.001	0.000	0.001	0.001	0.000	0.001	0.000	0.001	0.002	0.002	0.001	0.000	0.000	0.000	0.000	0.000	0.001	0.000	0.000	0.001	0.001	0.001	0.001	0.000	0.001	0.001	0.000	0.000	0.000	0.000	0.002
Ca^{2+}	0.001	0.001	0.001	0.001	0.000	0.000	0.000	0.001	0.000	0.000	0.000	0.000	0.000	0.001	0.000	0.000	0.000	0.000	0.000	0.000	0.001	0.000	0.000	0.002	0.002	0.000	0.000	0.000	0.001	0.001	0.000	0.000
K^{+}	0.000	0.000	0.000	0.000	0.000	0.000	0.000	0.000	0.000	0.000	0.000	0.000	0.000	0.000	0.000	0.000	0.000	0.001	0.000	0.001	0.000	0.000	0.000	0.001	0.001	0.000	0.000	0.000	0.000	0.001	0.000	0.000
Na^{+}	0.003	0.005	0.006	0.005	0.006	0.004	0.004	0.003	0.005	0.005	0.005	0.004	0.005	0.004	0.004	0.004	0.003	0.006	0.004	0.006	0.003	0.004	0.005	0.005	0.003	0.005	0.004	0.004	0.004	0.005	0.005	0.003
Li^{+}	1.011	1.001	0.995	1.006	1.002	1.003	1.001	1.005	1.001	0.995	0.995	0.990	0.988	0.988	0.988	0.990	0.991	0.995	0.997	0.991	0.997	0.999	0.998	1.004	0.995	0.993	0.992	0.995	0.990	0.986	0.986	0.991
M2 Total	1.022	1.008	1.006	1.014	1.013	1.012	1.009	1.012	1.010	1.007	1.003	1.000	0.994	1.000	0.997	0.999	1.001	1.010	1.009	1.006	1.010	1.010	1.011	1.020	1.010	1.002	0.999	1.006	1.000	0.999	0.997	1.001
Li wt%	3.68	3.67	3.68	3.72	3.69	3.72	3.71	3.73	3.70	3.69	3.66	3.65	3.63	3.64	3.63	3.65	3.62	3.64	3.67	3.64	3.68	3.67	3.68	3.72	3.67	3.64	3.66	3.71	3.68	3.66	3.67	3.70

Sample	#17B6	
Observations	Euhedral	
Zone	Pegmatite 2	
wt%	6	7
SiO_2	64.50	64.09
Al_2O_3	27.58	26.50
Fe_2O_3	0.06	0.23
Mn_2O_3	0.00	0.01
ZnO	0.07	0.00
FeO	0.20	0.00
MnO	0.00	0.00
CaO	0.02	0.02
K2O	0.00	0.00
Na_2O	0.07	0.06
Li_2O*	7.95	7.80
Total	100.45	98.72
a.p.f.u. (calculus done on the basis of 6 oxygen)		
Si^{4+}	1.993	2.011
Al^{3+}	0.007	0.000
Total-T	2.000	2.011
Fe^{3+}	0.002	0.006
Mn^{3+}	0.000	0.000
Al^{3+}	0.997	0.980
Zn^{2+}	0.002	0.000
Fe^{2+}	0.000	0.000
M1 Total	1.000	0.986
Fe^{2+}	0.005	0.000
Mn^{2+}	0.000	0.000
Ca^{2+}	0.001	0.001
K^{+}	0.000	0.000
Na^{+}	0.004	0.004
Li^{+}	0.988	0.984
M2 Total	0.998	0.989
Li wt%	3.69	3.62

II.II.II BERYL

Sample	#2cB5	#7aB5		#7bB5		#8bB2		#8bB6				#9bB1								#9bB5		#9bB9		#9cB1						#9cB2		
Zone	Pegmatite 1																															
Wt%	1	1	2	1	2	1	2	1	2	3	5	1	2	3	4	5	6	7	8	1	3	1	2	1	2	3	4	5	6	2	3	4
SiO_2	64.02	65.36	65.05	65.29	63.56	64.78	64.32	65.78	65.55	65.46	65.81	66.71	65.27	65.50	65.63	65.43	65.88	65.02	66.24	65.43	64.41	65.53	65.24	65.48	65.21	65.33	64.77	65.88	65.26	65.14	65.56	65.19
Al_2O_3	19.12	18.78	18.59	18.96	18.54	18.82	18.72	18.81	18.87	18.90	18.83	19.09	18.84	19.00	18.64	18.47	18.71	18.53	18.38	18.62	19.01	18.76	18.57	19.03	18.96	19.03	19.16	18.95	19.12	19.02	18.69	18.93
CaO	0.02	0.00	0.01	0.01	0.02	0.02	0.00	0.01	0.02	0.02	0.02	0.00	0.00	0.01	0.00	0.00	0.01	0.01	0.01	0.00	0.01	0.02	0.01	0.01	0.01	0.02	0.01	0.00	0.00	0.02	0.00	0.03
MnO	0.02	0.01	0.00	0.03	0.01	0.03	0.01	0.00	0.01	0.00	0.01	0.00	0.01	0.01	0.02	0.05	0.02	0.00	0.01	0.02	0.00	0.06	0.03	0.01	0.00	0.00	0.02	0.00	0.04	0.00	0.00	0.00
ZnO	0.03	0.13	0.05	0.03	0.00	0.04	0.00	0.00	0.00	0.00	0.02	0.00	0.07	0.00	0.02	0.06	0.09	0.01	0.00	0.08	0.00	0.02	0.00	0.00	0.03	0.03	0.03	0.05	0.00	0.07	0.15	0.00
MgO	0.00	0.01	0.00	0.00	0.01	0.00	0.00	0.00	0.00	0.00	0.00	0.00	0.00	0.00	0.00	0.00	0.00	0.00	0.00	0.00	0.00	0.00	0.00	0.00	0.00	0.00	0.02	0.00	0.00	0.00	0.00	0.01
FeO	0.04	0.06	0.01	0.01	0.04	0.04	0.02	0.25	0.29	0.17	0.24	0.09	0.07	0.21	0.25	0.16	0.07	0.21	0.16	0.30	0.12	0.34	0.30	0.17	0.19	0.11	0.15	0.15	0.13	0.27	0.25	0.31
Na_2O	1.25	1.21	1.74	0.61	1.56	1.76	1.94	0.73	0.96	1.15	0.96	0.50	1.50	1.15	1.12	1.21	0.93	1.16	1.04	0.97	1.10	0.87	1.32	0.69	1.03	1.12	0.97	1.27	1.30	0.99	1.10	1.06
K_2O	0.02	0.04	0.03	0.03	0.04	0.02	0.03	0.03	0.03	0.02	0.03	0.02	0.02	0.04	0.03	0.02	0.03	0.03	0.03	0.03	0.05	0.03	0.01	0.04	0.03	0.05	0.03	0.02	0.03	0.04	0.04	0.04
SnO_2	0.00	0.01	0.00	0.03	0.01	0.00	0.00	0.03	0.00	0.00	0.02	0.00	0.01	0.00	0.00	0.00	0.00	0.01	0.00	0.00	0.00	0.02	0.00	0.00	0.00	0.00	0.00	0.00	0.00	0.02	0.01	0.00
BaO	0.02	0.01	0.04	0.04	0.00	0.01	0.03	0.00	0.02	0.06	0.00	0.00	0.06	0.00	0.00	0.00	0.04	0.00	0.07	0.00	0.06	0.01	0.07	0.00	0.05	0.00	0.03	0.04	0.01	0.04	0.04	0.00
SrO	0.11	0.00	0.05	0.00	0.00	0.04	0.01	0.00	0.05	0.00	0.03	0.05	0.05	0.00	0.02	0.05	0.04	0.01	0.07	0.15	0.00	0.00	0.00	0.04	0.06	0.03	0.03	0.00	0.00	0.08	0.00	0.00
Cs_2O	0.16	0.28	0.14	0.31	0.54	0.13	0.13	0.12	0.12	0.07	0.10	0.04	0.19	0.13	0.12	0.11	0.12	0.09	0.14	0.11	0.08	0.07	0.06	0.08	0.14	0.23	0.11	0.09	0.15	0.10	0.13	0.08
Li_2O*	0.63	0.63	0.86	0.34	0.83	0.87	0.96	0.37	0.48	0.57	0.48	0.25	0.75	0.59	0.57	0.61	0.47	0.58	0.52	0.49	0.55	0.44	0.65	0.35	0.52	0.58	0.49	0.63	0.65	0.50	0.56	0.53
BeO*	12.13	12.47	12.05	12.96	11.77	11.94	11.76	12.98	12.69	12.57	12.77	13.41	12.23	12.57	12.61	12.52	12.85	12.46	12.86	12.67	12.36	12.73	12.37	12.92	12.56	12.52	12.49	12.55	12.37	12.53	12.56	12.49
CoO	0.00	0.02	0.00	0.02	0.00	0.00	0.00	0.00	0.00	0.00	0.00	0.00	0.02	0.00	0.01	0.00	0.00	0.03	0.03	0.00	0.00	0.00	0.00	0.00	0.00	0.02	0.02	0.00	0.00	0.00	0.00	0.02
Nb_2O_5	0.06	0.09	0.05	0.07	0.00	0.04	0.07	0.07	0.03	0.09	0.03	0.07	0.03	0.08	0.04	0.02	0.07	0.03	0.06	0.04	0.07	0.00	0.07	0.03	0.00	0.08	0.06	0.03	0.02	0.09	0.00	0.00
Ta_2O_5	0.09	0.00	0.06	0.06	0.04	0.09	0.23	0.00	0.08	0.00	0.01	0.00	0.08	0.15	0.02	0.06	0.00	0.00	0.00	0.25	0.00	0.00	0.00	0.05	0.16	0.00	0.01	0.00	0.00	0.03	0.00	0.00
GeO_2	0.00	0.00	0.02	0.00	0.00	0.00	0.00	0.00	0.00	0.00	0.02	0.00	0.00	0.00	0.03	0.00	0.00	0.00	0.00	0.03	0.03	0.00	0.00	0.00	0.00	0.02	0.03	0.00	0.04	0.00	0.01	0.00
Sc_2O_3	0.00	0.00	0.00	0.00	0.00	0.01	0.00	0.00	0.00	0.01	0.00	0.00	0.00	0.00	0.01	0.00	0.00	0.00	0.00	0.01	0.00	0.00	0.00	0.00	0.01	0.00	0.00	0.00	0.00	0.00	0.00	0.00
PbO	0.04	0.04	0.00	0.04	0.07	0.00	0.06	0.00	0.01	0.01	0.00	0.00	0.01	0.08	0.04	0.04	0.06	0.00	0.00	0.04	0.00	0.03	0.00	0.00	0.03	0.00	0.05	0.00	0.00	0.00	0.04	0.00
Cl	0.00	0.01	0.00	0.01	0.01	0.00	0.00	0.00	0.01	0.01	0.00	0.00	0.00	0.00	0.00	0.00	0.01	0.00	0.00	0.02	0.01	0.00	0.00	0.00	0.00	0.00	0.01	0.00	0.00	0.01	0.00	0.00
Total	97.74	99.15	98.76	98.86	97.03	98.63	98.28	99.17	99.19	99.11	99.38	100.23	99.21	99.50	99.17	98.82	99.40	98.18	99.61	99.23	97.85	98.91	98.69	98.90	98.99	99.16	98.49	99.67	99.12	98.95	99.14	98.69
a.p.f.u (Calculus done on the basis of 18 Oxygen)																																
Si^{4+}	5.945	5.980	5.983	5.969	5.969	5.970	5.961	5.984	5.978	5.974	5.986	5.985	5.978	5.966	5.991	5.996	5.991	5.990	6.011	5.982	5.957	5.987	5.990	5.972	5.969	5.969	5.954	5.982	5.964	5.965	5.990	5.976
Al^{IV}	0.056	0.020	0.015	0.031	0.031	0.030	0.039	0.016	0.022	0.026	0.013	0.015	0.022	0.034	0.008	0.004	0.010	0.010	0.000	0.017	0.041	0.013	0.010	0.029	0.031	0.030	0.044	0.018	0.034	0.035	0.010	0.025
Ge^{4+}	0.000	0.000	0.001	0.000	0.000	0.000	0.000	0.000	0.000	0.000	0.001	0.000	0.000	0.000	0.001	0.000	0.000	0.000	0.000	0.002	0.002	0.000	0.000	0.000	0.000	0.001	0.002	0.000	0.002	0.000	0.001	0.000
T-Total	6.000	6.000	6.000	6.000	6.000	6.000	6.000	6.000	6.000	6.000	6.000	6.000	6.000	6.000	6.000	6.000	6.000	6.000	6.012	6.000	6.000	6.000	6.000	6.000	6.000	6.000	6.000	6.000	6.000	6.000	6.000	6.000
Ta^{5+}	0.002	0.000	0.002	0.002	0.001	0.002	0.006	0.000	0.002	0.000	0.000	0.000	0.002	0.004	0.001	0.002	0.000	0.000	0.000	0.006	0.000	0.000	0.000	0.001	0.004	0.000	0.000	0.000	0.000	0.001	0.000	0.000
Nb^{5+}	0.002	0.004	0.002	0.003	0.000	0.002	0.003	0.003	0.001	0.004	0.001	0.003	0.001	0.003	0.002	0.001	0.003	0.001	0.002	0.002	0.003	0.000	0.003	0.001	0.000	0.003	0.003	0.001	0.001	0.004	0.000	0.000
Sc^{3+}	0.000	0.000	0.000	0.000	0.000	0.001	0.000	0.000	0.000	0.001	0.000	0.000	0.000	0.000	0.001	0.000	0.000	0.000	0.000	0.000	0.000	0.000	0.000	0.000	0.001	0.000	0.000	0.000	0.000	0.000	0.000	0.000
Al^{VI}	2.037	2.005	2.000	2.012	2.021	2.014	2.005	2.001	2.007	2.006	2.005	2.003	2.011	2.006	1.998	1.991	1.996	2.002	1.966	1.989	2.031	2.008	1.999	2.016	2.014	2.019	2.032	2.011	2.026	2.018	2.003	2.020
Co^{2+}	0.000	0.001	0.000	0.002	0.000	0.000	0.000	0.000	0.000	0.000	0.000	0.000	0.002	0.000	0.000	0.000	0.000	0.002	0.002	0.000	0.000	0.000	0.000	0.000	0.000	0.002	0.002	0.000	0.000	0.000	0.000	0.001
Ochtahedral Site	2.041	2.010	2.003	2.018	2.022	2.019	2.014	2.004	2.010	2.011	2.007	2.006	2.016	2.013	2.001	1.993	1.999	2.005	1.971	1.997	2.034	2.008	2.002	2.019	2.018	2.024	2.036	2.012	2.026	2.022	2.003	2.022
Sn^{4+}	0.000	0.000	0.000	0.001	0.000	0.000	0.000	0.001	0.000	0.000	0.001	0.000	0.000	0.000	0.000	0.000	0.000	0.000	0.000	0.000	0.000	0.001	0.000	0.000	0.000	0.000	0.000	0.000	0.000	0.001	0.001	0.000
Ba^{2+}	0.001	0.000	0.001	0.002	0.000	0.000	0.001	0.000	0.001	0.002	0.000	0.000	0.002	0.000	0.000	0.000	0.001	0.000	0.002	0.000	0.002	0.000	0.002	0.000	0.002	0.000	0.001	0.002	0.001	0.001	0.002	0.000
Sr^{2+}	0.006	0.000	0.003	0.000	0.000	0.002	0.001	0.000	0.002	0.000	0.002	0.002	0.003	0.000	0.001	0.003	0.002	0.001	0.004	0.008	0.000	0.000	0.000	0.002	0.003	0.001	0.002	0.000	0.000	0.004	0.000	0.000
Zn^{2+}	0.002	0.009	0.004	0.002	0.000	0.003	0.000	0.000	0.000	0.000	0.001	0.000	0.005	0.000	0.001	0.004	0.006	0.001	0.000	0.005	0.000	0.002	0.000	0.000	0.002	0.002	0.002	0.004	0.000	0.005	0.010	0.000
Fe^{2+}	0.003	0.004	0.001	0.001	0.003	0.003	0.001	0.019	0.022	0.013	0.018	0.007	0.006	0.016	0.019	0.013	0.006	0.016	0.012	0.023	0.009	0.026	0.023	0.013	0.014	0.009	0.012	0.012	0.010	0.021	0.019	0.024
Mn^{2+}	0.001	0.001	0.000	0.002	0.001	0.002	0.001	0.000	0.001	0.000	0.001	0.000	0.000	0.001	0.001	0.004	0.002	0.000	0.001	0.001	0.000	0.005	0.002	0.001	0.000	0.000	0.001	0.000	0.003	0.000	0.000	0.000
Ca^{2+}	0.002	0.000	0.001	0.001	0.002	0.002	0.000	0.001	0.002	0.002	0.002	0.000	0.000	0.001	0.000	0.000	0.001	0.001	0.001	0.000	0.001	0.002	0.001	0.001	0.001	0.002	0.001	0.000	0.000	0.002	0.000	0.003
Mg^{2+}	0.000	0.001	0.000	0.000	0.002	0.000	0.000	0.000	0.000	0.000	0.000	0.000	0.000	0.000	0.000	0.000	0.000	0.000	0.000	0.000	0.000	0.000	0.000	0.000	0.000	0.000	0.002	0.000	0.000	0.000	0.000	0.001
Be^{2+}	2.706	2.742	2.663	2.845	2.654	2.644	2.617	2.836	2.780	2.756	2.790	2.890	2.691	2.750	2.766	2.756	2.807	2.757	2.803	2.782	2.747	2.794	2.729	2.831	2.762	2.748	2.758	2.738	2.716	2.757	2.757	2.751
Li^{+}	0.234	0.231	0.320	0.125	0.312	0.322	0.359	0.136	0.178	0.208	0.177	0.091	0.277	0.214	0.208	0.224	0.174	0.215	0.191	0.181	0.205	0.161	0.238	0.129	0.192	0.212	0.183	0.229	0.239	0.185	0.204	0.195
T2-Total	2.955	2.988	2.992	2.979	2.974	2.978	2.979	2.993	2.985	2.983	2.991	2.991	2.984	2.982	2.997	3.003	2.998	2.990	3.015	3.000	2.964	2.989	2.996	2.976	2.977	2.975	2.962	2.985	2.968	2.976	2.992	2.974
Pb^{2+}	0.001	0.001	0.000	0.001	0.002	0.000	0.002	0.000	0.000	0.000	0.000	0.000	0.000	0.002	0.001	0.001	0.002	0.000	0.000	0.001	0.000	0.001	0.000	0.000	0.001	0.000	0.001	0.000	0.000	0.000	0.001	0.000
Cs^{+}	0.007	0.011	0.005	0.012	0.022	0.005	0.005	0.005	0.005	0.003	0.004	0.002	0.007	0.005	0.005	0.005	0.005	0.004	0.005	0.004	0.003	0.003	0.002	0.003	0.006	0.009	0.004	0.004	0.006	0.004	0.005	0.003
K^{+}	0.002	0.005	0.004	0.004	0.005	0.003	0.004	0.003	0.003	0.002	0.004	0.002	0.003	0.004	0.004	0.003	0.003	0.003	0.004	0.004	0.005	0.004	0.002	0.005	0.003	0.005	0.004	0.002	0.003	0.005	0.004	0.004
Na^{+}	0.225	0.214	0.311	0.108	0.283	0.314	0.348	0.128	0.170	0.203	0.170	0.088	0.266	0.203	0.199	0.216	0.164	0.208	0.183	0.172	0.197	0.154	0.234	0.121	0.183	0.198	0.173	0.224	0.230	0.176	0.194	0.188
2a Site total	0.235	0.231	0.320	0.125	0.312	0.322	0.359	0.136	0.178	0.208	0.177	0.091	0.277	0.214	0.208	0.224	0.174	0.215	0.191	0.181	0.205	0.161	0.238	0.129	0.192	0.212	0.182	0.229	0.239	0.185	0.204	0.195
Cl^{-}	0.001	0.001	0.000	0.002	0.001	0.000	0.000	0.000	0.001	0.001	0.000	0.000	0.000	0.000	0.000	0.000	0.001	0.000	0.000	0.002	0.001	0.000	0.001	0.001	0.000	0.000	0.002	0.000	0.000	0.001	0.000	0.001
A-Total	0.001	0.001	0.000	0.002	0.001	0.000	0.000	0.000	0.001	0.001	0.000	0.000	0.000	0.000	0.000	0.000	0.001	0.000	0.000	0.002	0.001	0.000	0.001	0.001	0.000	0.000	0.002	0.000	0.000	0.001	0.000	0.001

Sample	#11bB4		#11cB3		#13B1					#13B2		#13B3		#14B3			#17B2		#17B3		
Zone	Pegmatite 1				Pegmatite 2																
Wt%	1	2	1	2	1	2	3	5	6	1	3	1	2	1	3	4	1	2	1	2	3
SiO_2	65.95	66.46	66.14	66.19	65.97	66.31	65.30	65.66	65.24	65.70	65.03	65.89	65.97	65.01	64.83	65.25	66.00	65.92	65.33	65.41	65.39
Al_2O_3	19.02	19.09	19.02	18.87	19.37	19.09	19.00	19.27	19.10	19.17	18.97	19.31	19.23	18.38	18.41	18.24	19.15	19.06	19.13	19.05	19.11
CaO	0.02	0.03	0.03	0.02	0.01	0.02	0.00	0.01	0.02	0.00	0.01	0.02	0.02	0.00	0.00	0.00	0.03	0.04	0.00	0.00	0.00
MnO	0.00	0.02	0.01	0.04	0.00	0.02	0.00	0.01	0.00	0.00	0.03	0.02	0.01	0.03	0.00	0.00	0.01	0.02	0.00	0.00	0.02
ZnO	0.00	0.01	0.09	0.08	0.02	0.04	0.00	0.00	0.00	0.06	0.04	0.07	0.00	0.07	0.00	0.00	0.00	0.09	0.00	0.00	0.02
MgO	0.03	0.06	0.00	0.00	0.00	0.00	0.00	0.01	0.01	0.00	0.00	0.00	0.00	0.01	0.00	0.00	0.00	0.00	0.00	0.00	0.00
FeO	0.22	0.15	0.29	0.35	0.10	0.25	0.27	0.05	0.12	0.23	0.09	0.18	0.07	0.28	0.07	0.28	0.24	0.25	0.14	0.06	0.06
Na_2O	0.61	0.45	0.49	0.70	0.55	1.04	1.50	1.10	1.38	1.02	1.25	0.59	1.50	1.25	1.21	1.21	0.61	0.81	0.71	0.97	0.90
K_2O	0.01	0.00	0.01	0.02	0.02	0.03	0.03	0.03	0.02	0.03	0.04	0.04	0.04	0.03	0.03	0.04	0.03	0.02	0.02	0.03	0.04
SnO_2	0.01	0.00	0.00	0.01	0.01	0.00	0.00	0.02	0.03	0.01	0.00	0.01	0.03	0.00	0.01	0.00	0.00	0.01	0.00	0.00	0.01
BaO	0.05	0.02	0.00	0.00	0.02	0.01	0.05	0.05	0.06	0.00	0.01	0.09	0.02	0.00	0.01	0.00	0.03	0.00	0.00	0.00	0.02
SrO	0.00	0.04	0.00	0.01	0.05	0.00	0.00	0.08	0.01	0.00	0.08	0.00	0.00	0.02	0.00	0.04	0.02	0.02	0.04	0.00	0.01
Cs_2O	0.07	0.06	0.05	0.01	0.08	0.08	0.12	0.10	0.05	0.07	0.48	0.04	0.40	0.11	0.28	0.10	0.08	0.06	0.08	0.11	0.04
Li_2O*	0.31	0.22	0.25	0.35	0.28	0.52	0.75	0.55	0.68	0.51	0.67	0.30	0.78	0.62	0.63	0.61	0.31	0.41	0.36	0.49	0.45
BeO*	13.08	13.32	13.18	13.03	13.14	12.80	12.18	12.62	12.30	12.67	12.28	13.04	12.35	12.36	12.43	12.48	13.05	12.88	12.88	12.74	12.75
CoO	0.02	0.01	0.00	0.01	0.00	0.00	0.00	0.01	0.01	0.02	0.00	0.00	0.00	0.00	0.00	0.01	0.02	0.00	0.00	0.00	0.04
Nb_2O_5	0.06	0.02	0.00	0.00	0.04	0.10	0.00	0.03	0.00	0.06	0.00	0.07	0.07	0.06	0.05	0.00	0.00	0.01	0.04	0.05	0.01
Ta_2O_5	0.00	0.11	0.00	0.18	0.00	0.00	0.02	0.00	0.00	0.01	0.00	0.07	0.00	0.00	0.02	0.00	0.00	0.11	0.00	0.09	0.05
GeO_2	0.00	0.00	0.00	0.00	0.00	0.01	0.00	0.01	0.00	0.00	0.00	0.00	0.00	0.00	0.00	0.00	0.00	0.00	0.00	0.04	0.00
Sc_2O_3	0.00	0.01	0.00	0.01	0.00	0.00	0.01	0.00	0.02	0.00	0.00	0.00	0.00	0.00	0.00	0.00	0.00	0.00	0.00	0.00	0.00
PbO	0.02	0.00	0.05	0.00	0.00	0.01	0.00	0.00	0.03	0.00	0.03	0.00	0.02	0.00	0.10	0.00	0.00	0.03	0.00	0.00	0.00
Cl	0.01	0.00	0.00	0.00	0.01	0.01	0.01	0.01	0.00	0.01	0.01	0.00	0.00	0.00	0.00	0.01	0.01	0.00	0.00	0.00	0.01
Total	99.49	100.07	99.60	99.87	99.65	100.35	99.25	99.61	99.09	99.56	99.01	99.74	100.52	98.23	98.06	98.26	99.59	99.73	98.72	99.04	98.91
a.p.f.u (Calculus done on the basis of 18 Oxygen)																					
Si^{4+}	5.976	5.981	5.985	5.986	5.964	5.977	5.973	5.963	5.967	5.968	5.970	5.961	5.967	5.995	5.990	6.009	5.976	5.975	5.967	5.966	5.968
Al^{IV}	0.024	0.019	0.015	0.014	0.036	0.022	0.027	0.036	0.033	0.032	0.030	0.039	0.033	0.005	0.010	0.000	0.024	0.025	0.033	0.032	0.032
Ge^{4+}	0.000	0.000	0.000	0.000	0.000	0.000	0.000	0.000	0.000	0.000	0.000	0.000	0.000	0.000	0.000	0.000	0.000	0.000	0.000	0.002	0.000
T-Total	6.000	6.000	6.000	6.000	6.000	6.000	6.000	6.000	6.000	6.000	6.000	6.000	6.000	6.000	6.000	6.009	6.000	6.000	6.000	6.000	6.000
Ta^{5+}	0.000	0.003	0.000	0.004	0.000	0.000	0.001	0.000	0.000	0.000	0.000	0.002	0.000	0.000	0.001	0.000	0.000	0.003	0.000	0.002	0.001
Nb^{5+}	0.003	0.001	0.000	0.000	0.002	0.004	0.000	0.001	0.000	0.002	0.000	0.003	0.003	0.002	0.002	0.000	0.000	0.001	0.002	0.002	0.000
Sc^{3+}	0.000	0.001	0.000	0.000	0.000	0.000	0.001	0.000	0.002	0.000	0.000	0.000	0.000	0.000	0.000	0.000	0.000	0.000	0.000	0.000	0.000
Al^{VI}	2.007	2.005	2.013	1.998	2.028	2.006	2.021	2.026	2.026	2.020	2.021	2.020	2.016	1.993	1.995	1.980	2.019	2.012	2.026	2.017	2.023
Co^{2+}	0.002	0.000	0.000	0.001	0.000	0.000	0.000	0.001	0.001	0.001	0.000	0.000	0.000	0.000	0.000	0.001	0.001	0.000	0.000	0.000	0.003
Ochtahedral Site	2.011	2.010	2.013	2.004	2.030	2.010	2.023	2.028	2.028	2.025	2.022	2.024	2.019	1.996	1.997	1.981	2.021	2.015	2.027	2.021	2.027
Sn^{4+}	0.000	0.000	0.000	0.000	0.000	0.000	0.000	0.001	0.001	0.000	0.000	0.001	0.001	0.000	0.000	0.000	0.000	0.000	0.000	0.000	0.000
Ba^{2+}	0.002	0.001	0.000	0.000	0.001	0.000	0.002	0.002	0.002	0.000	0.000	0.003	0.001	0.000	0.001	0.000	0.001	0.000	0.000	0.000	0.001
Sr^{2+}	0.000	0.002	0.000	0.000	0.003	0.000	0.000	0.004	0.001	0.000	0.004	0.000	0.000	0.001	0.000	0.002	0.001	0.001	0.002	0.000	0.000
Zn^{2+}	0.000	0.001	0.006	0.005	0.002	0.003	0.000	0.000	0.000	0.004	0.003	0.005	0.000	0.005	0.000	0.000	0.000	0.006	0.000	0.000	0.001
Fe^{2+}	0.016	0.011	0.022	0.026	0.007	0.019	0.021	0.004	0.009	0.018	0.007	0.014	0.005	0.022	0.005	0.021	0.018	0.019	0.011	0.005	0.005
Mn^{2+}	0.000	0.002	0.001	0.003	0.000	0.002	0.000	0.001	0.000	0.000	0.002	0.001	0.001	0.003	0.000	0.000	0.001	0.001	0.000	0.000	0.001
Ca^{2+}	0.002	0.003	0.003	0.002	0.001	0.002	0.000	0.001	0.002	0.000	0.001	0.002	0.002	0.000	0.000	0.000	0.003	0.004	0.000	0.000	0.000
Mg^{2+}	0.005	0.008	0.000	0.000	0.000	0.000	0.000	0.001	0.001	0.000	0.000	0.000	0.000	0.001	0.000	0.000	0.000	0.000	0.000	0.000	0.000
Be^{2+}	2.847	2.879	2.865	2.832	2.854	2.772	2.677	2.753	2.702	2.765	2.708	2.834	2.683	2.738	2.758	2.761	2.838	2.804	2.826	2.793	2.795
Li^{+}	0.112	0.081	0.090	0.126	0.102	0.189	0.275	0.202	0.251	0.185	0.246	0.110	0.283	0.230	0.234	0.224	0.113	0.148	0.131	0.179	0.166
T2-Total	2.983	2.987	2.986	2.994	2.968	2.986	2.974	2.968	2.969	2.972	2.971	2.971	2.976	3.000	2.998	3.009	2.975	2.983	2.970	2.977	2.969
Pb^{2+}	0.001	0.000	0.001	0.000	0.000	0.000	0.000	0.000	0.001	0.000	0.001	0.000	0.001	0.000	0.002	0.000	0.000	0.001	0.000	0.000	0.000
Cs^{+}	0.003	0.002	0.002	0.000	0.003	0.003	0.005	0.004	0.002	0.003	0.019	0.001	0.016	0.004	0.011	0.004	0.003	0.002	0.003	0.004	0.002
K^{+}	0.001	0.000	0.001	0.002	0.003	0.004	0.004	0.004	0.003	0.003	0.004	0.005	0.004	0.004	0.004	0.005	0.003	0.003	0.002	0.004	0.004
Na^{+}	0.108	0.079	0.085	0.123	0.096	0.181	0.266	0.194	0.245	0.179	0.222	0.104	0.263	0.223	0.217	0.216	0.107	0.143	0.126	0.171	0.160
2a Site total	0.112	0.081	0.090	0.126	0.102	0.189	0.275	0.202	0.251	0.185	0.246	0.110	0.283	0.230	0.234	0.224	0.113	0.148	0.131	0.179	0.166
Cl^{-}	0.001	0.000	0.000	0.000	0.001	0.001	0.001	0.002	0.000	0.002	0.001	0.000	0.000	0.000	0.000	0.002	0.001	0.000	0.001	0.000	0.002
A-Total	0.001	0.000	0.000	0.000	0.001	0.001	0.001	0.002	0.000	0.002	0.001	0.000	0.000	0.000	0.000	0.002	0.001	0.000	0.001	0.000	0.002

II.II.III MICROCLINE

Sample	#2cB9				#4B1				#4B2							#4B3					#4B4			#4B5	#4B8			#5B2			
Zone	Pegmatite 1																														
wt%	1	2	3	4	4	5	6	10	2	6	8	10	11	17	18	3	5	6	7	11	1	3	5	2	2	3	4	1	2	4	5
SiO_2	64.63	64.15	63.86	63.66	63.00	62.31	63.50	63.37	64.04	63.86	63.56	64.36	64.01	64.34	63.44	63.03	63.10	62.95	62.81	62.82	63.41	63.22	62.67	63.77	62.88	63.32	63.06	64.33	65.37	64.06	63.90
Al_2O_3	17.85	17.94	17.65	17.90	17.98	17.75	17.80	16.89	17.29	17.70	17.59	17.53	17.75	17.56	17.47	17.45	17.50	17.39	17.82	17.52	17.58	17.36	17.24	17.77	17.96	17.77	17.86	18.52	18.06	17.62	18.02
P_2O_5	0.06	0.15	0.20	0.20	0.29	0.35	0.36	0.00	0.05	0.25	0.29	0.05	0.25	0.08	0.04	0.08	0.12	0.04	0.27	0.09	0.03	0.45	0.27	0.30	0.32	0.18	0.28	0.28	0.00	0.21	0.20
Fe_2O_3	0.00	0.01	0.00	0.00	0.00	0.00	0.00	0.00	0.00	0.00	0.00	0.00	0.00	0.00	0.00	0.00	0.00	0.00	0.00	0.00	0.00	0.00	0.00	0.00	0.00	0.00	0.00	0.00	0.00	0.00	0.00
K_2O	15.80	15.68	15.79	15.72	15.48	15.27	15.54	15.39	15.37	15.13	14.87	15.48	15.50	15.54	14.79	15.66	15.60	15.54	14.88	15.03	15.64	15.46	15.32	15.18	15.34	15.41	15.53	15.81	15.88	15.06	15.79
Na_2O	0.27	0.29	0.37	0.34	0.32	0.26	0.32	0.29	0.31	0.54	0.66	0.30	0.34	0.30	0.86	0.23	0.19	0.27	0.58	0.54	0.24	0.28	0.46	0.49	0.28	0.32	0.31	0.39	0.32	0.91	0.38
CaO	0.00	0.16	0.00	0.03	0.01	0.02	0.02	0.02	0.01	0.00	0.01	0.00	0.00	0.00	0.01	0.01	0.00	0.00	0.03	0.00	0.00	0.01	0.02	0.01	0.08	0.01	0.00	0.00	0.02	0.00	0.00
BaO	0.00	0.00	0.02	0.09	0.00	0.08	0.00	0.00	0.00	0.00	0.00	0.00	0.00	0.00	0.00	0.00	0.03	0.06	0.00	0.03	0.00	0.00	0.00	0.00	0.00	0.00	0.00	0.00	0.00	0.00	0.04
SrO	0.00	0.12	0.00	0.11	0.00	0.02	0.00	0.00	0.10	0.00	0.03	0.15	0.02	0.05	0.11	0.01	0.08	0.02	0.07	0.05	0.00	0.00	0.13	0.08	0.03	0.00	0.00	0.00	0.01	0.00	0.07
Cs_2O	0.00	0.00	0.00	0.00	0.00	0.00	0.00	0.01	0.05	0.01	0.02	0.07	0.06	0.03	0.00	0.00	0.03	0.04	0.08	0.04	0.00	0.04	0.00	0.02	0.00	0.03	0.05	0.00	0.00	0.00	0.00
ZnO	0.14	0.08	0.00	0.00	0.00	0.10	0.02	0.00	0.00	0.10	0.00	0.00	0.08	0.00	0.00	0.00	0.14	0.02	0.00	0.07	0.04	0.00	0.00	0.00	0.03	0.11	0.00	0.00	0.01	0.00	0.00
MnO	0.01	0.00	0.00	0.00	0.02	0.00	0.02	0.01	0.06	0.03	0.00	0.00	0.00	0.03	0.00	0.02	0.00	0.04	0.00	0.05	0.04	0.01	0.03	0.01	0.03	0.00	0.04	0.00	0.01	0.00	0.01
Total	98.76	98.59	97.90	98.05	97.10	96.16	97.58	95.99	97.28	97.63	97.04	97.94	98.01	97.93	96.71	96.48	96.78	96.38	96.52	96.24	96.99	96.82	96.13	97.63	96.95	97.14	97.13	99.33	99.69	97.87	98.40
a.p.f.u (Calculus done on the basis of 8 Oxygens)																															
Si^{4+}	3.016	3.002	3.008	2.998	2.989	2.986	2.997	3.040	3.032	3.008	3.009	3.027	3.008	3.025	3.017	3.013	3.009	3.016	2.994	3.008	3.014	3.005	3.006	3.004	2.987	3.003	2.993	2.984	3.019	3.011	2.997
Al^{3+}	0.982	0.989	0.980	0.994	1.005	1.003	0.990	0.955	0.965	0.983	0.981	0.972	0.983	0.973	0.979	0.983	0.984	0.982	1.001	0.989	0.985	0.972	0.975	0.986	1.005	0.993	0.999	1.013	0.983	0.976	0.996
P^{5+}	0.002	0.006	0.008	0.008	0.011	0.014	0.015	0.000	0.002	0.010	0.012	0.002	0.010	0.003	0.002	0.003	0.005	0.002	0.011	0.004	0.001	0.018	0.011	0.012	0.013	0.007	0.011	0.011	0.000	0.009	0.008
Fe^{3+}	0.001	0.002	0.001	0.000	0.001	0.002	0.000	0.001	0.000	0.000	0.001	0.000	0.001	0.000	0.001	0.001	0.002	0.000	0.001	0.000	0.003	0.003	0.002	0.000	0.002	0.001	0.001	0.000	0.001	0.000	0.000
Total-T	4.001	3.999	3.996	3.999	4.006	4.005	4.001	3.996	3.999	4.001	4.002	4.001	4.002	4.001	3.999	4.001	4.000	3.999	4.006	4.001	4.003	3.999	3.994	4.003	4.007	4.004	4.004	4.008	4.004	3.995	4.001
K^+	0.941	0.936	0.949	0.944	0.937	0.934	0.936	0.942	0.928	0.909	0.898	0.929	0.929	0.932	0.897	0.955	0.949	0.950	0.905	0.918	0.948	0.938	0.937	0.912	0.930	0.933	0.940	0.936	0.936	0.903	0.945
Na^+	0.025	0.026	0.034	0.031	0.030	0.024	0.030	0.027	0.029	0.049	0.061	0.027	0.031	0.027	0.079	0.022	0.018	0.025	0.054	0.050	0.022	0.025	0.043	0.045	0.026	0.029	0.028	0.035	0.029	0.083	0.035
Cs^+	0.000	0.000	0.000	0.000	0.000	0.000	0.000	0.000	0.001	0.000	0.000	0.001	0.001	0.001	0.000	0.000	0.001	0.001	0.002	0.001	0.000	0.001	0.000	0.000	0.000	0.001	0.001	0.000	0.000	0.000	0.000
Ca^{2+}	0.000	0.008	0.000	0.001	0.001	0.001	0.001	0.001	0.001	0.000	0.001	0.000	0.000	0.000	0.001	0.001	0.000	0.000	0.002	0.000	0.000	0.000	0.001	0.001	0.004	0.000	0.000	0.000	0.001	0.000	0.000
Ba^{2+}	0.000	0.000	0.000	0.002	0.000	0.002	0.000	0.000	0.000	0.000	0.000	0.000	0.000	0.000	0.000	0.000	0.001	0.001	0.000	0.001	0.000	0.000	0.000	0.000	0.000	0.000	0.000	0.000	0.000	0.000	0.001
Sr^{2+}	0.000	0.003	0.000	0.003	0.000	0.001	0.000	0.000	0.003	0.000	0.001	0.004	0.001	0.001	0.003	0.000	0.002	0.001	0.002	0.001	0.000	0.000	0.004	0.002	0.001	0.000	0.000	0.000	0.000	0.000	0.002
Mn^{2+}	0.001	0.000	0.000	0.000	0.001	0.000	0.001	0.000	0.002	0.001	0.000	0.000	0.000	0.001	0.000	0.001	0.000	0.002	0.000	0.002	0.002	0.001	0.001	0.001	0.001	0.000	0.002	0.000	0.001	0.000	0.000
Zn^{2+}	0.005	0.003	0.000	0.000	0.000	0.004	0.001	0.000	0.000	0.004	0.000	0.000	0.003	0.000	0.000	0.000	0.005	0.001	0.000	0.002	0.001	0.000	0.000	0.000	0.001	0.004	0.000	0.000	0.000	0.000	0.000
Total-A	0.971	0.977	0.983	0.981	0.968	0.965	0.968	0.970	0.963	0.964	0.961	0.962	0.965	0.963	0.980	0.978	0.975	0.980	0.963	0.976	0.974	0.965	0.986	0.960	0.963	0.967	0.971	0.971	0.967	0.987	0.982
% An	0.0	0.8	0.0	0.1	0.1	0.1	0.1	0.1	0.1	0.0	0.1	0.0	0.0	0.0	0.1	0.1	0.0	0.0	0.2	0.0	0.0	0.0	0.1	0.1	0.4	0.0	0.0	0.0	0.1	0.0	0.0
% Ab	2.5	2.7	3.5	3.2	3.1	2.5	3.1	2.7	3.0	5.1	6.3	2.8	3.3	2.8	8.1	2.2	1.8	2.6	5.6	5.2	2.3	2.6	4.3	4.6	2.7	3.0	2.9	3.6	3.0	8.4	3.5
% Or	97.5	96.4	96.5	96.7	96.9	97.4	96.8	97.1	96.9	94.8	93.6	97.2	96.7	97.2	91.8	97.7	98.2	97.4	94.3	94.8	97.7	97.3	95.6	95.3	96.9	96.9	97.1	96.4	96.9	91.5	96.5

Sample	#5B3		#9bB8				#13B4		
Zone	Pegmatite 1						Pegmatite 2		
wt%	1	2	1	2	3	4	1	2	4
SiO_2	64.83	64.30	63.96	63.71	63.55	63.66	64.44	64.10	64.38
Al_2O_3	18.18	17.85	18.27	18.12	18.55	18.26	18.55	18.35	18.77
P_2O_5	0.12	0.15	0.31	0.40	0.31	0.30	0.31	0.26	0.34
Fe_2O_3	0.00	0.00	0.00	0.00	0.00	0.00	0.00	0.00	0.00
K_2O	15.84	15.06	15.43	15.67	14.64	14.97	15.08	15.08	15.52
Na_2O	0.33	0.65	0.44	0.43	0.95	0.80	0.92	0.70	0.51
CaO	0.00	0.04	0.00	0.01	0.01	0.01	0.00	0.00	0.00
BaO	0.00	0.04	0.03	0.00	0.00	0.00	0.00	0.03	0.04
SrO	0.09	0.00	0.12	0.00	0.00	0.02	0.00	0.00	0.00
Cs_2O	0.00	0.00	0.00	0.00	0.00	0.00	0.00	0.00	0.00
ZnO	0.04	0.00	0.00	0.16	0.01	0.06	0.07	0.10	0.19
MnO	0.00	0.00	0.00	0.00	0.00	0.00	0.00	0.05	0.00
Total	99.43	98.09	98.55	98.49	98.01	98.08	99.38	98.68	99.74
a.p.f.u (Calculus done on the basis of 8 Oxygens)									
Si^{4+}	3.005	3.012	2.988	2.984	2.976	2.984	2.982	2.988	2.974
Al^{3+}	0.993	0.985	1.006	1.000	1.024	1.009	1.012	1.008	1.022
P^{5+}	0.005	0.006	0.012	0.016	0.012	0.012	0.012	0.010	0.013
Fe^{3+}	0.001	0.000	0.000	0.001	0.000	0.001	0.000	0.000	0.000
Total-T	4.004	4.004	4.007	4.000	4.012	4.006	4.005	4.006	4.009
K^+	0.937	0.900	0.920	0.936	0.875	0.895	0.890	0.897	0.914
Na^+	0.030	0.059	0.040	0.039	0.086	0.073	0.083	0.063	0.046
Cs^+	0.000	0.000	0.000	0.000	0.000	0.000	0.000	0.000	0.000
Ca^{2+}	0.000	0.002	0.000	0.000	0.000	0.000	0.000	0.000	0.000
Ba^{2+}	0.000	0.001	0.001	0.000	0.000	0.000	0.000	0.001	0.001
Sr^{2+}	0.002	0.000	0.003	0.000	0.000	0.001	0.000	0.000	0.000
Mn^{2+}	0.000	0.000	0.000	0.000	0.000	0.000	0.000	0.002	0.000
Zn^{2+}	0.001	0.000	0.000	0.006	0.000	0.002	0.003	0.004	0.006
Total-A	0.970	0.962	0.963	0.981	0.962	0.971	0.976	0.967	0.967
% An	0.0	0.2	0.0	0.0	0.0	0.0	0.0	0.0	0.0
% Ab	3.1	6.1	4.1	4.0	9.0	7.5	8.5	6.6	4.8
% Or	96.9	93.7	95.9	96.0	91.0	92.4	91.5	93.4	95.2

II.II.IV ALBITE

Sample	#1B2				#2cB5			#2cB6	#2cB7			#4B1						#4B2								#4B5	#4B8	#5B1			#5B2
Zone	Pegmatite 1																														
wt%	1	2	3	4	1	2	3	3	1	2	3	1	2	4	5	6	7	1	3	7	14	15	16	2	3	2	2	1	2	3	1
SiO_2	68.33	67.42	67.81	67.41	67.76	66.23	68.00	67.90	67.62	66.65	67.36	67.45	67.38	67.89	67.29	66.56	67.24	67.82	67.96	67.42	67.88	67.61	67.80	67.06	67.59	67.21	65.74	68.54	68.73	68.33	68.33
Al_2O_3	19.11	19.03	19.31	19.12	19.49	19.20	19.32	19.44	19.26	18.88	19.34	18.66	18.52	18.95	19.01	18.57	19.20	18.70	18.59	18.57	18.56	18.60	18.45	18.84	18.59	18.22	19.21	18.84	19.05	19.23	19.50
P_2O_5	0.14	0.10	0.11	0.21	0.12	0.32	0.02	0.15	0.09	0.15	0.14	0.00	0.00	0.02	0.23	0.00	0.31	0.10	0.08	0.16	0.07	0.00	0.08	0.22	0.01	0.01	0.22	0.00	0.00	0.00	0.10
Fe_2O_3	0.01	0.01	0.00	0.00	0.00	0.03	0.00	0.00	0.00	0.02	0.03	0.00	0.00	0.00	0.00	0.00	0.01	0.02	0.00	0.01	0.02	0.00	0.00	0.04	0.04	0.00	0.01	0.03	0.00	0.02	0.00
K_2O	0.07	0.07	0.10	0.09	0.10	0.11	0.12	0.08	0.16	0.14	0.19	0.13	0.10	0.11	0.10	0.13	0.08	0.11	0.11	0.18	0.12	0.13	0.15	0.28	0.13	0.12	0.17	0.06	0.09	0.08	0.08
Na_2O	11.49	11.34	11.14	11.22	11.63	10.99	11.68	11.14	11.45	11.32	11.71	11.16	11.05	11.33	11.23	11.10	11.30	11.11	11.29	11.23	11.29	11.25	11.03	11.34	11.40	11.07	11.29	11.40	11.70	11.63	11.61
CaO	0.06	0.05	0.13	0.06	0.05	0.15	0.06	0.06	0.09	0.06	0.06	0.01	0.04	0.00	0.06	0.02	0.08	0.00	0.00	0.00	0.03	0.03	0.00	0.10	0.02	0.03	0.11	0.03	0.01	0.01	0.03
BaO	0.10	0.06	0.01	0.00	0.00	0.01	0.03	0.00	0.00	0.00	0.00	0.00	0.00	0.05	0.00	0.00	0.01	0.06	0.00	0.00	0.03	0.00	0.00	0.00	0.00	0.00	0.00	0.07	0.00	0.00	0.00
SrO	0.04	0.04	0.00	0.00	0.05	0.00	0.00	0.01	0.10	0.06	0.04	0.13	0.00	0.05	0.09	0.05	0.00	0.14	0.12	0.05	0.04	0.02	0.11	0.05	0.13	0.00	0.17	0.04	0.00	0.00	0.06
Cs_2O	0.00	0.00	0.00	0.00	0.00	0.00	0.00	0.00	0.00	0.00	0.00	0.00	0.00	0.03	0.00	0.00	0.03	0.00	0.00	0.01	0.00	0.09	0.04	0.00	0.00	0.06	0.04	0.00	0.00	0.00	0.00
ZnO	0.04	0.01	0.07	0.00	0.05	0.06	0.01	0.03	0.06	0.16	0.06	0.06	0.16	0.00	0.00	0.04	0.02	0.00	0.00	0.00	0.02	0.17	0.04	0.00	0.00	0.15	0.00	0.06	0.00	0.00	0.00
MnO	0.00	0.03	0.00	0.03	0.03	0.01	0.00	0.00	0.01	0.00	0.00	0.01	0.00	0.01	0.00	0.03	0.00	0.00	0.06	0.01	0.02	0.02	0.00	0.06	0.07	0.01	0.00	0.01	0.04	0.00	0.00
Total	99.39	98.15	98.69	98.14	99.28	97.11	99.23	98.81	98.84	97.42	98.93	97.63	97.26	98.43	98.01	96.50	98.28	98.06	98.23	97.64	98.07	97.91	97.70	97.98	97.97	96.87	96.96	99.08	99.61	99.29	99.70
a.p.f.u (calculus done on the basis of 8 Oxygens)																															
Si^{4+}	3.002	2.999	2.996	2.994	2.983	2.976	2.994	2.994	2.991	2.991	2.979	3.015	3.020	3.010	2.995	3.010	2.985	3.016	3.019	3.012	3.019	3.017	3.025	2.992	3.015	3.027	2.968	3.018	3.011	3.004	2.992
Al^{3+}	0.990	0.998	1.006	1.001	1.011	1.017	1.002	1.010	1.004	0.998	1.008	0.983	0.978	0.990	0.997	0.990	1.005	0.980	0.973	0.978	0.973	0.978	0.971	0.991	0.977	0.967	1.022	0.978	0.983	0.996	1.006
p^{5+}	0.005	0.004	0.004	0.008	0.004	0.012	0.001	0.006	0.003	0.006	0.005	0.000	0.000	0.001	0.009	0.000	0.012	0.004	0.003	0.006	0.003	0.000	0.003	0.008	0.000	0.001	0.008	0.000	0.000	0.000	0.004
Fe^{3+}	0.000	0.000	0.000	0.000	0.000	0.001	0.000	0.000	0.000	0.001	0.001	0.000	0.000	0.000	0.000	0.000	0.000	0.001	0.000	0.000	0.001	0.000	0.000	0.001	0.001	0.000	0.000	0.001	0.000	0.001	0.000
Total-T	3.997	4.000	4.006	4.003	3.999	4.006	3.997	4.010	3.998	3.996	3.994	3.999	3.998	4.001	4.000	4.000	4.002	4.000	3.995	3.997	3.996	3.995	3.999	3.992	3.993	3.995	3.999	3.997	3.995	4.000	4.002
K^{+}	0.004	0.004	0.006	0.005	0.006	0.006	0.007	0.005	0.009	0.008	0.011	0.008	0.006	0.006	0.006	0.008	0.005	0.006	0.006	0.010	0.007	0.007	0.009	0.016	0.007	0.007	0.010	0.004	0.005	0.004	0.004
Na^{+}	0.979	0.978	0.954	0.966	0.993	0.958	0.997	0.953	0.982	0.985	1.004	0.968	0.960	0.974	0.969	0.973	0.973	0.958	0.973	0.973	0.973	0.973	0.954	0.981	0.986	0.967	0.989	0.974	0.994	0.991	0.985
Cs^{+}	0.000	0.000	0.000	0.000	0.000	0.000	0.000	0.000	0.000	0.000	0.000	0.000	0.000	0.001	0.000	0.000	0.001	0.000	0.000	0.000	0.000	0.002	0.001	0.000	0.000	0.001	0.001	0.000	0.000	0.000	0.000
Ca^{2+}	0.003	0.003	0.006	0.003	0.002	0.007	0.003	0.003	0.004	0.003	0.003	0.001	0.002	0.000	0.003	0.001	0.004	0.000	0.000	0.000	0.001	0.001	0.000	0.005	0.001	0.002	0.005	0.001	0.001	0.001	0.002
Ba^{2+}	0.002	0.001	0.000	0.000	0.000	0.000	0.001	0.000	0.000	0.000	0.000	0.000	0.000	0.001	0.000	0.000	0.000	0.001	0.000	0.000	0.001	0.000	0.000	0.000	0.000	0.000	0.000	0.001	0.000	0.000	0.000
Sr^{2+}	0.001	0.001	0.000	0.000	0.001	0.000	0.000	0.000	0.003	0.001	0.001	0.003	0.000	0.001	0.002	0.001	0.000	0.004	0.003	0.001	0.001	0.001	0.003	0.001	0.003	0.000	0.005	0.001	0.000	0.000	0.001
Mn^{2+}	0.000	0.001	0.000	0.001	0.001	0.001	0.000	0.000	0.000	0.000	0.000	0.000	0.000	0.000	0.000	0.001	0.000	0.000	0.002	0.000	0.001	0.001	0.000	0.002	0.003	0.000	0.000	0.000	0.001	0.000	0.000
Zn^{2+}	0.001	0.000	0.002	0.000	0.002	0.002	0.000	0.001	0.002	0.005	0.002	0.002	0.005	0.000	0.000	0.001	0.001	0.000	0.000	0.000	0.001	0.006	0.001	0.000	0.000	0.005	0.000	0.002	0.000	0.000	0.000
Total-A	0.989	0.988	0.968	0.975	1.005	0.974	1.007	0.961	1.000	1.002	1.021	0.982	0.973	0.983	0.980	0.985	0.983	0.969	0.984	0.985	0.984	0.990	0.967	1.005	1.000	0.981	1.009	0.983	1.001	0.996	0.992
% An	0.3	0.3	0.7	0.3	0.2	0.7	0.3	0.3	0.4	0.3	0.3	0.1	0.2	0.0	0.3	0.1	0.4	0.0	0.0	0.0	0.1	0.1	0.0	0.5	0.1	0.2	0.5	0.1	0.1	0.1	0.2
% Ab	99.3	99.3	98.8	99.2	99.2	98.6	99.1	99.2	98.7	98.9	98.7	99.2	99.2	99.4	99.1	99.1	99.1	99.4	99.4	99.0	99.2	99.1	99.1	97.9	99.2	99.1	98.5	99.5	99.4	99.5	99.4
% Or	0.4	0.4	0.6	0.5	0.6	0.7	0.7	0.5	0.9	0.8	1.1	0.8	0.6	0.6	0.6	0.8	0.5	0.6	0.6	1.0	0.7	0.7	0.9	1.6	0.7	0.7	1.0	0.4	0.5	0.4	0.4

Sample	#5B2	#7bB7				#8bB6	#8bB7			#8bB8		#9bB1							#9bB2									#9cB1			
Zone	Pegmatite 1																														
wt%	2	1	2	3	4	3	1	2	3	1	2	1	2	3	4	5	6	7	5	6	10	11	12	13	14	16	18	1	2	3	4
SiO_2	68.51	67.33	67.32	67.84	68.46	67.84	68.16	68.31	67.64	66.59	66.58	67.33	67.68	67.39	65.67	67.23	66.53	66.54	66.81	67.24	66.65	66.23	67.23	67.40	68.01	67.45	68.04	66.82	66.93	66.97	67.61
Al_2O_3	19.39	19.37	19.20	19.06	19.16	18.75	18.86	18.85	18.65	18.60	19.04	18.74	19.38	19.36	18.83	18.84	19.03	18.72	18.62	18.21	18.20	18.36	18.11	18.06	17.53	18.56	18.74	19.16	18.99	19.44	19.17
P_2O_5	0.12	0.37	0.39	0.00	0.10	0.20	0.08	0.04	0.02	0.07	0.24	0.24	0.31	0.35	0.28	0.04	0.16	0.19	0.05	0.28	0.24	0.30	0.22	0.00	0.06	0.03	0.10	0.45	0.28	0.16	0.07
Fe_2O_3	0.01	0.00	0.00	0.00	0.00	0.03	0.02	0.04	0.03	0.00	0.02	0.04	0.03	0.02	0.03	0.03	0.00	0.03	0.01	0.05	0.00	0.02	0.01	0.03	0.05	0.00	0.00	0.08	0.07	0.00	0.01
K_2O	0.07	0.08	0.09	0.09	0.09	0.08	0.14	0.12	0.08	0.07	0.08	0.06	0.06	0.08	0.06	0.12	0.11	0.05	0.13	0.13	0.10	0.11	0.10	0.14	0.08	0.09	0.11	0.11	0.15	0.08	0.08
Na_2O	11.67	11.25	11.24	11.57	11.68	11.03	11.08	11.21	11.32	10.99	11.17	11.13	11.23	11.28	11.03	11.35	10.96	11.25	11.20	11.13	11.11	11.07	11.34	11.59	11.10	11.04	11.21	11.26	11.46	11.21	11.36
CaO	0.03	0.08	0.04	0.01	0.00	0.04	0.12	0.12	0.01	0.06	0.05	0.37	0.18	0.20	0.10	0.04	0.25	0.01	0.01	0.07	0.16	0.15	0.08	0.02	0.02	0.01	0.02	0.24	0.19	0.19	0.06
BaO	0.00	0.06	0.00	0.00	0.08	0.03	0.00	0.00	0.00	0.00	0.08	0.00	0.00	0.10	0.05	0.00	0.00	0.03	0.03	0.07	0.02	0.00	0.05	0.01	0.03	0.00	0.00	0.00	0.07	0.00	0.00
SrO	0.00	0.00	0.07	0.12	0.03	0.20	0.06	0.00	0.00	0.05	0.00	0.09	0.00	0.00	0.00	0.12	0.00	0.00	0.00	0.00	0.00	0.00	0.02	0.20	0.05	0.08	0.00	0.03	0.00	0.08	0.11
Cs_2O	0.00	0.00	0.00	0.00	0.00	0.00	0.00	0.00	0.00	0.00	0.00	0.00	0.00	0.00	0.00	0.00	0.06	0.03	0.00	0.01	0.05	0.00	0.00	0.04	0.00	0.08	0.01	0.00	0.00	0.00	0.00
ZnO	0.03	0.11	0.00	0.00	0.00	0.07	0.02	0.00	0.00	0.00	0.01	0.00	0.08	0.08	0.10	0.00	0.00	0.17	0.00	0.08	0.12	0.00	0.00	0.00	0.08	0.01	0.00	0.00	0.14	0.17	0.11
MnO	0.00	0.06	0.03	0.00	0.00	0.05	0.00	0.00	0.03	0.02	0.00	0.00	0.00	0.00	0.00	0.00	0.00	0.03	0.00	0.00	0.02	0.02	0.01	0.01	0.00	0.00	0.01	0.11	0.06	0.00	0.01
Total	99.81	98.68	98.39	98.70	99.59	98.29	98.53	98.68	97.79	96.46	97.27	97.99	98.96	98.86	96.15	97.77	97.09	97.05	96.85	97.26	96.67	96.25	97.16	97.49	97.00	97.34	98.25	98.26	98.34	98.30	98.59
a.p.f.u (calculus done on the basis of 8 Oxygens)																															
Si^{4+}	2.995	2.978	2.984	3.003	3.002	3.011	3.015	3.017	3.016	3.009	2.987	2.999	2.983	2.978	2.982	3.003	2.990	2.995	3.009	3.017	3.010	3.001	3.019	3.025	3.055	3.021	3.017	2.972	2.980	2.978	2.996
Al^{3+}	0.999	1.010	1.003	0.994	0.990	0.981	0.983	0.981	0.980	0.991	1.007	0.984	1.007	1.008	1.008	0.992	1.008	0.993	0.988	0.963	0.969	0.981	0.959	0.955	0.928	0.980	0.979	1.004	0.997	1.019	1.001
P^{5+}	0.005	0.014	0.015	0.000	0.004	0.008	0.003	0.001	0.001	0.003	0.009	0.009	0.012	0.013	0.011	0.002	0.006	0.007	0.002	0.010	0.009	0.011	0.008	0.000	0.002	0.001	0.004	0.017	0.011	0.006	0.003
Fe^{3+}	0.000	0.000	0.000	0.000	0.000	0.001	0.001	0.001	0.001	0.000	0.001	0.001	0.001	0.001	0.001	0.001	0.000	0.001	0.001	0.002	0.000	0.001	0.000	0.001	0.002	0.000	0.000	0.003	0.002	0.000	0.000
Total-T	3.999	4.001	4.002	3.997	3.996	4.000	4.002	4.001	3.999	4.003	4.004	3.993	4.002	3.999	4.002	3.998	4.004	3.996	4.000	3.991	3.989	3.994	3.986	3.981	3.987	4.002	4.000	3.996	3.989	4.002	4.000
K^+	0.004	0.004	0.005	0.005	0.005	0.004	0.008	0.007	0.005	0.004	0.004	0.004	0.003	0.005	0.004	0.007	0.007	0.003	0.007	0.007	0.006	0.006	0.006	0.008	0.004	0.005	0.006	0.006	0.009	0.004	0.005
Na^+	0.989	0.964	0.966	0.993	0.993	0.949	0.950	0.960	0.979	0.963	0.972	0.961	0.960	0.966	0.971	0.983	0.955	0.982	0.978	0.968	0.973	0.973	0.988	1.008	0.966	0.959	0.964	0.971	0.989	0.966	0.976
Cs^+	0.000	0.000	0.000	0.000	0.000	0.000	0.000	0.000	0.000	0.000	0.000	0.000	0.000	0.000	0.000	0.000	0.001	0.001	0.000	0.000	0.001	0.000	0.000	0.001	0.000	0.002	0.000	0.000	0.000	0.000	0.000
Ca^{2+}	0.001	0.004	0.002	0.001	0.000	0.002	0.006	0.006	0.001	0.003	0.003	0.018	0.009	0.010	0.005	0.002	0.012	0.001	0.000	0.004	0.008	0.007	0.004	0.001	0.001	0.000	0.001	0.012	0.009	0.009	0.003
Ba^{2+}	0.000	0.001	0.000	0.000	0.001	0.001	0.000	0.000	0.000	0.000	0.001	0.000	0.000	0.002	0.001	0.000	0.000	0.001	0.001	0.001	0.000	0.000	0.001	0.000	0.001	0.000	0.000	0.000	0.001	0.000	0.000
Sr^{2+}	0.000	0.000	0.002	0.003	0.001	0.005	0.001	0.000	0.000	0.001	0.000	0.002	0.000	0.000	0.000	0.003	0.000	0.000	0.000	0.000	0.000	0.000	0.000	0.005	0.001	0.002	0.000	0.001	0.000	0.002	0.003
Mn^{2+}	0.000	0.002	0.001	0.000	0.000	0.002	0.000	0.000	0.001	0.001	0.000	0.000	0.000	0.000	0.000	0.000	0.000	0.001	0.000	0.000	0.001	0.001	0.000	0.000	0.000	0.000	0.001	0.004	0.002	0.000	0.000
Zn^{2+}	0.001	0.003	0.000	0.000	0.000	0.002	0.001	0.000	0.000	0.000	0.000	0.000	0.003	0.003	0.003	0.000	0.000	0.006	0.000	0.003	0.004	0.000	0.000	0.000	0.003	0.000	0.000	0.000	0.005	0.006	0.004
Total-A	0.995	0.979	0.976	1.002	1.000	0.965	0.966	0.972	0.985	0.972	0.981	0.985	0.974	0.985	0.984	0.995	0.975	0.993	0.986	0.983	0.992	0.987	0.999	1.024	0.976	0.968	0.972	0.993	1.015	0.987	0.990
% An	0.1	0.4	0.2	0.1	0.0	0.2	0.6	0.6	0.1	0.3	0.3	1.8	0.9	1.0	0.5	0.2	1.2	0.1	0.0	0.4	0.8	0.7	0.4	0.1	0.1	0.0	0.1	1.2	0.9	0.9	0.3
% Ab	99.5	99.2	99.3	99.4	99.5	99.4	98.6	98.7	99.4	99.3	99.3	97.8	98.8	98.6	99.2	99.1	98.1	99.6	99.2	98.9	98.7	98.6	99.0	99.1	99.4	99.5	99.3	98.2	98.2	98.6	99.2
% Or	0.4	0.4	0.5	0.5	0.5	0.5	0.8	0.7	0.5	0.4	0.4	0.4	0.3	0.5	0.4	0.7	0.7	0.3	0.8	0.8	0.6	0.6	0.6	0.8	0.5	0.5	0.6	0.6	0.9	0.4	0.5

Sample	#9cB2			#9cB6		#11cB1				#13B1	#13B2	#13B3			#13B5		#13B6		#14B1					#14B2				#14B3				#17B1
Zone	Pegmatite 1									Pegmatite 2																						
wt%	1	2	3	1	2	1	2	3	4	1	4	2	3	4	1	2	1	2	1	2	3	4	5	1	2	3	4	1	2	3	4	2
SiO_2	67.19	68.67	67.55	66.62	67.36	67.78	67.54	67.06	66.41	67.15	67.26	66.13	66.44	66.65	66.62	66.89	67.55	66.41	67.90	67.79	68.17	67.81	67.77	67.49	67.66	67.81	67.90	67.54	67.58	66.95	66.74	68.20
Al_2O_3	19.48	19.06	19.43	19.22	19.42	19.21	18.66	19.03	19.20	19.00	18.61	18.99	18.96	19.72	19.28	19.01	18.92	18.90	18.96	18.81	19.26	19.15	19.23	18.42	18.46	18.63	19.00	18.61	18.68	18.81	18.84	18.58
P_2O_5	0.27	0.03	0.58	0.33	0.29	0.07	0.03	0.25	0.28	0.30	0.23	0.32	0.27	0.22	0.27	0.20	0.07	0.20	0.10	0.06	0.20	0.20	0.21	0.00	0.08	0.00	0.13	0.18	0.04	0.19	0.12	0.00
Fe_2O_3	0.03	0.01	0.02	0.00	0.00	0.00	0.04	0.05	0.00	0.07	0.02	0.00	0.00	0.00	0.00	0.00	0.08	0.02	0.04	0.02	0.02	0.02	0.00	0.00	0.00	0.02	0.01	0.00	0.05	0.00	0.00	0.03
K_2O	0.09	0.06	0.09	0.14	0.11	0.08	0.07	0.08	0.06	0.10	0.12	0.08	0.09	0.12	0.15	0.06	0.08	0.14	0.08	0.07	0.11	0.05	0.09	0.11	0.10	0.08	0.10	0.08	0.08	0.10	0.10	0.13
Na_2O	11.28	11.34	11.60	11.19	11.18	11.43	11.25	11.29	11.23	11.44	10.88	11.20	10.92	11.05	10.86	11.21	11.24	11.15	11.29	11.45	11.59	11.88	11.53	10.98	11.31	11.25	11.28	11.20	11.36	11.06	11.15	11.20
CaO	0.16	0.00	0.56	0.16	0.20	0.05	0.00	0.10	0.21	0.10	0.23	0.27	0.09	0.33	0.31	0.17	0.09	0.10	0.05	0.04	0.09	0.05	0.07	0.04	0.06	0.01	0.04	0.01	0.04	0.08	0.13	0.01
BaO	0.00	0.00	0.04	0.00	0.00	0.00	0.02	0.00	0.05	0.01	0.01	0.00	0.00	0.00	0.00	0.05	0.00	0.00	0.00	0.05	0.00	0.00	0.00	0.00	0.00	0.00	0.03	0.08	0.05	0.00	0.04	0.00
SrO	0.00	0.00	0.00	0.04	0.00	0.12	0.13	0.10	0.06	0.00	0.00	0.02	0.00	0.06	0.02	0.02	0.00	0.07	0.01	0.14	0.05	0.03	0.05	0.11	0.05	0.04	0.12	0.00	0.07	0.05	0.13	0.00
Cs_2O	0.00	0.00	0.00	0.00	0.00	0.00	0.00	0.08	0.00	0.00	0.00	0.00	0.04	0.00	0.00	0.01	0.02	0.00	0.00	0.00	0.00	0.00	0.00	0.00	0.00	0.00	0.00	0.00	0.00	0.00	0.00	0.00
ZnO	0.00	0.00	0.06	0.06	0.05	0.00	0.00	0.09	0.00	0.04	0.03	0.01	0.00	0.09	0.00	0.14	0.04	0.00	0.00	0.00	0.00	0.04	0.00	0.00	0.02	0.03	0.11	0.00	0.00	0.00	0.00	0.00
MnO	0.00	0.00	0.00	0.00	0.01	0.02	0.00	0.00	0.00	0.03	0.02	0.00	0.02	0.08	0.00	0.00	0.03	0.00	0.00	0.02	0.03	0.00	0.01	0.00	0.00	0.00	0.05	0.00	0.00	0.00	0.05	0.00
Total	98.50	99.17	99.91	97.76	98.61	98.76	97.74	98.11	97.51	98.23	97.40	97.03	96.82	98.33	97.51	97.77	98.11	96.98	98.42	98.43	99.52	99.23	98.95	97.14	97.74	97.86	98.76	97.70	97.96	97.23	97.29	98.15
a.p.f.u (calculus done on the basis of 8 Oxygens)																																
Si^{4+}	2.977	3.016	2.958	2.976	2.980	2.997	3.015	2.988	2.975	2.986	3.009	2.976	2.990	2.963	2.979	2.989	3.005	2.990	3.007	3.009	2.992	2.987	2.990	3.026	3.020	3.021	3.002	3.013	3.012	3.001	2.997	3.027
Al^{3+}	1.017	0.986	1.003	1.012	1.013	1.001	0.982	0.999	1.014	0.996	0.981	1.007	1.006	1.033	1.016	1.001	0.992	1.003	0.990	0.984	0.996	0.994	1.000	0.973	0.971	0.978	0.990	0.979	0.981	0.994	0.997	0.972
P^{5+}	0.010	0.001	0.022	0.012	0.011	0.003	0.001	0.010	0.011	0.011	0.009	0.012	0.010	0.008	0.010	0.008	0.002	0.007	0.004	0.002	0.007	0.007	0.008	0.000	0.003	0.000	0.005	0.007	0.002	0.007	0.004	0.000
Fe^{3+}	0.001	0.000	0.001	0.000	0.000	0.000	0.001	0.002	0.000	0.002	0.001	0.000	0.000	0.000	0.000	0.000	0.003	0.001	0.001	0.001	0.001	0.001	0.000	0.000	0.000	0.001	0.000	0.000	0.002	0.000	0.000	0.001
Total-T	4.005	4.004	3.984	4.000	4.003	4.000	3.999	3.998	4.000	3.996	3.999	3.996	4.006	4.005	4.006	3.998	4.002	4.001	4.002	3.995	3.996	3.990	3.998	4.000	3.994	4.000	3.998	3.999	3.997	4.002	3.998	4.000
K^+	0.005	0.003	0.005	0.008	0.006	0.004	0.004	0.004	0.004	0.005	0.007	0.005	0.005	0.007	0.008	0.003	0.005	0.008	0.005	0.004	0.006	0.003	0.005	0.006	0.006	0.005	0.006	0.005	0.004	0.006	0.006	0.007
Na^+	0.969	0.965	0.985	0.969	0.959	0.980	0.974	0.975	0.976	0.987	0.943	0.977	0.953	0.953	0.942	0.971	0.969	0.973	0.970	0.986	0.986	1.015	0.986	0.955	0.979	0.971	0.967	0.969	0.982	0.961	0.971	0.964
Cs^+	0.000	0.000	0.000	0.000	0.000	0.000	0.000	0.001	0.000	0.000	0.000	0.000	0.001	0.000	0.000	0.000	0.000	0.000	0.000	0.000	0.000	0.000	0.000	0.000	0.000	0.000	0.000	0.000	0.000	0.000	0.000	0.000
Ca^{2+}	0.008	0.000	0.026	0.008	0.009	0.002	0.000	0.005	0.010	0.005	0.011	0.013	0.004	0.016	0.015	0.008	0.004	0.005	0.002	0.002	0.004	0.002	0.003	0.002	0.003	0.001	0.002	0.001	0.002	0.004	0.006	0.001
Ba^{2+}	0.000	0.000	0.001	0.000	0.000	0.000	0.000	0.000	0.001	0.000	0.000	0.000	0.000	0.000	0.000	0.001	0.000	0.000	0.000	0.001	0.000	0.000	0.000	0.000	0.000	0.000	0.001	0.001	0.001	0.000	0.001	0.000
Sr^{2+}	0.000	0.000	0.000	0.001	0.000	0.003	0.003	0.003	0.002	0.000	0.000	0.001	0.000	0.002	0.000	0.001	0.000	0.002	0.000	0.004	0.001	0.001	0.001	0.003	0.001	0.001	0.003	0.000	0.002	0.001	0.003	0.000
Mn^{2+}	0.000	0.000	0.000	0.000	0.000	0.001	0.000	0.000	0.000	0.001	0.001	0.000	0.001	0.003	0.000	0.000	0.001	0.000	0.000	0.001	0.001	0.000	0.000	0.000	0.000	0.000	0.002	0.000	0.000	0.000	0.002	0.000
Zn^{2+}	0.000	0.000	0.002	0.002	0.002	0.000	0.000	0.003	0.000	0.001	0.001	0.000	0.000	0.003	0.000	0.005	0.001	0.000	0.000	0.000	0.000	0.001	0.000	0.000	0.001	0.001	0.004	0.000	0.000	0.000	0.000	0.000
Total-A	0.982	0.969	1.018	0.988	0.976	0.990	0.982	0.991	0.992	0.999	0.963	0.996	0.964	0.983	0.966	0.989	0.981	0.988	0.977	0.996	0.999	1.022	0.996	0.965	0.989	0.978	0.984	0.975	0.991	0.972	0.988	0.972
% An	0.8	0.0	2.6	0.8	1.0	0.2	0.0	0.5	1.0	0.5	1.2	1.3	0.4	1.6	1.6	0.8	0.4	0.5	0.2	0.2	0.4	0.2	0.3	0.2	0.3	0.1	0.2	0.1	0.2	0.4	0.6	0.1
% Ab	98.7	99.6	96.9	98.4	98.4	99.3	99.6	99.1	98.6	99.0	98.2	98.2	99.1	97.7	97.6	98.8	99.1	98.7	99.3	99.5	99.0	99.5	99.2	99.2	99.2	99.5	99.2	99.5	99.4	99.0	98.8	99.2
% Or	0.5	0.4	0.5	0.8	0.6	0.4	0.4	0.4	0.4	0.5	0.7	0.5	0.5	0.7	0.9	0.3	0.5	0.8	0.5	0.4	0.6	0.3	0.5	0.7	0.6	0.5	0.6	0.5	0.4	0.6	0.6	0.8

Sample	#17B1		#17B2			#17B3	
Zone	Pegmatite 2						
wt%	3	4	1	2	4	2	3
SiO_2	67.61	67.46	68.43	67.86	68.94	67.43	67.27
Al_2O_3	18.74	18.79	19.15	19.27	19.26	18.74	18.73
P_2O_5	0.06	0.08	0.11	0.24	0.07	0.00	0.05
Fe_2O_3	0.02	0.01	0.03	0.06	0.00	0.02	0.00
K_2O	0.11	0.12	0.13	0.11	0.10	0.54	0.08
Na_2O	11.24	11.26	11.25	11.18	11.53	10.87	11.05
CaO	0.04	0.05	0.03	0.20	0.05	0.00	0.04
BaO	0.07	0.00	0.05	0.05	0.00	0.00	0.00
SrO	0.01	0.20	0.00	0.06	0.08	0.14	0.10
Cs_2O	0.00	0.00	0.00	0.00	0.00	0.00	0.00
ZnO	0.11	0.00	0.10	0.14	0.11	0.07	0.06
MnO	0.02	0.04	0.00	0.00	0.05	0.00	0.00
Total	98.03	98.00	99.27	99.17	100.18	97.80	97.38
a.p.f.u (calculus done on the basis of 8 Oxygens)							
Si^{4+}	3.011	3.007	3.007	2.989	3.005	3.013	3.012
Al^{3+}	0.983	0.987	0.992	1.000	0.989	0.987	0.989
P^{5+}	0.002	0.003	0.004	0.009	0.003	0.000	0.002
Fe^{3+}	0.001	0.000	0.001	0.002	0.000	0.001	0.000
Total-T	3.997	3.997	4.003	4.000	3.997	4.001	4.002
K^+	0.006	0.007	0.007	0.006	0.005	0.031	0.005
Na^+	0.971	0.973	0.958	0.955	0.975	0.941	0.959
Cs^+	0.000	0.000	0.000	0.000	0.000	0.000	0.000
Ca^{2+}	0.002	0.002	0.002	0.010	0.002	0.000	0.002
Ba^{2+}	0.001	0.000	0.001	0.001	0.000	0.000	0.000
Sr^{2+}	0.000	0.005	0.000	0.001	0.002	0.004	0.003
Mn^{2+}	0.001	0.002	0.000	0.000	0.002	0.000	0.000
Zn^{2+}	0.004	0.000	0.003	0.005	0.004	0.002	0.002
Total-A	0.985	0.988	0.971	0.978	0.990	0.978	0.971
% An	0.2	0.2	0.2	1.0	0.2	0.0	0.2
% Ab	99.2	99.1	99.1	98.4	99.2	96.9	99.3
% Or	0.7	0.7	0.7	0.6	0.5	3.1	0.5

II.II.V MUSCOVITE

Sample	#1B1			#1B2						#1B4	#2cB1				#2cB2						#2cB3				#2cB4				#2cB5			
Domain	Pegmatite 1																															
wt%	1	2	3	1	2	3	4	5	6	1	1	2	3	4	1	2	3	4	5	6	1	2	3	4	1	2	3	4	1	2	3	4
SiO_2	46.36	46.48	45.63	46.53	47.36	45.98	45.78	46.54	46.22	45.14	46.26	46.38	46.51	47.09	47.29	46.94	47.78	47.10	47.51	47.41	46.86	46.51	46.99	45.84	47.38	46.51	46.49	46.28	46.32	45.62	46.09	45.80
Al_2O_3	38.32	38.38	36.50	38.01	37.90	37.04	36.48	36.73	37.06	38.16	37.80	37.29	37.83	37.74	38.91	37.77	37.39	37.39	36.56	37.15	38.47	37.31	37.50	37.93	37.38	37.57	38.21	37.69	38.57	37.95	37.84	37.76
K_2O	9.55	9.33	10.09	8.93	8.77	10.00	10.81	9.96	10.35	9.84	10.08	10.86	10.67	10.78	9.64	10.61	10.15	10.46	10.29	10.70	9.80	10.29	10.02	10.26	9.62	9.87	9.84	10.17	10.07	9.98	10.43	10.02
Fe_2O_3	0.00	0.00	0.85	0.00	0.00	0.00	0.68	0.00	0.00	0.79	0.00	0.00	0.00	0.00	0.00	0.00	0.00	0.00	0.00	0.00	0.00	0.00	0.00	0.00	0.00	0.00	0.00	0.00	0.00	0.00	0.00	0.00
FeO	1.23	1.14	0.66	0.81	0.82	1.37	0.34	1.24	0.95	0.05	0.39	0.34	0.45	0.42	0.49	0.64	0.51	0.37	0.51	0.56	0.67	0.83	1.12	0.99	1.30	0.90	0.72	0.93	0.90	1.08	0.69	1.03
MgO	0.01	0.01	0.01	0.00	0.00	0.01	0.00	0.00	0.00	0.01	0.00	0.00	0.00	0.00	0.00	0.02	0.00	0.00	0.00	0.00	0.01	0.00	0.00	0.00	0.00	0.00	0.01	0.02	0.01	0.00	0.01	0.00
Mn_2O_3	0.00	0.00	0.00	0.00	0.00	0.00	0.00	0.00	0.00	0.00	0.00	0.00	0.00	0.00	0.00	0.00	0.00	0.00	0.00	0.00	0.00	0.00	0.00	0.00	0.00	0.00	0.00	0.00	0.00	0.00	0.00	0.00
MnO	0.03	0.07	0.03	0.02	0.03	0.14	0.03	0.03	0.03	0.04	0.01	0.06	0.02	0.01	0.04	0.03	0.02	0.02	0.06	0.06	0.02	0.03	0.07	0.00	0.06	0.01	0.06	0.01	0.02	0.02	0.02	0.04
CaO	0.03	0.03	0.02	0.00	0.01	0.02	0.01	0.00	0.03	0.02	0.01	0.00	0.00	0.01	0.05	0.00	0.06	0.01	0.03	0.00	0.00	0.00	0.01	0.01	0.01	0.00	0.02	0.03	0.01	0.03	0.01	0.00
Na_2O	0.34	0.32	0.51	0.32	0.30	0.52	0.39	0.42	0.54	0.19	0.24	0.27	0.27	0.27	0.22	0.24	0.29	0.26	0.24	0.19	0.19	0.37	0.49	0.59	0.44	0.41	0.40	0.51	0.41	0.56	0.44	0.47
BaO	0.00	0.00	0.01	0.05	0.02	0.01	0.00	0.04	0.03	0.01	0.01	0.06	0.06	0.04	0.00	0.03	0.01	0.00	0.06	0.08	0.04	0.00	0.01	0.07	0.02	0.00	0.02	0.00	0.00	0.00	0.04	0.00
SnO_2	0.00	0.04	0.09	0.04	0.09	0.03	0.00	0.00	0.01	0.00	0.00	0.00	0.00	0.00	0.00	0.00	0.03	0.00	0.00	0.00	0.00	0.07	0.04	0.02	0.03	0.01	0.06	0.03	0.04	0.03	0.05	0.00
TiO_2	0.00	0.01	0.03	0.00	0.02	0.02	0.01	0.00	0.00	0.00	0.00	0.00	0.03	0.00	0.01	0.01	0.01	0.00	0.00	0.01	0.01	0.03	0.02	0.03	0.00	0.03	0.04	0.04	0.01	0.02	0.02	0.00
Cr_2O_3	0.07	0.04	0.08	0.08	0.07	0.03	0.06	0.04	0.06	0.04	0.03	0.06	0.05	0.02	0.07	0.09	0.06	0.07	0.05	0.04	0.06	0.05	0.07	0.07	0.06	0.08	0.06	0.02	0.03	0.05	0.03	0.05
V_2O_3	0.00	0.00	0.00	0.00	0.00	0.00	0.00	0.00	0.00	0.00	0.00	0.00	0.00	0.00	0.00	0.00	0.00	0.00	0.00	0.00	0.00	0.00	0.00	0.00	0.00	0.00	0.00	0.00	0.00	0.00	0.00	0.00
ZnO	0.07	0.11	0.11	0.11	0.07	0.19	0.00	0.08	0.00	0.05	0.00	0.04	0.01	0.09	0.10	0.06	0.06	0.00	0.02	0.04	0.00	0.01	0.06	0.02	0.15	0.06	0.12	0.16	0.01	0.11	0.08	0.12
Li_2O*	0.00	0.00	0.88	0.00	0.00	0.00	0.66	0.00	0.00	0.95	0.34	0.00	0.00	0.00	0.00	0.00	0.00	0.00	0.00	0.00	0.00	0.00	0.00	0.00	0.00	0.00	0.00	0.00	0.00	0.00	0.00	0.00
Ta_2O_5	0.08	0.00	0.00	0.00	0.07	0.00	0.00	0.00	0.08	0.10	0.02	0.00	0.00	0.00	0.08	0.00	0.00	0.03	0.00	0.02	0.00	0.00	0.02	0.17	0.02	0.11	0.18	0.15	0.15	0.09	0.00	0.13
Nb_2O_5	0.03	0.00	0.00	0.00	0.07	0.05	0.11	0.08	0.08	0.08	0.00	0.00	0.06	0.10	0.01	0.04	0.00	0.10	0.04	0.00	0.01	0.02	0.02	0.09	0.02	0.12	0.03	0.03	0.10	0.08	0.05	0.01
PbO	0.00	0.07	0.04	0.00	0.03	0.00	0.02	0.01	0.00	0.01	0.00	0.02	0.00	0.00	0.00	0.00	0.00	0.02	0.00	0.00	0.00	0.00	0.00	0.06	0.00	0.00	0.00	0.00	0.00	0.00	0.04	0.02
SrO	0.00	0.04	0.01	0.05	0.01	0.03	0.02	0.02	0.05	0.05	0.00	0.00	0.00	0.01	0.01	0.00	0.00	0.04	0.09	0.00	0.02	0.00	0.07	0.01	0.03	0.00	0.03	0.00	0.00	0.00	0.00	0.00
CoO	0.00	0.03	0.00	0.01	0.00	0.00	0.02	0.00	0.00	0.00	0.02	0.01	0.00	0.00	0.00	0.04	0.02	0.00	0.01	0.02	0.01	0.00	0.01	0.01	0.01	0.00	0.03	0.00	0.00	0.00	0.00	0.03
Cl	0.00	0.00	0.01	0.01	0.00	0.00	0.01	0.00	0.00	0.00	0.00	0.01	0.00	0.00	0.00	0.00	0.01	0.02	0.00	0.00	0.00	0.01	0.02	0.00	0.00	0.01	0.00	0.00	0.02	0.00	0.00	0.01
F	0.25	0.13	0.38	0.29	0.00	0.18	0.03	0.23	0.06	0.09	0.22	0.00	0.12	0.16	0.05	0.19	0.12	0.02	0.08	0.03	0.16	0.11	0.27	0.12	0.11	0.05	0.06	0.04	0.02	0.26	0.12	0.22
Total	96.34	96.21	95.93	95.26	95.62	95.62	95.45	95.43	95.57	95.62	95.43	95.40	96.08	96.73	96.96	96.71	96.52	95.90	95.52	96.29	96.33	95.64	96.80	96.29	96.63	95.73	96.39	96.08	96.68	95.89	95.96	95.71
a.p.f.u (calculus done on the basis of 11 oxygens)																																
Si^{4+}	3.032	3.037	3.017	3.061	3.088	3.048	3.032	3.082	3.058	2.966	3.044	3.067	3.053	3.072	3.051	3.064	3.107	3.088	3.126	3.101	3.051	3.067	3.069	3.017	3.087	3.057	3.038	3.042	3.020	3.013	3.035	3.028
Al^{3+}	0.968	0.963	0.983	0.939	0.912	0.952	0.968	0.917	0.942	1.034	0.956	0.933	0.947	0.928	0.949	0.936	0.892	0.913	0.874	0.899	0.949	0.934	0.931	0.983	0.913	0.943	0.962	0.958	0.980	0.987	0.965	0.972
Fe^{3+}	0.000	0.000	0.000	0.000	0.000	0.000	0.000	0.000	0.000	0.000	0.000	0.000	0.000	0.000	0.000	0.000	0.000	0.000	0.000	0.000	0.000	0.000	0.000	0.000	0.000	0.000	0.000	0.000	0.000	0.000	0.000	0.000
Total IV	4.000	4.000	4.000	4.000	4.000	4.000	4.000	3.999	4.000	4.000	4.000	4.000	4.000	4.000	4.000	4.000	3.999	4.000	4.000	4.000	4.000	4.000	4.000	4.000	4.000	4.000	4.000	4.000	4.000	4.000	4.000	4.000
Ta^{5+}	0.001	0.000	0.000	0.000	0.001	0.000	0.000	0.000	0.001	0.002	0.000	0.000	0.000	0.000	0.001	0.000	0.000	0.001	0.000	0.000	0.000	0.000	0.000	0.003	0.000	0.002	0.003	0.003	0.003	0.002	0.000	0.002
Nb^{5+}	0.001	0.000	0.000	0.000	0.002	0.002	0.003	0.003	0.002	0.003	0.000	0.000	0.002	0.003	0.000	0.001	0.000	0.003	0.001	0.000	0.000	0.001	0.001	0.003	0.001	0.004	0.001	0.001	0.003	0.002	0.001	0.000
Sn^{4+}	0.000	0.001	0.002	0.001	0.002	0.001	0.000	0.000	0.000	0.000	0.000	0.000	0.000	0.000	0.000	0.000	0.001	0.000	0.000	0.000	0.000	0.002	0.001	0.001	0.001	0.000	0.002	0.001	0.001	0.001	0.001	0.000
Ti^{4+}	0.000	0.000	0.001	0.000	0.001	0.001	0.001	0.000	0.000	0.000	0.000	0.000	0.001	0.000	0.000	0.001	0.001	0.000	0.000	0.000	0.001	0.001	0.001	0.001	0.000	0.001	0.002	0.002	0.000	0.001	0.001	0.000
Fe^{3+}	0.000	0.000	0.042	0.000	0.000	0.000	0.034	0.000	0.000	0.039	0.000	0.000	0.000	0.000	0.000	0.000	0.000	0.000	0.000	0.000	0.000	0.000	0.000	0.000	0.000	0.000	0.000	0.000	0.000	0.000	0.000	0.000
Mn^{3+}	0.000	0.000	0.000	0.000	0.000	0.000	0.000	0.000	0.000	0.000	0.000	0.000	0.000	0.000	0.000	0.000	0.000	0.000	0.000	0.000	0.000	0.000	0.000	0.000	0.000	0.000	0.000	0.000	0.000	0.000	0.000	0.000
Cr^{3+}	0.003	0.002	0.004	0.004	0.004	0.001	0.003	0.002	0.003	0.002	0.002	0.003	0.002	0.001	0.004	0.005	0.003	0.003	0.002	0.002	0.003	0.003	0.004	0.004	0.003	0.004	0.003	0.001	0.002	0.003	0.002	0.003
Al^{3+}	1.986	1.993	1.862	2.008	2.001	1.942	1.880	1.950	1.948	1.922	1.975	1.973	1.980	1.973	2.011	1.971	1.973	1.976	1.961	1.964	2.004	1.966	1.955	1.959	1.958	1.968	1.980	1.962	1.983	1.968	1.972	1.970
Zn^{2+}	0.003	0.005	0.005	0.005	0.004	0.009	0.000	0.004	0.000	0.002	0.000	0.002	0.000	0.004	0.005	0.003	0.003	0.000	0.001	0.002	0.000	0.000	0.003	0.001	0.007	0.003	0.006	0.008	0.001	0.005	0.004	0.006
Co^{2+}	0.000	0.002	0.000	0.001	0.000	0.000	0.001	0.000	0.000	0.000	0.001	0.001	0.000	0.000	0.000	0.002	0.001	0.000	0.000	0.001	0.000	0.000	0.000	0.001	0.001	0.000	0.002	0.000	0.000	0.000	0.000	0.002
Fe^{2+}	0.067	0.062	0.037	0.045	0.045	0.076	0.019	0.069	0.053	0.003	0.021	0.019	0.025	0.023	0.027	0.035	0.028	0.020	0.028	0.030	0.037	0.046	0.061	0.055	0.071	0.049	0.040	0.051	0.049	0.060	0.038	0.057
Mn^{2+}	0.002	0.004	0.001	0.001	0.002	0.008	0.002	0.002	0.002	0.002	0.001	0.003	0.001	0.001	0.002	0.002	0.001	0.001	0.003	0.003	0.001	0.002	0.004	0.000	0.003	0.001	0.004	0.000	0.001	0.001	0.001	0.002
Mg^{2+}	0.001	0.001	0.001	0.000	0.000	0.001	0.000	0.000	0.000	0.001	0.000	0.000	0.000	0.000	0.000	0.002	0.000	0.000	0.000	0.000	0.001	0.000	0.000	0.000	0.000	0.000	0.001	0.002	0.001	0.000	0.001	0.000
Li^{+}	0.000	0.000	0.233	0.000	0.000	0.000	0.177	0.000	0.000	0.251	0.090	0.000	0.000	0.000	0.000	0.000	0.000	0.000	0.000	0.000	0.000	0.000	0.000	0.000	0.000	0.000	0.000	0.000	0.000	0.000	0.000	0.000
Total VI	2.064	2.069	2.190	2.065	2.061	2.041	2.119	2.028	2.010	2.226	2.090	2.001	2.011	2.005	2.050	2.021	2.011	2.004	1.997	2.004	2.047	2.020	2.031	2.026	2.044	2.032	2.042	2.029	2.044	2.042	2.021	2.041
Pb^{2+}	0.000	0.001	0.001	0.000	0.001	0.000	0.000	0.000	0.000	0.000	0.000	0.000	0.000	0.000	0.000	0.000	0.000	0.000	0.000	0.000	0.000	0.000	0.000	0.001	0.000	0.000	0.000	0.000	0.000	0.000	0.001	0.000
Ba^{2+}	0.000	0.000	0.000	0.001	0.000	0.000	0.000	0.001	0.001	0.000	0.000	0.002	0.002	0.001	0.000	0.001	0.000	0.000	0.002	0.002	0.001	0.000	0.000	0.002	0.001	0.000	0.001	0.000	0.000	0.000	0.001	0.000
Sr^{2+}	0.000	0.001	0.000	0.002	0.001	0.001	0.001	0.001	0.002	0.002	0.000	0.000	0.000	0.000	0.000	0.000	0.000	0.002	0.004	0.000	0.001	0.000	0.003	0.001	0.001	0.000	0.001	0.000	0.000	0.000	0.000	0.000
Ca^{2+}	0.002	0.002	0.002	0.000	0.001	0.001	0.000	0.000	0.002	0.001	0.000	0.000	0.000	0.001	0.003	0.000	0.004	0.000	0.002	0.000	0.000	0.000	0.001	0.001	0.001	0.000	0.001	0.002	0.000	0.002	0.001	0.000
K^{+}	0.796	0.778	0.851	0.749	0.729	0.846	0.913	0.841	0.874	0.825	0.846	0.916	0.894	0.897	0.793	0.884	0.842	0.875	0.864	0.893	0.814	0.866	0.835	0.862	0.799	0.828	0.820	0.853	0.837	0.841	0.877	0.845
Na^{+}	0.044	0.041	0.066	0.041	0.038	0.067	0.050	0.054	0.070	0.025	0.031	0.035	0.035	0.035	0.027	0.030	0.037	0.033	0.031	0.024	0.024	0.047	0.062	0.076	0.055	0.052	0.051	0.065	0.052	0.072	0.056	0.060
Total X	0.842	0.823	0.919	0.793	0.769	0.916	0.964	0.897	0.948	0.853	0.878	0.953	0.930	0.933	0.824	0.915	0.883	0.910	0.901	0.919	0.840	0.913	0.901	0.941	0.857	0.880	0.874	0.920	0.889	0.915	0.935	0.905
OH^{-}	1.949	1.972	1.917	1.939	1.999	1.963	1.993	1.951	1.986	1.982	1.954	1.999	1.974	1.968	1.990	1.961	1.974	1.994	1.984	1.994	1.967	1.975	1.941	1.975	1.977	1.986	1.986	1.991	1.994	1.944	1.975	1.953
Cl^{-}	0.000	0.000	0.002	0.001	0.000	0.000	0.001	0.000	0.000	0.000	0.000	0.001	0.000	0.000	0.000	0.000	0.001	0.002	0.000	0.000	0.000	0.001	0.002	0.000	0.000	0.001	0.000	0.000	0.002	0.000	0.000	0.001
F^{-}	0.051	0.028	0.080	0.061	0.000	0.037	0.006	0.049	0.013	0.018	0.046	0.000	0.025	0.032	0.009	0.038	0.025	0.004	0.016	0.006	0.032	0.022	0.057	0.024	0.023	0.011	0.012	0.007	0.004	0.055	0.025	0.046
$O2^{-}$	0.000	0.000	0.001	0.000	0.001	0.001	0.001	0.000	0.000	0.000	0.000	0.000	0.001	0.000	0.000	0.001	0.001	0.000	0.000	0.000	0.001	0.001	0.001	0.001	0.000	0.001	0.002	0.002	0.000	0.001	0.001	0.000
Total Y	2.000	2.000	2.000	2.000	2.000	2.000	2.000	2.000	2.000	2.000	2.000	2.000	2.000	2.000	2.000	2.000	2.000	2.000	2.000	2.000	2.000	2.000	2.000	2.000	2.000	2.000	2.000	2.000	2.000	2.000	2.000	2.000

Sample	#2cB9		#4B1				#4B2				#4B3				#4B5			#4B8		#5B1	#5B1.2	#5B2			#5B2.2			#5B4				
Domain	Pegmatite 1																															
wt%	1	2	1	2	3	4	1	2	3	4	1	2	3	5	1	2	3	1	2	1	1	1	2	3	1	2	3	1	2	3	4	5
SiO_2	46.81	46.32	47.10	45.42	45.87	46.32	45.74	46.28	45.16	45.59	46.52	45.61	46.09	46.05	46.22	45.78	45.89	46.13	46.94	47.37	46.99	46.90	46.22	45.73	47.26	46.49	46.57	46.59	45.90	45.80	46.15	46.44
Al_2O_3	38.01	37.99	37.91	38.89	36.84	35.70	38.29	37.51	37.43	36.57	36.86	36.55	36.94	36.90	38.29	37.98	38.00	38.45	36.83	38.64	37.24	38.95	37.86	38.01	37.51	37.03	37.69	38.37	37.74	37.26	37.60	36.90
K_2O	10.21	10.61	9.39	10.31	10.31	10.28	9.78	10.36	10.60	10.26	9.34	10.68	9.79	10.10	9.52	10.21	10.22	9.55	10.08	9.09	9.94	10.04	10.30	10.54	8.70	10.35	10.40	9.45	10.36	10.17	10.20	10.49
Fe_2O_3	0.00	0.00	0.00	0.00	0.60	1.02	0.32	0.00	0.03	0.52	1.31	0.12	0.96	0.73	0.00	0.00	0.00	0.00	0.00	0.00	0.00	0.00	0.00	0.00	0.24	0.00	0.00	0.00	0.00	0.00	0.00	0.00
FeO	1.06	0.41	0.50	0.27	0.00	0.00	0.00	0.56	0.60	0.62	0.00	0.59	0.18	0.28	0.84	0.59	0.36	0.81	0.92	1.07	1.13	0.73	0.89	1.14	0.60	1.28	0.84	1.13	1.12	1.18	1.25	1.27
MgO	0.00	0.01	0.00	0.00	0.00	0.01	0.00	0.01	0.00	0.01	0.00	0.00	0.02	0.01	0.01	0.00	0.00	0.02	0.02	0.02	0.02	0.04	0.00	0.01	0.02	0.04	0.00	0.00	0.03	0.01	0.01	0.01
Mn_2O_3	0.00	0.00	0.00	0.00	0.00	0.03	0.00	0.00	0.00	0.00	0.03	0.00	0.00	0.00	0.00	0.00	0.00	0.00	0.00	0.00	0.00	0.00	0.00	0.00	0.00	0.00	0.00	0.00	0.00	0.00	0.00	0.00
MnO	0.07	0.00	0.03	0.00	0.00	0.00	0.01	0.00	0.01	0.03	0.00	0.00	0.03	0.03	0.02	0.05	0.00	0.00	0.02	0.01	0.04	0.02	0.04	0.01	0.03	0.03	0.04	0.00	0.00	0.01	0.03	0.02
CaO	0.02	0.02	0.00	0.01	0.03	0.03	0.01	0.00	0.03	0.05	0.01	0.00	0.02	0.01	0.01	0.01	0.00	0.00	0.03	0.01	0.01	0.01	0.03	0.01	0.02	0.03	0.00	0.00	0.02	0.04	0.02	0.00
Na_2O	0.44	0.34	0.30	0.34	0.56	0.29	0.39	0.25	0.23	0.17	0.28	0.25	0.33	0.44	0.19	0.43	0.35	0.20	0.24	0.29	0.31	0.23	0.57	0.50	0.16	0.50	0.44	0.32	0.42	0.47	0.39	0.44
BaO	0.04	0.02	0.00	0.00	0.05	0.00	0.00	0.00	0.07	0.00	0.00	0.04	0.00	0.00	0.00	0.01	0.01	0.00	0.04	0.01	0.02	0.00	0.03	0.03	0.01	0.00	0.00	0.00	0.00	0.02	0.00	0.01
SnO_2	0.00	0.01	0.00	0.00	0.08	0.03	0.02	0.00	0.00	0.00	0.02	0.00	0.04	0.01	0.00	0.06	0.00	0.00	0.04	0.04	0.02	0.00	0.05	0.07	0.00	0.03	0.07	0.07	0.02	0.01	0.03	0.02
TiO_2	0.04	0.00	0.01	0.00	0.00	0.00	0.00	0.01	0.00	0.02	0.03	0.00	0.03	0.00	0.00	0.00	0.01	0.01	0.01	0.00	0.04	0.00	0.04	0.02	0.00	0.05	0.01	0.04	0.03	0.01	0.03	0.00
Cr_2O_3	0.07	0.04	0.03	0.06	0.01	0.07	0.05	0.05	0.06	0.06	0.06	0.04	0.04	0.04	0.01	0.01	0.04	0.03	0.07	0.02	0.06	0.07	0.06	0.04	0.07	0.01	0.10	0.07	0.08	0.06	0.06	0.02
V_2O_3	0.00	0.00	0.00	0.00	0.00	0.00	0.00	0.00	0.00	0.00	0.00	0.00	0.00	0.00	0.00	0.00	0.00	0.00	0.00	0.00	0.00	0.00	0.00	0.00	0.00	0.00	0.00	0.00	0.00	0.00	0.00	0.00
ZnO	0.03	0.09	0.07	0.03	0.03	0.07	0.04	0.04	0.04	0.00	0.00	0.00	0.12	0.05	0.03	0.00	0.11	0.03	0.09	0.05	0.04	0.08	0.09	0.06	0.03	0.10	0.07	0.06	0.07	0.07	0.04	0.15
Li_2O*	0.00	0.00	0.00	0.00	0.80	1.41	0.51	0.00	1.00	1.51	0.95	1.22	0.73	0.62	0.00	0.00	0.00	0.00	0.00	0.00	0.00	0.00	0.00	0.00	0.51	0.00	0.00	0.00	0.00	0.00	0.00	0.00
Ta_2O_5	0.00	0.00	0.00	0.07	0.13	0.18	0.00	0.06	0.00	0.00	0.02	0.17	0.14	0.00	0.03	0.10	0.00	0.00	0.00	0.13	0.05	0.00	0.04	0.14	0.04	0.04	0.19	0.00	0.00	0.00	0.00	0.16
Nb_2O_5	0.06	0.07	0.01	0.00	0.06	0.08	0.05	0.00	0.08	0.04	0.05	0.06	0.04	0.11	0.08	0.09	0.05	0.04	0.03	0.02	0.09	0.05	0.00	0.06	0.06	0.01	0.01	0.05	0.13	0.06	0.09	0.04
PbO	0.04	0.00	0.00	0.02	0.00	0.02	0.00	0.01	0.00	0.00	0.00	0.01	0.04	0.01	0.02	0.02	0.01	0.00	0.01	0.09	0.02	0.07	0.00	0.00	0.00	0.03	0.04	0.00	0.05	0.01	0.02	0.00
SrO	0.00	0.01	0.00	0.00	0.07	0.06	0.02	0.04	0.00	0.01	0.03	0.00	0.00	0.03	0.00	0.04	0.00	0.09	0.00	0.00	0.01	0.00	0.03	0.00	0.00	0.00	0.04	0.06	0.00	0.08	0.02	0.00
CoO	0.01	0.00	0.00	0.00	0.00	0.01	0.01	0.00	0.00	0.01	0.04	0.00	0.00	0.00	0.00	0.02	0.00	0.01	0.00	0.00	0.01	0.02	0.00	0.00	0.00	0.00	0.00	0.02	0.01	0.00	0.00	0.00
Cl	0.00	0.00	0.01	0.00	0.01	0.01	0.00	0.00	0.01	0.01	0.00	0.01	0.00	0.01	0.03	0.01	0.00	0.01	0.00	0.00	0.03	0.01	0.00	0.00	0.01	0.00	0.00	0.02	0.00	0.01	0.00	0.00
F	0.10	0.04	0.11	0.08	0.20	0.00	0.21	0.11	0.06	0.08	0.08	0.12	0.08	0.04	0.09	0.06	0.07	0.19	0.12	0.05	0.13	0.19	0.17	0.20	0.17	0.13	0.15	0.10	0.11	0.07	0.11	0.07
Total	97.02	95.99	95.49	95.50	95.66	95.61	95.46	95.27	95.40	95.56	95.63	95.45	95.62	95.46	95.39	95.45	95.13	95.57	95.47	96.90	96.18	97.40	96.42	96.55	95.43	96.14	96.67	96.35	96.10	95.31	96.04	96.04
a.p.f.u (calculus done on the basis of 11 oxygens)																																
Si^{4+}	3.047	3.042	3.083	2.994	3.028	3.050	3.004	3.059	2.987	3.004	3.042	3.017	3.032	3.036	3.038	3.026	3.035	3.031	3.097	3.060	3.081	3.031	3.033	3.008	3.082	3.063	3.049	3.038	3.025	3.040	3.039	3.065
Al^{3+}	0.953	0.959	0.917	1.006	0.972	0.950	0.996	0.941	1.013	0.996	0.958	0.983	0.968	0.964	0.962	0.975	0.965	0.969	0.903	0.941	0.919	0.969	0.967	0.992	0.918	0.937	0.950	0.962	0.975	0.960	0.961	0.935
Fe^{3+}	0.000	0.000	0.000	0.000	0.000	0.000	0.000	0.000	0.000	0.000	0.000	0.000	0.000	0.000	0.000	0.000	0.000	0.000	0.000	0.000	0.000	0.000	0.000	0.000	0.000	0.000	0.000	0.000	0.000	0.000	0.000	0.000
Total IV	4.000	4.000	4.000	4.000	4.000	4.000	4.000	4.000	4.000	4.000	4.000	4.000	4.000	4.000	4.000	4.000	4.000	4.000	4.000	4.000	4.000	4.000	4.000	4.000	4.000	4.000	3.999	4.000	4.000	4.000	4.000	3.999
Ta^{5+}	0.000	0.000	0.000	0.001	0.002	0.003	0.000	0.001	0.000	0.000	0.000	0.003	0.003	0.000	0.001	0.002	0.000	0.000	0.000	0.002	0.001	0.000	0.001	0.003	0.001	0.001	0.003	0.000	0.000	0.000	0.000	0.003
Nb^{5+}	0.002	0.002	0.000	0.000	0.002	0.002	0.002	0.000	0.002	0.001	0.001	0.002	0.001	0.003	0.002	0.003	0.002	0.001	0.001	0.001	0.003	0.001	0.000	0.002	0.002	0.000	0.000	0.002	0.004	0.002	0.003	0.001
Sn^{4+}	0.000	0.000	0.000	0.000	0.002	0.001	0.001	0.000	0.000	0.000	0.001	0.000	0.001	0.000	0.000	0.002	0.000	0.000	0.001	0.001	0.001	0.000	0.001	0.002	0.000	0.001	0.002	0.002	0.001	0.000	0.001	0.001
Ti^{4+}	0.002	0.000	0.000	0.000	0.000	0.000	0.000	0.000	0.000	0.001	0.002	0.000	0.001	0.000	0.000	0.000	0.000	0.001	0.001	0.000	0.002	0.000	0.002	0.001	0.000	0.002	0.001	0.002	0.002	0.000	0.002	0.000
Fe^{3+}	0.000	0.000	0.000	0.000	0.030	0.050	0.016	0.000	0.002	0.026	0.065	0.006	0.048	0.036	0.000	0.000	0.000	0.000	0.000	0.000	0.000	0.000	0.000	0.000	0.012	0.000	0.000	0.000	0.000	0.000	0.000	0.000
Mn^{3+}	0.000	0.000	0.000	0.000	0.000	0.002	0.000	0.000	0.000	0.000	0.001	0.000	0.000	0.000	0.000	0.000	0.000	0.000	0.000	0.000	0.000	0.000	0.000	0.000	0.000	0.000	0.000	0.000	0.000	0.000	0.000	0.000
Cr^{3+}	0.004	0.002	0.002	0.003	0.001	0.003	0.003	0.002	0.003	0.003	0.003	0.002	0.002	0.002	0.001	0.001	0.002	0.002	0.003	0.001	0.003	0.003	0.003	0.002	0.004	0.000	0.005	0.004	0.004	0.003	0.003	0.001
Al^{3+}	1.963	1.981	2.008	2.015	1.894	1.820	1.967	1.982	1.905	1.844	1.883	1.867	1.896	1.903	2.004	1.983	1.997	2.009	1.960	2.001	1.958	1.998	1.962	1.956	1.966	1.939	1.958	1.987	1.955	1.955	1.958	1.935
Zn^{2+}	0.002	0.004	0.003	0.002	0.002	0.004	0.002	0.002	0.002	0.000	0.000	0.000	0.006	0.003	0.002	0.000	0.005	0.001	0.004	0.002	0.002	0.004	0.004	0.003	0.001	0.005	0.003	0.003	0.004	0.003	0.002	0.008
Co^{2+}	0.000	0.000	0.000	0.000	0.000	0.001	0.000	0.000	0.000	0.000	0.002	0.000	0.000	0.000	0.000	0.001	0.000	0.000	0.000	0.000	0.000	0.001	0.000	0.000	0.000	0.000	0.000	0.001	0.000	0.000	0.000	0.000
Fe^{2+}	0.058	0.022	0.027	0.015	0.000	0.000	0.000	0.031	0.033	0.034	0.000	0.032	0.010	0.015	0.046	0.033	0.020	0.045	0.051	0.058	0.062	0.039	0.049	0.063	0.033	0.070	0.046	0.062	0.062	0.066	0.069	0.070
Mn^{2+}	0.004	0.000	0.002	0.000	0.000	0.000	0.000	0.000	0.001	0.002	0.000	0.000	0.002	0.002	0.001	0.003	0.000	0.000	0.001	0.001	0.002	0.001	0.002	0.001	0.002	0.002	0.002	0.000	0.000	0.000	0.002	0.001
Mg^{2+}	0.000	0.001	0.000	0.000	0.000	0.001	0.000	0.001	0.000	0.001	0.000	0.000	0.002	0.001	0.001	0.000	0.000	0.002	0.002	0.002	0.002	0.004	0.000	0.001	0.002	0.004	0.000	0.000	0.003	0.001	0.001	0.001
Li^{+}	0.000	0.000	0.000	0.000	0.213	0.372	0.135	0.000	0.266	0.401	0.251	0.324	0.194	0.163	0.000	0.000	0.000	0.000	0.000	0.000	0.000	0.000	0.000	0.000	0.135	0.000	0.000	0.000	0.000	0.000	0.000	0.000
Total VI	2.035	2.014	2.042	2.035	2.146	2.260	2.126	2.020	2.214	2.313	2.209	2.236	2.165	2.128	2.058	2.027	2.026	2.061	2.024	2.068	2.035	2.051	2.024	2.032	2.156	2.025	2.021	2.062	2.034	2.031	2.039	2.021
Pb^{2+}	0.001	0.000	0.000	0.000	0.000	0.000	0.000	0.000	0.000	0.000	0.000	0.000	0.001	0.000	0.000	0.000	0.000	0.000	0.000	0.002	0.000	0.001	0.000	0.000	0.000	0.001	0.001	0.000	0.001	0.000	0.000	0.000
Ba^{2+}	0.001	0.001	0.000	0.000	0.001	0.000	0.000	0.000	0.002	0.000	0.000	0.001	0.000	0.000	0.000	0.000	0.000	0.000	0.001	0.000	0.000	0.000	0.001	0.001	0.000	0.000	0.000	0.000	0.000	0.001	0.001	0.000
Sr^{2+}	0.000	0.000	0.000	0.000	0.003	0.002	0.001	0.002	0.000	0.001	0.001	0.000	0.000	0.001	0.000	0.002	0.000	0.003	0.000	0.000	0.000	0.000	0.001	0.000	0.000	0.000	0.001	0.002	0.000	0.003	0.001	0.000
Ca^{2+}	0.001	0.001	0.000	0.001	0.002	0.002	0.001	0.000	0.002	0.003	0.001	0.000	0.001	0.001	0.001	0.001	0.000	0.000	0.002	0.001	0.001	0.001	0.002	0.001	0.001	0.002	0.000	0.000	0.002	0.003	0.001	0.000
K^{+}	0.848	0.888	0.784	0.867	0.868	0.863	0.819	0.873	0.895	0.862	0.779	0.901	0.822	0.849	0.799	0.861	0.862	0.801	0.849	0.749	0.832	0.828	0.863	0.884	0.724	0.870	0.868	0.786	0.871	0.861	0.857	0.883
Na^{+}	0.056	0.043	0.039	0.044	0.072	0.037	0.050	0.032	0.030	0.022	0.036	0.032	0.042	0.056	0.024	0.055	0.045	0.025	0.030	0.036	0.039	0.029	0.072	0.063	0.020	0.064	0.056	0.040	0.054	0.060	0.050	0.056
Total X	0.906	0.934	0.823	0.912	0.946	0.904	0.871	0.907	0.928	0.888	0.817	0.934	0.865	0.907	0.823	0.919	0.907	0.829	0.882	0.787	0.873	0.859	0.938	0.949	0.745	0.937	0.927	0.828	0.928	0.928	0.909	0.940
OH^{-}	1.978	1.993	1.975	1.983	1.957	1.999	1.956	1.978	1.987	1.982	1.983	1.975	1.981	1.991	1.979	1.987	1.986	1.959	1.976	1.990	1.967	1.961	1.963	1.958	1.963	1.970	1.967	1.977	1.976	1.985	1.976	1.986
Cl^{-}	0.000	0.000	0.002	0.000	0.001	0.001	0.000	0.000	0.002	0.001	0.000	0.001	0.000	0.001	0.004	0.001	0.000	0.001	0.000	0.000	0.003	0.001	0.000	0.000	0.001	0.000	0.000	0.002	0.000	0.001	0.000	0.000
F^{-}	0.020	0.007	0.023	0.018	0.042	0.000	0.044	0.022	0.012	0.016	0.016	0.024	0.018	0.008	0.018	0.012	0.014	0.039	0.024	0.010	0.028	0.039	0.036	0.042	0.036	0.028	0.032	0.020	0.022	0.014	0.022	0.014
$O2^{-}$	0.002	0.000	0.000	0.000	0.000	0.000	0.000	0.000	0.000	0.001	0.002	0.000	0.001	0.000	0.000	0.000	0.000	0.001	0.001	0.000	0.002	0.000	0.002	0.001	0.000	0.002	0.001	0.002	0.002	0.000	0.002	0.000
Total Y	2.000	2.000	2.000	2.000	2.000	2.000	2.000	2.000	2.000	2.000	2.000	2.000	2.000	2.000	2.000	2.000	2.000	2.000	2.000	2.000	2.000	2.000	2.000	2.000	2.000	2.000	2.000	2.000	2.000	2.000	2.000	2.000

Sample	#5B5				#7aB5			#7bB2				#7bB3						#7bB5			#9bB1						#9bB3					
Domain	Pegmatite 1																															
wt%	1	2	3	4	1	2	5	1	2	3	4	1	2	3	4	5	6	1	2	3	1	2	3	4	5	6	1	2	3	4	5	6
SiO_2	46.79	46.44	46.56	46.54	46.92	46.15	47.08	46.91	46.26	45.98	46.40	46.53	46.13	45.54	45.67	45.84	45.85	46.03	46.36	46.22	45.90	45.47	46.09	44.84	46.36	46.26	46.81	46.73	46.25	45.89	47.52	45.98
Al_2O_3	38.68	38.07	37.68	38.23	38.21	38.08	36.64	39.26	39.41	37.90	37.99	38.31	38.21	36.93	37.42	37.75	37.88	39.02	39.11	37.60	38.86	37.24	37.62	37.48	36.89	36.28	38.63	36.39	36.63	37.01	34.71	36.73
K_2O	9.62	10.37	10.41	10.03	9.86	10.68	10.15	9.60	9.32	9.78	9.60	8.65	8.49	9.97	9.75	10.26	10.12	9.25	9.10	10.25	8.45	10.57	10.45	10.07	10.33	10.26	9.45	10.36	10.46	10.44	10.02	10.47
Fe_2O_3	0.00	0.00	0.00	0.00	0.00	0.00	0.08	0.00	0.00	0.00	0.23	0.00	0.06	0.03	0.03	0.00	0.00	0.00	0.00	0.00	0.47	0.00	0.00	0.58	0.00	1.18	0.00	0.00	0.71	0.00	0.00	0.00
FeO	0.94	0.78	1.03	0.96	0.42	0.42	0.26	0.68	0.69	0.19	0.00	0.67	0.61	0.58	0.56	0.57	0.56	0.62	0.61	0.61	0.57	1.09	0.90	0.46	0.93	0.00	1.13	1.21	0.28	1.26	2.01	1.21
MgO	0.01	0.01	0.02	0.01	0.01	0.00	0.06	0.00	0.01	0.01	0.01	0.01	0.02	0.00	0.00	0.05	0.04	0.00	0.00	0.01	0.00	0.00	0.00	0.01	0.00	0.00	0.00	0.00	0.01	0.00	0.01	0.00
Mn_2O_3	0.00	0.00	0.00	0.00	0.00	0.00	0.00	0.00	0.00	0.00	0.04	0.00	0.00	0.00	0.00	0.00	0.00	0.00	0.00	0.00	0.00	0.00	0.00	0.00	0.00	0.00	0.00	0.00	0.00	0.00	0.00	0.00
MnO	0.00	0.05	0.00	0.05	0.02	0.04	0.02	0.09	0.04	0.04	0.00	0.05	0.05	0.02	0.06	0.03	0.04	0.05	0.03	0.04	0.05	0.05	0.06	0.07	0.08	0.06	0.05	0.06	0.00	0.05	0.08	0.05
CaO	0.02	0.02	0.02	0.00	0.01	0.01	0.08	0.00	0.00	0.02	0.01	0.02	0.02	0.05	0.00	0.06	0.03	0.04	0.04	0.00	0.01	0.00	0.01	0.03	0.00	0.02	0.00	0.01	0.01	0.01	0.01	0.02
Na_2O	0.32	0.49	0.35	0.51	0.19	0.27	0.26	0.20	0.20	0.24	0.22	0.33	0.33	0.57	0.49	0.25	0.23	0.27	0.29	0.20	0.32	0.39	0.43	0.44	0.44	0.40	0.36	0.46	0.45	0.50	0.44	0.45
BaO	0.00	0.02	0.01	0.00	0.03	0.01	0.02	0.00	0.03	0.06	0.02	0.01	0.00	0.00	0.00	0.01	0.03	0.02	0.00	0.00	0.01	0.00	0.02	0.00	0.00	0.02	0.00	0.00	0.00	0.02	0.03	0.00
SnO_2	0.03	0.00	0.02	0.05	0.02	0.00	0.02	0.02	0.03	0.00	0.01	0.10	0.09	0.06	0.01	0.04	0.08	0.08	0.03	0.13	0.06	0.02	0.04	0.02	0.04	0.01	0.03	0.04	0.03	0.01	0.07	0.06
TiO_2	0.02	0.04	0.00	0.02	0.00	0.00	0.00	0.01	0.00	0.00	0.00	0.06	0.03	0.03	0.04	0.02	0.00	0.00	0.02	0.04	0.03	0.02	0.00	0.00	0.02	0.01	0.01	0.04	0.02	0.04	0.00	0.01
Cr_2O_3	0.05	0.08	0.08	0.06	0.07	0.04	0.04	0.04	0.11	0.05	0.02	0.06	0.07	0.05	0.08	0.09	0.01	0.00	0.05	0.05	0.08	0.05	0.07	0.06	0.03	0.05	0.05	0.03	0.04	0.04	0.08	0.06
V_2O_3	0.00	0.00	0.00	0.00	0.00	0.00	0.00	0.00	0.00	0.00	0.00	0.00	0.00	0.00	0.00	0.00	0.00	0.00	0.00	0.00	0.00	0.00	0.00	0.00	0.00	0.00	0.00	0.00	0.00	0.00	0.00	0.00
ZnO	0.09	0.00	0.06	0.12	0.06	0.04	0.12	0.08	0.06	0.00	0.05	0.05	0.02	0.06	0.12	0.06	0.12	0.06	0.09	0.02	0.03	0.04	0.03	0.01	0.03	0.01	0.03	0.02	0.00	0.05	0.08	0.12
Li_2O*	0.00	0.00	0.00	0.00	0.00	0.00	0.37	0.00	0.00	0.98	0.55	0.00	1.07	1.38	0.99	0.00	0.00	0.00	0.00	0.00	0.38	0.00	0.00	1.31	0.00	0.89	0.00	0.00	0.52	0.00	0.00	0.00
Ta_2O_5	0.00	0.10	0.06	0.03	0.04	0.15	0.00	0.00	0.15	0.00	0.04	0.00	0.00	0.00	0.00	0.00	0.00	0.06	0.04	0.00	0.01	0.09	0.00	0.00	0.10	0.00	0.00	0.03	0.00	0.02	0.07	0.00
Nb_2O_5	0.09	0.06	0.12	0.06	0.07	0.00	0.02	0.02	0.11	0.03	0.08	0.00	0.00	0.08	0.01	0.00	0.00	0.03	0.12	0.08	0.08	0.04	0.07	0.08	0.07	0.06	0.08	0.15	0.00	0.09	0.05	0.08
PbO	0.08	0.00	0.00	0.00	0.03	0.01	0.07	0.04	0.00	0.00	0.02	0.00	0.00	0.00	0.00	0.08	0.00	0.07	0.00	0.00	0.00	0.00	0.00	0.05	0.00	0.05	0.01	0.03	0.02	0.00	0.07	0.07
SrO	0.00	0.01	0.00	0.00	0.03	0.00	0.00	0.00	0.04	0.00	0.00	0.08	0.00	0.00	0.00	0.00	0.01	0.00	0.01	0.00	0.00	0.03	0.06	0.00	0.00	0.03	0.02	0.00	0.03	0.01	0.04	0.09
CoO	0.01	0.00	0.00	0.00	0.01	0.00	0.01	0.00	0.01	0.03	0.02	0.03	0.01	0.00	0.00	0.00	0.00	0.00	0.00	0.00	0.04	0.00	0.00	0.02	0.04	0.01	0.00	0.00	0.00	0.00	0.01	0.03
Cl	0.00	0.00	0.00	0.00	0.00	0.00	0.00	0.00	0.02	0.02	0.03	0.00	0.01	0.01	0.03	0.02	0.01	0.01	0.01	0.00	0.01	0.00	0.00	0.01	0.01	0.03	0.01	0.00	0.02	0.01	0.03	0.03
F	0.13	0.12	0.21	0.17	0.00	0.04	0.13	0.00	0.13	0.10	0.00	0.24	0.09	0.00	0.12	0.00	0.11	0.21	0.05	0.22	0.21	0.18	0.19	0.02	0.14	0.12	0.16	0.14	0.14	0.15	0.23	0.23
Total	96.85	96.64	96.62	96.84	95.97	95.93	95.42	96.95	96.61	95.40	95.33	95.20	95.30	95.34	95.37	95.13	95.12	95.81	95.95	95.45	95.58	95.28	96.02	95.55	95.51	95.74	96.83	95.69	95.61	95.60	95.53	95.69
a.p.f.u (calculus done on the basis of 11 oxygens)																																
Si^{4+}	3.036	3.035	3.048	3.034	3.062	3.034	3.099	3.028	3.003	3.015	3.039	3.053	3.009	3.001	3.008	3.034	3.036	3.014	3.019	3.053	2.999	3.029	3.038	2.958	3.070	3.047	3.037	3.092	3.054	3.046	3.161	3.056
Al^{3+}	0.964	0.965	0.952	0.966	0.938	0.966	0.901	0.972	0.997	0.985	0.961	0.946	0.991	0.999	0.992	0.966	0.964	0.986	0.981	0.946	1.001	0.971	0.961	1.042	0.930	0.953	0.963	0.908	0.946	0.954	0.839	0.944
Fe^{3+}	0.000	0.000	0.000	0.000	0.000	0.000	0.000	0.000	0.000	0.000	0.000	0.000	0.000	0.000	0.000	0.000	0.000	0.000	0.000	0.000	0.000	0.000	0.000	0.000	0.000	0.000	0.000	0.000	0.000	0.000	0.000	0.000
Total IV	4.000	4.000	4.000	4.000	4.000	4.000	4.000	4.000	4.000	4.000	3.999	3.999	4.000	4.000	4.000	4.000	4.000	4.000	4.000	4.000	4.000	4.000	3.999	4.000	4.000	4.000	4.000	4.000	4.000	4.000	4.000	4.000
Ta^{5+}	0.000	0.002	0.001	0.001	0.001	0.003	0.000	0.000	0.003	0.000	0.001	0.000	0.000	0.000	0.000	0.000	0.000	0.001	0.001	0.000	0.000	0.002	0.000	0.000	0.002	0.000	0.000	0.001	0.000	0.000	0.001	0.000
Nb^{5+}	0.003	0.002	0.004	0.002	0.002	0.000	0.000	0.001	0.003	0.001	0.002	0.000	0.000	0.002	0.000	0.000	0.000	0.001	0.003	0.002	0.002	0.001	0.002	0.002	0.002	0.002	0.002	0.004	0.000	0.003	0.002	0.002
Sn^{4+}	0.001	0.000	0.001	0.001	0.000	0.000	0.001	0.001	0.001	0.000	0.000	0.003	0.002	0.001	0.000	0.001	0.002	0.002	0.001	0.003	0.002	0.001	0.001	0.000	0.001	0.000	0.001	0.001	0.001	0.000	0.002	0.002
Ti^{4+}	0.001	0.002	0.000	0.001	0.000	0.000	0.000	0.001	0.000	0.000	0.000	0.003	0.001	0.001	0.002	0.001	0.000	0.000	0.001	0.002	0.002	0.001	0.000	0.000	0.001	0.000	0.001	0.002	0.001	0.002	0.000	0.000
Fe^{3+}	0.000	0.000	0.000	0.000	0.000	0.000	0.004	0.000	0.000	0.000	0.011	0.000	0.003	0.002	0.002	0.000	0.000	0.000	0.000	0.000	0.023	0.000	0.000	0.029	0.000	0.059	0.000	0.000	0.035	0.000	0.000	0.000
Mn^{3+}	0.000	0.000	0.000	0.000	0.000	0.000	0.000	0.000	0.000	0.000	0.002	0.000	0.000	0.000	0.000	0.000	0.000	0.000	0.000	0.000	0.000	0.000	0.000	0.000	0.000	0.000	0.000	0.000	0.000	0.000	0.000	0.000
Cr^{3+}	0.003	0.004	0.004	0.003	0.004	0.002	0.002	0.002	0.006	0.003	0.001	0.003	0.004	0.003	0.004	0.005	0.000	0.000	0.003	0.003	0.004	0.002	0.004	0.003	0.001	0.002	0.003	0.001	0.002	0.002	0.004	0.003
Al^{3+}	1.994	1.967	1.956	1.971	2.000	1.985	1.941	2.014	2.019	1.944	1.972	2.017	1.947	1.870	1.913	1.979	1.992	2.024	2.021	1.981	1.991	1.954	1.961	1.871	1.949	1.864	1.992	1.930	1.904	1.941	1.881	1.933
Zn^{2+}	0.004	0.000	0.003	0.006	0.003	0.002	0.006	0.004	0.003	0.000	0.003	0.002	0.001	0.003	0.006	0.003	0.006	0.003	0.004	0.001	0.001	0.002	0.001	0.001	0.002	0.000	0.002	0.001	0.000	0.003	0.004	0.006
Co^{2+}	0.001	0.000	0.000	0.000	0.001	0.000	0.001	0.000	0.001	0.001	0.001	0.002	0.001	0.000	0.000	0.000	0.000	0.000	0.000	0.000	0.002	0.000	0.000	0.001	0.002	0.001	0.000	0.000	0.000	0.000	0.001	0.001
Fe^{2+}	0.051	0.042	0.056	0.053	0.023	0.023	0.014	0.037	0.037	0.010	0.000	0.037	0.033	0.032	0.031	0.032	0.031	0.034	0.033	0.033	0.031	0.061	0.049	0.025	0.051	0.000	0.062	0.067	0.015	0.070	0.112	0.067
Mn^{2+}	0.000	0.003	0.000	0.003	0.001	0.002	0.001	0.005	0.002	0.002	0.000	0.003	0.003	0.001	0.003	0.002	0.002	0.003	0.002	0.002	0.003	0.003	0.003	0.004	0.004	0.003	0.003	0.003	0.000	0.003	0.004	0.003
Mg^{2+}	0.001	0.001	0.002	0.001	0.001	0.000	0.006	0.000	0.001	0.001	0.001	0.001	0.002	0.000	0.000	0.005	0.004	0.000	0.000	0.001	0.000	0.000	0.000	0.001	0.000	0.000	0.000	0.000	0.001	0.000	0.001	0.000
Li^{+}	0.000	0.000	0.000	0.000	0.000	0.000	0.099	0.000	0.000	0.258	0.145	0.000	0.280	0.366	0.263	0.000	0.000	0.000	0.000	0.000	0.101	0.000	0.000	0.348	0.000	0.235	0.000	0.000	0.138	0.000	0.000	0.000
Total VI	2.058	2.023	2.026	2.041	2.034	2.017	2.075	2.063	2.075	2.220	2.139	2.070	2.276	2.281	2.224	2.027	2.038	2.068	2.069	2.028	2.163	2.026	2.022	2.285	2.015	2.166	2.063	2.011	2.098	2.024	2.011	2.018
Pb^{2+}	0.001	0.000	0.000	0.000	0.001	0.000	0.001	0.001	0.000	0.000	0.000	0.000	0.000	0.000	0.000	0.001	0.000	0.001	0.000	0.000	0.000	0.000	0.000	0.001	0.000	0.001	0.000	0.001	0.000	0.000	0.001	0.001
Ba^{2+}	0.000	0.000	0.000	0.000	0.001	0.000	0.001	0.000	0.001	0.002	0.000	0.000	0.000	0.000	0.000	0.000	0.001	0.000	0.000	0.000	0.000	0.000	0.001	0.000	0.000	0.000	0.000	0.000	0.000	0.001	0.001	0.000
Sr^{2+}	0.000	0.001	0.000	0.000	0.001	0.000	0.000	0.000	0.001	0.000	0.000	0.003	0.000	0.000	0.000	0.000	0.000	0.000	0.000	0.000	0.000	0.001	0.002	0.000	0.000	0.001	0.001	0.000	0.001	0.001	0.001	0.004
Ca^{2+}	0.001	0.001	0.001	0.000	0.000	0.001	0.006	0.000	0.000	0.001	0.001	0.002	0.001	0.003	0.000	0.004	0.002	0.003	0.003	0.000	0.001	0.000	0.001	0.002	0.000	0.002	0.000	0.001	0.000	0.001	0.001	0.002
K^{+}	0.796	0.865	0.870	0.834	0.820	0.896	0.853	0.791	0.771	0.818	0.802	0.724	0.706	0.838	0.819	0.866	0.855	0.773	0.756	0.864	0.704	0.899	0.879	0.847	0.873	0.862	0.782	0.875	0.882	0.884	0.850	0.888
Na^{+}	0.040	0.062	0.045	0.065	0.024	0.034	0.033	0.025	0.025	0.030	0.028	0.042	0.042	0.072	0.062	0.032	0.030	0.034	0.036	0.026	0.040	0.051	0.055	0.056	0.057	0.052	0.045	0.058	0.058	0.064	0.056	0.057
Total X	0.838	0.929	0.915	0.899	0.847	0.932	0.893	0.816	0.799	0.852	0.832	0.771	0.749	0.914	0.882	0.905	0.888	0.811	0.795	0.890	0.745	0.951	0.937	0.906	0.930	0.918	0.828	0.935	0.941	0.950	0.910	0.951
OH^{-}	1.972	1.974	1.956	1.964	2.000	1.993	1.973	2.000	1.971	1.978	1.997	1.946	1.979	1.998	1.971	1.997	1.976	1.955	1.987	1.952	1.954	1.961	1.960	1.995	1.968	1.972	1.965	1.968	1.969	1.965	1.949	1.948
Cl^{-}	0.000	0.000	0.000	0.000	0.000	0.000	0.000	0.000	0.002	0.002	0.003	0.000	0.001	0.001	0.003	0.002	0.002	0.001	0.001	0.000	0.001	0.000	0.000	0.002	0.001	0.003	0.001	0.000	0.002	0.001	0.003	0.003
F^{-}	0.027	0.024	0.044	0.035	0.000	0.007	0.027	0.000	0.027	0.020	0.000	0.050	0.018	0.000	0.024	0.000	0.022	0.044	0.011	0.046	0.043	0.038	0.040	0.004	0.030	0.024	0.033	0.030	0.028	0.032	0.049	0.049
$O2^{-}$	0.001	0.002	0.000	0.001	0.000	0.000	0.000	0.001	0.000	0.000	0.000	0.003	0.001	0.001	0.002	0.001	0.000	0.000	0.001	0.002	0.002	0.001	0.000	0.000	0.001	0.000	0.001	0.002	0.001	0.002	0.000	0.000
Total Y	2.000	2.000	2.000	2.000	2.000	2.000	2.000	2.000	2.000	2.000	2.000	2.000	2.000	2.000	2.000	2.000	2.000	2.000	2.000	2.000	2.000	2.000	2.000	2.000	2.000	2.000	2.000	2.000	2.000	2.000	2.000	2.000

Sample	#9bB3			#9bB9				#9cB1					#9cB4		#9cB6		#11bB1				#11bB2		#11bB3			#11bB4						#11bB6
Domain	Pegmatite 1																MAZ									Pegmatite 1						MAZ
wt%	7	8	9	1	2	3	4	1	2	3	4	5	1	2	1	2	1	2	3	4	1	2	1	2	3	1	2	3	4	5	6	1
SiO_2	44.48	45.99	46.41	47.14	46.82	46.84	45.80	46.99	46.48	46.42	46.46	46.91	46.13	46.42	46.70	46.03	47.03	45.70	46.60	46.40	46.38	46.28	44.31	45.82	46.53	46.99	46.80	46.59	46.60	46.49	46.37	46.63
Al_2O_3	36.52	36.23	35.98	38.19	37.03	36.57	37.69	36.44	36.52	36.80	36.65	36.06	36.91	35.87	38.00	37.10	35.42	34.86	34.44	34.33	35.18	35.92	33.76	34.07	34.06	37.67	37.10	36.84	37.53	36.43	37.55	35.53
K_2O	10.19	10.47	10.34	9.44	9.68	9.88	9.97	9.71	10.49	10.23	10.53	10.26	9.61	10.16	9.25	10.31	8.91	9.82	9.92	9.66	8.81	9.48	8.38	9.60	9.70	9.37	9.88	9.41	9.90	9.72	9.58	9.01
Fe_2O_3	1.16	0.74	1.39	0.00	0.00	0.80	0.00	0.00	0.00	0.00	0.00	0.00	0.00	1.69	0.00	0.00	0.00	1.72	0.00	0.00	0.00	0.00	3.99	0.00	0.00	0.00	0.00	0.00	0.00	0.00	0.00	1.50
FeO	0.00	0.54	0.00	0.92	1.22	0.18	0.81	1.31	1.54	1.33	1.15	1.54	1.63	0.00	0.95	0.92	2.30	0.00	1.50	1.85	2.05	1.34	0.25	2.58	1.92	1.08	0.75	1.30	0.76	1.03	0.85	0.00
MgO	0.00	0.01	0.00	0.01	0.00	0.00	0.00	0.00	0.00	0.01	0.00	0.00	0.00	0.00	0.00	0.01	1.21	0.91	0.93	1.02	0.97	0.59	1.23	1.23	0.90	0.04	0.06	0.03	0.06	0.25	0.12	0.66
Mn_2O_3	0.08	0.00	0.13	0.00	0.00	0.00	0.00	0.00	0.00	0.00	0.00	0.00	0.00	0.10	0.00	0.00	0.00	0.01	0.00	0.00	0.00	0.00	0.00	0.00	0.00	0.00	0.00	0.00	0.00	0.00	0.00	0.08
MnO	0.00	0.00	0.00	0.05	0.07	0.01	0.04	0.05	0.07	0.04	0.06	0.08	0.07	0.00	0.05	0.08	0.02	0.00	0.00	0.00	0.03	0.04	0.03	0.05	0.00	0.02	0.03	0.00	0.06	0.00	0.00	0.00
CaO	0.04	0.02	0.00	0.03	0.00	0.02	0.01	0.00	0.03	0.04	0.01	0.01	0.00	0.02	0.01	0.01	0.00	0.02	0.03	0.03	0.01	0.03	0.02	0.00	0.00	0.03	0.00	0.04	0.01	0.01	0.00	0.01
Na_2O	0.44	0.30	0.46	0.34	0.42	0.38	0.33	0.35	0.49	0.40	0.42	0.52	0.36	0.45	0.37	0.51	0.57	0.77	0.61	0.71	0.62	0.87	0.62	0.66	0.75	0.79	0.85	0.86	0.92	1.04	1.05	0.74
BaO	0.03	0.00	0.01	0.04	0.00	0.03	0.02	0.03	0.02	0.00	0.02	0.00	0.08	0.00	0.03	0.03	0.35	0.21	0.28	0.23	0.32	0.33	0.27	0.36	0.39	0.04	0.00	0.00	0.02	0.06	0.07	0.16
SnO_2	0.04	0.01	0.04	0.04	0.05	0.02	0.06	0.03	0.03	0.00	0.03	0.04	0.05	0.03	0.02	0.02	0.10	0.04	0.04	0.12	0.07	0.00	0.03	0.10	0.09	0.02	0.00	0.07	0.02	0.00	0.06	0.00
TiO_2	0.00	0.00	0.02	0.03	0.02	0.00	0.02	0.03	0.01	0.01	0.02	0.00	0.01	0.00	0.02	0.03	0.57	0.54	0.31	0.53	0.67	0.21	0.85	0.65	0.59	0.00	0.00	0.00	0.00	0.00	0.00	0.23
Cr_2O_3	0.07	0.04	0.04	0.06	0.06	0.02	0.05	0.08	0.04	0.08	0.07	0.02	0.07	0.04	0.05	0.05	0.05	0.10	0.07	0.07	0.06	0.06	0.05	0.04	0.05	0.05	0.07	0.06	0.06	0.05	0.04	0.07
V_2O_3	0.00	0.00	0.00	0.00	0.00	0.00	0.00	0.00	0.00	0.00	0.00	0.00	0.00	0.00	0.00	0.00	0.00	0.00	0.00	0.00	0.00	0.00	0.00	0.00	0.00	0.00	0.00	0.00	0.00	0.00	0.00	0.00
ZnO	0.08	0.02	0.04	0.04	0.06	0.05	0.12	0.13	0.04	0.05	0.01	0.10	0.07	0.05	0.00	0.10	0.00	0.00	0.00	0.00	0.03	0.00	0.11	0.00	0.00	0.04	0.06	0.06	0.08	0.00	0.03	0.05
Li_2O*	2.05	1.05	0.26	0.00	0.00	0.55	0.00	0.00	0.00	0.00	0.00	0.00	0.00	0.23	0.00	0.00	0.00	0.53	0.00	0.00	0.00	0.00	1.53	0.00	0.00	0.00	0.00	0.00	0.00	0.00	0.00	0.38
Ta_2O_5	0.00	0.00	0.00	0.00	0.02	0.00	0.17	0.05	0.11	0.05	0.00	0.12	0.03	0.14	0.01	0.06	0.00	0.00	0.19	0.00	0.00	0.04	0.12	0.03	0.00	0.00	0.00	0.04	0.05	0.00	0.00	0.00
Nb_2O_5	0.10	0.00	0.11	0.15	0.11	0.07	0.05	0.06	0.02	0.04	0.03	0.03	0.09	0.04	0.04	0.09	0.07	0.05	0.00	0.04	0.11	0.01	0.00	0.03	0.02	0.05	0.07	0.02	0.07	0.10	0.01	0.11
PbO	0.00	0.04	0.00	0.02	0.01	0.02	0.03	0.00	0.02	0.01	0.00	0.00	0.00	0.00	0.02	0.09	0.00	0.07	0.00	0.02	0.00	0.02	0.03	0.00	0.00	0.02	0.00	0.00	0.00	0.00	0.00	0.08
SrO	0.00	0.01	0.00	0.04	0.00	0.04	0.07	0.02	0.01	0.09	0.04	0.00	0.00	0.00	0.06	0.00	0.05	0.06	0.09	0.02	0.00	0.07	0.01	0.03	0.00	0.00	0.00	0.00	0.05	0.00	0.02	0.00
CoO	0.00	0.00	0.00	0.02	0.00	0.02	0.03	0.01	0.02	0.02	0.01	0.03	0.00	0.00	0.00	0.00	0.01	0.00	0.02	0.00	0.00	0.00	0.01	0.00	0.00	0.02	0.00	0.00	0.01	0.03	0.02	0.01
Cl	0.02	0.02	0.00	0.01	0.00	0.01	0.01	0.00	0.00	0.01	0.00	0.00	0.00	0.00	0.00	0.02	0.00	0.01	0.01	0.02	0.01	0.02	0.01	0.00	0.01	0.00	0.00	0.01	0.00	0.01	0.01	0.00
F	0.08	0.26	0.12	0.22	0.19	0.05	0.10	0.12	0.20	0.11	0.10	0.16	0.20	0.26	0.10	0.12	0.29	0.09	0.39	0.33	0.44	0.35	0.32	0.39	0.28	0.26	0.06	0.24	0.14	0.25	0.12	0.41
Total	95.36	95.74	95.35	96.78	95.74	95.54	95.38	95.40	96.10	95.72	95.62	95.86	95.31	95.51	95.69	95.57	96.93	95.48	95.41	95.36	95.75	95.66	95.92	95.64	95.29	96.50	95.74	95.56	96.34	95.47	95.87	95.67
a.p.f.u (calculus done on the basis of 11 oxygens)																																
Si^{4+}	2.941	3.038	3.075	3.061	3.082	3.078	3.032	3.104	3.075	3.070	3.077	3.104	3.061	3.076	3.060	3.051	3.085	3.038	3.115	3.104	3.081	3.075	2.949	3.077	3.117	3.067	3.077	3.077	3.054	3.080	3.048	3.077
Al^{3+}	1.059	0.962	0.925	0.939	0.918	0.922	0.967	0.895	0.925	0.930	0.923	0.896	0.939	0.922	0.940	0.949	0.915	0.962	0.885	0.896	0.919	0.925	1.051	0.923	0.884	0.933	0.923	0.923	0.946	0.920	0.952	0.923
Fe^{3+}	0.000	0.000	0.000	0.000	0.000	0.000	0.000	0.000	0.000	0.000	0.000	0.000	0.000	0.000	0.000	0.000	0.000	0.000	0.000	0.000	0.000	0.000	0.000	0.000	0.000	0.000	0.000	0.000	0.000	0.000	0.000	0.000
Total IV	4.000	4.000	4.000	4.000	4.000	4.000	3.999	3.999	4.000	4.000	4.000	4.000	4.000	3.999	4.000	4.000	4.000	4.000	4.000	4.000	4.000	4.000	4.000	4.000	4.000	4.000	4.000	4.000	4.000	4.000	4.000	4.000
Ta^{5+}	0.000	0.000	0.000	0.000	0.000	0.000	0.003	0.001	0.002	0.001	0.000	0.002	0.001	0.003	0.000	0.001	0.000	0.000	0.004	0.000	0.000	0.001	0.002	0.001	0.000	0.000	0.000	0.001	0.001	0.000	0.000	0.000
Nb^{5+}	0.003	0.000	0.003	0.004	0.003	0.002	0.002	0.002	0.001	0.001	0.001	0.001	0.003	0.001	0.001	0.003	0.002	0.002	0.000	0.001	0.003	0.000	0.000	0.001	0.001	0.002	0.002	0.001	0.002	0.003	0.000	0.003
Sn^{4+}	0.001	0.000	0.001	0.001	0.001	0.001	0.002	0.001	0.001	0.000	0.001	0.001	0.001	0.001	0.001	0.001	0.003	0.001	0.001	0.003	0.002	0.000	0.001	0.003	0.003	0.001	0.000	0.002	0.001	0.000	0.002	0.000
Ti^{4+}	0.000	0.000	0.001	0.001	0.001	0.000	0.001	0.001	0.000	0.000	0.001	0.000	0.000	0.000	0.001	0.002	0.028	0.027	0.016	0.027	0.033	0.011	0.043	0.033	0.030	0.000	0.000	0.000	0.000	0.000	0.000	0.012
Fe^{3+}	0.058	0.037	0.069	0.000	0.000	0.040	0.000	0.000	0.000	0.000	0.000	0.000	0.000	0.084	0.000	0.000	0.000	0.086	0.000	0.000	0.000	0.000	0.200	0.000	0.000	0.000	0.000	0.000	0.000	0.000	0.000	0.075
Mn^{3+}	0.004	0.000	0.007	0.000	0.000	0.000	0.000	0.000	0.000	0.000	0.000	0.000	0.000	0.005	0.000	0.000	0.000	0.001	0.000	0.000	0.000	0.000	0.000	0.000	0.000	0.000	0.000	0.000	0.000	0.000	0.000	0.004
Cr^{3+}	0.004	0.002	0.002	0.003	0.003	0.001	0.003	0.004	0.002	0.004	0.004	0.001	0.004	0.002	0.003	0.002	0.003	0.005	0.004	0.004	0.003	0.003	0.003	0.002	0.003	0.003	0.004	0.003	0.003	0.003	0.002	0.004
Al^{3+}	1.787	1.858	1.886	1.984	1.955	1.910	1.975	1.942	1.922	1.939	1.938	1.915	1.948	1.880	1.994	1.949	1.823	1.769	1.829	1.811	1.835	1.888	1.597	1.774	1.806	1.964	1.952	1.945	1.952	1.924	1.957	1.840
Zn^{2+}	0.004	0.001	0.002	0.002	0.003	0.003	0.006	0.006	0.002	0.002	0.001	0.005	0.003	0.002	0.000	0.005	0.000	0.000	0.000	0.000	0.002	0.000	0.005	0.000	0.000	0.002	0.003	0.003	0.004	0.000	0.001	0.003
Co^{2+}	0.000	0.000	0.000	0.001	0.000	0.001	0.002	0.001	0.001	0.001	0.001	0.001	0.000	0.000	0.000	0.000	0.001	0.000	0.001	0.000	0.000	0.000	0.000	0.000	0.000	0.001	0.000	0.000	0.001	0.001	0.001	0.001
Fe^{2+}	0.000	0.030	0.000	0.050	0.067	0.010	0.045	0.072	0.085	0.074	0.064	0.085	0.091	0.000	0.052	0.051	0.126	0.000	0.084	0.103	0.114	0.074	0.014	0.145	0.107	0.059	0.042	0.072	0.042	0.057	0.047	0.000
Mn^{2+}	0.000	0.000	0.000	0.003	0.004	0.000	0.002	0.003	0.004	0.002	0.003	0.004	0.004	0.000	0.003	0.005	0.001	0.000	0.000	0.000	0.002	0.002	0.002	0.003	0.000	0.001	0.002	0.000	0.003	0.000	0.000	0.000
Mg^{2+}	0.000	0.001	0.000	0.001	0.000	0.000	0.000	0.000	0.000	0.001	0.000	0.000	0.000	0.000	0.000	0.001	0.118	0.091	0.092	0.102	0.096	0.059	0.122	0.123	0.090	0.004	0.006	0.003	0.006	0.025	0.011	0.065
Li^{+}	0.545	0.279	0.069	0.000	0.000	0.145	0.000	0.000	0.000	0.000	0.000	0.000	0.000	0.061	0.000	0.000	0.000	0.141	0.000	0.000	0.000	0.000	0.409	0.000	0.000	0.000	0.000	0.000	0.000	0.000	0.000	0.101
Total VI	2.405	2.208	2.040	2.051	2.038	2.112	2.039	2.033	2.019	2.026	2.012	2.016	2.054	2.039	2.054	2.019	2.104	2.121	2.029	2.051	2.090	2.038	2.397	2.083	2.038	2.035	2.010	2.029	2.013	2.012	2.022	2.106
Pb^{2+}	0.000	0.001	0.000	0.000	0.000	0.000	0.001	0.000	0.000	0.000	0.000	0.000	0.000	0.000	0.000	0.002	0.000	0.001	0.000	0.000	0.000	0.000	0.001	0.000	0.000	0.000	0.000	0.000	0.000	0.000	0.000	0.002
Ba^{2+}	0.001	0.000	0.000	0.001	0.000	0.001	0.001	0.001	0.000	0.000	0.001	0.000	0.002	0.000	0.001	0.001	0.009	0.005	0.007	0.006	0.008	0.009	0.007	0.010	0.010	0.001	0.000	0.000	0.001	0.002	0.002	0.004
Sr^{2+}	0.000	0.000	0.000	0.001	0.000	0.001	0.003	0.001	0.000	0.003	0.001	0.000	0.000	0.000	0.002	0.000	0.002	0.002	0.003	0.001	0.000	0.003	0.000	0.001	0.000	0.000	0.000	0.000	0.002	0.000	0.001	0.000
Ca^{2+}	0.003	0.002	0.000	0.002	0.000	0.002	0.001	0.000	0.002	0.003	0.001	0.001	0.000	0.001	0.001	0.001	0.000	0.001	0.002	0.002	0.001	0.002	0.001	0.000	0.000	0.002	0.000	0.003	0.001	0.001	0.000	0.001
K^{+}	0.859	0.882	0.874	0.782	0.813	0.828	0.842	0.818	0.885	0.863	0.889	0.866	0.813	0.859	0.773	0.871	0.745	0.833	0.846	0.824	0.747	0.804	0.711	0.822	0.829	0.780	0.829	0.793	0.828	0.822	0.803	0.758
Na^{+}	0.057	0.038	0.059	0.043	0.054	0.049	0.042	0.044	0.063	0.051	0.054	0.067	0.047	0.058	0.047	0.066	0.072	0.100	0.079	0.092	0.079	0.112	0.080	0.087	0.098	0.100	0.108	0.110	0.117	0.133	0.133	0.095
Total X	0.920	0.923	0.933	0.830	0.867	0.881	0.888	0.864	0.951	0.920	0.947	0.934	0.862	0.919	0.824	0.940	0.828	0.942	0.938	0.925	0.835	0.929	0.800	0.920	0.937	0.884	0.937	0.905	0.948	0.957	0.939	0.860
OH^{-}	1.982	1.943	1.975	1.952	1.960	1.990	1.978	1.973	1.957	1.976	1.978	1.967	1.958	1.946	1.978	1.972	1.912	1.953	1.900	1.902	1.875	1.913	1.889	1.884	1.909	1.946	1.988	1.950	1.972	1.947	1.975	1.903
Cl^{-}	0.002	0.003	0.000	0.001	0.000	0.001	0.002	0.000	0.000	0.001	0.000	0.000	0.000	0.000	0.000	0.002	0.000	0.001	0.001	0.002	0.001	0.002	0.001	0.000	0.001	0.000	0.000	0.001	0.000	0.001	0.001	0.000
F^{-}	0.016	0.055	0.024	0.045	0.040	0.010	0.020	0.025	0.042	0.023	0.021	0.033	0.042	0.054	0.021	0.025	0.060	0.019	0.083	0.070	0.092	0.074	0.067	0.083	0.060	0.054	0.012	0.049	0.028	0.052	0.025	0.086
$O2^{-}$	0.000	0.000	0.001	0.001	0.001	0.000	0.001	0.001	0.000	0.000	0.001	0.000	0.000	0.000	0.001	0.002	0.028	0.027	0.016	0.027	0.033	0.011	0.043	0.033	0.030	0.000	0.000	0.000	0.000	0.000	0.000	0.012
Total Y	2.000	2.000	2.000	2.000	2.000	2.000	2.000	2.000	2.000	2.000	2.000	2.000	2.000	2.000	2.000	2.000	2.000	2.000	2.000	2.000	2.000	2.000	2.000	2.000	2.000	2.000	2.000	2.000	2.000	2.000	2.000	2.000

Sample	#11bB6		#11cB1						#11cB2			#11cB3				#11cB8											#12B1					
Domain	MAZ		Pegmatite 1													MAZ																	
wt%	2	3	1	2	3	4	5	6	1	2	3	1	2	3	4	1	2	3	4	5	6	7	8	9	10	11	1	2	3	4	5	6
SiO_2	46.95	46.89	46.43	45.44	46.23	46.31	46.21	45.87	46.32	46.73	45.94	46.50	46.51	46.14	46.38	47.91	46.92	46.92	47.01	45.70	46.23	45.21	46.69	46.31	46.04	46.91	46.29	46.24	46.14	46.46	46.81	46.51
Al_2O_3	35.14	35.19	38.40	37.11	37.00	37.47	36.62	36.96	37.81	36.50	36.84	38.75	37.00	37.42	37.62	35.29	35.26	34.96	34.91	34.26	35.41	33.18	35.26	33.31	35.03	34.90	34.27	34.42	33.50	34.06	33.87	34.99
K_2O	9.66	9.58	8.96	9.72	9.81	9.83	9.75	9.77	8.38	9.72	9.45	8.77	9.64	9.66	9.55	9.34	9.78	9.79	9.58	9.76	9.69	9.79	9.59	10.00	9.67	9.62	9.84	9.93	9.97	9.92	9.97	9.65
Fe_2O_3	0.00	0.00	0.00	0.56	0.00	0.00	0.00	0.00	0.75	0.00	0.80	0.00	0.00	0.00	0.00	0.00	0.00	0.00	0.00	1.51	0.00	1.47	1.38	0.00	0.37	0.00	0.00	2.08	0.43	2.20	0.00	0.00
FeO	1.27	1.41	1.01	0.42	1.18	1.03	1.52	0.92	0.04	1.38	0.07	0.94	0.99	0.82	0.84	1.56	1.52	1.45	1.52	0.00	1.46	0.00	0.00	2.70	1.19	1.64	2.24	0.00	2.03	0.00	2.13	1.97
MgO	0.73	0.78	0.00	0.02	0.00	0.00	0.01	0.00	0.03	0.00	0.04	0.03	0.00	0.01	0.00	0.98	0.75	0.74	0.83	0.71	0.80	0.77	0.65	1.16	0.80	0.85	1.23	1.10	1.40	1.10	1.20	1.10
Mn_2O_3	0.00	0.00	0.00	0.00	0.00	0.00	0.00	0.00	0.00	0.00	0.00	0.00	0.00	0.00	0.00	0.00	0.00	0.00	0.00	0.00	0.00	0.10	0.01	0.00	0.00	0.00	0.00	0.03	0.00	0.05	0.00	0.00
MnO	0.00	0.05	0.06	0.04	0.02	0.00	0.06	0.05	0.00	0.04	0.01	0.05	0.05	0.03	0.01	0.01	0.05	0.00	0.03	0.00	0.01	0.00	0.00	0.02	0.05	0.06	0.02	0.00	0.05	0.00	0.01	0.07
CaO	0.02	0.00	0.01	0.00	0.02	0.00	0.03	0.01	0.06	0.01	0.01	0.00	0.01	0.01	0.01	0.01	0.02	0.02	0.01	0.01	0.01	0.00	0.01	0.00	0.00	0.03	0.00	0.00	0.00	0.00	0.00	0.00
Na_2O	0.81	0.82	0.70	1.00	0.94	0.83	0.84	0.97	0.66	0.69	1.07	0.77	0.96	0.97	1.01	0.61	0.87	0.78	0.76	0.80	0.80	0.68	0.81	0.63	0.74	0.77	0.69	0.76	0.66	0.70	0.74	0.68
BaO	0.24	0.17	0.03	0.03	0.00	0.01	0.01	0.02	0.05	0.00	0.09	0.04	0.00	0.01	0.06	0.21	0.11	0.10	0.25	0.17	0.18	0.23	0.13	0.26	0.23	0.21	0.08	0.13	0.11	0.15	0.01	0.13
SnO_2	0.00	0.05	0.03	0.02	0.01	0.04	0.05	0.03	0.06	0.02	0.00	0.04	0.08	0.03	0.01	0.03	0.06	0.08	0.03	0.06	0.07	0.04	0.06	0.07	0.02	0.05	0.07	0.07	0.04	0.08	0.06	0.06
TiO_2	0.20	0.24	0.00	0.03	0.06	0.05	0.04	0.04	0.02	0.03	0.00	0.02	0.06	0.00	0.00	0.25	0.27	0.27	0.38	0.34	0.39	0.33	0.27	0.42	0.45	0.45	0.29	0.28	0.19	0.24	0.19	0.23
Cr_2O_3	0.05	0.02	0.02	0.06	0.04	0.03	0.00	0.07	0.03	0.06	0.04	0.07	0.04	0.07	0.04	0.08	0.03	0.09	0.05	0.05	0.06	0.06	0.06	0.08	0.05	0.05	0.05	0.05	0.06	0.06	0.06	0.07
V_2O_3	0.00	0.00	0.00	0.00	0.00	0.00	0.00	0.00	0.00	0.00	0.00	0.00	0.00	0.00	0.00	0.00	0.00	0.00	0.00	0.00	0.00	0.00	0.00	0.00	0.00	0.00	0.00	0.00	0.00	0.00	0.00	0.00
ZnO	0.00	0.00	0.03	0.03	0.00	0.06	0.04	0.07	0.00	0.01	0.12	0.04	0.07	0.00	0.03	0.00	0.00	0.01	0.00	0.00	0.05	0.00	0.00	0.06	0.04	0.04	0.03	0.07	0.02	0.05	0.05	0.03
Li_2O*	0.00	0.00	0.00	0.82	0.00	0.00	0.00	0.00	1.12	0.00	0.74	0.00	0.00	0.00	0.00	0.00	0.00	0.00	0.00	2.01	0.00	3.48	0.25	0.00	0.76	0.00	0.00	0.26	0.83	0.34	0.00	0.00
Ta_2O_5	0.14	0.00	0.00	0.10	0.17	0.00	0.09	0.00	0.03	0.00	0.10	0.00	0.06	0.01	0.00	0.00	0.09	0.04	0.00	0.00	0.00	0.00	0.00	0.02	0.00	0.00	0.00	0.00	0.02	0.00	0.00	0.04
Nb_2O_5	0.00	0.01	0.06	0.05	0.08	0.01	0.00	0.00	0.02	0.00	0.10	0.04	0.09	0.00	0.08	0.10	0.08	0.00	0.07	0.01	0.06	0.08	0.06	0.02	0.03	0.06	0.01	0.00	0.04	0.05	0.02	0.09
PbO	0.08	0.02	0.05	0.01	0.02	0.00	0.00	0.11	0.04	0.00	0.01	0.02	0.00	0.00	0.00	0.05	0.02	0.00	0.00	0.00	0.05	0.04	0.00	0.00	0.00	0.00	0.00	0.01	0.00	0.00	0.00	0.01
SrO	0.05	0.03	0.00	0.01	0.04	0.00	0.05	0.02	0.03	0.06	0.05	0.07	0.10	0.00	0.00	0.00	0.02	0.00	0.00	0.03	0.11	0.06	0.00	0.08	0.00	0.03	0.02	0.00	0.00	0.00	0.08	0.04
CoO	0.01	0.01	0.02	0.00	0.02	0.00	0.00	0.00	0.00	0.00	0.01	0.00	0.00	0.01	0.01	0.00	0.03	0.01	0.00	0.02	0.00	0.02	0.00	0.00	0.00	0.00	0.01	0.00	0.00	0.03	0.01	0.02
Cl	0.00	0.00	0.02	0.01	0.02	0.00	0.00	0.01	0.02	0.01	0.02	0.03	0.01	0.02	0.01	0.01	0.03	0.02	0.03	0.05	0.02	0.12	0.04	0.01	0.02	0.00	0.00	0.00	0.00	0.00	0.01	0.00
F	0.40	0.43	0.30	0.23	0.20	0.26	0.30	0.30	0.16	0.12	0.13	0.30	0.11	0.35	0.11	0.37	0.12	0.20	0.28	0.21	0.32	0.25	0.32	0.15	0.22	0.41	0.47	0.42	0.47	0.55	0.67	0.32
Total	95.75	95.70	96.10	95.68	95.84	95.93	95.63	95.22	95.63	95.39	95.64	96.47	95.78	95.56	95.77	96.80	96.01	95.47	95.72	95.70	95.71	95.90	95.59	95.28	95.71	96.09	95.64	95.86	95.96	96.05	95.89	96.01
a.p.f.u (calculus done on the basis of 11 oxygens)																																
Si^{4+}	3.117	3.112	3.034	3.000	3.055	3.051	3.066	3.051	3.016	3.093	3.026	3.026	3.067	3.050	3.049	3.134	3.102	3.118	3.117	3.021	3.074	2.984	3.090	3.119	3.054	3.109	3.098	3.073	3.077	3.086	3.128	3.087
Al^{3+}	0.883	0.888	0.966	1.000	0.945	0.949	0.934	0.948	0.984	0.907	0.974	0.974	0.933	0.950	0.951	0.866	0.898	0.882	0.883	0.979	0.926	1.016	0.910	0.881	0.946	0.891	0.903	0.927	0.923	0.914	0.872	0.913
Fe^{3+}	0.000	0.000	0.000	0.000	0.000	0.000	0.000	0.000	0.000	0.000	0.000	0.000	0.000	0.000	0.000	0.000	0.000	0.000	0.000	0.000	0.000	0.000	0.000	0.000	0.000	0.000	0.000	0.000	0.000	0.000	0.000	0.000
Total IV	4.000	4.000	4.000	4.000	4.000	4.000	4.000	3.999	4.000	4.000	4.000	4.000	4.000	4.000	4.000	4.000	4.000	4.000	4.000	4.000	4.000	4.000	4.000	4.000	4.000	4.000	4.000	4.000	4.000	4.000	4.000	4.000
Ta^{5+}	0.003	0.000	0.000	0.002	0.003	0.000	0.002	0.000	0.001	0.000	0.002	0.000	0.001	0.000	0.000	0.000	0.002	0.001	0.000	0.000	0.000	0.000	0.000	0.000	0.000	0.000	0.000	0.000	0.000	0.000	0.000	0.001
Nb^{5+}	0.000	0.000	0.002	0.001	0.003	0.000	0.000	0.000	0.001	0.000	0.003	0.001	0.003	0.000	0.002	0.003	0.002	0.000	0.002	0.000	0.002	0.002	0.002	0.001	0.001	0.002	0.000	0.000	0.001	0.002	0.001	0.003
Sn^{4+}	0.000	0.001	0.001	0.000	0.000	0.001	0.001	0.001	0.001	0.001	0.000	0.001	0.002	0.001	0.000	0.001	0.002	0.002	0.001	0.002	0.002	0.001	0.002	0.002	0.000	0.001	0.002	0.002	0.001	0.002	0.002	0.002
Ti^{4+}	0.010	0.012	0.000	0.002	0.003	0.002	0.002	0.002	0.001	0.001	0.000	0.001	0.003	0.000	0.000	0.012	0.014	0.014	0.019	0.017	0.020	0.016	0.013	0.021	0.023	0.022	0.015	0.014	0.010	0.012	0.010	0.012
Fe^{3+}	0.000	0.000	0.000	0.028	0.000	0.000	0.000	0.000	0.037	0.000	0.040	0.000	0.000	0.000	0.000	0.000	0.000	0.000	0.000	0.075	0.000	0.073	0.069	0.000	0.018	0.000	0.000	0.104	0.022	0.110	0.000	0.000
Mn^{3+}	0.000	0.000	0.000	0.000	0.000	0.000	0.000	0.000	0.000	0.000	0.000	0.000	0.000	0.000	0.000	0.000	0.000	0.000	0.000	0.000	0.000	0.005	0.001	0.000	0.000	0.000	0.000	0.001	0.000	0.003	0.000	0.000
Cr^{3+}	0.003	0.001	0.001	0.003	0.002	0.002	0.000	0.004	0.002	0.003	0.002	0.003	0.002	0.004	0.002	0.004	0.001	0.005	0.003	0.003	0.003	0.003	0.003	0.004	0.003	0.003	0.003	0.003	0.003	0.003	0.003	0.004
Al^{3+}	1.867	1.864	1.992	1.887	1.937	1.960	1.930	1.950	1.918	1.939	1.886	1.999	1.942	1.965	1.964	1.855	1.849	1.856	1.846	1.691	1.850	1.566	1.840	1.763	1.793	1.836	1.800	1.769	1.711	1.753	1.796	1.825
Zn^{2+}	0.000	0.000	0.002	0.001	0.000	0.003	0.002	0.003	0.000	0.001	0.006	0.002	0.003	0.000	0.002	0.000	0.000	0.000	0.000	0.000	0.002	0.000	0.000	0.003	0.002	0.002	0.002	0.004	0.001	0.003	0.002	0.001
Co^{2+}	0.000	0.001	0.001	0.000	0.001	0.000	0.000	0.000	0.000	0.000	0.001	0.000	0.000	0.000	0.001	0.000	0.002	0.001	0.000	0.001	0.000	0.001	0.000	0.000	0.000	0.000	0.001	0.000	0.000	0.002	0.001	0.001
Fe^{2+}	0.071	0.078	0.055	0.023	0.065	0.057	0.085	0.051	0.002	0.076	0.004	0.051	0.055	0.045	0.046	0.085	0.084	0.080	0.084	0.000	0.081	0.000	0.000	0.152	0.066	0.091	0.125	0.000	0.113	0.000	0.119	0.110
Mn^{2+}	0.000	0.003	0.003	0.002	0.001	0.000	0.003	0.003	0.000	0.002	0.000	0.003	0.003	0.002	0.001	0.001	0.003	0.000	0.002	0.000	0.001	0.000	0.000	0.001	0.003	0.004	0.001	0.000	0.003	0.000	0.001	0.004
Mg^{2+}	0.072	0.077	0.000	0.002	0.000	0.000	0.001	0.000	0.003	0.000	0.003	0.003	0.000	0.001	0.000	0.096	0.074	0.074	0.082	0.070	0.080	0.076	0.064	0.116	0.079	0.084	0.123	0.109	0.139	0.109	0.120	0.109
Li^{+}	0.000	0.000	0.000	0.218	0.000	0.000	0.000	0.000	0.294	0.000	0.197	0.000	0.000	0.000	0.000	0.000	0.000	0.000	0.000	0.534	0.000	0.924	0.065	0.000	0.204	0.000	0.000	0.071	0.223	0.090	0.000	0.000
Total VI	2.025	2.038	2.056	2.170	2.016	2.025	2.026	2.014	2.259	2.023	2.144	2.064	2.014	2.018	2.018	2.056	2.032	2.032	2.038	2.392	2.040	2.668	2.059	2.063	2.191	2.044	2.072	2.075	2.227	2.088	2.053	2.070
Pb^{2+}	0.001	0.000	0.001	0.000	0.000	0.000	0.000	0.002	0.001	0.000	0.000	0.000	0.000	0.000	0.000	0.001	0.000	0.000	0.000	0.000	0.001	0.001	0.000	0.000	0.000	0.000	0.000	0.000	0.000	0.000	0.000	0.000
Ba^{2+}	0.006	0.004	0.001	0.001	0.000	0.000	0.000	0.001	0.001	0.000	0.002	0.001	0.000	0.000	0.002	0.005	0.003	0.003	0.007	0.004	0.005	0.006	0.003	0.007	0.006	0.006	0.002	0.004	0.003	0.004	0.000	0.003
Sr^{2+}	0.002	0.001	0.000	0.000	0.002	0.000	0.002	0.001	0.001	0.002	0.002	0.003	0.004	0.000	0.000	0.000	0.001	0.000	0.000	0.001	0.004	0.002	0.000	0.003	0.000	0.001	0.001	0.000	0.000	0.000	0.003	0.002
Ca^{2+}	0.002	0.000	0.001	0.000	0.001	0.000	0.002	0.001	0.004	0.001	0.001	0.000	0.001	0.001	0.000	0.001	0.001	0.001	0.001	0.001	0.001	0.000	0.001	0.000	0.000	0.002	0.000	0.000	0.000	0.000	0.000	0.000
K^{+}	0.819	0.811	0.747	0.819	0.828	0.826	0.825	0.829	0.696	0.821	0.794	0.728	0.811	0.815	0.801	0.780	0.825	0.830	0.811	0.823	0.822	0.824	0.810	0.859	0.818	0.814	0.840	0.842	0.848	0.840	0.850	0.817
Na^{+}	0.105	0.105	0.088	0.128	0.120	0.106	0.108	0.125	0.083	0.089	0.136	0.097	0.122	0.125	0.129	0.077	0.112	0.101	0.098	0.103	0.103	0.087	0.104	0.082	0.095	0.099	0.090	0.098	0.086	0.090	0.096	0.088
Total X	0.934	0.922	0.837	0.948	0.951	0.932	0.938	0.958	0.787	0.913	0.936	0.829	0.938	0.941	0.933	0.864	0.942	0.935	0.916	0.932	0.935	0.921	0.918	0.950	0.919	0.921	0.933	0.943	0.937	0.934	0.950	0.910
OH^{-}	1.906	1.897	1.937	1.949	1.954	1.944	1.936	1.934	1.965	1.973	1.970	1.933	1.972	1.926	1.976	1.910	1.960	1.942	1.920	1.933	1.911	1.919	1.916	1.945	1.929	1.891	1.886	1.898	1.891	1.873	1.849	1.920
Cl^{-}	0.000	0.000	0.002	0.002	0.002	0.000	0.000	0.001	0.002	0.001	0.003	0.003	0.002	0.002	0.001	0.001	0.003	0.002	0.003	0.006	0.003	0.013	0.004	0.001	0.002	0.000	0.000	0.001	0.000	0.000	0.001	0.001
F^{-}	0.084	0.090	0.061	0.048	0.042	0.054	0.062	0.063	0.032	0.025	0.028	0.063	0.024	0.072	0.024	0.077	0.024	0.043	0.058	0.044	0.067	0.051	0.066	0.033	0.046	0.086	0.099	0.088	0.099	0.115	0.141	0.068
$O2^{-}$	0.010	0.012	0.000	0.002	0.003	0.002	0.002	0.002	0.001	0.001	0.000	0.001	0.003	0.000	0.000	0.012	0.014	0.014	0.019	0.017	0.020	0.016	0.013	0.021	0.023	0.022	0.015	0.014	0.010	0.012	0.010	0.012
Total Y	2.000	2.000	2.000	2.000	2.000	2.000	2.000	2.000	2.000	2.000	2.000	2.000	2.000	2.000	2.000	2.000	2.000	2.000	2.000	2.000	2.000	2.000	2.000	2.000	2.000	2.000	2.000	2.000	2.000	2.000	2.000	2.000

Sample	#12B2						#13B1	#13B2							#13B5				#14B2			#14B3	#14B4	#14B5			#14B6				#17B1	
Domain	MAZ						Pegmatite 2																									
wt%	1	2	3	4	5	6	1	1	2	3	4	5	7	8	1	2	3	4	1	2	3	1	1	1	2	3	1	2	3	4	1	2
SiO_2	47.22	46.94	46.82	46.86	47.28	45.97	47.04	46.38	45.82	46.32	46.16	46.25	45.96	45.80	45.60	46.70	46.70	46.41	45.53	45.80	45.89	46.55	45.79	46.12	46.04	45.17	46.50	46.15	46.30	45.79	46.07	45.73
Al_2O_3	35.34	33.67	35.04	34.34	33.13	33.53	38.34	37.74	36.81	37.56	37.61	36.34	36.69	36.38	37.52	36.33	37.24	37.08	37.76	36.98	36.42	37.09	37.68	36.95	36.64	35.71	37.53	36.68	36.57	36.70	37.48	36.92
K_2O	9.32	9.84	9.89	9.83	9.64	9.96	8.70	9.42	10.40	9.89	9.73	10.53	10.33	10.43	9.32	9.18	10.23	10.21	9.87	10.19	10.22	9.53	9.57	9.37	10.12	10.25	9.68	10.43	10.60	10.38	9.75	10.44
Fe_2O_3	0.00	0.00	0.00	0.00	0.00	2.62	0.00	0.00	0.94	0.00	0.00	0.97	0.00	0.32	1.30	0.06	0.00	0.00	0.32	0.31	0.43	0.00	0.74	0.96	0.46	1.68	0.00	0.00	0.00	0.00	0.00	0.00
FeO	2.04	2.64	1.57	1.85	2.80	0.13	1.27	1.16	0.18	1.19	1.20	0.20	1.05	0.87	0.00	0.39	0.96	1.03	0.48	0.53	0.91	1.25	0.50	0.11	0.29	0.00	0.99	0.97	1.03	1.27	1.18	1.01
MgO	1.11	1.45	0.96	1.18	1.44	1.36	0.01	0.01	0.00	0.01	0.00	0.00	0.01	0.01	0.00	0.00	0.01	0.03	0.00	0.00	0.05	0.04	0.01	0.01	0.00	0.05	0.00	0.03	0.03	0.02	0.00	0.02
Mn_2O_3	0.00	0.00	0.00	0.00	0.00	0.00	0.00	0.00	0.00	0.00	0.00	0.00	0.00	0.00	0.07	0.00	0.00	0.00	0.00	0.00	0.00	0.00	0.00	0.00	0.00	0.05	0.00	0.00	0.00	0.00	0.00	0.00
MnO	0.00	0.05	0.01	0.00	0.06	0.04	0.13	0.05	0.04	0.11	0.08	0.05	0.04	0.01	0.00	0.02	0.05	0.01	0.07	0.06	0.07	0.00	0.00	0.04	0.04	0.00	0.00	0.00	0.04	0.03	0.02	0.01
CaO	0.03	0.01	0.01	0.00	0.03	0.03	0.07	0.01	0.01	0.01	0.00	0.02	0.01	0.03	0.02	0.21	0.02	0.01	0.01	0.00	0.01	0.02	0.00	0.02	0.01	0.03	0.02	0.02	0.00	0.00	0.01	0.00
Na_2O	0.60	0.65	0.79	0.74	0.61	0.65	0.25	0.37	0.43	0.36	0.35	0.35	0.42	0.48	0.36	0.22	0.32	0.42	0.42	0.51	0.43	0.24	0.35	0.40	0.42	0.52	0.37	0.37	0.49	0.46	0.44	0.55
BaO	0.17	0.08	0.12	0.07	0.13	0.00	0.00	0.00	0.03	0.07	0.00	0.00	0.02	0.01	0.02	0.00	0.04	0.00	0.01	0.03	0.00	0.00	0.04	0.00	0.00	0.00	0.02	0.07	0.02	0.03	0.00	0.00
SnO_2	0.05	0.07	0.04	0.08	0.08	0.10	0.06	0.02	0.00	0.04	0.02	0.01	0.04	0.00	0.04	0.00	0.03	0.03	0.04	0.05	0.00	0.01	0.00	0.00	0.03	0.01	0.05	0.02	0.00	0.02	0.06	0.01
TiO_2	0.22	0.24	0.10	0.22	0.35	0.27	0.02	0.00	0.00	0.01	0.01	0.01	0.00	0.00	0.02	0.01	0.01	0.01	0.01	0.03	0.00	0.03	0.05	0.05	0.03	0.01	0.00	0.01	0.04	0.00	0.02	0.01
Cr_2O_3	0.06	0.02	0.08	0.03	0.07	0.05	0.02	0.04	0.05	0.07	0.05	0.08	0.07	0.03	0.07	0.03	0.07	0.07	0.05	0.05	0.04	0.06	0.05	0.04	0.04	0.03	0.03	0.06	0.10	0.08	0.07	0.07
V_2O_3	0.00	0.00	0.00	0.00	0.00	0.00	0.00	0.00	0.00	0.00	0.00	0.00	0.00	0.00	0.00	0.00	0.00	0.00	0.00	0.00	0.00	0.00	0.00	0.00	0.00	0.00	0.00	0.00	0.00	0.00	0.00	0.00
ZnO	0.00	0.08	0.00	0.04	0.00	0.03	0.06	0.00	0.05	0.07	0.16	0.02	0.00	0.03	0.07	0.00	0.06	0.00	0.00	0.06	0.00	0.01	0.05	0.07	0.04	0.07	0.01	0.01	0.08	0.13	0.05	0.06
Li_2O*	0.00	0.00	0.00	0.00	0.00	0.75	0.00	0.00	0.48	0.00	0.00	0.64	0.00	0.83	0.62	2.03	0.00	0.00	0.75	0.63	0.98	0.00	0.47	1.14	1.13	1.38	0.00	0.00	0.00	0.00	0.00	0.00
Ta_2O_5	0.09	0.02	0.00	0.09	0.00	0.05	0.15	0.00	0.12	0.00	0.06	0.00	0.26	0.09	0.04	0.00	0.04	0.08	0.05	0.10	0.00	0.00	0.00	0.07	0.00	0.22	0.00	0.06	0.00	0.02	0.17	0.05
Nb_2O_5	0.03	0.01	0.03	0.05	0.00	0.08	0.02	0.01	0.08	0.00	0.10	0.02	0.06	0.03	0.06	0.10	0.07	0.03	0.00	0.06	0.01	0.09	0.08	0.10	0.09	0.11	0.12	0.11	0.02	0.06	0.10	0.07
PbO	0.01	0.00	0.05	0.00	0.05	0.07	0.00	0.05	0.04	0.00	0.05	0.00	0.00	0.00	0.00	0.03	0.00	0.00	0.00	0.00	0.01	0.05	0.00	0.10	0.05	0.06	0.00	0.03	0.02	0.00	0.00	0.00
SrO	0.00	0.03	0.00	0.00	0.03	0.00	0.09	0.05	0.02	0.01	0.06	0.04	0.01	0.00	0.07	0.00	0.00	0.00	0.01	0.00	0.00	0.09	0.01	0.00	0.01	0.04	0.01	0.07	0.09	0.00	0.00	0.02
CoO	0.01	0.00	0.00	0.00	0.00	0.00	0.00	0.01	0.00	0.00	0.00	0.00	0.01	0.03	0.00	0.01	0.03	0.00	0.02	0.00	0.00	0.00	0.02	0.01	0.01	0.00	0.01	0.05	0.02	0.00	0.00	0.02
Cl	0.01	0.01	0.03	0.01	0.02	0.02	0.02	0.02	0.03	0.00	0.00	0.01	0.00	0.02	0.01	0.02	0.02	0.02	0.00	0.00	0.00	0.00	0.01	0.00	0.00	0.01	0.00	0.01	0.01	0.00	0.02	0.00
F	0.53	0.56	0.31	0.35	0.50	0.54	0.20	0.24	0.17	0.27	0.15	0.11	0.14	0.24	0.23	0.23	0.00	0.29	0.07	0.05	0.06	0.12	0.20	0.08	0.17	0.27	0.03	0.07	0.07	0.07	0.13	0.12
Total	96.82	96.36	95.86	95.74	96.22	96.21	96.44	95.56	95.71	95.99	95.78	95.64	95.10	95.63	95.40	95.55	95.87	95.71	95.45	95.44	95.52	95.17	95.62	95.63	95.59	95.68	95.36	95.21	95.53	95.04	95.56	95.10
a.p.f.u (calculus done on the basis of 11 oxygens)																																
Si^{4+}	3.104	3.125	3.107	3.119	3.150	3.057	3.057	3.055	3.030	3.051	3.043	3.053	3.062	3.034	3.004	3.047	3.071	3.067	2.999	3.027	3.031	3.078	3.013	3.023	3.032	2.997	3.062	3.069	3.072	3.053	3.044	3.047
Al^{3+}	0.896	0.875	0.893	0.881	0.850	0.943	0.943	0.945	0.970	0.949	0.957	0.947	0.938	0.966	0.995	0.954	0.928	0.933	1.001	0.973	0.969	0.922	0.987	0.978	0.969	1.003	0.938	0.931	0.928	0.947	0.956	0.953
Fe^{3+}	0.000	0.000	0.000	0.000	0.000	0.000	0.000	0.000	0.000	0.000	0.000	0.000	0.000	0.000	0.000	0.000	0.000	0.000	0.000	0.000	0.000	0.000	0.000	0.000	0.000	0.000	0.000	0.000	0.000	0.000	0.000	0.000
Total IV	4.000	4.000	4.000	4.000	4.000	4.000	4.000	4.000	4.000	4.000	4.000	4.000	4.000	4.000	4.000	4.000	4.000	4.000	4.000	4.000	4.000	4.000	4.000	4.000	4.000	4.000	4.000	4.000	4.000	4.000	4.000	4.000
Ta^{5+}	0.002	0.000	0.000	0.002	0.000	0.001	0.003	0.000	0.002	0.000	0.001	0.000	0.005	0.002	0.001	0.000	0.001	0.001	0.001	0.002	0.000	0.000	0.000	0.001	0.000	0.004	0.000	0.001	0.000	0.000	0.003	0.001
Nb^{5+}	0.001	0.000	0.001	0.002	0.000	0.002	0.001	0.000	0.002	0.000	0.003	0.001	0.002	0.001	0.002	0.003	0.002	0.001	0.000	0.002	0.000	0.003	0.002	0.003	0.003	0.003	0.004	0.003	0.001	0.002	0.003	0.002
Sn^{4+}	0.001	0.002	0.001	0.002	0.002	0.003	0.002	0.001	0.000	0.001	0.001	0.000	0.001	0.000	0.001	0.000	0.001	0.001	0.001	0.001	0.000	0.000	0.000	0.000	0.001	0.000	0.001	0.001	0.000	0.001	0.001	0.000
Ti^{4+}	0.011	0.012	0.005	0.011	0.018	0.013	0.001	0.000	0.000	0.001	0.000	0.000	0.000	0.000	0.001	0.000	0.001	0.000	0.000	0.002	0.000	0.001	0.003	0.002	0.002	0.000	0.000	0.001	0.002	0.000	0.001	0.000
Fe^{3+}	0.000	0.000	0.000	0.000	0.000	0.131	0.000	0.000	0.047	0.000	0.000	0.048	0.000	0.016	0.064	0.003	0.000	0.000	0.016	0.016	0.022	0.000	0.037	0.048	0.023	0.084	0.000	0.000	0.000	0.000	0.000	0.000
Mn^{3+}	0.000	0.000	0.000	0.000	0.000	0.000	0.000	0.000	0.000	0.000	0.000	0.000	0.000	0.000	0.004	0.000	0.000	0.000	0.000	0.000	0.000	0.000	0.000	0.000	0.000	0.003	0.000	0.000	0.000	0.000	0.000	0.000
Cr^{3+}	0.003	0.001	0.004	0.002	0.004	0.002	0.001	0.002	0.003	0.004	0.003	0.004	0.004	0.001	0.003	0.002	0.004	0.004	0.003	0.003	0.002	0.003	0.003	0.002	0.002	0.001	0.002	0.003	0.005	0.004	0.004	0.004
Al^{3+}	1.842	1.766	1.847	1.813	1.751	1.684	1.993	1.985	1.899	1.966	1.966	1.881	1.943	1.874	1.918	1.840	1.958	1.955	1.930	1.908	1.867	1.968	1.935	1.877	1.875	1.789	1.975	1.944	1.933	1.938	1.962	1.946
Zn^{2+}	0.000	0.004	0.000	0.002	0.000	0.002	0.003	0.000	0.002	0.004	0.008	0.001	0.000	0.001	0.003	0.000	0.003	0.000	0.000	0.003	0.000	0.001	0.003	0.003	0.002	0.004	0.001	0.000	0.004	0.006	0.002	0.003
Co^{2+}	0.001	0.000	0.000	0.000	0.000	0.000	0.000	0.001	0.000	0.000	0.000	0.000	0.000	0.001	0.000	0.001	0.002	0.000	0.001	0.000	0.000	0.000	0.001	0.000	0.001	0.000	0.000	0.003	0.001	0.000	0.000	0.001
Fe^{2+}	0.112	0.147	0.087	0.103	0.156	0.007	0.069	0.064	0.010	0.066	0.066	0.011	0.059	0.048	0.000	0.021	0.053	0.057	0.026	0.029	0.050	0.069	0.028	0.006	0.016	0.000	0.054	0.054	0.057	0.071	0.065	0.056
Mn^{2+}	0.000	0.003	0.001	0.000	0.003	0.002	0.007	0.003	0.003	0.006	0.005	0.003	0.002	0.000	0.000	0.001	0.003	0.001	0.004	0.004	0.004	0.000	0.000	0.002	0.002	0.000	0.000	0.000	0.002	0.001	0.001	0.001
Mg^{2+}	0.109	0.144	0.095	0.117	0.143	0.134	0.001	0.001	0.000	0.001	0.000	0.000	0.001	0.001	0.000	0.000	0.001	0.003	0.000	0.000	0.005	0.003	0.001	0.001	0.000	0.005	0.000	0.003	0.003	0.002	0.000	0.002
Li^{+}	0.000	0.000	0.000	0.000	0.000	0.200	0.000	0.000	0.128	0.000	0.000	0.170	0.000	0.221	0.163	0.533	0.000	0.000	0.198	0.167	0.260	0.000	0.123	0.300	0.300	0.369	0.000	0.000	0.000	0.000	0.000	0.000
Total VI	2.081	2.080	2.041	2.053	2.078	2.182	2.080	2.055	2.096	2.048	2.052	2.119	2.016	2.167	2.160	2.403	2.027	2.022	2.180	2.136	2.209	2.048	2.134	2.246	2.225	2.264	2.037	2.012	2.008	2.024	2.043	2.016
Pb^{2+}	0.000	0.000	0.001	0.000	0.001	0.001	0.000	0.001	0.001	0.000	0.001	0.000	0.000	0.000	0.000	0.001	0.000	0.000	0.000	0.000	0.000	0.001	0.000	0.002	0.001	0.001	0.000	0.001	0.000	0.000	0.000	0.000
Ba^{2+}	0.004	0.002	0.003	0.002	0.004	0.000	0.000	0.000	0.001	0.002	0.000	0.000	0.001	0.000	0.001	0.000	0.001	0.000	0.000	0.001	0.000	0.000	0.001	0.000	0.000	0.000	0.001	0.002	0.000	0.001	0.000	0.000
Sr^{2+}	0.000	0.001	0.000	0.000	0.001	0.000	0.003	0.002	0.001	0.000	0.002	0.002	0.000	0.000	0.003	0.000	0.000	0.000	0.000	0.000	0.000	0.003	0.000	0.000	0.000	0.002	0.000	0.003	0.003	0.000	0.000	0.001
Ca^{2+}	0.002	0.001	0.001	0.000	0.002	0.002	0.005	0.001	0.001	0.001	0.000	0.002	0.000	0.002	0.001	0.014	0.001	0.000	0.001	0.000	0.001	0.002	0.000	0.002	0.001	0.002	0.002	0.001	0.000	0.000	0.001	0.000
K^{+}	0.781	0.836	0.837	0.835	0.819	0.845	0.721	0.792	0.877	0.831	0.818	0.887	0.878	0.882	0.783	0.764	0.858	0.861	0.829	0.859	0.861	0.803	0.803	0.784	0.850	0.868	0.813	0.885	0.897	0.883	0.821	0.888
Na^{+}	0.076	0.084	0.101	0.095	0.078	0.084	0.032	0.047	0.056	0.046	0.045	0.045	0.055	0.061	0.046	0.028	0.040	0.054	0.053	0.065	0.056	0.030	0.045	0.051	0.054	0.067	0.047	0.048	0.063	0.059	0.056	0.071
Total X	0.864	0.923	0.943	0.931	0.905	0.931	0.761	0.841	0.936	0.879	0.867	0.935	0.934	0.945	0.834	0.807	0.901	0.915	0.884	0.925	0.918	0.839	0.849	0.838	0.906	0.939	0.863	0.939	0.964	0.943	0.878	0.959
OH^{-}	1.878	1.870	1.927	1.914	1.874	1.872	1.956	1.947	1.962	1.943	1.968	1.976	1.971	1.947	1.950	1.951	1.998	1.937	1.986	1.988	1.988	1.974	1.954	1.982	1.964	1.942	1.994	1.984	1.983	1.985	1.969	1.975
Cl^{-}	0.001	0.001	0.003	0.001	0.003	0.002	0.002	0.002	0.004	0.000	0.000	0.001	0.000	0.002	0.001	0.002	0.002	0.002	0.000	0.000	0.000	0.000	0.001	0.000	0.000	0.001	0.000	0.001	0.001	0.000	0.002	0.000
F^{-}	0.110	0.117	0.066	0.074	0.106	0.113	0.041	0.050	0.035	0.056	0.032	0.023	0.029	0.051	0.048	0.047	0.000	0.060	0.014	0.010	0.012	0.025	0.043	0.016	0.035	0.057	0.006	0.014	0.014	0.015	0.028	0.024
$O2^{-}$	0.011	0.012	0.005	0.011	0.018	0.013	0.001	0.000	0.000	0.001	0.000	0.000	0.000	0.000	0.001	0.000	0.001	0.000	0.000	0.002	0.000	0.001	0.003	0.002	0.002	0.000	0.000	0.001	0.002	0.000	0.001	0.000
Total Y	2.000	2.000	2.000	2.000	2.000	2.000	2.000	2.000	2.000	2.000	2.000	2.000	2.000	2.000	2.000	2.000	2.000	2.000	2.000	2.000	2.000	2.000	2.000	2.000	2.000	2.000	2.000	2.000	2.000	2.000	2.000	2.000

Sample	#17B1					#17B2				#17B3			#18aB1					#18aB2				#18aB4		#19B3		#19B4			#19B5	
Domain	Pegmatite 2												Host Rock																
wt%	3	4	5	6	7	1	2	3	4	1	2	3	1	3	4	5	6	1	2	3	4	1	2	1	2	1	2	3	1	2
SiO_2	45.52	46.02	45.82	46.25	45.73	46.58	46.00	46.55	45.98	46.31	46.84	46.09	47.50	45.60	47.13	46.21	46.75	46.23	46.59	46.60	45.99	46.91	46.80	45.55	45.73	46.13	46.78	46.79	46.46	46.80
Al_2O_3	37.32	37.41	36.76	34.05	36.40	38.05	36.60	37.15	37.44	37.52	36.43	37.21	37.73	35.18	35.68	36.13	35.76	37.68	37.73	35.77	36.24	38.01	38.14	33.93	33.83	35.77	35.84	36.06	37.88	37.98
K_2O	10.26	10.60	10.14	10.05	9.80	9.30	10.13	10.42	10.44	9.55	10.26	10.36	9.06	10.03	10.15	10.25	10.05	9.32	9.18	10.03	10.03	8.64	8.34	8.25	8.05	9.51	9.31	9.54	8.83	8.63
Fe_2O_3	0.00	0.00	0.64	2.14	0.29	0.00	0.90	0.00	0.00	0.00	0.00	0.00	0.00	0.00	0.00	0.00	0.00	0.00	0.00	0.00	0.00	0.00	1.16	5.80	5.84	1.12	1.05	0.00	0.00	0.00
FeO	1.03	0.89	0.36	0.00	0.77	1.20	0.39	1.02	1.03	1.30	1.32	1.02	1.02	2.42	1.22	1.32	1.11	1.05	1.02	1.06	1.07	1.01	0.00	0.00	0.00	0.00	0.00	0.92	1.17	1.14
MgO	0.01	0.02	0.06	0.02	0.02	0.04	0.03	0.02	0.01	0.01	0.02	0.01	0.46	0.78	0.62	0.55	0.54	0.51	0.51	0.51	0.50	0.44	0.46	1.43	1.44	0.48	0.49	0.38	0.47	0.47
Mn_2O_3	0.00	0.00	0.00	0.10	0.00	0.00	0.00	0.00	0.00	0.00	0.00	0.00	0.00	0.00	0.00	0.00	0.00	0.00	0.00	0.00	0.00	0.00	0.01	0.03	0.00	0.05	0.00	0.00	0.00	0.00
MnO	0.04	0.04	0.05	0.00	0.06	0.05	0.07	0.05	0.00	0.03	0.05	0.05	0.04	0.03	0.00	0.02	0.03	0.00	0.02	0.00	0.00	0.00	0.00	0.00	0.00	0.00	0.00	0.02	0.01	0.00
CaO	0.00	0.00	0.09	0.02	0.02	0.03	0.07	0.00	0.01	0.00	0.03	0.03	0.01	0.01	0.02	0.01	0.03	0.00	0.00	0.01	0.03	0.00	0.01	0.02	0.01	0.00	0.01	0.01	0.00	0.00
Na_2O	0.49	0.38	0.47	0.40	0.57	0.39	0.50	0.57	0.53	0.35	0.50	0.52	0.46	0.42	0.42	0.43	0.48	0.44	0.42	0.54	0.56	0.42	0.41	0.21	0.20	0.44	0.43	0.54	0.39	0.38
BaO	0.00	0.01	0.00	0.02	0.08	0.04	0.00	0.00	0.00	0.00	0.00	0.00	0.23	0.23	0.26	0.23	0.18	0.19	0.28	0.19	0.20	0.17	0.24	0.20	0.21	0.19	0.16	0.20	0.20	0.27
SnO_2	0.04	0.04	0.04	0.10	0.04	0.02	0.03	0.04	0.05	0.01	0.00	0.02	0.01	0.00	0.00	0.00	0.00	0.00	0.00	0.00	0.00	0.00	0.02	0.00	0.00	0.00	0.00	0.00	0.00	0.00
TiO_2	0.00	0.03	0.06	0.04	0.01	0.01	0.00	0.02	0.02	0.01	0.02	0.07	0.44	0.20	0.23	0.35	0.29	0.22	0.24	0.31	0.30	0.37	0.38	0.45	0.48	0.33	0.33	0.41	0.34	0.40
Cr_2O_3	0.07	0.05	0.05	0.01	0.04	0.07	0.02	0.02	0.03	0.04	0.08	0.01	0.06	0.05	0.08	0.07	0.06	0.07	0.08	0.08	0.05	0.04	0.00	0.05	0.10	0.04	0.07	0.09	0.05	0.06
V_2O_3	0.00	0.00	0.00	0.00	0.00	0.00	0.00	0.00	0.00	0.00	0.00	0.00	0.00	0.00	0.00	0.00	0.00	0.00	0.00	0.00	0.00	0.00	0.00	0.00	0.00	0.00	0.00	0.00	0.00	0.00
ZnO	0.07	0.03	0.07	0.05	0.07	0.00	0.17	0.09	0.06	0.07	0.06	0.02	0.09	0.06	0.05	0.04	0.12	0.06	0.01	0.04	0.00	0.00	0.01	0.04	0.12	0.11	0.00	0.00	0.00	0.00
Li_2O*	0.00	0.00	0.68	2.19	1.40	0.00	0.49	0.00	0.00	0.00	0.00	0.00	0.00	0.00	0.00	0.00	0.00	0.00	0.00	0.00	0.00	0.00	0.29	0.60	0.44	0.98	1.04	0.00	0.00	0.00
Ta_2O_5	0.17	0.01	0.04	0.07	0.04	0.00	0.03	0.00	0.07	0.17	0.04	0.00	0.01	0.01	0.01	0.00	0.15	0.00	0.00	0.00	0.04	0.01	0.00	0.02	0.00	0.00	0.00	0.00	0.00	0.00
Nb_2O_5	0.01	0.12	0.10	0.03	0.05	0.06	0.06	0.07	0.00	0.07	0.06	0.00	0.05	0.02	0.00	0.04	0.00	0.13	0.12	0.10	0.04	0.02	0.03	0.00	0.07	0.02	0.00	0.02	0.04	0.06
PbO	0.01	0.00	0.03	0.00	0.00	0.01	0.03	0.01	0.00	0.06	0.03	0.00	0.06	0.06	0.00	0.00	0.00	0.00	0.02	0.00	0.01	0.02	0.00	0.01	0.02	0.04	0.05	0.00	0.00	0.00
SrO	0.06	0.00	0.01	0.05	0.00	0.03	0.00	0.00	0.00	0.00	0.00	0.09	0.00	0.05	0.06	0.04	0.08	0.08	0.02	0.01	0.06	0.00	0.05	0.00	0.00	0.04	0.04	0.03	0.00	0.01
CoO	0.00	0.00	0.00	0.01	0.01	0.00	0.02	0.00	0.00	0.00	0.02	0.00	0.01	0.00	0.01	0.00	0.00	0.00	0.02	0.00	0.02	0.03	0.02	0.00	0.01	0.01	0.02	0.01	0.00	0.01
Cl	0.00	0.00	0.01	0.00	0.00	0.01	0.00	0.00	0.01	0.00	0.01	0.00	0.01	0.02	0.03	0.02	0.00	0.00	0.00	0.00	0.00	0.00	0.01	0.00	0.01	0.01	0.00	0.01	0.00	0.01
F	0.12	0.02	0.12	0.17	0.08	0.26	0.30	0.23	0.19	0.07	0.23	0.15	0.00	0.09	0.30	0.06	0.00	0.02	0.12	0.03	0.05	0.13	0.18	0.02	0.00	0.07	0.15	0.08	0.00	0.01
Total	95.21	95.65	95.59	95.78	95.48	96.14	95.83	96.26	95.87	95.58	95.98	95.63	97.24	95.23	96.26	95.75	95.60	95.99	96.38	95.27	95.20	96.23	96.58	96.58	96.55	95.34	95.76	95.09	95.85	96.22
a.p.f.u (calculus done on the basis of 11 oxygens)																														
Si^{4+}	3.030	3.042	3.026	3.050	3.016	3.049	3.040	3.063	3.039	3.053	3.093	3.051	3.068	3.060	3.109	3.065	3.096	3.032	3.043	3.092	3.061	3.052	3.028	2.998	3.009	3.045	3.065	3.100	3.037	3.045
Al^{3+}	0.970	0.958	0.974	0.950	0.984	0.951	0.960	0.937	0.961	0.947	0.907	0.949	0.932	0.940	0.891	0.935	0.904	0.969	0.958	0.908	0.939	0.948	0.972	1.002	0.991	0.955	0.935	0.901	0.963	0.955
Fe^{3+}	0.000	0.000	0.000	0.000	0.000	0.000	0.000	0.000	0.000	0.000	0.000	0.000	0.000	0.000	0.000	0.000	0.000	0.000	0.000	0.000	0.000	0.000	0.000	0.000	0.000	0.000	0.000	0.000	0.000	0.000
Total IV	4.000	4.000	4.000	4.000	4.000	4.000	4.000	4.000	4.000	4.000	4.000	4.000	4.000	4.000	4.000	4.000	4.000	4.000	4.000	4.000	4.000	4.000	4.000	4.000	4.000	4.000	4.000	4.000	4.000	4.000
Ta^{5+}	0.003	0.000	0.001	0.001	0.001	0.000	0.001	0.000	0.001	0.002	0.001	0.000	0.000	0.000	0.000	0.000	0.003	0.000	0.000	0.000	0.001	0.000	0.000	0.000	0.000	0.000	0.000	0.000	0.000	0.000
Nb^{5+}	0.000	0.003	0.003	0.001	0.002	0.002	0.002	0.002	0.000	0.002	0.002	0.000	0.002	0.001	0.000	0.001	0.000	0.004	0.004	0.003	0.001	0.001	0.001	0.000	0.002	0.001	0.000	0.001	0.001	0.002
Sn^{4+}	0.001	0.001	0.001	0.003	0.001	0.001	0.001	0.001	0.001	0.000	0.000	0.000	0.000	0.000	0.000	0.000	0.000	0.000	0.000	0.000	0.000	0.000	0.001	0.000	0.000	0.000	0.000	0.000	0.000	0.000
Ti^{4+}	0.000	0.001	0.003	0.002	0.001	0.000	0.000	0.001	0.001	0.001	0.001	0.003	0.022	0.010	0.011	0.017	0.014	0.011	0.012	0.016	0.015	0.018	0.019	0.022	0.024	0.017	0.016	0.020	0.017	0.019
Fe^{3+}	0.000	0.000	0.032	0.106	0.015	0.000	0.045	0.000	0.000	0.000	0.000	0.000	0.000	0.000	0.000	0.000	0.000	0.000	0.000	0.000	0.000	0.000	0.057	0.287	0.289	0.056	0.052	0.000	0.000	0.000
Mn^{3+}	0.000	0.000	0.000	0.005	0.000	0.000	0.000	0.000	0.000	0.000	0.000	0.000	0.000	0.000	0.000	0.000	0.000	0.000	0.000	0.000	0.000	0.000	0.001	0.001	0.000	0.003	0.000	0.000	0.000	0.000
Cr^{3+}	0.004	0.003	0.002	0.001	0.002	0.004	0.001	0.001	0.002	0.002	0.004	0.000	0.003	0.003	0.004	0.004	0.003	0.003	0.004	0.004	0.003	0.002	0.000	0.003	0.005	0.002	0.003	0.005	0.003	0.003
Al^{3+}	1.957	1.957	1.887	1.697	1.846	1.983	1.891	1.945	1.955	1.968	1.928	1.954	1.940	1.843	1.883	1.889	1.887	1.944	1.946	1.889	1.903	1.965	1.936	1.629	1.633	1.828	1.833	1.915	1.956	1.958
Zn^{2+}	0.003	0.001	0.003	0.003	0.003	0.000	0.008	0.004	0.003	0.003	0.003	0.001	0.004	0.003	0.002	0.002	0.006	0.003	0.001	0.002	0.000	0.000	0.001	0.002	0.006	0.005	0.000	0.000	0.000	0.000
Co^{2+}	0.000	0.000	0.000	0.001	0.001	0.000	0.001	0.000	0.000	0.000	0.001	0.000	0.000	0.000	0.000	0.000	0.000	0.000	0.001	0.000	0.001	0.002	0.001	0.000	0.001	0.000	0.001	0.001	0.000	0.001
Fe^{2+}	0.057	0.049	0.020	0.000	0.043	0.066	0.022	0.056	0.057	0.072	0.073	0.057	0.055	0.136	0.068	0.073	0.061	0.058	0.056	0.059	0.059	0.055	0.000	0.000	0.000	0.000	0.000	0.051	0.064	0.062
Mn^{2+}	0.002	0.002	0.003	0.000	0.004	0.003	0.004	0.003	0.000	0.002	0.003	0.003	0.002	0.002	0.000	0.001	0.002	0.000	0.001	0.000	0.000	0.000	0.000	0.000	0.000	0.000	0.000	0.001	0.000	0.000
Mg^{2+}	0.001	0.002	0.006	0.002	0.002	0.004	0.003	0.002	0.001	0.001	0.002	0.001	0.044	0.078	0.061	0.055	0.053	0.050	0.050	0.050	0.050	0.043	0.044	0.140	0.141	0.047	0.048	0.038	0.046	0.045
Li^{+}	0.000	0.000	0.182	0.582	0.371	0.000	0.131	0.000	0.000	0.000	0.000	0.000	0.000	0.000	0.000	0.000	0.000	0.000	0.000	0.000	0.000	0.000	0.074	0.158	0.116	0.260	0.274	0.000	0.000	0.000
Total VI	2.028	2.020	2.142	2.402	2.289	2.062	2.108	2.015	2.022	2.053	2.016	2.019	2.072	2.075	2.029	2.042	2.029	2.072	2.074	2.023	2.033	2.087	2.133	2.242	2.217	2.219	2.228	2.031	2.087	2.090
Pb^{2+}	0.000	0.000	0.001	0.000	0.000	0.000	0.001	0.000	0.000	0.001	0.001	0.000	0.001	0.001	0.000	0.000	0.000	0.000	0.000	0.000	0.000	0.000	0.000	0.000	0.000	0.001	0.001	0.000	0.000	0.000
Ba^{2+}	0.000	0.000	0.000	0.001	0.002	0.001	0.000	0.000	0.000	0.000	0.000	0.000	0.006	0.006	0.007	0.006	0.005	0.005	0.007	0.005	0.005	0.004	0.006	0.005	0.005	0.005	0.004	0.005	0.005	0.007
Sr^{2+}	0.002	0.000	0.000	0.002	0.000	0.001	0.000	0.000	0.000	0.000	0.000	0.003	0.000	0.002	0.002	0.002	0.003	0.003	0.001	0.000	0.003	0.000	0.002	0.000	0.000	0.001	0.001	0.001	0.000	0.001
Ca^{2+}	0.000	0.000	0.007	0.001	0.001	0.002	0.005	0.000	0.001	0.000	0.002	0.002	0.001	0.001	0.002	0.001	0.002	0.000	0.000	0.001	0.002	0.000	0.001	0.001	0.001	0.000	0.001	0.001	0.000	0.000
K^{+}	0.871	0.894	0.854	0.846	0.825	0.776	0.854	0.875	0.880	0.804	0.865	0.875	0.746	0.859	0.854	0.867	0.849	0.780	0.765	0.849	0.852	0.717	0.688	0.693	0.676	0.801	0.778	0.806	0.737	0.716
Na^{+}	0.063	0.049	0.060	0.051	0.073	0.049	0.064	0.073	0.068	0.045	0.064	0.067	0.058	0.054	0.054	0.055	0.061	0.056	0.053	0.070	0.072	0.053	0.052	0.027	0.026	0.056	0.054	0.069	0.050	0.048
Total X	0.937	0.944	0.922	0.901	0.901	0.830	0.924	0.948	0.949	0.850	0.931	0.947	0.812	0.923	0.918	0.931	0.920	0.844	0.826	0.924	0.933	0.775	0.749	0.726	0.708	0.865	0.839	0.882	0.791	0.772
OH^{-}	1.974	1.995	1.971	1.963	1.983	1.945	1.937	1.951	1.958	1.985	1.949	1.966	1.977	1.970	1.922	1.969	1.986	1.985	1.964	1.978	1.974	1.955	1.944	1.974	1.975	1.967	1.952	1.962	1.983	1.978
Cl^{-}	0.000	0.000	0.002	0.000	0.000	0.001	0.000	0.000	0.001	0.000	0.002	0.000	0.001	0.002	0.004	0.002	0.000	0.000	0.000	0.000	0.000	0.000	0.001	0.000	0.001	0.001	0.000	0.001	0.000	0.001
F^{-}	0.026	0.004	0.024	0.035	0.017	0.054	0.063	0.048	0.040	0.014	0.049	0.031	0.000	0.018	0.063	0.012	0.000	0.004	0.024	0.006	0.011	0.027	0.036	0.004	0.000	0.015	0.032	0.017	0.000	0.002
$O2^{-}$	0.000	0.001	0.003	0.002	0.001	0.000	0.000	0.001	0.001	0.001	0.001	0.003	0.022	0.010	0.011	0.017	0.014	0.011	0.012	0.016	0.015	0.018	0.019	0.022	0.024	0.017	0.016	0.020	0.017	0.019
Total Y	2.000	2.000	2.000	2.000	2.000	2.000	2.000	2.000	2.000	2.000	2.000	2.000	2.000	2.000	2.000	2.000	2.000	2.000	2.000	2.000	2.000	2.000	2.000	2.000	2.000	2.000	2.000	2.000	2.000	2.000

II.II.VI BIOTITE

Sample	#12B2						#12B2.2						#18aB3	#18aB5			#18aB6				#19B1				#19B2			#19B3					#19B4			
Zone	MAZ												Host Rock																							
wt%	1	2	3	4	5	6	1	2	3	4	5	6	1	1	2	3	1	2	3	4	1	2	3	4	1	2	3	1	2	3	4	5	1	2	3	4
SiO_2	36.84	36.86	36.73	36.40	37.22	37.46	36.16	37.58	37.44	36.33	38.15	35.91	35.35	34.66	34.67	33.70	34.94	34.91	34.91	35.42	35.35	34.98	35.37	35.39	33.09	33.10	35.05	35.26	35.13	34.52	34.37	34.63	33.97	33.65	35.08	34.42
Al_2O_3	20.51	20.14	20.55	20.62	20.44	20.12	20.73	20.15	20.40	20.42	19.75	20.43	21.68	21.41	21.33	21.08	20.75	20.82	20.62	20.37	20.70	20.70	20.50	20.51	20.20	20.10	19.32	20.30	20.25	19.99	20.33	20.38	20.36	20.33	20.40	20.51
MgO	5.24	5.63	5.11	5.23	5.37	5.46	5.18	5.58	5.42	5.50	5.92	5.41	7.36	5.66	5.67	6.21	5.28	5.29	5.18	4.95	5.48	5.50	5.52	5.48	6.47	6.53	5.54	5.68	5.73	5.50	5.81	5.74	5.98	5.97	5.72	5.73
K_2O	8.07	8.36	8.42	8.15	8.08	8.25	8.02	8.23	8.15	7.48	8.58	7.87	6.35	7.94	7.94	5.19	7.53	7.44	7.48	8.03	8.21	8.15	7.95	8.16	6.39	6.45	8.39	7.98	8.01	7.69	7.94	7.72	7.26	7.32	7.81	7.80
FeO	11.64	11.23	11.79	12.92	11.94	9.03	8.24	11.86	11.32	11.56	20.41	14.20	11.86	13.60	14.66	16.01	14.98	14.15	11.59	14.08	12.86	15.07	15.44	14.83	16.76	15.66	14.56	14.71	15.21	11.56	14.10	14.48	16.64	14.57	13.18	15.11
Fe_2O_3	10.70	11.33	10.94	10.04	10.25	12.77	16.02	10.59	10.60	12.05	0.00	9.67	11.83	10.99	9.68	10.19	9.29	10.08	13.19	9.91	11.90	9.51	9.25	9.52	9.85	10.84	9.70	9.76	8.94	13.07	10.38	10.16	8.88	11.18	11.28	9.21
Mn_2O_3	0.00	0.00	0.00	0.00	0.00	0.00	0.00	0.00	0.00	0.00	0.00	0.00	0.00	0.00	0.00	0.00	0.00	0.00	0.00	0.00	0.00	0.00	0.00	0.00	0.00	0.00	0.00	0.00	0.00	0.00	0.00	0.00	0.00	0.00	0.00	0.00
MnO	0.30	0.24	0.22	0.23	0.23	0.28	0.22	0.21	0.27	0.25	0.15	0.25	0.27	0.23	0.25	0.28	0.25	0.24	0.29	0.23	0.20	0.16	0.16	0.14	0.22	0.10	0.13	0.14	0.14	0.19	0.12	0.16	0.17	0.17	0.15	0.10
CaO	0.01	0.02	0.01	0.04	0.01	0.02	0.03	0.02	0.03	0.05	0.02	0.04	0.31	0.01	0.03	0.13	0.13	0.15	0.07	0.04	0.00	0.01	0.03	0.00	0.00	0.00	0.00	0.00	0.01	0.05	0.00	0.02	0.00	0.06	0.01	0.04
Na_2O	0.08	0.05	0.10	0.11	0.13	0.10	0.10	0.11	0.12	0.11	0.08	0.10	0.08	0.11	0.09	0.75	0.12	0.16	0.11	0.08	0.07	0.06	0.07	0.10	0.05	0.01	0.04	0.02	0.03	0.09	0.08	0.05	0.08	0.09	0.05	0.06
BaO	0.08	0.08	0.08	0.05	0.12	0.01	0.10	0.10	0.07	0.08	0.09	0.05	0.05	0.04	0.03	0.02	0.01	0.10	0.10	0.09	0.11	0.11	0.09	0.12	0.06	0.08	0.10	0.04	0.03	0.04	0.09	0.05	0.04	0.11	0.05	0.12
Cs_2O	0.00	0.02	0.00	0.00	0.03	0.12	0.00	0.00	0.00	0.00	0.23	0.00	0.00	0.00	0.00	0.00	0.00	0.00	0.00	0.00	0.00	0.00	0.00	0.00	0.00	0.00	0.00	0.00	0.00	0.00	0.00	0.00	0.00	0.00	0.00	0.00
TiO_2	1.69	1.63	1.54	1.75	1.71	1.42	1.74	1.65	1.78	1.57	1.70	1.54	0.07	0.62	0.58	0.61	1.72	1.67	1.72	1.76	1.50	1.56	1.69	1.55	1.37	1.40	1.68	1.62	1.56	1.74	1.63	1.61	1.60	1.57	1.57	1.58
Cr_2O_3	0.07	0.06	0.08	0.09	0.06	0.09	0.09	0.09	0.05	0.05	0.10	0.04	0.06	0.08	0.05	0.05	0.06	0.08	0.10	0.08	0.07	0.10	0.11	0.05	0.09	0.09	0.05	0.04	0.09	0.11	0.12	0.08	0.10	0.10	0.09	0.10
ZnO	0.00	0.04	0.09	0.06	0.07	0.10	0.09	0.05	0.07	0.14	0.12	0.23	0.29	0.13	0.03	0.05	0.08	0.03	0.11	0.05	0.07	0.00	0.06	0.02	0.03	0.03	0.02	0.04	0.00	0.10	0.01	0.00	0.10	0.11	0.08	0.01
Li_2O*	0.94	0.93	0.56	0.21	0.20	1.89	0.00	0.13	0.15	1.39	0.00	0.26	1.12	1.00	1.07	0.00	1.00	1.28	0.00	1.39	0.24	0.17	0.17	0.23	0.00	0.00	0.00	0.93	1.07	0.00	0.00	0.00	0.00	0.00	1.64	0.00
Ta_2O_5	0.00	0.04	0.06	0.00	0.06	0.00	0.00	0.00	0.05	0.10	0.09	0.10	0.01	0.00	0.00	0.13	0.02	0.16	0.00	0.00	0.16	0.04	0.19	0.00	0.01	0.00	0.00	0.00	0.00	0.12	0.09	0.15	0.03	0.00	0.18	0.00
Nb_2O_5	0.13	0.04	0.06	0.10	0.10	0.08	0.10	0.04	0.19	0.04	0.04	0.00	0.05	0.04	0.05	0.07	0.06	0.06	0.09	0.08	0.09	0.08	0.07	0.08	0.07	0.00	0.07	0.00	0.06	0.03	0.10	0.00	0.03	0.08	0.01	0.11
Ga_2O_3	0.00	0.04	0.00	0.04	0.00	0.00	0.00	0.02	0.00	0.00	0.00	0.00	0.00	0.04	0.03	0.00	0.06	0.01	0.00	0.03	0.00	0.00	0.05	0.01	0.03	0.05	0.00	0.00	0.02	0.05	0.00	0.00	0.01	0.00	0.00	0.00
PbO	0.03	0.02	0.03	0.00	0.00	0.00	0.00	0.00	0.00	0.03	0.00	0.00	0.06	0.02	0.00	0.05	0.00	0.03	0.00	0.03	0.02	0.00	0.04	0.00	0.00	0.00	0.01	0.00	0.00	0.03	0.05	0.00	0.01	0.01	0.07	0.00
SrO	0.00	0.02	0.00	0.00	0.00	0.06	0.11	0.02	0.01	0.03	0.09	0.00	0.00	0.01	0.00	0.00	0.00	0.00	0.08	0.00	0.03	0.00	0.00	0.00	0.04	0.06	0.03	0.01	0.00	0.09	0.02	0.03	0.00	0.05	0.01	0.01
CoO	0.05	0.04	0.04	0.05	0.03	0.04	0.06	0.02	0.02	0.05	0.07	0.04	0.03	0.04	0.01	0.07	0.05	0.04	0.05	0.03	0.06	0.05	0.06	0.07	0.04	0.05	0.03	0.04	0.04	0.03	0.03	0.04	0.04	0.05	0.05	0.06
Cl	0.01	0.00	0.01	0.00	0.00	0.01	0.00	0.01	0.00	0.03	0.01	0.03	0.03	0.01	0.00	0.03	0.00	0.00	0.01	0.00	0.01	0.00	0.01	0.01	0.00	0.00	0.01	0.01	0.01	0.00	0.00	0.01	0.02	0.02	0.01	0.01
F	1.48	1.28	1.26	1.42	1.27	1.69	1.10	1.27	1.39	1.05	1.60	1.06	0.54	0.53	0.31	0.33	0.29	0.29	0.29	0.40	0.11	0.20	0.28	0.19	0.02	0.21	0.12	0.29	0.25	0.29	0.11	0.26	0.14	0.10	0.19	0.21
Total	97.87	98.09	97.67	97.50	97.29	99.02	98.08	97.72	97.53	98.31	97.21	97.21	97.39	97.17	96.48	94.95	96.60	96.97	95.99	97.06	97.23	96.43	97.10	96.44	94.77	94.76	94.82	96.88	96.56	95.29	95.39	95.57	95.47	95.53	97.61	95.19
a.p.f.u (Calculus done on a basis of 11 oxygens)																																				
Si^{4+}	2.717	2.712	2.722	2.715	2.761	2.711	2.661	2.776	2.769	2.658	2.889	2.692	2.581	2.578	2.593	2.569	2.615	2.598	2.628	2.637	2.630	2.637	2.652	2.662	2.548	2.548	2.691	2.633	2.632	2.625	2.619	2.634	2.598	2.569	2.588	2.630
Al^{3+}	1.283	1.288	1.279	1.285	1.239	1.289	1.339	1.224	1.231	1.342	1.111	1.308	1.419	1.422	1.407	1.431	1.385	1.402	1.372	1.363	1.370	1.363	1.348	1.338	1.452	1.452	1.309	1.367	1.368	1.375	1.381	1.367	1.402	1.431	1.412	1.370
Fe^{3+}	0.000	0.000	0.000	0.000	0.000	0.000	0.000	0.000	0.000	0.000	0.000	0.000	0.000	0.000	0.000	0.000	0.000	0.000	0.000	0.000	0.000	0.000	0.000	0.000	0.000	0.000	0.000	0.000	0.000	0.000	0.000	0.000	0.000	0.000	0.000	0.000
Total IV	4.000	4.000	4.000	4.000	4.000	4.000	4.000	4.000	4.000	4.000	4.000	4.000	4.000	4.000	4.000	4.000	4.000	4.000	4.000	4.000	4.000	4.000	4.000	4.000	4.000	4.000	4.000	4.000	4.000	4.000	4.000	4.000	4.000	4.000	4.000	4.000
Ta^{5+}	0.000	0.001	0.001	0.000	0.001	0.000	0.000	0.000	0.001	0.002	0.002	0.002	0.000	0.000	0.000	0.003	0.000	0.003	0.000	0.000	0.003	0.001	0.004	0.000	0.000	0.000	0.000	0.000	0.000	0.002	0.002	0.003	0.001	0.000	0.004	0.000
Nb^{5+}	0.004	0.001	0.002	0.003	0.003	0.003	0.003	0.001	0.006	0.001	0.001	0.000	0.002	0.001	0.002	0.003	0.002	0.002	0.003	0.003	0.003	0.003	0.002	0.003	0.002	0.000	0.002	0.000	0.002	0.001	0.003	0.000	0.001	0.003	0.000	0.004
Ti^{4+}	0.094	0.090	0.086	0.098	0.096	0.078	0.096	0.092	0.099	0.087	0.097	0.087	0.004	0.034	0.033	0.035	0.097	0.093	0.097	0.099	0.084	0.088	0.096	0.088	0.079	0.081	0.097	0.091	0.088	0.100	0.094	0.092	0.092	0.090	0.087	0.091
Fe^{3+}	0.594	0.627	0.610	0.564	0.572	0.696	0.887	0.588	0.590	0.663	0.000	0.545	0.650	0.615	0.545	0.585	0.523	0.565	0.747	0.556	0.667	0.539	0.522	0.539	0.571	0.628	0.560	0.549	0.504	0.748	0.596	0.581	0.511	0.642	0.626	0.529
Mn^{3+}	0.000	0.000	0.000	0.000	0.000	0.000	0.000	0.000	0.000	0.000	0.000	0.000	0.000	0.000	0.000	0.000	0.000	0.000	0.000	0.000	0.000	0.000	0.000	0.000	0.000	0.000	0.000	0.000	0.000	0.000	0.000	0.000	0.000	0.000	0.000	0.000
Ga^{3+}	0.000	0.002	0.000	0.002	0.000	0.000	0.000	0.001	0.000	0.000	0.000	0.000	0.000	0.002	0.001	0.000	0.003	0.000	0.000	0.002	0.000	0.000	0.003	0.000	0.001	0.003	0.000	0.000	0.001	0.002	0.000	0.000	0.001	0.000	0.000	0.000
Cr^{3+}	0.004	0.003	0.005	0.005	0.003	0.005	0.005	0.005	0.003	0.003	0.006	0.003	0.004	0.005	0.003	0.003	0.003	0.005	0.006	0.005	0.004	0.006	0.006	0.003	0.005	0.006	0.003	0.002	0.005	0.007	0.007	0.005	0.006	0.006	0.005	0.006
Al^{3+}	0.499	0.459	0.516	0.528	0.548	0.428	0.458	0.530	0.547	0.420	0.652	0.497	0.446	0.455	0.473	0.463	0.446	0.424	0.457	0.424	0.445	0.475	0.464	0.480	0.381	0.372	0.439	0.420	0.420	0.417	0.445	0.460	0.434	0.398	0.361	0.477
Zn^{2+}	0.000	0.002	0.005	0.003	0.004	0.005	0.005	0.003	0.004	0.007	0.007	0.013	0.016	0.007	0.001	0.003	0.005	0.002	0.006	0.003	0.004	0.000	0.003	0.001	0.001	0.002	0.001	0.002	0.000	0.006	0.000	0.000	0.006	0.006	0.004	0.001
Fe^{2+}	0.718	0.691	0.731	0.806	0.741	0.547	0.507	0.733	0.700	0.708	1.293	0.890	0.724	0.846	0.917	1.021	0.938	0.880	0.729	0.877	0.800	0.950	0.969	0.933	1.079	1.009	0.935	0.919	0.953	0.735	0.899	0.921	1.064	0.930	0.813	0.966
Mn^{2+}	0.019	0.015	0.014	0.015	0.014	0.017	0.014	0.013	0.017	0.015	0.010	0.016	0.017	0.014	0.016	0.018	0.016	0.015	0.019	0.015	0.012	0.010	0.010	0.009	0.014	0.006	0.008	0.009	0.009	0.012	0.008	0.011	0.011	0.011	0.009	0.006
Co^{2+}	0.003	0.002	0.002	0.003	0.002	0.002	0.003	0.001	0.001	0.003	0.004	0.002	0.002	0.003	0.001	0.004	0.003	0.002	0.003	0.002	0.004	0.003	0.004	0.005	0.003	0.003	0.002	0.002	0.003	0.002	0.002	0.002	0.003	0.003	0.003	0.004
Mg^{2+}	0.577	0.617	0.564	0.581	0.594	0.589	0.569	0.614	0.598	0.601	0.668	0.604	0.801	0.628	0.632	0.705	0.589	0.587	0.581	0.550	0.608	0.618	0.617	0.614	0.743	0.750	0.634	0.632	0.640	0.624	0.660	0.651	0.682	0.679	0.629	0.653
Li^{+}	0.278	0.275	0.167	0.062	0.059	0.549	0.000	0.040	0.044	0.410	0.000	0.078	0.328	0.301	0.322	0.000	0.301	0.384	0.000	0.418	0.071	0.050	0.053	0.070	0.000	0.000	0.000	0.281	0.321	0.000	0.000	0.000	0.000	0.000	0.488	0.000
Total VI	2.789	2.786	2.701	2.670	2.636	2.918	2.548	2.622	2.610	2.920	2.740	2.737	2.991	2.911	2.946	2.842	2.925	2.962	2.649	2.951	2.705	2.743	2.752	2.744	2.881	2.859	2.681	2.906	2.946	2.656	2.716	2.726	2.811	2.769	3.029	2.736
Ba^{2+}	0.002	0.002	0.002	0.002	0.004	0.000	0.003	0.003	0.002	0.002	0.003	0.001	0.001	0.001	0.001	0.001	0.000	0.003	0.003	0.003	0.003	0.003	0.003	0.003	0.002	0.002	0.003	0.001	0.001	0.001	0.003	0.002	0.001	0.003	0.001	0.004
Ca^{2+}	0.001	0.001	0.001	0.003	0.001	0.001	0.002	0.001	0.003	0.004	0.002	0.003	0.024	0.001	0.002	0.011	0.010	0.012	0.005	0.003	0.000	0.001	0.002	0.000	0.000	0.000	0.000	0.000	0.001	0.004	0.000	0.002	0.000	0.005	0.001	0.004
Pb^{2+}	0.001	0.000	0.001	0.000	0.000	0.000	0.000	0.000	0.000	0.001	0.000	0.000	0.001	0.000	0.000	0.001	0.000	0.001	0.000	0.001	0.000	0.000	0.001	0.000	0.000	0.000	0.000	0.000	0.000	0.001	0.001	0.000	0.000	0.000	0.001	0.000
Sr^{2+}	0.000	0.001	0.000	0.000	0.000	0.002	0.005	0.001	0.000	0.001	0.004	0.000	0.000	0.001	0.000	0.000	0.000	0.000	0.004	0.000	0.001	0.000	0.000	0.000	0.002	0.003	0.002	0.001	0.000	0.004	0.001	0.001	0.000	0.002	0.001	0.000
Cs^{+}	0.000	0.001	0.000	0.000	0.001	0.004	0.000	0.000	0.000	0.000	0.007	0.000	0.000	0.000	0.000	0.000	0.000	0.000	0.000	0.000	0.000	0.000	0.000	0.000	0.000	0.000	0.000	0.000	0.000	0.000	0.000	0.000	0.000	0.000	0.000	0.000
K+	0.759	0.785	0.796	0.776	0.765	0.762	0.753	0.776	0.769	0.699	0.829	0.752	0.592	0.754	0.757	0.504	0.719	0.706	0.718	0.763	0.779	0.784	0.760	0.783	0.627	0.634	0.822	0.760	0.766	0.747	0.772	0.749	0.708	0.713	0.735	0.760
Na^{+}	0.012	0.007	0.014	0.015	0.018	0.014	0.014	0.016	0.017	0.016	0.012	0.015	0.011	0.016	0.014	0.110	0.017	0.023	0.017	0.011	0.010	0.009	0.010	0.014	0.007	0.001	0.005	0.003	0.004	0.014	0.012	0.008	0.012	0.013	0.007	0.010
Total X	0.775	0.798	0.814	0.796	0.788	0.784	0.776	0.797	0.790	0.723	0.857	0.771	0.630	0.773	0.774	0.627	0.747	0.744	0.747	0.780	0.794	0.797	0.776	0.801	0.638	0.639	0.832	0.765	0.772	0.770	0.788	0.761	0.722	0.737	0.746	0.777
$O2^{-}$	0.094	0.090	0.086	0.098	0.096	0.078	0.096	0.092	0.099	0.087	0.097	0.087	0.004	0.034	0.033	0.035	0.097	0.093	0.097	0.099	0.084	0.088	0.096	0.088	0.079	0.081	0.097	0.091	0.088	0.100	0.094	0.092	0.092	0.090	0.087	0.091
F^{-}	0.346	0.298	0.296	0.335	0.297	0.388	0.257	0.296	0.326	0.243	0.384	0.251	0.125	0.124	0.072	0.080	0.069	0.069	0.070	0.095	0.025	0.048	0.067	0.044	0.005	0.052	0.030	0.068	0.059	0.069	0.025	0.063	0.033	0.024	0.045	0.051
Cl^{-}	0.001	0.000	0.002	0.000	0.000	0.001	0.000	0.001	0.000	0.004	0.001	0.003	0.004	0.001	0.000	0.004	0.000	0.000	0.001	0.000	0.002	0.000	0.002	0.002	0.000	0.000	0.001	0.002	0.001	0.000	0.001	0.001	0.002	0.002	0.001	0.002
OH^{-}	1.560	1.612	1.617	1.567	1.608	1.534	1.647	1.611	1.575	1.667	1.518	1.659	1.868	1.840	1.895	1.881	1.835	1.838	1.832	1.807	1.889	1.864	1.836	1.867	1.915	1.867	1.872	1.840	1.852	1.831	1.881	1.844	1.873	1.884	1.867	1.857
Total Y	2.000	2.000	2.000	2.000	2.000	2.000	2.000	2.000	2.000	2.000	2.000	2.000	2.000	2.000	2.000	2.000	2.000	2.000	2.000	2.000	2.000	2.000	2.000	2.000	2.000	2.000	2.000	2.000	2.000	2.000	2.000	2.000	2.000	2.000	2.000	2.000

II.II.VII GARNET

Sample	#19B1						#19B3				#19B4				#19B5	
Position	Core	Mid	Rim	Core	Mid	Rim	Core	Mid 1	Mid 2	Rim	Core	Mid 1	Mid 2	Rim	Core	Rim
wt%	1	2	3	4	5	6	1	2	3	4	1	2	3	4	1	2
SiO_2	36.34	36.19	36.26	36.49	36.24	36.60	34.96	34.87	35.65	35.81	35.72	35.57	35.55	35.79	35.95	36.04
TiO_2	0.13	0.02	0.02	0.01	0.03	0.01	0.06	0.05	0.03	0.00	0.02	0.04	0.01	0.05	0.03	0.05
Al_2O_3	20.71	20.94	20.84	20.76	20.92	20.84	20.04	20.17	20.69	20.73	20.67	20.41	20.56	20.44	20.56	20.55
Cr_2O_3	0.10	0.07	0.09	0.05	0.04	0.08	0.06	0.09	0.07	0.09	0.04	0.08	0.06	0.09	0.06	0.08
Fe_2O_3	0.04	0.00	0.00	0.00	0.00	0.00	0.00	0.00	0.00	0.00	0.00	0.00	0.00	0.00	0.00	0.00
FeO	29.75	29.10	29.85	31.08	31.12	31.02	27.46	27.60	28.51	31.04	27.14	27.21	27.71	29.11	27.77	27.75
MnO	9.52	10.24	9.26	7.75	7.89	7.90	10.63	10.82	10.16	7.61	10.77	10.71	10.60	8.85	10.55	10.64
MgO	1.18	1.15	1.18	1.27	1.37	1.34	1.10	1.05	1.10	1.30	0.93	1.03	0.99	1.09	1.07	1.08
CaO	1.94	1.90	1.95	1.88	1.93	1.92	1.81	1.79	1.84	1.64	1.71	1.71	1.78	2.00	2.00	1.95
Y_2O_3	0.00	0.00	0.00	0.00	0.00	0.00	0.11	0.09	0.00	0.15	0.28	0.28	0.11	0.00	0.04	0.00
Total	99.71	99.61	99.44	99.28	99.53	99.70	96.24	96.54	98.04	98.37	97.28	97.02	97.36	97.42	98.02	98.13
a.p.f.u (calculus done on the basis of 8 Oxygen)																
Si^{4+}	2.964	2.942	2.958	2.993	2.946	2.985	2.950	2.924	2.946	2.951	2.997	2.992	2.970	2.994	2.987	2.994
Al^{IV}	0.008	0.001	0.001	0.003	0.002	0.001	0.004	0.003	0.002	0.000	0.002	0.003	0.002	0.003	0.003	0.003
T-Total	2.972	2.943	2.959	2.995	2.947	2.986	2.954	2.927	2.948	2.951	2.999	2.994	2.972	2.997	2.990	2.997
Al^{VI}	1.983	2.006	2.003	2.004	2.002	2.003	1.988	1.991	2.014	2.013	2.042	2.020	2.022	2.012	2.010	2.009
Ti^{4+}	0.008	0.001	0.001	0.000	0.002	0.001	0.004	0.003	0.002	0.000	0.002	0.003	0.001	0.003	0.002	0.003
Fe^{3+}	0.003	0.000	0.000	0.000	0.000	0.000	0.000	0.000	0.000	0.000	0.000	0.000	0.000	0.000	0.000	0.000
Cr^{3+}	0.007	0.005	0.006	0.003	0.003	0.005	0.004	0.006	0.005	0.006	0.003	0.005	0.004	0.006	0.004	0.005
Fe^{2+}	0.000	0.000	0.000	0.000	0.000	0.000	0.004	0.000	0.000	0.000	0.000	0.000	0.000	0.000	0.000	0.000
$[R^{3+}]^{VI}$	2.000	2.012	2.010	2.007	2.007	2.009	2.000	2.000	2.020	2.019	2.046	2.028	2.027	2.021	2.016	2.017
Fe^{2+}	2.029	1.979	2.037	2.132	2.116	2.116	1.934	1.936	1.970	2.139	1.904	1.914	1.935	2.036	1.929	1.928
Mn^{2+}	0.658	0.705	0.640	0.538	0.543	0.545	0.760	0.768	0.711	0.531	0.766	0.763	0.750	0.627	0.742	0.748
Mg^{2+}	0.144	0.139	0.143	0.155	0.166	0.162	0.138	0.131	0.136	0.159	0.117	0.129	0.123	0.136	0.132	0.133
Ca^{2+}	0.169	0.166	0.171	0.165	0.168	0.168	0.164	0.161	0.163	0.145	0.153	0.154	0.159	0.180	0.178	0.173
Y^{3+}	0.000	0.000	0.000	0.000	0.000	0.000	0.005	0.004	0.000	0.006	0.013	0.012	0.005	0.000	0.002	0.000
$[R^{2+}]^{VIII}$	3.000	2.989	2.991	2.990	2.993	2.991	3.000	3.000	2.980	2.981	2.952	2.972	2.972	2.979	2.983	2.983

II.II.VIII TOURMALINE

Sample	#11bB1						#11bB1.1		#11bB2						#11bB3								#11cB8								#11cR	
Zone															MAZ																	
Position	Core	Rim	Core	Rim	Core	Rim	Core	Rim	Core	Rim	Core	Rim	Core	Rim	Core	Rim	Core	Rim	Core	Rim	Core	Rim	Core	Interval 1	Interval 2	Rim	Interval 1	Interval 2	Interval 3	Rim	Core	Interval 1
Wt%	1	2	3	4	5	6	1	2	1	2	3	4	5	6	1	2	3	4	5	6	7	8	1	2	3	4	5	6	7	8	1	2
SiO_2	35.33	35.37	35.74	35.29	35.10	35.07	35.76	35.24	35.47	35.46	35.67	35.51	35.53	35.45	35.58	35.25	35.34	35.65	35.17	36.17	35.45	35.13	35.42	35.29	35.16	34.84	35.35	35.47	34.93	34.98	35.59	35.21
Al_2O_3	33.42	33.13	34.30	33.52	32.55	32.31	34.14	32.56	33.30	33.53	34.22	33.66	33.25	33.03	32.01	32.89	33.77	33.05	32.72	32.91	32.49	32.41	32.95	33.82	33.25	32.97	34.41	33.91	33.69	32.95	34.55	33.57
Fe_2O_3	0.00	0.00	0.00	0.00	0.00	0.00	0.00	0.00	0.00	0.00	0.00	0.00	0.00	0.00	0.89	0.00	0.00	0.00	0.00	1.11	0.57	0.00	0.00	0.00	0.00	0.00	0.00	0.00	0.00	0.00	0.00	0.00
FeO	10.48	10.39	7.75	8.57	9.97	10.23	8.57	10.65	10.93	11.02	9.82	8.42	8.80	9.54	8.21	9.47	7.93	8.73	9.61	7.89	9.72	10.13	10.84	10.44	9.06	10.85	9.97	9.24	8.62	10.86	9.53	10.12
MgO	3.36	3.37	4.62	4.58	4.00	3.84	4.06	3.35	2.87	2.80	3.51	4.58	4.38	4.00	4.55	4.10	4.91	4.38	4.13	4.80	3.68	3.93	3.04	2.80	4.27	3.02	2.93	3.63	4.40	2.99	3.11	3.26
B_2O_3	10.40	10.38	10.56	10.47	10.34	10.32	10.46	10.32	10.41	10.42	10.53	10.52	10.48	10.45	10.46	10.42	10.50	10.46	10.40	10.53	10.42	10.35	10.38	10.37	10.41	10.32	10.42	10.46	10.42	10.32	10.47	10.38
MnO	0.08	0.10	0.03	0.07	0.03	0.09	0.02	0.08	0.08	0.06	0.04	0.09	0.06	0.04	0.00	0.06	0.07	0.01	0.06	0.00	0.08	0.08	0.12	0.05	0.03	0.04	0.11	0.02	0.08	0.11	0.02	0.04
K_2O	0.01	0.03	0.02	0.01	0.02	0.03	0.01	0.05	0.01	0.02	0.02	0.02	0.04	0.04	0.01	0.01	0.02	0.02	0.00	0.02	0.02	0.02	0.19	0.03	0.03	0.02	0.04	0.03	0.03	0.05	0.01	0.01
Na_2O	1.68	1.67	1.67	1.49	1.73	1.79	1.30	1.63	1.77	1.77	1.70	1.46	1.72	1.89	2.01	1.93	1.38	1.80	2.04	1.68	1.89	1.84	1.70	1.68	1.69	1.80	1.48	1.75	1.57	1.73	1.52	1.84
CaO	0.07	0.07	0.16	0.37	0.15	0.17	0.12	0.12	0.05	0.05	0.06	0.41	0.30	0.12	0.09	0.13	0.39	0.10	0.10	0.07	0.10	0.15	0.11	0.03	0.27	0.12	0.03	0.09	0.33	0.10	0.02	0.03
Cr_2O_3	0.06	0.11	0.06	0.09	0.05	0.07	0.05	0.08	0.05	0.05	0.08	0.07	0.02	0.06	0.08	0.06	0.08	0.09	0.12	0.04	0.10	0.08	0.02	0.02	0.03	0.07	0.06	0.04	0.08	0.09	0.06	0.10
TiO_2	0.47	0.55	0.43	0.85	0.78	0.85	0.24	0.80	0.60	0.52	0.40	0.89	0.74	0.86	1.38	0.87	0.81	0.81	0.94	0.36	0.80	0.79	0.62	0.32	0.77	0.87	0.23	0.47	0.73	0.77	0.19	0.39
ZnO	0.06	0.00	0.04	0.07	0.03	0.04	0.01	0.06	0.05	0.03	0.03	0.05	0.02	0.00	0.06	0.10	0.09	0.07	0.02	0.00	0.10	0.08	0.08	0.01	0.02	0.04	0.06	0.07	0.05	0.02	0.07	0.05
CoO	0.03	0.02	0.04	0.03	0.00	0.02	0.02	0.03	0.02	0.01	0.01	0.05	0.01	0.00	0.00	0.04	0.05	0.03	0.01	0.00	0.03	0.00	0.02	0.02	0.01	0.00	0.04	0.01	0.01	0.03	0.00	0.00
WO_3	0.00	0.00	0.04	0.03	0.00	0.07	0.06	0.00	0.00	0.00	0.00	0.02	0.10	0.11	0.00	0.00	0.00	0.04	0.03	0.00	0.13	0.12	0.01	0.01	0.08	0.09	0.00	0.00	0.10	0.01	0.06	0.00
Nb_2O_5	0.01	0.10	0.00	0.01	0.08	0.02	0.02	0.00	0.09	0.00	0.00	0.02	0.10	0.01	0.03	0.05	0.04	0.06	0.05	0.03	0.03	0.02	0.04	0.06	0.05	0.00	0.01	0.04	0.04	0.07	0.09	0.00
SnO_2	0.01	0.03	0.00	0.01	0.00	0.01	0.03	0.00	0.06	0.02	0.00	0.02	0.00	0.03	0.00	0.02	0.00	0.06	0.01	0.00	0.00	0.00	0.03	0.05	0.00	0.04	0.01	0.00	0.04	0.00	0.07	0.01
V_2O_3	0.02	0.01	0.01	0.03	0.10	0.00	0.06	0.07	0.00	0.03	0.07	0.05	0.07	0.04	0.04	0.06	0.09	0.01	0.00	0.06	0.01	0.10	0.00	0.00	0.02	0.00	0.02	0.03	0.00	0.05	0.00	0.01
SrO	0.05	0.00	0.03	0.00	0.03	0.07	0.04	0.03	0.04	0.03	0.07	0.06	0.00	0.12	0.11	0.08	0.00	0.00	0.05	0.03	0.03	0.04	0.00	0.05	0.12	0.00	0.00	0.05	0.04	0.02	0.07	0.00
Li_2O*	0.12	0.14	0.20	0.10	0.08	0.10	0.16	0.12	0.19	0.20	0.17	0.13	0.18	0.17	0.24	0.14	0.08	0.18	0.15	0.20	0.20	0.10	0.19	0.23	0.14	0.16	0.19	0.22	0.11	0.15	0.22	0.19
F	0.40	0.20	0.04	0.30	0.30	0.32	0.17	0.43	0.25	0.22	0.16	0.14	0.27	0.34	0.11	0.32	0.03	0.07	0.41	0.10	0.36	0.29	0.26	0.31	0.21	0.18	0.08	0.20	0.29	0.32	0.05	0.34
Total	96.04	95.66	95.75	95.88	95.35	95.41	95.27	95.62	96.24	96.24	96.56	96.15	96.07	96.31	95.85	95.98	95.58	95.62	96.01	95.99	96.20	95.66	96.01	95.58	95.59	95.41	95.45	95.74	95.55	95.61	95.69	95.55
a.p.f.u (calculus done on the basis of 12 cations Z+T)																																
Total B	3.000	3.000	3.000	3.000	3.000	3.000	3.000	3.000	3.000	3.000	3.000	3.000	3.000	3.000	3.000	3.000	3.000	3.000	3.000	3.000	3.000	3.000	3.000	3.000	3.000	3.000	3.000	3.000	3.000	3.000	3.000	3.000
Si^{4+}	5.908	5.924	5.884	5.859	5.902	5.909	5.940	5.933	5.920	5.915	5.888	5.866	5.893	5.897	5.911	5.882	5.850	5.926	5.876	5.969	5.910	5.902	5.932	5.912	5.868	5.869	5.894	5.891	5.825	5.890	5.909	5.897
Al^{3+}	0.092	0.076	0.114	0.140	0.098	0.091	0.060	0.067	0.080	0.085	0.111	0.135	0.104	0.102	0.089	0.114	0.150	0.074	0.121	0.031	0.082	0.098	0.065	0.088	0.130	0.130	0.104	0.109	0.176	0.110	0.090	0.103
Total T	6.000	6.000	5.999	5.998	5.999	6.000	6.000	6.000	6.000	6.000	6.000	6.000	5.997	5.999	6.000	5.995	6.000	6.000	5.997	5.999	5.992	6.000	5.997	6.000	5.998	5.999	5.998	6.000	6.000	6.000	5.999	6.000
Fe^{3+}	0.000	0.000	0.000	0.000	0.000	0.000	0.000	0.000	0.000	0.000	0.000	0.000	0.000	0.000	0.000	0.000	0.000	0.000	0.000	0.000	0.000	0.000	0.000	0.000	0.000	0.000	0.000	0.000	0.000	0.000	0.000	0.000
Cr^{3+}	0.008	0.014	0.008	0.012	0.007	0.010	0.007	0.011	0.006	0.007	0.010	0.009	0.003	0.008	0.010	0.008	0.011	0.011	0.016	0.005	0.013	0.011	0.002	0.003	0.004	0.009	0.008	0.006	0.011	0.012	0.008	0.014
V^{3+}	0.003	0.001	0.002	0.004	0.013	0.000	0.008	0.010	0.000	0.004	0.010	0.006	0.010	0.005	0.005	0.007	0.012	0.002	0.000	0.007	0.002	0.013	0.000	0.000	0.003	0.000	0.003	0.004	0.000	0.007	0.000	0.001
Al^{3+}	5.989	5.985	5.990	5.985	5.980	5.990	5.985	5.980	5.994	5.989	5.980	5.985	5.987	5.987	5.985	5.984	5.977	5.987	5.985	5.988	5.985	5.976	5.998	5.998	5.993	5.991	5.989	5.991	5.989	5.982	5.993	5.985
Total Z	6.000	6.000	6.000	6.000	6.000	6.000	6.000	6.000	6.000	6.000	6.000	6.000	6.000	6.000	6.000	6.000	6.000	6.000	6.000	6.000	6.000	6.000	6.000	6.000	6.000	6.000	6.000	6.000	6.000	6.000	6.000	6.000
W^{6+}	0.000	0.000	0.002	0.001	0.000	0.003	0.003	0.000	0.000	0.000	0.000	0.001	0.004	0.005	0.000	0.000	0.000	0.002	0.001	0.000	0.005	0.005	0.001	0.001	0.003	0.004	0.000	0.000	0.005	0.001	0.003	0.000
Nb^{5+}	0.001	0.007	0.000	0.001	0.006	0.002	0.002	0.000	0.007	0.000	0.000	0.002	0.007	0.001	0.002	0.004	0.003	0.005	0.004	0.002	0.002	0.002	0.003	0.005	0.004	0.000	0.001	0.003	0.003	0.005	0.006	0.000
Sn^{4+}	0.001	0.002	0.000	0.001	0.000	0.000	0.002	0.000	0.004	0.002	0.000	0.001	0.000	0.002	0.000	0.002	0.000	0.004	0.000	0.000	0.000	0.000	0.002	0.003	0.000	0.003	0.001	0.000	0.003	0.000	0.005	0.001
Ti^{4+}	0.059	0.070	0.053	0.106	0.099	0.108	0.030	0.101	0.075	0.066	0.050	0.110	0.092	0.107	0.172	0.109	0.101	0.101	0.118	0.045	0.100	0.100	0.078	0.041	0.097	0.110	0.029	0.059	0.092	0.097	0.023	0.050
Pr^{3+}	0.004	0.001	0.004	0.002	0.004	0.003	0.000	0.000	0.002	0.000	0.001	0.001	0.001	0.000	0.001	0.000	0.000	0.000	0.001	0.005	0.001	0.000	0.003	0.000	0.000	0.001	0.000	0.002	0.000	0.000	0.000	0.000
Fe^{3+}	0.000	0.000	0.000	0.000	0.000	0.000	0.000	0.000	0.000	0.000	0.000	0.000	0.000	0.000	0.112	0.000	0.000	0.000	0.000	0.138	0.071	0.000	0.000	0.000	0.000	0.000	0.000	0.000	0.000	0.000	0.000	0.000
Sc^{3+}	0.002	0.000	0.000	0.000	0.000	0.000	0.000	0.000	0.000	0.000	0.000	0.000	0.001	0.000	0.001	0.000	0.004	0.001	0.002	0.000	0.002	0.000	0.000	0.000	0.000	0.002	0.000	0.002	0.000	0.000	0.000	0.001
Al^{3+}	0.503	0.478	0.551	0.436	0.374	0.335	0.638	0.414	0.476	0.517	0.566	0.434	0.409	0.385	0.195	0.371	0.460	0.413	0.339	0.381	0.318	0.344	0.440	0.592	0.418	0.426	0.669	0.537	0.456	0.446	0.679	0.539
Zn^{2+}	0.007	0.000	0.005	0.009	0.004	0.005	0.001	0.008	0.006	0.004	0.003	0.006	0.002	0.000	0.008	0.013	0.011	0.008	0.002	0.000	0.013	0.010	0.010	0.002	0.002	0.005	0.007	0.009	0.007	0.003	0.009	0.006
Co^{2+}	0.004	0.002	0.006	0.003	0.000	0.003	0.002	0.005	0.002	0.002	0.002	0.006	0.001	0.000	0.000	0.005	0.006	0.004	0.001	0.000	0.004	0.000	0.003	0.003	0.002	0.000	0.006	0.002	0.002	0.005	0.000	0.000
Fe^{2+}	1.465	1.455	1.067	1.190	1.402	1.441	1.190	1.500	1.526	1.537	1.356	1.163	1.221	1.327	1.141	1.322	1.098	1.213	1.343	1.089	1.356	1.424	1.518	1.463	1.264	1.528	1.390	1.284	1.202	1.529	1.323	1.418
Mn^{2+}	0.011	0.014	0.004	0.010	0.005	0.013	0.002	0.012	0.011	0.009	0.006	0.012	0.009	0.006	0.000	0.008	0.010	0.002	0.009	0.000	0.012	0.011	0.016	0.007	0.004	0.005	0.015	0.002	0.011	0.015	0.003	0.006
Mg^{2+}	0.838	0.840	1.134	1.134	1.001	0.964	1.005	0.840	0.714	0.697	0.863	1.128	1.084	0.991	1.126	1.019	1.212	1.085	1.028	1.181	0.915	0.984	0.759	0.699	1.062	0.758	0.729	0.899	1.094	0.750	0.771	0.815
Li^{+}	0.079	0.094	0.134	0.064	0.056	0.068	0.105	0.080	0.130	0.132	0.116	0.086	0.123	0.117	0.158	0.095	0.052	0.119	0.098	0.135	0.135	0.066	0.129	0.153	0.094	0.106	0.127	0.150	0.071	0.103	0.150	0.131
Total Y	2.973	2.964	2.959	2.956	2.951	2.945	2.979	2.959	2.953	2.964	2.962	2.951	2.954	2.942	2.916	2.947	2.957	2.957	2.946	2.977	2.931	2.946	2.962	2.967	2.948	2.948	2.973	2.948	2.944	2.953	2.972	2.965
Sr^{2+}	0.005	0.000	0.003	0.000	0.003	0.007	0.004	0.003	0.004	0.003	0.007	0.006	0.000	0.012	0.011	0.008	0.000	0.000	0.005	0.003	0.003	0.004	0.000	0.005	0.011	0.000	0.000	0.005	0.004	0.002	0.006	0.000
Ca^{2+}	0.012	0.013	0.028	0.066	0.027	0.030	0.021	0.021	0.010	0.008	0.011	0.072	0.054	0.022	0.016	0.022	0.069	0.018	0.019	0.013	0.018	0.028	0.019	0.005	0.048	0.022	0.006	0.016	0.058	0.018	0.003	0.005
K^{+}	0.001	0.007	0.004	0.002	0.003	0.005	0.002	0.010	0.003	0.004	0.004	0.004	0.009	0.009	0.002	0.003	0.004	0.005	0.001	0.004	0.004	0.005	0.041	0.005	0.006	0.005	0.009	0.005	0.005	0.011	0.002	0.003
Na^{+}	0.545	0.541	0.534	0.479	0.565	0.585	0.417	0.533	0.572	0.574	0.544	0.467	0.553	0.610	0.646	0.623	0.441	0.580	0.662	0.538	0.612	0.599	0.552	0.544	0.548	0.588	0.478	0.564	0.507	0.564	0.489	0.596
X□	0.437	0.439	0.431	0.453	0.402	0.373	0.556	0.434	0.411	0.411	0.434	0.451	0.385	0.348	0.326	0.344	0.486	0.397	0.314	0.443	0.363	0.365	0.389	0.440	0.387	0.386	0.507	0.410	0.425	0.405	0.500	0.396
Total X	0.563	0.561	0.569	0.547	0.598	0.627	0.444	0.567	0.589	0.589	0.566	0.549	0.615	0.652	0.674	0.656	0.514	0.603	0.686	0.557	0.637	0.635	0.611	0.560	0.613	0.615	0.493	0.590	0.575	0.596	0.500	0.604
OH^{-}	3.789	3.892	3.978	3.839	3.838	3.831	3.909	3.769	3.869	3.883	3.918	3.923	3.858	3.823	3.943	3.834	3.982	3.961	3.784	3.950	3.809	3.848	3.851	3.832	3.890	3.903	3.956	3.893	3.847	3.830	3.971	3.817
F^{-}	0.211	0.107	0.020	0.159	0.162	0.170	0.088	0.231	0.130	0.117	0.082	0.074	0.142	0.177	0.057	0.166	0.016	0.038	0.216	0.050	0.191	0.152	0.138	0.166	0.109	0.095	0.044	0.107	0.151	0.168	0.027	0.180
Total W	4.000	3.999	3.998	3.998	3.999	4.000	3.998	4.000	3.999	4.000	4.000	3.998	4.000	4.000	4.000	4.000	3.998	3.999	4.000	4.000	4.000	4.000	3.989	3.998	4.000	3.998	4.000	4.000	3.998	3.998	3.998	3.997

Sample	#11cR			#18aB6				#18aB7					
Zone	MAZ			Host Rock									
Position	Interval 2	Rim	Interval 3	Core	Rim	Core	Rim	Core	Rim	Core	Rim	Core	Rim
Wt%	3	4	5	1	2	3	4	1	2	3	4	5	6
SiO_2	34.99	34.78	35.44	35.68	35.72	34.87	35.59	35.23	35.54	34.62	35.42	35.46	35.37
Al_2O_3	33.60	32.79	33.21	31.81	31.65	33.67	34.35	34.32	34.30	34.32	34.16	34.11	34.46
Fe_2O_3	0.00	0.00	0.00	1.83	3.43	0.00	0.00	0.00	0.00	0.00	0.00	0.00	0.00
FeO	8.26	10.24	9.55	7.14	5.54	8.07	8.24	8.31	8.23	8.05	8.17	8.06	7.97
MgO	4.47	3.36	3.76	4.83	4.86	4.32	3.96	4.24	4.25	4.45	4.38	4.29	4.18
B_2O_3	10.43	10.28	10.43	10.44	10.49	10.40	10.47	10.48	10.50	10.44	10.53	10.51	10.51
MnO	0.05	0.09	0.09	0.02	0.05	0.03	0.07	0.09	0.05	0.04	0.08	0.01	0.02
K_2O	0.02	0.03	0.03	0.03	0.03	0.02	0.03	0.03	0.03	0.02	0.05	0.04	0.05
Na_2O	1.54	1.78	1.82	1.68	1.68	1.12	1.06	1.15	1.05	1.12	1.37	1.16	1.05
CaO	0.46	0.11	0.09	0.21	0.21	0.78	0.36	0.46	0.49	0.72	0.54	0.64	0.64
Cr_2O_3	0.07	0.05	0.02	0.13	0.09	0.07	0.08	0.10	0.05	0.07	0.10	0.06	0.09
TiO_2	0.86	0.79	0.75	1.00	0.94	0.93	0.45	0.61	0.60	0.86	0.60	0.82	0.65
ZnO	0.02	0.02	0.02	0.07	0.09	0.09	0.02	0.06	0.00	0.02	0.03	0.02	0.06
CoO	0.03	0.03	0.02	0.01	0.01	0.02	0.02	0.00	0.02	0.02	0.01	0.02	0.03
WO_3	0.07	0.02	0.00	0.00	0.00	0.01	0.00	0.09	0.00	0.00	0.07	0.02	0.15
Nb_2O_5	0.01	0.00	0.03	0.01	0.00	0.07	0.00	0.10	0.05	0.05	0.01	0.05	0.07
SnO_2	0.00	0.03	0.03	0.00	0.00	0.03	0.00	0.00	0.00	0.00	0.00	0.02	0.00
V_2O_3	0.02	0.02	0.00	0.03	0.00	0.00	0.03	0.00	0.00	0.05	0.06	0.00	0.00
SrO	0.05	0.00	0.00	0.06	0.09	0.05	0.03	0.00	0.01	0.01	0.07	0.09	0.00
Li_2O*	0.17	0.15	0.19	0.27	0.42	0.19	0.19	0.12	0.15	0.12	0.20	0.22	0.21
F	0.16	0.27	0.22	0.08	0.04	0.00	0.00	0.07	0.04	0.01	0.07	0.00	0.09
Total	95.27	94.85	95.71	95.34	95.35	94.74	94.94	95.44	95.36	94.98	95.93	95.59	95.58
a.p.f.u (calculus done on the basis of 12 cations Z+T)													
Total B	3.000	3.000	3.000	3.000	3.000	3.000	3.000	3.000	3.000	3.000	3.000	3.000	3.000
Si^{4+}	5.832	5.880	5.908	5.939	5.919	5.830	5.907	5.842	5.880	5.764	5.848	5.862	5.851
Al^{3+}	0.167	0.120	0.091	0.061	0.081	0.168	0.090	0.158	0.120	0.231	0.152	0.139	0.149
Total T	5.999	6.000	5.999	6.000	6.000	5.997	5.996	6.000	6.000	5.995	6.000	6.000	6.000
Fe^{3+}	0.000	0.000	0.000	0.000	0.000	0.000	0.000	0.000	0.000	0.000	0.000	0.000	0.000
Cr^{3+}	0.010	0.007	0.002	0.017	0.012	0.009	0.010	0.013	0.006	0.009	0.013	0.008	0.012
V^{3+}	0.003	0.003	0.000	0.004	0.000	0.000	0.004	0.000	0.000	0.006	0.008	0.000	0.000
Al^{3+}	5.987	5.990	5.998	5.979	5.988	5.991	5.986	5.988	5.994	5.985	5.979	5.992	5.989
Total Z	6.000	6.000	6.000	6.000	6.000	6.000	6.000	6.000	6.000	6.000	6.000	6.000	6.000
W^{6+}	0.003	0.001	0.000	0.000	0.000	0.000	0.000	0.004	0.000	0.000	0.003	0.001	0.006
Nb^{5+}	0.000	0.000	0.003	0.001	0.000	0.005	0.000	0.007	0.003	0.004	0.001	0.004	0.005
Sn^{4+}	0.000	0.002	0.002	0.000	0.000	0.002	0.000	0.000	0.000	0.000	0.000	0.001	0.000
Ti^{4+}	0.108	0.100	0.094	0.126	0.117	0.117	0.056	0.076	0.074	0.107	0.074	0.102	0.081
Pr^{3+}	0.004	0.006	0.004	0.000	0.002	0.000	0.000	0.000	0.000	0.001	0.002	0.000	0.001
Fe^{3+}	0.000	0.000	0.000	0.229	0.428	0.000	0.000	0.000	0.000	0.000	0.000	0.000	0.000
Sc^{3+}	0.000	0.000	0.000	0.000	0.004	0.000	0.000	0.001	0.002	0.002	0.001	0.004	0.000
Al^{3+}	0.446	0.422	0.435	0.201	0.112	0.476	0.643	0.563	0.576	0.519	0.515	0.514	0.580
Zn^{2+}	0.003	0.002	0.002	0.008	0.011	0.011	0.002	0.007	0.000	0.003	0.003	0.002	0.007
Co^{2+}	0.004	0.005	0.003	0.002	0.002	0.002	0.003	0.000	0.002	0.003	0.002	0.002	0.004
Fe^{2+}	1.152	1.448	1.331	0.994	0.768	1.129	1.143	1.153	1.139	1.120	1.128	1.114	1.103
Mn^{2+}	0.006	0.013	0.013	0.003	0.007	0.004	0.009	0.012	0.007	0.006	0.012	0.002	0.003
Mg^{2+}	1.111	0.847	0.933	1.199	1.201	1.077	0.980	1.048	1.049	1.103	1.077	1.056	1.029
Li^{+}	0.111	0.101	0.129	0.179	0.277	0.129	0.125	0.082	0.102	0.079	0.135	0.148	0.141
Total Y	2.948	2.947	2.949	2.942	2.927	2.951	2.961	2.954	2.955	2.946	2.954	2.948	2.960
Sr^{2+}	0.005	0.000	0.000	0.006	0.009	0.005	0.002	0.000	0.001	0.001	0.006	0.008	0.000
Ca^{2+}	0.081	0.020	0.016	0.038	0.037	0.140	0.065	0.082	0.087	0.129	0.095	0.113	0.113
K^{+}	0.003	0.006	0.007	0.007	0.007	0.004	0.006	0.006	0.006	0.005	0.011	0.009	0.010
Na^{+}	0.496	0.583	0.588	0.541	0.539	0.364	0.342	0.370	0.336	0.363	0.440	0.373	0.335
X□	0.415	0.390	0.389	0.409	0.408	0.487	0.585	0.542	0.570	0.502	0.448	0.498	0.542
Total X	0.585	0.610	0.612	0.591	0.592	0.513	0.415	0.458	0.430	0.498	0.552	0.503	0.458
OH^{-}	3.914	3.856	3.874	3.956	3.977	4.000	3.997	3.966	3.977	3.997	3.964	3.997	3.953
F^{-}	0.086	0.142	0.118	0.044	0.023	0.000	0.000	0.034	0.023	0.003	0.037	0.000	0.047
Total W	4.000	3.999	3.992	4.000	4.000	4.000	3.997	4.000	4.000	4.000	4.000	3.997	4.000

II.II.IX APATITE

Sample	#11bB2		#11bB4				#11bB6		#11bB7		#11cB8		#12B3						#18aB4		#18aB7		#5B1		#5B2			#9cB1	#11bB6	#14B5		#18aB4
Zone	MAZ		Pegmatite 1				MAZ		Pegmatite 1		MAZ								Host Rock				Pegmatite 1						MAZ	Pegmatite 2		Host Rock
Species	Fluorapatite																												Hydroxylapatite			
wt%	2	3	1	3	6	7	5	8	3	4	1	2	1	2	3	4	5	6	1	3	1	2	1	3	4	7	1	2	2
CaO	53.64	54.74	51.48	50.67	52.86	52.36	53.08	53.26	50.56	51.60	53.81	53.21	54.07	54.71	53.35	54.49	54.20	54.32	53.29	52.95	55.09	54.72	53.15	54.44	52.91	53.73	55.07	54.25	54.40
P_2O_5	39.48	39.31	39.64	40.17	40.64	39.65	39.44	39.43	39.56	39.65	39.72	39.83	42.83	42.58	42.74	43.04	42.97	42.27	40.37	40.82	43.40	43.33	43.01	41.74	39.71	39.67	41.95	42.83	40.51
FeO	0.00	0.00	1.42	1.88	0.64	0.64	0.32	0.00	3.14	2.20	0.00	0.12	0.38	0.28	0.36	0.28	0.28	0.22	0.00	0.17	0.07	0.06	0.26	0.00	0.56	0.00	0.21	0.00	0.00
Fe_2O_3	0.38	0.23	0.00	0.00	0.00	0.00	0.00	0.32	0.00	0.00	0.33	0.17	0.00	0.00	0.00	0.00	0.00	0.00	0.15	0.00	0.00	0.00	0.00	0.00	0.00	0.13	0.00	0.00	0.10
SrO	0.24	0.09	0.30	0.32	0.43	0.37	0.12	0.14	0.22	0.20	0.18	0.13	0.20	0.00	0.84	0.17	0.10	0.14	0.29	0.19	0.00	0.00	0.02	0.00	0.06	0.18	0.00	0.22	0.15
SiO_2	0.05	0.05	0.02	0.19	0.00	0.00	0.03	0.15	0.00	0.05	0.03	0.02	0.00	0.00	0.00	0.00	0.00	0.00	0.05	0.08	0.00	0.00	0.00	0.00	0.03	0.00	0.00	0.00	0.07
MnO	0.00	0.00	0.02	0.03	0.01	0.01	0.00	0.00	0.04	0.03	0.00	0.00	0.62	0.54	0.48	0.30	0.40	0.27	0.00	0.00	1.02	1.15	2.31	0.00	0.01	0.00	0.00	0.00	0.00
Mn_2O_5	1.71	0.81	0.01	0.00	0.01	0.02	1.66	1.26	0.01	0.02	1.03	1.14	0.00	0.00	0.00	0.00	0.00	0.00	0.18	0.41	0.00	0.00	0.00	0.00	0.01	0.73	0.00	0.00	0.31
Mn_2O_3	0.00	0.00	0.00	0.00	0.00	0.00	0.00	0.00	0.00	0.00	0.00	0.00	0.00	0.00	0.00	0.00	0.00	0.00	0.00	0.00	0.00	0.00	0.00	0.34	0.00	0.00	0.00	0.00	0.00
Na_2O	0.05	0.06	0.08	0.17	0.00	0.03	0.06	0.04	0.00	0.01	0.11	0.09	0.00	0.02	0.00	0.00	0.03	0.02	0.02	0.00	0.03	0.03	0.24	0.17	0.02	0.06	0.00	0.16	0.21
MgO	0.00	0.00	0.11	0.00	0.03	0.01	0.01	0.04	0.00	0.00	0.00	0.00	0.02	0.01	0.00	0.02	0.03	0.03	0.04	0.08	0.00	0.00	0.02	0.03	0.00	0.02	0.00	0.02	0.00
K_2O	0.01	0.02	0.00	0.00	0.02	0.01	0.00	0.01	0.00	0.00	0.07	0.02	0.00	0.00	0.00	0.00	0.00	0.00	0.06	0.00	0.00	0.00	0.00	0.00	0.00	0.00	0.00	0.00	0.05
PbO	0.00	0.00	0.00	0.00	0.11	0.16	0.00	0.03	0.06	0.07	0.01	0.04	0.00	0.00	0.00	0.00	0.00	0.00	0.31	0.13	0.00	0.00	0.00	0.00	0.02	0.03	0.00	0.00	0.03
BaO	0.00	0.04	0.09	0.33	0.05	0.00	0.00	0.00	0.02	0.05	0.09	0.09	0.12	0.07	0.05	0.01	0.02	0.01	0.05	0.30	0.07	0.12	0.00	0.26	0.00	0.00	0.00	0.00	0.00
Al_2O_3	0.01	0.01	0.02	0.00	0.11	0.10	0.00	0.04	0.00	0.00	0.01	0.00	0.00	0.00	0.00	0.00	0.00	0.01	0.00	0.08	0.00	0.01	0.00	0.00	0.01	0.01	0.00	0.02	0.08
Nb_2O_5	0.00	0.00	0.64	0.16	0.00	0.00	0.11	0.02	0.00	0.09	0.01	0.16	0.00	0.00	0.00	0.00	0.00	0.00	0.00	0.00	0.00	0.00	0.00	0.00	0.00	0.05	0.00	0.00	0.00
SO_3	0.00	0.03	0.06	0.00	0.14	0.00	0.00	0.01	0.00	0.01	0.00	0.04	0.00	0.00	0.00	0.00	0.00	0.00	0.20	0.13	0.00	0.00	0.00	0.00	0.07	0.02	0.00	0.00	0.20
Cl	0.00	0.02	0.03	0.04	0.08	0.00	0.02	0.00	0.01	0.01	0.00	0.00	0.00	0.01	0.00	0.00	0.00	0.02	0.00	0.00	0.00	0.01	0.00	0.00	0.00	0.01	0.03	0.01	0.00
F	2.31	2.02	3.39	3.16	2.55	2.96	2.25	2.39	2.91	2.86	3.51	3.03	2.40	2.66	2.71	2.84	2.80	2.45	3.10	3.06	2.74	2.97	2.07	3.64	2.76	1.67	1.46	1.07	0.80
Total	97.88	97.41	97.32	97.10	97.67	96.33	97.10	97.15	96.53	96.86	98.90	98.10	100.63	100.88	100.54	101.16	100.84	99.76	98.08	98.38	102.42	102.40	101.08	100.63	96.16	96.30	98.72	98.58	96.90
a.p.f.u (calculus done on the basis of 8 cations)																																
S^{6+}	0.000	0.002	0.004	0.000	0.009	0.000	0.000	0.001	0.000	0.001	0.000	0.003	0.000	0.000	0.000	0.000	0.000	0.000	0.013	0.008	0.000	0.000	0.000	0.000	0.005	0.002	0.000	0.000	0.012
Mn^{5+}	0.093	0.045	0.001	0.000	0.001	0.001	0.092	0.070	0.001	0.001	0.057	0.063	0.000	0.000	0.000	0.000	0.000	0.000	0.010	0.022	0.000	0.000	0.000	0.000	0.001	0.040	0.000	0.000	0.017
P^{5+}	2.886	2.888	2.940	2.969	2.932	2.935	2.901	2.898	2.965	2.955	2.909	2.918	3.026	3.013	3.037	3.032	3.032	3.013	2.908	2.921	3.021	3.024	3.023	2.992	2.958	2.923	2.997	3.037	2.877
Si^{4+}	0.004	0.004	0.002	0.016	0.000	0.000	0.002	0.013	0.000	0.004	0.003	0.002	0.000	0.000	0.000	0.000	0.000	0.000	0.004	0.006	0.000	0.000	0.000	0.000	0.003	0.000	0.000	0.000	0.006
Al^{3+}	0.001	0.001	0.002	0.000	0.011	0.011	0.000	0.004	0.000	0.000	0.001	0.000	0.000	0.000	0.000	0.000	0.000	0.000	0.000	0.008	0.000	0.000	0.000	0.000	0.001	0.001	0.000	0.000	0.007
Z Total	2.984	2.939	2.949	2.986	2.953	2.947	2.995	2.985	2.966	2.960	2.970	2.985	3.026	3.013	3.037	3.032	3.032	3.013	2.934	2.965	3.021	3.024	3.023	2.993	2.967	2.966	2.997	3.037	2.919
Nb^{5+}	0.000	0.000	0.025	0.006	0.000	0.000	0.004	0.001	0.000	0.004	0.000	0.006	0.000	0.000	0.000	0.000	0.000	0.000	0.000	0.000	0.000	0.000	0.000	0.000	0.000	0.002	0.000	0.000	0.000
Fe^{3+}	0.025	0.015	0.000	0.000	0.000	0.000	0.000	0.021	0.000	0.000	0.021	0.011	0.000	0.000	0.000	0.000	0.000	0.000	0.010	0.000	0.000	0.000	0.000	0.000	0.000	0.008	0.000	0.000	0.006
Mn^{3+}	0.000	0.000	0.000	0.000	0.000	0.000	0.000	0.000	0.000	0.000	0.000	0.000	0.000	0.000	0.000	0.000	0.000	0.000	0.000	0.000	0.000	0.000	0.000	0.022	0.000	0.000	0.000	0.000	0.000
Al^{3+}	0.000	0.000	0.000	0.000	0.000	0.000	0.000	0.000	0.000	0.000	0.000	0.000	0.000	0.000	0.000	0.000	0.000	0.001	0.000	0.000	0.000	0.001	0.000	0.000	0.000	0.000	0.000	0.002	0.000
Pb^{2+}	0.000	0.000	0.000	0.000	0.003	0.004	0.000	0.001	0.001	0.002	0.000	0.001	0.000	0.000	0.000	0.000	0.000	0.000	0.007	0.003	0.000	0.000	0.000	0.000	0.001	0.001	0.000	0.000	0.001
Ba^{2+}	0.000	0.001	0.003	0.011	0.002	0.000	0.000	0.000	0.001	0.002	0.003	0.003	0.004	0.002	0.002	0.000	0.001	0.001	0.002	0.010	0.002	0.004	0.000	0.009	0.000	0.000	0.000	0.000	0.000
Sr^{2+}	0.012	0.005	0.015	0.016	0.021	0.019	0.006	0.007	0.011	0.010	0.009	0.006	0.010	0.000	0.041	0.008	0.005	0.007	0.014	0.009	0.000	0.000	0.001	0.000	0.003	0.009	0.000	0.011	0.007
Fe^{2+}	0.000	0.000	0.104	0.137	0.046	0.047	0.023	0.000	0.233	0.162	0.000	0.009	0.026	0.020	0.025	0.020	0.020	0.015	0.000	0.012	0.005	0.004	0.018	0.000	0.041	0.000	0.015	0.000	0.000
Mn^{2+}	0.000	0.000	0.002	0.002	0.001	0.001	0.000	0.000	0.003	0.002	0.000	0.000	0.044	0.038	0.034	0.021	0.028	0.019	0.000	0.000	0.071	0.080	0.163	0.000	0.001	0.000	0.000	0.000	0.000
Ca^{2+}	4.963	5.088	4.832	4.740	4.827	4.905	4.942	4.953	4.795	4.866	4.988	4.933	4.836	4.900	4.798	4.858	4.840	4.900	4.859	4.795	4.853	4.834	4.728	4.939	4.988	5.010	4.979	4.868	4.889
Mg^{2+}	0.000	0.000	0.014	0.000	0.004	0.002	0.001	0.005	0.000	0.000	0.000	0.000	0.003	0.001	0.000	0.002	0.004	0.004	0.005	0.010	0.000	0.000	0.002	0.004	0.000	0.002	0.000	0.003	0.000
K^{+}	0.001	0.002	0.000	0.000	0.002	0.001	0.000	0.001	0.000	0.000	0.008	0.002	0.000	0.000	0.000	0.000	0.000	0.000	0.006	0.000	0.000	0.000	0.000	0.000	0.000	0.000	0.000	0.000	0.006
Na^{+}	0.009	0.010	0.013	0.029	0.000	0.005	0.010	0.006	0.001	0.002	0.018	0.015	0.000	0.003	0.000	0.001	0.005	0.002	0.003	0.000	0.005	0.005	0.039	0.028	0.003	0.011	0.000	0.026	0.035
M Total	5.009	5.121	5.008	4.943	4.905	4.983	4.987	4.995	5.045	5.050	5.047	4.986	4.923	4.964	4.900	4.910	4.903	4.949	4.905	4.839	4.936	4.927	4.951	5.001	5.036	5.043	4.994	4.909	4.943
OH^{-}	0.370	0.445	0.056	0.122	0.301	0.181	0.378	0.344	0.185	0.203	0.040	0.170	0.367	0.296	0.281	0.251	0.261	0.344	0.167	0.182	0.287	0.226	0.457	0.024	0.232	0.539	0.607	0.717	0.788
Cl^{-}	0.001	0.002	0.004	0.005	0.011	0.000	0.003	0.000	0.001	0.002	0.000	0.000	0.000	0.001	0.000	0.001	0.000	0.003	0.000	0.000	0.000	0.001	0.000	0.000	0.000	0.002	0.004	0.001	0.000
F^{-}	0.630	0.553	0.940	0.872	0.688	0.819	0.619	0.656	0.814	0.795	0.960	0.830	0.633	0.703	0.719	0.748	0.739	0.652	0.833	0.818	0.713	0.773	0.543	0.976	0.768	0.460	0.389	0.282	0.212
X Total	1.000	1.000	1.000	1.000	1.000	1.000	1.000	1.000	1.000	1.000	1.000	1.000	1.000	1.000	1.000	1.000	1.000	1.000	1.000	1.000	1.000	1.000	1.000	1.000	1.000	1.000	1.000	1.000	1.000

II.II.X LITHIOPHILITE-TRIPHYLITE

Sample	#1B2	#2cB7							#4B2						#4B3							#4B4					#4B5			#9bB2			
Species	Triphylite													Lithiophilite	Triphylite			Lithiophilite	Triphylite		Lithiophilite	Triphylite					Triphylite						
wt%	2	1	2	3	4	5	6	7	1	2	4	6	7	9	1	2	3	4	5	6		1	2	3	4	5	1	2	3	1	2	3	4
P_2O_5	43.69	44.01	43.59	43.92	43.95	43.97	43.94	43.78	43.79	44.19	43.95	43.42	43.48	42.37	43.63	43.37	43.02	43.18	44.20	43.15		43.82	43.54	43.81	42.80	43.91	44.21	43.25	44.47	43.36	43.43	43.40	43.33
FeO	26.69	28.80	28.86	29.27	28.22	28.91	27.51	27.95	21.81	22.82	23.30	23.27	23.07	3.77	23.37	23.41	23.34	9.77	23.49	18.74		22.73	22.90	22.78	23.48	22.75	22.99	23.21	23.06	27.07	27.25	27.05	27.21
Fe_2O_3	0.00	0.00	0.00	0.00	0.00	0.00	0.00	0.00	0.00	0.00	0.00	0.00	0.00	0.00	0.00	0.00	0.00	0.00	0.00	0.00		0.00	0.00	0.00	0.00	0.00	0.00	0.00	0.00	0.00	0.00	0.00	0.00
MnO	16.09	15.95	16.36	15.79	16.75	15.98	17.16	17.04	21.15	21.34	21.25	20.97	21.27	39.50	19.81	19.93	19.80	34.39	19.85	24.48		21.18	21.28	21.04	20.56	21.22	21.16	21.04	21.17	17.69	17.71	17.64	17.38
CaO	0.03	0.01	0.01	0.01	0.00	0.00	0.05	0.00	0.03	0.03	0.01	0.00	0.04	0.07	0.02	0.05	0.04	0.00	0.02	0.03		0.02	0.03	0.02	0.01	0.03	0.02	0.04	0.01	0.02	0.02	0.05	0.02
MgO	0.21	0.02	0.00	0.01	0.05	0.02	0.02	0.00	0.05	0.07	0.04	0.06	0.08	0.00	0.09	0.05	0.10	0.04	0.06	0.11		0.05	0.08	0.02	0.03	0.05	0.02	0.04	0.06	0.00	0.00	0.01	0.04
K_2O	0.00	0.00	0.00	0.01	0.00	0.01	0.00	0.00	0.09	0.00	0.00	0.02	0.00	0.01	0.04	0.05	0.08	0.02	0.01	0.06		0.00	0.00	0.01	0.00	0.00	0.00	0.00	0.00	0.00	0.00	0.00	0.00
Na_2O	0.20	0.03	0.00	0.04	0.03	0.02	0.05	0.05	0.09	0.07	0.00	0.02	0.00	0.03	0.13	0.05	0.14	0.05	0.02	0.12		0.00	0.01	0.07	0.09	0.03	0.02	0.04	0.01	0.02	0.06	0.01	0.00
PbO	0.10	0.00	0.03	0.00	0.05	0.04	0.00	0.00	0.00	0.00	0.03	0.01	0.01	0.03	0.05	0.05	0.00	0.00	0.00	0.03		0.00	0.04	0.08	0.05	0.00	0.00	0.02	0.00	0.01	0.06	0.03	0.00
SiO_2	0.03	0.11	0.05	0.11	0.08	0.15	0.04	0.00	0.98	0.02	0.23	0.38	0.31	0.83	0.34	0.27	0.70	0.20	0.30	0.64		0.02	0.04	0.02	0.08	0.03	0.06	0.03	0.05	0.05	0.06	0.16	0.08
UO_3	0.00	0.00	0.01	0.05	0.00	0.00	0.04	0.00	0.00	0.00	0.01	0.01	0.00	0.04	0.01	0.04	0.00	0.00	0.00	0.03		0.00	0.02	0.01	0.01	0.00	0.02	0.03	0.05	0.00	0.06	0.00	0.00
Er_2O_3	0.00	0.00	0.00	0.18	0.10	0.06	0.00	0.12	0.00	0.04	0.06	0.00	0.00	0.00	0.07	0.00	0.08	0.00	0.00	0.00		0.00	0.00	0.00	0.22	0.04	0.13	0.05	0.03	0.00	0.00	0.00	0.00
Eu_2O_3	0.00	0.02	0.15	0.14	0.08	0.12	0.00	0.19	0.16	0.17	0.16	0.10	0.12	0.30	0.13	0.13	0.12	0.34	0.22	0.05		0.17	0.12	0.31	0.16	0.16	0.02	0.12	0.20	0.07	0.18	0.09	0.06
Li_2O*	8.97	9.51	9.78	9.60	9.58	9.53	9.45	9.65	8.93	9.26	9.46	9.48	9.55	9.40	8.99	9.10	9.09	9.54	9.00	9.13		9.24	9.46	9.16	9.50	9.23	9.25	9.54	9.25	9.63	9.70	9.60	9.61
Total	96.01	98.44	98.83	99.12	98.87	98.81	98.25	98.78	97.07	98.01	98.50	97.72	97.91	96.34	96.65	96.50	96.51	97.53	97.16	96.57		97.23	97.52	97.32	96.99	97.44	97.89	97.41	98.34	97.91	98.52	98.04	97.73
a.p.f.u (calculus done on the basis of 4 oxygens)																																	
P^{5+}	0.996	0.990	0.981	0.987	0.988	0.988	0.992	0.986	0.986	0.998	0.989	0.981	0.984	0.971	0.994	0.990	0.980	0.980	0.999	0.984		0.998	0.989	0.998	0.982	0.997	0.999	0.983	1.000	0.984	0.981	0.983	0.984
Si^{4+}	0.001	0.003	0.001	0.003	0.002	0.004	0.001	0.000	0.026	0.001	0.006	0.010	0.008	0.023	0.009	0.007	0.019	0.005	0.008	0.017		0.000	0.001	0.001	0.002	0.001	0.002	0.001	0.001	0.001	0.002	0.004	0.002
Total	0.996	0.992	0.982	0.990	0.990	0.992	0.993	0.986	1.012	0.999	0.995	0.991	0.992	0.994	1.003	0.997	0.999	0.985	1.007	1.001		0.998	0.990	0.999	0.984	0.998	1.000	0.984	1.001	0.985	0.983	0.987	0.986
U^{6+}	0.000	0.000	0.000	0.000	0.000	0.000	0.000	0.000	0.000	0.000	0.000	0.000	0.000	0.000	0.000	0.000	0.000	0.000	0.000	0.000		0.000	0.000	0.000	0.000	0.000	0.000	0.000	0.000	0.000	0.000	0.000	0.000
$Er3^{+}$	0.000	0.000	0.000	0.002	0.001	0.001	0.000	0.001	0.000	0.000	0.001	0.000	0.000	0.000	0.001	0.000	0.001	0.000	0.000	0.000		0.000	0.000	0.000	0.002	0.000	0.001	0.000	0.000	0.000	0.000	0.000	0.000
Eu^{3+}	0.000	0.000	0.001	0.001	0.001	0.001	0.000	0.002	0.001	0.002	0.001	0.001	0.001	0.003	0.001	0.001	0.001	0.003	0.002	0.000		0.002	0.001	0.003	0.002	0.002	0.000	0.001	0.002	0.001	0.002	0.001	0.001
Fe^{3+}	0.000	0.000	0.000	0.000	0.000	0.000	0.000	0.000	0.000	0.000	0.000	0.000	0.000	0.000	0.000	0.000	0.000	0.000	0.000	0.000		0.000	0.000	0.000	0.000	0.000	0.000	0.000	0.000	0.000	0.000	0.000	0.000
Pb^{2+}	0.001	0.000	0.000	0.000	0.000	0.000	0.000	0.000	0.000	0.000	0.000	0.000	0.000	0.000	0.000	0.000	0.000	0.000	0.000	0.000		0.000	0.000	0.001	0.000	0.000	0.000	0.000	0.000	0.000	0.000	0.000	0.000
Fe^{2+}	0.601	0.640	0.642	0.650	0.626	0.642	0.614	0.622	0.485	0.509	0.518	0.520	0.516	0.085	0.526	0.528	0.525	0.219	0.525	0.422		0.511	0.514	0.513	0.532	0.510	0.513	0.521	0.512	0.607	0.608	0.605	0.611
Mn^{2+}	0.367	0.359	0.368	0.355	0.376	0.360	0.388	0.384	0.476	0.482	0.478	0.474	0.481	0.906	0.451	0.455	0.451	0.781	0.449	0.559		0.483	0.484	0.479	0.472	0.482	0.478	0.478	0.476	0.402	0.400	0.400	0.395
Ca^{2+}	0.001	0.000	0.000	0.000	0.000	0.000	0.001	0.000	0.001	0.001	0.000	0.000	0.001	0.002	0.001	0.002	0.001	0.000	0.001	0.001		0.001	0.001	0.001	0.000	0.001	0.000	0.001	0.000	0.001	0.001	0.001	0.001
Mg^{2+}	0.009	0.001	0.000	0.001	0.002	0.001	0.001	0.000	0.002	0.003	0.002	0.002	0.003	0.000	0.004	0.002	0.004	0.002	0.003	0.005		0.002	0.003	0.001	0.001	0.002	0.001	0.002	0.002	0.000	0.000	0.001	0.001
Total	0.978	0.999	1.012	1.009	1.006	1.004	1.004	1.008	0.966	0.997	1.000	0.997	1.002	0.997	0.983	0.988	0.984	1.005	0.979	0.987		0.998	1.003	0.997	1.010	0.997	0.994	1.004	0.993	1.010	1.011	1.007	1.008
K^{+}	0.000	0.000	0.000	0.000	0.000	0.000	0.000	0.000	0.003	0.000	0.000	0.001	0.000	0.000	0.001	0.002	0.003	0.001	0.000	0.002		0.000	0.000	0.000	0.000	0.000	0.000	0.000	0.000	0.000	0.000	0.000	0.000
Na^{+}	0.010	0.001	0.000	0.002	0.002	0.001	0.003	0.003	0.005	0.004	0.000	0.001	0.000	0.002	0.007	0.003	0.007	0.003	0.001	0.006		0.000	0.001	0.004	0.005	0.002	0.001	0.002	0.000	0.001	0.003	0.001	0.000
Li^{+}	0.971	1.016	1.045	1.025	1.022	1.018	1.013	1.032	0.955	0.993	1.011	1.018	1.026	1.024	0.973	0.987	0.984	1.028	0.966	0.989		1.000	1.021	0.991	1.036	0.996	0.992	1.029	0.988	1.037	1.040	1.033	1.037
Total	0.981	1.017	1.045	1.028	1.024	1.019	1.016	1.034	0.963	0.997	1.011	1.020	1.026	1.026	0.981	0.991	0.994	1.032	0.967	0.997		1.000	1.021	0.995	1.040	0.997	0.993	1.031	0.988	1.038	1.043	1.033	1.037
Li wt%	4.17	4.42	4.54	4.46	4.45	4.43	4.39	4.48	4.15	4.30	4.39	4.40	4.44	4.37	4.18	4.23	4.22	4.43	4.18	4.24		4.29	4.39	4.26	4.41	4.29	4.30	4.43	4.30	4.47	4.50	4.46	4.46

Sample	#9bB2														#9bB9				#9cB2	#11cB3							#13B2							
Species	Triphylite																																
wt%	5	6	7	8	9	10	11	12	13	15	16	17	18	19	2	3	4	5	2	1	2	3	4	5	6	7	1	2	3	4	5	6	7	8
P_2O_5	43.48	43.78	43.58	43.55	43.58	43.62	44.15	44.12	43.22	43.68	43.75	43.90	43.65	43.80	44.88	44.40	43.99	44.75	44.88	44.46	44.09	44.34	43.98	43.69	44.14	43.93	44.49	44.56	44.60	44.91	44.48	44.28	44.72	44.08
FeO	27.22	27.09	27.23	27.18	27.64	27.18	26.76	27.19	24.49	27.07	27.30	27.13	27.15	27.02	22.85	28.42	24.10	24.21	27.56	24.60	24.76	22.06	25.52	24.61	24.29	25.65	27.52	25.98	27.47	27.48	24.38	27.87	25.54	27.66
Fe_2O_3	0.00	0.00	0.00	0.00	0.00	0.00	0.00	0.00	0.00	0.00	0.00	0.00	0.00	0.00	5.86	0.00	4.39	4.52	0.00	0.00	0.00	3.25	0.00	0.00	0.00	0.00	0.00	1.65	0.00	0.00	3.46	0.00	2.38	0.00
MnO	17.53	17.51	17.41	17.68	17.34	17.35	17.46	17.00	16.04	17.54	17.53	17.41	17.34	17.26	14.44	14.77	14.88	14.49	15.00	19.52	19.90	19.51	18.98	19.72	19.58	19.14	17.39	17.39	17.21	17.07	17.20	17.11	17.09	17.37
CaO	0.06	0.03	0.01	0.02	0.00	0.19	0.10	0.15	2.69	0.00	0.04	0.07	0.07	0.09	0.08	0.08	0.08	0.19	0.15	0.09	0.10	0.05	0.10	0.15	0.20	0.11	0.08	0.10	0.09	0.02	0.07	0.05	0.18	0.20
MgO	0.03	0.00	0.03	0.02	0.02	0.01	0.02	0.01	0.06	0.01	0.02	0.03	0.00	0.00	0.00	0.00	0.00	0.00	0.15	0.17	0.15	0.12	0.16	0.17	0.11	0.18	0.03	0.00	0.03	0.06	0.04	0.06	0.05	0.03
K_2O	0.00	0.00	0.00	0.00	0.00	0.00	0.00	0.00	0.00	0.00	0.00	0.00	0.00	0.00	0.04	0.00	0.00	0.05	0.04	0.00	0.00	0.00	0.00	0.00	0.00	0.00	0.00	0.00	0.00	0.00	0.00	0.00	0.01	0.00
Na_2O	0.03	0.02	0.01	0.00	0.00	0.07	0.04	0.30	0.09	0.00	0.05	0.03	0.04	0.03	0.22	0.00	0.00	0.00	0.24	0.08	0.06	0.00	0.06	0.33	0.04	0.03	0.06	0.01	0.00	0.08	0.04	0.04	0.04	0.01
PbO	0.07	0.00	0.00	0.00	0.00	0.09	0.00	0.01	0.07	0.06	0.03	0.05	0.00	0.03	0.14	0.13	0.00	0.08	0.04	0.01	0.02	0.06	0.03	0.01	0.00	0.00	0.00	0.06	0.06	0.03	0.04	0.04	0.05	0.00
SiO_2	0.12	0.10	0.07	0.09	0.07	0.11	0.02	0.11	0.15	0.07	0.13	0.12	0.08	0.15	0.02	0.39	0.00	0.22	0.04	0.18	0.11	0.30	0.10	0.23	0.17	0.18	0.10	0.20	0.15	0.11	0.08	0.07	0.12	0.05
UO_3	0.00	0.01	0.00	0.06	0.02	0.02	0.00	0.02	0.04	0.03	0.03	0.00	0.01	0.00	0.00	0.00	0.02	0.00	0.24	0.00	0.03	0.06	0.00	0.02	0.00	0.02	0.03	0.00	0.00	0.00	0.05	0.07	0.05	0.00
Er_2O_3	0.02	0.09	0.20	0.07	0.00	0.04	0.03	0.00	0.00	0.06	0.00	0.00	0.11	0.04	0.00	0.00	0.12	0.00	0.27	0.03	0.01	0.05	0.01	0.09	0.07	0.00	0.00	0.00	0.07	0.00	0.00	0.00	0.00	0.06
Eu_2O_3	0.23	0.15	0.20	0.14	0.17	0.17	0.03	0.11	0.07	0.00	0.21	0.06	0.10	0.03	0.00	0.38	0.42	0.29	0.36	0.18	0.05	0.17	0.18	0.14	0.12	0.07	0.06	0.08	0.10	0.13	0.16	0.12	0.06	0.16
Li_2O*	9.69	9.50	9.59	9.67	9.69	9.55	9.29	9.16	9.36	9.48	9.61	9.48	9.52	9.37	7.50	8.95	8.12	7.93	8.53	9.30	9.59	8.91	9.56	9.44	9.30	9.67	9.47	9.15	9.38	9.24	8.76	9.55	9.02	9.67
Total	98.48	98.27	98.30	98.47	98.52	98.39	97.88	98.17	96.28	97.98	98.69	98.29	98.09	97.80	96.02	97.52	96.11	96.73	97.50	98.60	98.85	98.87	98.68	98.59	98.02	98.98	99.22	99.19	99.16	99.11	98.73	99.25	99.29	99.29
a.p.f.u (calculus done on the basis of 4 oxygens)																																		
P^{5+}	0.981	0.988	0.983	0.983	0.982	0.986	0.997	0.995	0.986	0.989	0.985	0.988	0.987	0.992	1.010	0.999	0.993	1.004	1.009	0.996	0.986	0.988	0.988	0.982	0.995	0.983	0.992	0.992	0.995	1.001	0.992	0.991	0.994	0.985
Si^{4+}	0.003	0.003	0.002	0.002	0.002	0.003	0.001	0.003	0.004	0.002	0.003	0.003	0.002	0.004	0.001	0.010	0.000	0.006	0.001	0.005	0.003	0.008	0.003	0.006	0.004	0.005	0.003	0.005	0.004	0.003	0.002	0.002	0.003	0.001
Total	0.984	0.990	0.985	0.986	0.984	0.989	0.998	0.998	0.990	0.990	0.989	0.992	0.989	0.995	1.011	1.009	0.993	1.009	1.010	1.000	0.989	0.996	0.990	0.988	1.000	0.988	0.994	0.997	1.000	1.004	0.994	0.993	0.997	0.987
U^{6+}	0.000	0.000	0.000	0.000	0.000	0.000	0.000	0.000	0.000	0.000	0.000	0.000	0.000	0.000	0.000	0.000	0.000	0.000	0.001	0.000	0.000	0.000	0.000	0.000	0.000	0.000	0.000	0.000	0.000	0.000	0.000	0.000	0.000	0.000
$Er3^{+}$	0.000	0.001	0.002	0.001	0.000	0.000	0.000	0.000	0.000	0.001	0.000	0.000	0.001	0.000	0.000	0.000	0.001	0.000	0.002	0.000	0.000	0.000	0.000	0.001	0.001	0.000	0.000	0.000	0.001	0.000	0.000	0.000	0.000	0.001
Eu^{3+}	0.002	0.001	0.002	0.001	0.002	0.002	0.000	0.001	0.001	0.000	0.002	0.001	0.001	0.000	0.000	0.004	0.004	0.003	0.003	0.002	0.000	0.002	0.002	0.001	0.001	0.001	0.001	0.001	0.001	0.001	0.001	0.001	0.001	0.001
Fe^{3+}	0.000	0.000	0.000	0.000	0.000	0.000	0.000	0.000	0.000	0.000	0.000	0.000	0.000	0.000	0.117	0.000	0.088	0.090	0.000	0.000	0.000	0.064	0.000	0.000	0.000	0.000	0.000	0.033	0.000	0.000	0.069	0.000	0.047	0.000
Pb^{2+}	0.001	0.000	0.000	0.000	0.000	0.001	0.000	0.000	0.001	0.000	0.000	0.000	0.000	0.000	0.001	0.001	0.000	0.001	0.000	0.000	0.000	0.000	0.000	0.000	0.000	0.000	0.000	0.000	0.001	0.000	0.000	0.000	0.000	0.000
Fe^{2+}	0.607	0.604	0.607	0.606	0.615	0.607	0.597	0.606	0.552	0.605	0.607	0.603	0.606	0.604	0.508	0.632	0.537	0.536	0.612	0.544	0.547	0.486	0.566	0.547	0.541	0.567	0.606	0.571	0.606	0.605	0.537	0.616	0.561	0.611
Mn^{2+}	0.396	0.395	0.393	0.399	0.391	0.392	0.395	0.384	0.366	0.397	0.395	0.392	0.392	0.391	0.325	0.333	0.336	0.325	0.338	0.437	0.445	0.435	0.426	0.444	0.442	0.428	0.388	0.387	0.384	0.381	0.384	0.383	0.380	0.389
Ca^{2+}	0.002	0.001	0.000	0.001	0.000	0.005	0.003	0.004	0.078	0.000	0.001	0.002	0.002	0.003	0.002	0.002	0.002	0.005	0.004	0.003	0.003	0.002	0.003	0.004	0.006	0.003	0.002	0.003	0.003	0.001	0.002	0.002	0.005	0.006
Mg^{2+}	0.001	0.000	0.001	0.001	0.001	0.000	0.001	0.000	0.003	0.000	0.001	0.001	0.000	0.000	0.000	0.000	0.000	0.000	0.006	0.007	0.006	0.005	0.006	0.007	0.005	0.007	0.001	0.000	0.001	0.002	0.002	0.002	0.002	0.001
Total	1.008	1.002	1.005	1.009	1.009	1.007	0.996	0.995	0.999	1.004	1.007	1.000	1.003	0.999	0.954	0.971	0.969	0.960	0.967	0.993	1.002	0.994	1.004	1.003	0.995	1.006	0.999	0.995	0.995	0.990	0.995	1.005	0.996	1.008
K^{+}	0.000	0.000	0.000	0.000	0.000	0.000	0.000	0.000	0.000	0.000	0.000	0.000	0.000	0.000	0.001	0.000	0.000	0.002	0.001	0.000	0.000	0.000	0.000	0.000	0.000	0.000	0.000	0.000	0.000	0.000	0.000	0.000	0.000	0.000
Na^{+}	0.001	0.001	0.000	0.000	0.000	0.004	0.002	0.016	0.005	0.000	0.003	0.002	0.002	0.001	0.011	0.000	0.000	0.000	0.012	0.004	0.003	0.000	0.003	0.017	0.002	0.002	0.003	0.001	0.000	0.004	0.002	0.002	0.002	0.001
Li^{+}	1.038	1.018	1.028	1.037	1.038	1.025	0.996	0.982	1.014	1.019	1.028	1.014	1.022	1.007	0.802	0.957	0.871	0.845	0.912	0.989	1.019	0.943	1.020	1.009	0.996	1.028	1.003	0.968	0.995	0.979	0.929	1.015	0.952	1.027
Total	1.040	1.019	1.028	1.037	1.038	1.029	0.998	0.997	1.019	1.019	1.030	1.015	1.025	1.009	0.815	0.957	0.871	0.846	0.925	0.993	1.022	0.943	1.023	1.026	0.998	1.030	1.006	0.968	0.995	0.983	0.930	1.017	0.954	1.028
Li wt%	4.50	4.41	4.45	4.49	4.50	4.44	4.31	4.25	4.35	4.40	4.46	4.40	4.42	4.35	3.49	4.16	3.77	3.68	3.96	4.32	4.46	4.14	4.44	4.39	4.32	4.49	4.40	4.25	4.36	4.29	4.07	4.43	4.19	4.49

Sample	#13B6		#13B3		#13B5	#17B5
Species	Triphylite					
wt%	1	2	4	5	2	1
P_2O_5	43.48	43.74	44.55	44.48	44.15	44.83
FeO	27.96	28.50	27.86	27.96	28.11	25.44
Fe_2O_3	0.00	0.00	0.00	0.27	0.00	0.00
MnO	16.62	16.13	15.99	15.53	14.12	16.56
CaO	0.08	0.15	0.04	0.01	0.15	0.20
MgO	0.07	0.15	0.02	0.05	0.00	0.17
K_2O	0.00	0.00	0.01	0.05	0.00	0.00
Na_2O	0.11	0.33	0.09	0.13	0.00	0.10
PbO	0.01	0.07	0.15	0.10	0.00	0.00
SiO_2	0.21	0.13	0.00	0.03	0.37	0.00
UO_3	0.00	0.00	0.12	0.07	0.00	0.00
Er_2O_3	0.08	0.16	0.02	0.17	0.38	0.30
Eu_2O_3	0.04	0.13	0.00	0.28	0.18	0.04
Li_2O*	9.58	9.57	9.02	8.99	8.58	8.43
Total	98.24	99.05	97.87	98.11	96.04	96.06
a.p.f.u (calculus done on the basis of 4 oxygens)						
P^{5+}	0.983	0.982	1.003	0.999	1.008	1.016
Si^{4+}	0.006	0.003	0.000	0.001	0.010	0.000
Total	0.988	0.986	1.003	0.999	1.018	1.016
U^{6+}	0.000	0.000	0.001	0.000	0.000	0.000
$Er3^{+}$	0.001	0.001	0.000	0.001	0.003	0.003
Eu^{3+}	0.000	0.001	0.000	0.003	0.002	0.000
Fe^{3+}	0.000	0.000	0.000	0.005	0.000	0.000
Pb^{2+}	0.000	0.001	0.001	0.001	0.000	0.000
Fe^{2+}	0.624	0.632	0.619	0.620	0.634	0.569
Mn^{2+}	0.376	0.363	0.360	0.349	0.323	0.375
Ca^{2+}	0.002	0.004	0.001	0.000	0.004	0.006
Mg^{2+}	0.003	0.006	0.001	0.002	0.000	0.007
Total	1.006	1.008	0.984	0.982	0.966	0.960
K^{+}	0.000	0.000	0.000	0.002	0.000	0.000
Na^{+}	0.006	0.017	0.005	0.007	0.000	0.005
Li^{+}	1.028	1.021	0.965	0.958	0.931	0.907
Total	1.034	1.038	0.970	0.967	0.931	0.912
Li wt%	4.45	4.44	4.19	4.18	3.99	3.92

II.II.XI HETEROSITE-PURPURITE

Sample	#5B2					#11bB7		#13B2				#13B3		#9bB2							
Species	Purpurite					Heterosite															
wt%	1	2	3	4	5	1	2	1	2	3	4	1	2	1	2	3	4	5	6	7	8
P_2O_5	45.93	47.65	46.54	46.37	47.66	41.28	41.49	46.51	47.64	46.46	47.79	46.88	47.24	46.53	46.65	46.83	47.12	46.79	46.95	46.33	46.84
Fe_2O_3	24.51	25.64	25.59	26.51	25.75	28.29	29.39	30.47	30.62	30.62	29.61	30.52	30.28	28.41	29.63	29.05	29.12	29.54	30.10	30.14	28.40
MnO	-	-	-	-	-	13.08	13.50	0.00	0.00	0.00	0.00	0.00	0.00	0.00	0.00	0.00	0.00	0.00	0.00	0.00	0.00
Mn_2O_3	30.38	30.32	29.56	29.06	29.54	3.44	2.20	23.22	24.04	24.11	23.62	22.74	22.00	24.16	24.88	24.07	23.46	23.90	23.84	23.01	24.27
CaO	0.00	0.01	0.03	0.06	0.03	1.28	1.42	0.14	0.08	0.13	0.38	0.10	0.07	0.07	0.02	0.09	0.04	0.14	0.00	0.03	0.07
MgO	0.03	0.07	0.12	0.01	0.07	0.28	0.36	0.07	0.14	0.00	0.00	0.02	0.02	0.00	0.05	0.00	0.07	0.03	0.09	0.01	0.09
Na_2O	0.04	0.12	0.10	0.00	0.08	8.10	8.41	0.00	0.10	0.14	0.06	0.00	0.00	0.05	0.12	0.00	0.06	0.08	0.20	0.00	0.00
Ce_2O_3	2.00	0.00	2.18	0.58	0.19	1.54	1.74	0.00	0.00	0.36	0.19	0.00	2.03	0.78	0.00	0.00	0.39	0.00	0.00	0.00	2.44
Li_2O*	-	-	-	-	-	0.00	0.00	0.00	0.00	0.00	0.00	0.00	0.00	0.00	0.00	0.00	0.00	0.00	0.00	0.00	0.00
Total	102.88	103.80	104.14	102.59	103.32	97.27	98.52	100.41	102.61	101.83	101.64	100.26	101.64	100.00	101.35	100.04	100.25	100.47	101.18	99.52	102.11
a.p.f.u (calcus done on the basis of 4 oxygens)																					
P^{5+}	0.967	0.978	0.966	0.971	0.983	0.946	0.945	0.985	0.987	0.975	0.997	0.991	0.995	0.991	0.982	0.994	0.998	0.987	0.987	0.990	0.986
Total	0.967	0.978	0.969	0.971	0.983	0.957	0.952	0.985	0.987	0.978	0.997	0.992	0.995	0.992	0.982	0.994	0.998	0.991	0.987	0.990	0.986
Ce^{3+}	0.018	0.000	0.020	0.005	0.002	0.015	0.017	0.000	0.000	0.003	0.002	0.000	0.018	0.007	0.000	0.000	0.004	0.000	0.000	0.000	0.022
Fe^{3+}	0.459	0.468	0.472	0.494	0.472	0.576	0.595	0.573	0.564	0.571	0.549	0.573	0.567	0.538	0.554	0.548	0.548	0.554	0.562	0.572	0.532
Mn^{3+}	0.575	0.560	0.552	0.547	0.548	0.071	0.045	0.442	0.448	0.455	0.443	0.432	0.417	0.463	0.471	0.459	0.447	0.454	0.451	0.442	0.460
Mn^{2+}	0.000	0.000	0.000	0.000	0.000	0.300	0.308	0.000	0.000	0.000	0.000	0.000	0.000	0.000	0.000	0.000	0.000	0.000	0.000	0.000	0.000
Ca^{2+}	0.000	0.000	0.001	0.002	0.001	0.037	0.041	0.004	0.002	0.004	0.010	0.003	0.002	0.002	0.001	0.002	0.001	0.004	0.000	0.001	0.002
Mg^{2+}	0.001	0.002	0.005	0.000	0.002	0.011	0.015	0.003	0.005	0.000	0.000	0.001	0.001	0.000	0.002	0.000	0.003	0.001	0.003	0.000	0.004
Total	1.053	1.030	1.049	1.048	1.024	1.010	1.020	1.021	1.019	1.033	1.004	1.009	1.005	1.009	1.027	1.009	1.002	1.012	1.016	1.015	1.019
Na^{+}	0.002	0.005	0.005	0.000	0.004	0.425	0.439	0.000	0.005	0.007	0.003	0.000	0.000	0.002	0.006	0.000	0.003	0.004	0.010	0.000	0.000
Li^{+}	0.000	0.000	0.000	0.000	0.000	0.000	0.000	0.000	0.000	0.000	0.000	0.000	0.000	0.000	0.000	0.000	0.000	0.000	0.000	0.000	0.000
Total	0.002	0.005	0.005	0.000	0.004	0.425	0.439	0.000	0.005	0.007	0.003	0.000	0.000	0.002	0.006	0.000	0.003	0.004	0.010	0.000	0.000

II.II.XII FAIRFIELDITE-MESSELITE

Sample	#9bB1				#9bB2									#9cB2	#13B1			#13B2								#13B3			#13B5	#17B1	#17B5		
Species	Fairfieldite			Messelite	Fairfieldite								Messelite	Fairfieldite				Messelite								Fairfieldite			Messelite				
wt%	1	2	3	4	6	1	3	6	7	11	14	16	17	1	1	6	7	2	3	4	5	6	8	10	1	2	6	7	5	1	5	7	8
P_2O_5	36.01	38.02	37.54	38.13	37.21	37.86	37.47	37.14	37.67	37.39	36.64	38.10	36.80	37.99	36.27	37.45	36.43	37.21	38.36	38.17	38.57	37.92	37.69	37.34	37.90	37.75	37.12	38.00	37.42	37.42	37.49	38.16	37.63
CaO	30.05	30.54	29.90	29.14	29.79	30.56	31.52	30.21	30.38	29.10	30.72	30.14	29.89	30.76	31.35	29.87	31.38	29.33	31.14	30.37	29.90	30.25	31.14	30.99	30.68	30.93	30.69	30.78	30.27	30.77	30.32	29.61	30.34
FeO	8.42	8.34	9.14	10.20	7.82	5.94	6.47	5.66	5.72	8.65	6.98	8.53	9.20	7.90	11.81	10.99	9.89	10.10	10.65	13.85	11.30	9.05	10.90	12.15	9.08	7.50	12.36	12.29	10.51	9.63	10.79	10.15	10.81
MnO	8.90	8.85	9.24	7.36	9.29	10.87	10.97	11.25	11.51	9.32	10.67	9.23	8.33	11.84	5.82	6.39	7.98	6.08	6.13	3.53	6.17	8.54	5.60	5.06	7.72	9.06	5.04	5.32	6.70	7.55	7.88	7.81	6.85
MgO	0.09	0.01	0.05	0.13	0.00	0.01	0.08	0.01	0.00	0.12	0.00	0.00	0.13	0.05	0.29	0.24	0.21	0.50	0.34	0.17	0.43	0.28	0.18	0.31	0.30	0.21	0.13	0.01	0.09	0.14	0.25	0.14	0.26
K_2O	0.03	0.05	0.03	0.00	0.00	0.00	0.02	0.01	0.01	0.04	0.01	0.02	0.00	0.00	0.01	0.03	0.03	0.00	0.05	0.01	0.00	0.00	0.00	0.07	0.04	0.00	0.00	0.00	0.02	0.00	0.00	0.03	0.07
Al_2O_3	0.01	0.00	0.12	0.17	0.02	0.04	0.05	0.03	0.00	0.24	0.13	0.00	0.05	0.01	0.09	0.08	0.03	0.00	0.00	0.02	0.09	0.00	0.17	0.02	0.00	0.01	0.00	0.00	0.00	0.06	0.00	0.07	0.00
Na_2O	0.26	0.16	0.09	0.28	0.10	0.00	0.03	0.00	0.03	0.14	0.00	0.03	0.17	0.06	0.27	0.07	0.00	0.21	0.07	0.00	0.17	0.00	0.16	0.09	0.04	0.07	0.12	0.00	0.11	0.12	0.00	0.00	0.00
PbO	0.00	0.45	0.00	0.00	0.25	0.00	0.02	0.00	0.33	0.16	0.31	0.00	0.14	0.00	0.00	0.01	0.00	0.17	0.05	0.00	0.00	0.02	0.08	0.24	0.00	0.06	0.07	0.03	0.15	0.00	0.06	0.00	0.04
SrO	0.00	0.02	0.08	0.33	0.00	0.15	0.00	0.18	0.00	0.14	0.11	0.00	0.00	0.00	0.03	0.09	0.18	0.80	0.38	0.00	0.84	0.06	0.00	0.47	0.05	0.18	0.05	0.17	0.00	0.03	0.16	0.00	0.32
SiO_2	3.89	0.07	0.35	0.04	0.70	0.17	0.18	0.13	0.20	0.86	0.09	0.41	0.49	0.08	0.42	0.24	0.00	0.11	0.10	0.46	0.09	0.00	0.03	0.17	0.10	0.00	0.02	0.07	0.00	0.08	0.00	0.15	0.05
Nd_2O_3	0.80	0.19	0.00	0.66	1.37	0.33	0.00	0.00	0.00	0.00	0.19	1.23	0.00	0.00	0.66	0.66	0.90	0.00	0.00	0.47	0.00	0.57	0.00	0.00	0.76	0.00	0.00	0.85	0.00	0.76	0.00	0.00	0.00
Er_2O_3	0.06	0.33	0.15	0.00	0.00	0.17	0.00	0.00	0.00	0.12	0.00	0.08	0.35	0.15	0.00	0.00	0.04	0.33	0.00	0.08	0.00	0.46	0.03	0.32	0.22	0.19	0.71	0.00	0.00	0.04	0.02	0.04	0.00
Dy_2O_3	1.91	1.06	0.42	0.00	0.61	1.17	0.00	1.77	0.65	0.00	0.67	0.92	1.51	0.00	0.00	0.76	0.00	2.66	0.00	2.15	0.38	0.00	0.48	0.00	0.19	0.97	1.31	0.60	1.14	0.00	0.28	0.33	1.27
Total	90.41	88.08	87.11	86.43	87.16	87.26	86.81	86.38	86.49	86.27	86.50	88.68	87.07	88.84	87.00	86.87	87.07	87.50	87.25	89.28	87.94	87.14	86.45	87.23	87.07	86.93	87.61	88.11	86.41	86.60	87.25	86.49	87.62
a.p.f.u (calculus done on the basis of 8 oxygen																																	
P^{5+}	1.824	1.965	1.970	1.970	1.951	1.978	1.961	1.941	1.962	1.945	1.955	1.971	1.937	1.967	1.901	1.958	1.910	1.966	1.985	1.959	1.976	1.966	1.971	1.940	1.971	1.953	1.964	1.963	1.967	1.956	1.953	1.971	1.938
Si^{4+}	0.233	0.005	0.022	0.002	0.044	0.010	0.011	0.008	0.012	0.053	0.005	0.025	0.030	0.005	0.026	0.015	0.000	0.007	0.006	0.028	0.005	0.000	0.002	0.011	0.006	0.000	0.001	0.004	0.000	0.005	0.000	0.009	0.003
Total	2.056	1.970	1.992	1.973	1.995	1.988	1.973	1.949	1.974	1.998	1.960	1.996	1.968	1.972	1.927	1.973	1.910	1.973	1.991	1.987	1.981	1.966	1.972	1.951	1.977	1.953	1.965	1.967	1.967	1.961	1.953	1.980	1.941
Er^{3+}	0.001	0.006	0.003	0.000	0.000	0.003	0.000	0.000	0.000	0.002	0.000	0.001	0.007	0.003	0.000	0.000	0.001	0.007	0.000	0.001	0.000	0.009	0.001	0.006	0.004	0.004	0.014	0.000	0.000	0.001	0.000	0.001	0.000
Dy^{3+}	0.037	0.021	0.009	0.000	0.012	0.023	0.000	0.035	0.013	0.000	0.014	0.018	0.030	0.000	0.000	0.015	0.000	0.053	0.000	0.042	0.007	0.000	0.010	0.000	0.004	0.019	0.026	0.012	0.023	0.000	0.006	0.007	0.025
Nd^{3+}	0.017	0.004	0.000	0.014	0.030	0.007	0.000	0.000	0.000	0.000	0.004	0.027	0.000	0.000	0.015	0.015	0.020	0.000	0.000	0.010	0.000	0.012	0.000	0.000	0.017	0.000	0.000	0.019	0.000	0.017	0.000	0.000	0.000
Al^{3+}	0.001	0.000	0.008	0.012	0.001	0.003	0.004	0.002	0.000	0.018	0.009	0.000	0.004	0.000	0.007	0.006	0.002	0.000	0.000	0.002	0.007	0.000	0.012	0.002	0.000	0.001	0.000	0.000	0.000	0.004	0.000	0.005	0.000
Pb^{2+}	0.000	0.007	0.000	0.000	0.004	0.000	0.000	0.000	0.006	0.003	0.005	0.000	0.002	0.000	0.000	0.000	0.000	0.003	0.001	0.000	0.000	0.000	0.001	0.004	0.000	0.001	0.001	0.001	0.003	0.000	0.001	0.000	0.001
Sr^{2+}	0.000	0.001	0.003	0.012	0.000	0.005	0.000	0.006	0.000	0.005	0.004	0.000	0.000	0.000	0.001	0.003	0.007	0.029	0.013	0.000	0.029	0.002	0.000	0.017	0.002	0.007	0.002	0.006	0.000	0.001	0.006	0.000	0.011
Fe^{2+}	0.421	0.426	0.474	0.521	0.405	0.307	0.335	0.292	0.294	0.445	0.368	0.436	0.478	0.404	0.611	0.568	0.513	0.527	0.545	0.702	0.572	0.463	0.563	0.624	0.466	0.383	0.646	0.627	0.546	0.497	0.555	0.518	0.550
Mn^{2+}	0.451	0.458	0.485	0.381	0.488	0.568	0.574	0.588	0.600	0.485	0.569	0.477	0.439	0.613	0.305	0.334	0.419	0.321	0.317	0.182	0.316	0.443	0.293	0.263	0.402	0.469	0.267	0.275	0.352	0.395	0.411	0.403	0.353
Mg^{2+}	0.008	0.001	0.005	0.012	0.000	0.001	0.007	0.001	0.000	0.011	0.000	0.000	0.012	0.005	0.026	0.022	0.019	0.047	0.031	0.016	0.039	0.025	0.016	0.028	0.028	0.019	0.012	0.001	0.009	0.013	0.023	0.013	0.024
K^+	0.003	0.004	0.002	0.000	0.000	0.000	0.002	0.001	0.001	0.003	0.001	0.002	0.000	0.000	0.000	0.003	0.002	0.000	0.004	0.000	0.000	0.000	0.000	0.005	0.003	0.000	0.000	0.000	0.001	0.000	0.000	0.002	0.005
Total	0.938	0.927	0.989	0.951	0.940	0.917	0.922	0.925	0.913	0.971	0.974	0.962	0.973	1.026	0.965	0.965	0.982	0.987	0.911	0.955	0.971	0.955	0.896	0.949	0.926	0.903	0.968	0.940	0.933	0.928	1.002	0.949	0.968
Sr^{2+}	0.000	0.001	0.003	0.012	0.000	0.005	0.000	0.006	0.000	0.005	0.004	0.000	0.000	0.000	0.001	0.003	0.007	0.029	0.013	0.000	0.029	0.002	0.000	0.017	0.002	0.007	0.002	0.006	0.000	0.001	0.006	0.000	0.011
Ca^{2+}	1.926	1.998	1.985	1.905	1.977	2.021	2.088	1.997	2.003	1.916	2.074	1.973	1.992	2.015	2.079	1.976	2.083	1.962	2.039	1.972	1.939	1.984	2.061	2.038	2.019	2.025	2.055	2.012	2.014	2.036	2.000	1.935	1.978
K^+	0.003	0.004	0.002	0.000	0.000	0.000	0.002	0.001	0.001	0.003	0.001	0.002	0.000	0.000	0.000	0.003	0.002	0.000	0.004	0.000	0.000	0.000	0.000	0.005	0.003	0.000	0.000	0.000	0.001	0.000	0.000	0.002	0.005
Na^+	0.030	0.019	0.010	0.034	0.011	0.000	0.004	0.000	0.004	0.017	0.000	0.003	0.021	0.007	0.032	0.008	0.000	0.026	0.009	0.000	0.020	0.000	0.019	0.011	0.005	0.008	0.015	0.000	0.013	0.015	0.000	0.000	0.000
Total	1.958	2.021	2.001	1.950	1.988	2.026	2.094	2.004	2.007	1.941	2.079	1.978	2.013	2.022	2.113	1.990	2.091	2.016	2.065	1.973	1.988	1.987	2.080	2.071	2.029	2.040	2.072	2.018	2.028	2.051	2.005	1.937	1.994

II.II.XIII LUDLAMITE

Sample	#13B2			#13B3			#13B5	#13B6	#17B2									#17B5							
Wt%	2	4	5	1	2	3	3	2	2	3	4	5	6	7	8	9	11	1	2	3	5	6	7	8	9
P_2O_5	32.11	32.41	33.04	32.05	32.86	31.33	33.62	31.45	34.12	32.41	32.49	31.96	32.42	31.91	33.56	31.67	33.59	32.21	32.25	31.25	30.3	33.86	31.03	31.88	31.71
FeO	41.76	42.18	34.66	40.82	39.89	37.18	35.82	40.59	38.4	40.7	39.19	39.23	38.74	39	38.68	37.82	39.14	30.93	35.49	36.8	35.84	34.9	36.37	34.94	37.37
Fe_2O_3	0	0	0	2.82	0.65	5.04	0	3.61	0	0	0	0	0	0	0	1.24	0	4.01	0	0	2.44	0	2.53	0	0.46
MnO	4.24	3.89	4.29	5.97	8.46	7.88	9.67	3.02	8.6	5	8.33	8.24	8.85	8.33	8	8.33	7.42	8.87	10.25	8.97	8.64	10.81	8.78	11.17	8.68
CaO	0.06	0.05	5.39	0.06	0.02	0.15	0.17	0.08	0.38	1.03	0.12	0.09	0.07	0.05	0.15	0.09	0.12	5.54	0.28	0.13	0.17	0.12	0.14	0.12	0.39
MgO	0.31	0.42	0.3	0.37	0.3	0.21	0.15	0.95	0.38	0.33	0.3	0.28	0.43	0.25	0.44	0.25	0.3	0.27	0.47	0.42	0.46	0.35	0.39	0.45	0.37
K_2O	0.04	0.08	0.13	0	0.04	0.03	0.01	0.13	0.07	0.07	0.04	0	0.01	0.01	0.05	0.08	0.1	0.03	0.02	0	0.02	0	0	0.01	0.02
Al_2O_3	0.03	0	0.05	0.02	0.02	0	0.11	0.07	0	0.02	0.04	0.01	0	0.02	0.01	0	0.03	0.07	0.03	0.08	0.08	0.03	0.03	0.02	0.02
Na_2O	0.14	0.1	0.14	0.16	0.17	0.27	0.16	0.31	0.31	0.3	0.17	0.07	0.04	0.09	0.14	0.26	0.2	0.18	0.12	0.12	0.13	0.17	0.22	0.21	0.23
PbO	0.06	0.07	0	0	0.09	0.02	0.09	0.12	0.02	0.03	0.03	0	0.09	0	0	0.09	0.02	0.01	0	0	0.03	0	0.03	0.01	0
SiO_2	0.16	0.22	0.26	0.02	0.14	0.1	0.15	0	0.08	0.39	0.1	0.03	0.08	0.04	0.02	0.24	0.15	0.13	0.45	0.92	0.69	0.57	0.33	0.43	0.29
UO_3	0.07	0	0	0.08	0.02	0	0	0.07	0.01	0.01	0.04	0.09	0	0	0.03	0.01	0	0	0.04	0.07	0.07	0.06	0	0	0.02
Er_2O_3	0.29	0	0.25	0.26	0.12	0.09	0.04	0.14	0.1	0.05	0.08	0.09	0	0.01	0.05	0.22	0.1	0.01	0.09	0.04	0.02	0.13	0.02	0	0.04
Nd_2O_3	0.31	0	0	0.09	0	0	0.38	0.46	0.2	0.09	0	0	0	0	0.01	0.01	0.04	0.14	0.06	0.09	0.2	0	0.04	0.02	0
Total	79.58	79.42	78.51	82.72	82.78	82.3	80.37	81	82.67	80.43	80.93	80.09	80.73	79.71	81.14	80.31	81.21	82.4	79.55	78.89	79.09	81	79.91	79.26	79.6
a.p.f.u (calculus done basis on 8 oxygens)																									
P^{5+}	1.999	2.000	2.023	1.934	1.987	1.905	2.046	1.935	2.033	1.995	1.998	1.993	2.002	2.000	2.036	1.970	2.031	1.924	1.993	1.957	1.914	2.033	1.938	1.990	1.979
Si^{4+}	0.012	0.016	0.019	0.001	0.010	0.007	0.011	0.000	0.005	0.028	0.007	0.002	0.006	0.003	0.001	0.017	0.011	0.009	0.033	0.068	0.051	0.040	0.025	0.032	0.022
Total	2.010	2.016	2.041	1.935	1.997	1.912	2.057	1.935	2.038	2.023	2.005	1.995	2.008	2.003	2.037	1.988	2.041	1.934	2.026	2.025	1.965	2.074	1.963	2.021	2.000
U^{6+}	0.001	0.000	0.000	0.001	0.000	0.000	0.000	0.001	0.000	0.000	0.001	0.001	0.000	0.000	0.001	0.000	0.000	0.000	0.001	0.001	0.001	0.001	0.000	0.000	0.000
Er^{3+}	0.007	0.000	0.006	0.006	0.003	0.002	0.001	0.003	0.002	0.001	0.002	0.002	0.000	0.000	0.001	0.005	0.002	0.000	0.002	0.001	0.001	0.003	0.001	0.000	0.001
Nd^{3+}	0.008	0.000	0.000	0.002	0.000	0.000	0.010	0.012	0.005	0.002	0.000	0.000	0.000	0.000	0.000	0.000	0.001	0.004	0.002	0.002	0.005	0.000	0.001	0.001	0.000
Fe^{3+}	0.000	0.000	0.000	0.151	0.035	0.272	0.000	0.197	0.000	0.000	0.000	0.000	0.000	0.000	0.000	0.068	0.000	0.213	0.000	0.000	0.137	0.000	0.140	0.000	0.026
Al^{3+}	0.002	0.000	0.004	0.002	0.002	0.000	0.009	0.006	0.000	0.002	0.003	0.001	0.000	0.001	0.001	0.000	0.003	0.005	0.003	0.007	0.007	0.003	0.003	0.001	0.002
Pb^{2+}	0.001	0.001	0.000	0.000	0.002	0.000	0.002	0.002	0.000	0.001	0.001	0.000	0.002	0.000	0.000	0.002	0.000	0.000	0.000	0.000	0.001	0.000	0.001	0.000	0.000
Fe^{2+}	2.567	2.571	2.096	2.433	2.382	2.233	2.154	2.468	2.260	2.475	2.381	2.417	2.363	2.415	2.317	2.325	2.337	1.825	2.167	2.277	2.236	2.070	2.244	2.154	2.304
Mn^{2+}	0.264	0.240	0.263	0.360	0.512	0.479	0.589	0.186	0.513	0.308	0.512	0.514	0.546	0.523	0.486	0.518	0.449	0.530	0.634	0.562	0.546	0.649	0.548	0.697	0.542
Ca^{2+}	0.005	0.004	0.418	0.004	0.002	0.011	0.013	0.006	0.029	0.080	0.010	0.007	0.005	0.004	0.011	0.007	0.009	0.419	0.022	0.010	0.014	0.009	0.011	0.010	0.031
Mg^{2+}	0.034	0.045	0.033	0.040	0.032	0.023	0.016	0.103	0.040	0.036	0.032	0.031	0.047	0.028	0.047	0.027	0.032	0.029	0.052	0.046	0.051	0.037	0.042	0.050	0.041
K^{+}	0.004	0.008	0.012	0.000	0.004	0.003	0.001	0.012	0.006	0.006	0.004	0.000	0.001	0.001	0.004	0.007	0.009	0.003	0.002	0.000	0.002	0.000	0.000	0.001	0.002
Na^{+}	0.020	0.014	0.020	0.023	0.024	0.038	0.023	0.043	0.043	0.042	0.024	0.010	0.005	0.012	0.019	0.037	0.028	0.024	0.018	0.017	0.019	0.023	0.031	0.030	0.033
Total	2.914	2.883	2.850	3.021	2.996	3.062	2.816	3.039	2.899	2.954	2.968	2.984	2.969	2.983	2.887	2.997	2.870	3.052	2.901	2.923	3.018	2.795	3.022	2.943	2.980

II.II.XIV MONTEBRASITE

Sample	#4B7									#7aB1	#7aB1	#7aB2	#7aB4			
wt%	1	2	3	5	6	7	8	9	15	1	2	2	3	4	5	8
P_2O_5	47.55	46.77	47.47	48.21	47.51	47.02	47.12	48.70	47.35	48.99	48.85	46.95	46.40	45.83	47.68	47.63
Al_2O_3	36.17	34.94	35.68	35.62	35.34	35.65	36.57	35.35	35.27	37.00	36.40	35.13	35.87	36.19	36.27	36.76
Li_2O*	9.59	9.63	9.60	9.88	9.79	9.62	9.29	10.11	9.65	9.93	10.09	9.65	9.24	8.92	9.62	9.60
FeO	0.00	0.00	0.00	0.00	0.05	0.10	0.15	0.00	0.01	0.00	0.00	0.13	0.03	0.19	0.06	0.00
Fe_2O_3	0.00	0.00	0.00	0.00	0.00	0.00	0.00	0.00	0.00	0.00	0.00	0.00	0.00	0.00	0.00	0.00
CaO	0.00	0.00	0.01	0.09	0.00	0.18	0.00	0.00	0.15	0.15	0.00	0.00	0.00	0.02	0.09	0.00
MgO	0.03	0.00	0.00	0.00	0.00	0.09	0.10	0.02	0.08	0.00	0.02	0.09	0.03	0.08	0.00	0.00
K_2O	0.00	0.04	0.04	0.00	0.06	0.07	0.05	0.00	0.04	0.00	0.00	0.00	0.00	0.01	0.01	0.02
Na_2O	0.06	0.07	0.05	0.00	0.00	0.05	0.07	0.04	0.00	0.21	0.00	0.01	0.06	0.07	0.05	0.00
Ta_2O_5	1.38	0.65	0.00	0.00	0.00	0.00	0.00	0.36	0.89	0.00	0.00	0.40	1.00	0.01	0.00	0.00
Nb_2O_5	0.00	0.28	0.00	0.19	0.19	0.74	0.65	0.00	0.00	0.19	0.19	0.00	1.11	0.09	0.00	0.00
SiO_2	0.09	0.31	0.02	0.00	0.18	0.60	0.00	0.02	0.12	0.22	0.06	0.10	0.02	0.00	0.02	0.00
Lu_2O_3	0.00	0.38	0.00	0.00	0.53	0.00	0.26	0.00	0.01	0.00	0.00	0.89	0.85	0.87	0.61	0.27
Dy_2O_3	0.00	0.00	0.43	0.96	0.00	0.62	1.17	0.00	0.00	0.00	0.00	0.00	0.00	1.21	0.00	0.00
Nd_2O_3	0.38	0.24	1.58	0.48	0.34	0.00	0.14	0.00	1.05	0.63	0.97	0.98	0.00	0.10	0.00	0.58
Ce_2O_3	2.21	0.00	0.57	1.16	0.00	0.59	1.12	0.00	0.83	0.00	0.00	0.00	2.82	1.71	1.98	0.00
La_2O_3	0.20	0.14	0.34	0.22	0.14	0.34	0.00	0.00	0.13	0.00	0.00	0.00	0.00	0.11	0.11	0.35
Cl	0.00	0.06	0.00	0.00	0.03	0.00	0.02	0.01	0.00	0.00	0.00	0.00	0.00	0.00	0.00	0.06
F	1.03	1.26	1.05	0.72	1.93	0.01	0.69	0.37	0.36	0.55	0.35	1.27	0.00	1.21	0.53	0.91
Total	98.69	94.76	96.84	97.53	96.07	95.67	97.40	94.97	95.94	97.87	96.92	95.58	97.44	96.62	97.02	96.18
a.p.f.u. (calculus done on the basis of 4 oxygens)																
P^{5+}	0.967	0.972	0.976	0.981	0.978	0.962	0.959	0.985	0.975	0.976	0.981	0.976	0.954	0.954	0.970	0.974
Si^{4+}	0.002	0.008	0.001	0.000	0.004	0.015	0.000	0.000	0.003	0.005	0.002	0.003	0.001	0.000	0.001	0.000
Total	0.969	0.980	0.976	0.981	0.982	0.976	0.959	0.986	0.978	0.981	0.983	0.979	0.954	0.954	0.970	0.974
Ta^{5+}	0.009	0.004	0.000	0.000	0.000	0.000	0.000	0.002	0.006	0.000	0.000	0.003	0.007	0.000	0.000	0.000
Nb^{5+}	0.000	0.003	0.000	0.002	0.002	0.008	0.007	0.000	0.000	0.002	0.002	0.000	0.012	0.001	0.000	0.000
Lu^{3+}	0.000	0.003	0.000	0.000	0.004	0.000	0.002	0.000	0.000	0.000	0.000	0.007	0.006	0.006	0.004	0.002
Dy^{3+}	0.000	0.000	0.003	0.007	0.000	0.005	0.009	0.000	0.000	0.000	0.000	0.000	0.000	0.010	0.000	0.000
Nd^{3+}	0.003	0.002	0.014	0.004	0.003	0.000	0.001	0.000	0.009	0.005	0.008	0.009	0.000	0.001	0.000	0.005
Ce^{3+}	0.019	0.000	0.005	0.010	0.000	0.005	0.010	0.000	0.007	0.000	0.000	0.000	0.025	0.015	0.017	0.000
La^{3+}	0.002	0.001	0.003	0.002	0.001	0.003	0.000	0.000	0.001	0.000	0.000	0.000	0.000	0.001	0.001	0.003
Fe^{3+}	0.000	0.000	0.000	0.000	0.000	0.000	0.000	0.000	0.000	0.000	0.000	0.000	0.000	0.000	0.000	0.000
Al^{3+}	1.023	1.011	1.021	1.009	1.012	1.015	1.037	0.996	1.011	1.026	1.018	1.017	1.026	1.049	1.027	1.046
Fe^{2+}	0.000	0.000	0.000	0.000	0.001	0.002	0.003	0.000	0.000	0.000	0.000	0.003	0.001	0.004	0.001	0.000
Ca^{2+}	0.000	0.000	0.000	0.002	0.000	0.005	0.000	0.000	0.004	0.004	0.000	0.000	0.000	0.000	0.002	0.000
Mg^{2+}	0.001	0.000	0.000	0.000	0.000	0.003	0.004	0.001	0.003	0.000	0.001	0.003	0.001	0.003	0.000	0.000
K^{+}	0.000	0.001	0.001	0.000	0.002	0.002	0.001	0.000	0.001	0.000	0.000	0.000	0.000	0.000	0.000	0.001
Na^{+}	0.003	0.003	0.002	0.000	0.000	0.002	0.003	0.002	0.000	0.010	0.000	0.001	0.003	0.003	0.002	0.000
Li^{+}	0.926	0.951	0.937	0.955	0.956	0.935	0.899	0.972	0.943	0.940	0.963	0.953	0.903	0.883	0.929	0.932
Total	1.987	1.980	1.987	1.992	1.982	1.985	1.976	1.973	1.986	1.986	1.991	1.994	1.983	1.977	1.985	1.989
OH^{-}	0.922	0.900	0.919	0.945	0.850	1.000	0.947	0.972	0.973	0.959	0.974	0.901	1.000	0.906	0.960	0.928
Cl^{-}	0	0.003	0.000	0.000	0.001	0.000	0.001	0.000	0.000	0.000	0.000	0.000	0.000	0.000	0.000	0.002
F^{-}	0.078	0.098	0.081	0.055	0.149	0.001	0.053	0.028	0.027	0.041	0.026	0.099	0.000	0.094	0.040	0.070
Total	1.000	1.000	1.000	1.000	1.000	1.000	1.000	1.000	1.000	1.000	1.000	1.000	1.000	1.000	1.000	1.000
Li wt.%	4.46	4.47	4.46	4.59	4.55	4.47	4.32	4.70	4.48	4.62	4.69	4.48	4.30	4.15	4.47	4.46

II.II.XV ILMENITE

Sample	#18aB1					#18aB2				#19B2	#19B3			
wt%	1	2	3	4	5	1	2	3	4	1	1	2	3	4
TiO_2	52.69	52.89	52.87	52.58	52.97	51.64	51.77	52.28	49.82	52.32	51.58	51.52	51.10	51.15
FeO	42.75	42.68	42.70	42.61	42.69	41.49	41.32	42.54	41.73	42.89	42.65	42.83	42.50	42.28
MnO	3.31	3.49	3.25	3.31	3.39	3.30	3.21	3.18	3.36	2.50	2.46	2.36	2.50	2.54
MgO	0.00	0.01	0.01	0.00	0.03	0.03	0.02	0.00	0.04	0.00	0.00	0.02	0.03	0.00
ZnO	0.04	0.02	0.01	0.00	0.00	0.00	0.12	0.02	0.09	0.04	0.06	0.01	0.16	0.10
Nb_2O_5	0.14	0.11	0.17	0.10	0.17	0.05	0.08	0.13	0.00	0.15	0.19	0.17	0.13	0.16
WO_3	0.10	0.00	0.00	0.00	0.00	0.18	0.00	0.03	0.15	0.17	0.00	0.15	0.27	0.18
BaO	0.02	0.04	0.11	0.01	0.00	0.10	0.07	0.10	0.04	0.06	0.09	0.08	0.14	0.03
Al_2O_3	0.00	0.00	0.00	0.01	0.01	0.20	0.18	0.01	0.07	0.00	0.02	0.03	0.01	0.01
Na_2O	0.02	0.03	0.01	0.01	0.00	0.02	0.01	0.00	0.03	0.01	0.03	0.00	0.00	0.00
SiO_2	0.04	0.04	0.05	0.04	0.05	0.11	0.11	0.07	0.32	0.04	0.04	0.02	0.03	0.08
ZrO_2	0.00	0.00	0.01	0.01	0.05	0.00	0.00	0.03	0.01	0.05	0.03	0.03	0.00	0.04
CoO	0.06	0.04	0.03	0.03	0.06	0.04	0.06	0.10	0.02	0.03	0.09	0.03	0.06	0.06
PbO	0.12	0.04	0.00	0.00	0.06	0.00	0.00	0.03	0.09	0.04	0.01	0.04	0.03	0.05
Ta_2O_5	0.01	0.00	0.00	0.00	0.00	0.00	0.00	0.10	0.00	0.20	0.15	0.01	0.12	0.13
UO_2	0.00	0.02	0.00	0.00	0.08	0.09	0.06	0.00	0.00	0.13	0.08	0.04	0.00	0.00
HfO_2	0.16	0.00	0.00	0.16	0.00	0.00	0.07	0.22	0.15	0.00	0.00	0.00	0.10	0.00
Total	99.45	99.40	99.23	98.86	99.55	97.24	97.08	98.82	95.92	98.62	97.47	97.35	97.18	96.81
a.p.f.u (calculus done on the basis of 6 oxygens)														
Ti^{4+}	2.009	2.012	2.015	2.012	2.013	2.006	2.013	2.006	1.971	2.010	2.006	2.005	1.997	2.002
Si^{4+}	0.002	0.002	0.002	0.002	0.003	0.006	0.006	0.004	0.017	0.002	0.002	0.001	0.001	0.004
Ti Position	2.010	2.014	2.017	2.014	2.015	2.012	2.019	2.009	1.988	2.012	2.008	2.006	1.999	2.006
W^{6+}	0.001	0.000	0.000	0.000	0.000	0.002	0.000	0.000	0.002	0.002	0.000	0.002	0.004	0.002
Nb^{5+}	0.003	0.003	0.004	0.002	0.004	0.001	0.002	0.003	0.000	0.004	0.004	0.004	0.003	0.004
Ta^{5+}	0.000	0.000	0.000	0.000	0.000	0.000	0.000	0.001	0.000	0.003	0.002	0.000	0.002	0.002
Zr^{4+}	0.000	0.000	0.000	0.000	0.001	0.000	0.000	0.001	0.000	0.001	0.001	0.001	0.000	0.001
U^{4+}	0.000	0.000	0.000	0.000	0.001	0.001	0.001	0.000	0.000	0.002	0.001	0.001	0.000	0.000
Hf^{4+}	0.002	0.000	0.000	0.002	0.000	0.000	0.001	0.003	0.002	0.000	0.000	0.000	0.002	0.000
Al^{3+}	0.000	0.000	0.000	0.001	0.001	0.012	0.011	0.001	0.005	0.000	0.001	0.002	0.001	0.001
Fe^{2+}	1.812	1.805	1.809	1.813	1.803	1.792	1.786	1.814	1.835	1.831	1.844	1.853	1.847	1.839
Mn^{2+}	0.142	0.150	0.140	0.142	0.145	0.145	0.140	0.137	0.150	0.108	0.108	0.104	0.110	0.112
Mg^{2+}	0.000	0.001	0.000	0.000	0.002	0.002	0.002	0.000	0.003	0.000	0.000	0.002	0.002	0.000
Zn^{2+}	0.002	0.001	0.000	0.000	0.000	0.000	0.005	0.001	0.004	0.002	0.002	0.000	0.006	0.004
Ba^{2+}	0.001	0.001	0.002	0.000	0.000	0.002	0.002	0.002	0.001	0.001	0.002	0.002	0.003	0.001
Co^{2+}	0.002	0.002	0.001	0.001	0.003	0.002	0.003	0.004	0.001	0.001	0.004	0.001	0.003	0.003
Pb^{2+}	0.002	0.001	0.000	0.000	0.001	0.000	0.000	0.000	0.001	0.001	0.000	0.001	0.000	0.001
Na^{+}	0.002	0.003	0.001	0.001	0.000	0.002	0.001	0.000	0.003	0.001	0.003	0.000	0.000	0.000
Fe Position	1.969	1.965	1.958	1.963	1.960	1.960	1.952	1.968	2.007	1.956	1.971	1.971	1.982	1.969

II.II.XVI COLUMBITE-TANTALITE

Sample	#7aB5	#7bB7		#13B1	
Zone	Pegmatite 1			Pegmatite 2	
wt%	4	1	2	1	2
Ta_2O_5	19.71	42.75	42.23	45.65	41.15
Nb_2O_5	59.41	40.22	40.15	29.95	37.21
Fe_2O_3	0.00	0.00	0.00	4.99	3.04
FeO	11.84	10.74	10.79	6.68	8.48
MnO	6.75	5.99	6.09	6.13	5.82
TiO_2	0.41	0.33	0.51	0.56	0.29
SiO_2	0.11	0.25	0.24	0.41	1.47
Tm_2O_3	0.42	0.77	0.31	0.70	0.66
Ce_2O_3	0.48	0.30	0.00	0.70	0.55
UO_2	0.01	0.14	0.01	0.10	0.10
PbO_2	0.11	0.10	0.02	0.13	0.07
ZrO_2	0.08	0.14	0.13	0.05	0.02
Y_2O_3	0.18	0.12	0.15	0.06	0.15
Total	99.51	101.84	100.62	96.10	99.01
a.p.f.u (calculus done on the basis of 6 oxygen)					
U^{4+}	0.000	0.002	0.000	0.002	0.002
Pb^{4+}	0.002	0.002	0.000	0.002	0.001
Zr^{4+}	0.003	0.005	0.004	0.002	0.001
Si^{4+}	0.007	0.016	0.016	0.029	0.096
Tm^{3+}	0.008	0.016	0.007	0.016	0.013
Ce^{3+}	0.011	0.007	0.000	0.018	0.013
Y^{3+}	0.006	0.004	0.005	0.002	0.005
Fe^{3+}	0.000	0.000	0.000	0.151	0.031
Fe^{2+}	0.604	0.590	0.597	0.397	0.466
Mn^{2+}	0.349	0.334	0.341	0.369	0.324
Total A	0.989	0.976	0.971	0.987	0.953
Ta^{5+}	0.327	0.764	0.760	0.882	0.735
Nb^{5+}	1.638	1.196	1.201	0.962	1.106
Ti^{4+}	0.019	0.016	0.025	0.030	0.014
Fe^{3+}	0.000	0.000	0.000	0.116	0.119
Total B	1.984	1.976	1.987	1.989	1.974

II.II.XVII PYRITE

Sample	#11bB5				#11cB1	#11cB3			#12B6		
Zone	Proximal MAZ								Distal MAZ		
wt%	2	3	4	5	1	1	2	3	1	2	3
Fe	45.10	44.29	44.84	44.97	44.79	45.08	44.83	44.63	45.24	46.17	45.53
S	51.74	49.32	50.79	50.99	50.75	51.92	52.31	51.96	52.14	52.73	52.09
As	0.05	3.15	0.10	0.07	0.05	0.16	0.15	0.15	0.10	0.10	0.02
Ni	0.03	0.00	0.34	0.30	0.02	0.00	0.05	0.02	0.64	0.05	0.04
Pb	0.00	0.00	0.00	0.10	0.23	0.00	0.02	0.00	0.03	0.00	0.09
W	0.13	0.07	0.00	0.12	0.00	0.04	0.21	0.18	0.00	0.00	0.00
Mo	0.04	0.06	0.07	0.05	0.09	0.03	0.08	0.05	0.04	0.08	0.06
Zn	0.00	0.09	0.00	0.09	0.03	0.15	0.01	0.00	0.00	0.00	0.02
Mn	0.00	0.02	0.00	0.00	0.01	0.06	0.13	0.03	0.00	0.02	0.04
Co	0.00	0.00	0.03	0.02	0.00	0.00	0.02	0.00	0.05	0.00	0.00
Cu	0.08	0.00	0.02	0.03	0.07	0.03	0.00	0.00	0.02	0.00	0.34
Total	97.18	96.99	96.18	96.74	96.04	97.47	97.79	97.01	98.27	99.14	98.22
a.p.f.u (calculus done on the basis of 3 ions)											
Fe	0.999	1.002	1.006	1.004	1.007	0.995	0.986	0.989	0.992	1.002	0.999
S	1.996	1.942	1.984	1.983	1.987	1.996	2.004	2.005	1.991	1.994	1.991
As	0.001	0.053	0.002	0.001	0.001	0.003	0.003	0.002	0.002	0.002	0.000
Ni	0.001	0.000	0.007	0.006	0.001	0.000	0.001	0.000	0.013	0.001	0.001
Pb	0.000	0.000	0.000	0.001	0.001	0.000	0.000	0.000	0.000	0.000	0.001
W	0.001	0.001	0.000	0.001	0.000	0.000	0.001	0.001	0.000	0.000	0.000
Mo	0.001	0.001	0.001	0.001	0.001	0.000	0.001	0.001	0.001	0.001	0.001
Zn	0.000	0.002	0.000	0.002	0.001	0.003	0.000	0.000	0.000	0.000	0.000
Mn	0.000	0.000	0.000	0.000	0.000	0.001	0.003	0.001	0.000	0.000	0.001
Co	0.000	0.000	0.001	0.001	0.000	0.000	0.000	0.000	0.001	0.000	0.000
Cu	0.002	0.000	0.001	0.001	0.001	0.001	0.000	0.000	0.001	0.000	0.007

II.II.XVIII ARSENOPYRITE

Sample	#11bB2		#12B3			#12B5		#12B6
Zone	Proximal MAZ		Distal MAZ					
wt%	1	2	1	2	3	1	2	1
As	50.00	49.32	48.90	47.89	48.73	46.51	45.65	44.51
Fe	26.43	30.41	28.03	27.90	27.66	32.29	34.21	33.34
S	15.53	16.11	16.68	17.16	17.19	18.37	19.58	19.60
Co	2.34	1.62	0.82	0.97	2.77	0.98	0.05	0.36
Ni	4.61	1.13	4.82	5.09	3.62	0.72	0.20	1.01
Sb	0.00	0.06	0.00	0.05	0.04	0.00	0.00	0.05
Pb	0.00	0.04	0.00	0.02	0.01	0.06	0.10	0.00
Au	0.00	0.00	0.06	0.00	0.02	0.07	0.05	0.03
Ag	0.00	0.04	0.00	0.05	0.02	0.03	0.00	0.00
Mo	0.00	0.02	0.00	0.05	0.02	0.01	0.02	0.01
In	0.00	0.00	0.00	0.05	0.00	0.00	0.03	0.00
Mn	0.04	0.00	0.02	0.04	0.00	0.01	0.00	0.02
Cu	0.00	0.00	0.03	0.02	0.00	0.00	0.00	0.00
Total	98.97	98.76	99.40	99.38	100.08	99.04	100.17	99.00
a.p.f.u (calculus done on the basis of 3 ions)								
Fe	0.814	0.932	0.850	0.842	0.830	0.963	0.999	0.980
Ni	0.135	0.033	0.139	0.146	0.103	0.020	0.006	0.028
Co	0.068	0.047	0.024	0.028	0.079	0.028	0.001	0.010
Cu	0.000	0.000	0.001	0.001	0.000	0.000	0.000	0.000
Pb	0.000	0.000	0.000	0.000	0.000	0.001	0.001	0.000
Mo	0.000	0.000	0.000	0.001	0.000	0.000	0.000	0.000
In	0.000	0.000	0.000	0.001	0.000	0.000	0.000	0.000
Mn	0.001	0.000	0.001	0.001	0.000	0.000	0.000	0.001
Au	0.000	0.000	0.001	0.000	0.000	0.001	0.000	0.000
Ag	0.000	0.001	0.000	0.001	0.000	0.000	0.000	0.000
Fe Position	1.019	1.013	1.014	1.020	1.012	1.013	1.008	1.019
As	1.000	0.999	1.000	0.999	1.000	1.000	0.993	0.976
S	0.000	0.000	0.000	0.000	0.000	0.000	0.000	0.004
Sb	0.000	0.001	0.000	0.001	0.001	0.000	0.000	0.001
As Position	1.000	1.000	1.000	1.000	1.000	1.000	0.993	0.980
As	0.148	0.127	0.105	0.078	0.090	0.034	0.000	0.000
S	0.833	0.860	0.880	0.902	0.898	0.954	0.995	1.000
S Position	0.981	0.987	0.985	0.979	0.988	0.987	0.995	1.000

II.II.XIX SPHALERITE

Sample	#8bB7	#9bB9	#13B3			#14B6				
Zone	Pegmatite 1		Pegmatite 2							
wt%	1	1	1	2	3	1	2	3	4	5
Zn	62.88	62.68	60.39	60.78	60.62	60.83	60.73	60.04	60.47	60.92
S	32.83	33.31	33.57	33.57	33.70	33.11	33.09	33.08	33.04	33.56
Fe	0.60	0.98	5.48	5.46	5.50	3.45	3.38	3.23	3.29	3.14
Cd	0.10	0.02	0.22	0.22	0.21	0.22	0.34	0.26	0.28	0.30
Cu	0.12	0.18	0.00	0.00	0.00	0.23	0.13	0.17	0.16	0.19
Mn	0.00	0.36	0.05	0.02	0.02	0.06	0.06	0.00	0.06	0.03
Sn	0.01	0.03	0.02	0.00	0.00	0.00	0.02	0.01	0.00	0.00
Pb	0.00	0.02	0.00	0.05	0.08	0.00	0.00	0.02	0.01	0.06
Au	0.03	0.00	0.00	0.00	0.00	0.01	0.00	0.00	0.00	0.00
Ag	0.06	0.01	0.00	0.02	0.00	0.02	0.00	0.00	0.01	0.01
Mo	0.13	0.08	0.13	0.14	0.09	0.13	0.11	0.13	0.13	0.13
In	0.00	0.07	0.00	0.00	0.00	0.09	0.01	0.00	0.04	0.00
As	0.02	0.00	0.01	0.04	0.01	0.00	0.03	0.00	0.01	0.00
Se	0.01	0.00	0.00	0.00	0.01	0.01	0.00	0.00	0.00	0.02
Sb	0.00	0.00	0.07	0.01	0.04	0.03	0.00	0.00	0.09	0.04
Co	0.00	0.00	0.01	0.01	0.00	0.00	0.03	0.03	0.02	0.01
Ga	0.00	0.00	0.00	0.01	0.02	0.00	0.00	0.00	0.03	0.09
Total	96.79	97.74	99.95	100.33	100.29	98.17	97.94	96.97	97.63	98.50
a.p.f.u (calculus done on the basis of 3 ions)										
S	1.023	1.025	1.010	1.007	1.010	1.015	1.017	1.024	1.018	1.024
Se	0.000	0.000	0.000	0.000	0.000	0.000	0.000	0.000	0.000	0.000
Sb	0.000	0.000	0.001	0.000	0.000	0.000	0.000	0.000	0.001	0.000
S Position	1.023	1.025	1.010	1.007	1.010	1.016	1.017	1.024	1.019	1.024
Zn	0.961	0.946	0.891	0.894	0.891	0.915	0.915	0.911	0.914	0.911
Fe	0.011	0.017	0.095	0.094	0.095	0.061	0.060	0.057	0.058	0.055
Cd	0.001	0.000	0.002	0.002	0.002	0.002	0.003	0.002	0.002	0.003
Cu	0.002	0.003	0.000	0.000	0.000	0.004	0.002	0.003	0.003	0.003
Mn	0.000	0.006	0.001	0.000	0.000	0.001	0.001	0.000	0.001	0.001
Sn	0.000	0.000	0.000	0.000	0.000	0.000	0.000	0.000	0.000	0.000
Pb	0.000	0.000	0.000	0.000	0.000	0.000	0.000	0.000	0.000	0.000
Au	0.000	0.000	0.000	0.000	0.000	0.000	0.000	0.000	0.000	0.000
Ag	0.001	0.000	0.000	0.000	0.000	0.000	0.000	0.000	0.000	0.000
Mo	0.001	0.001	0.001	0.001	0.001	0.001	0.001	0.001	0.001	0.001
In	0.000	0.001	0.000	0.000	0.000	0.001	0.000	0.000	0.000	0.000
As	0.000	0.000	0.000	0.001	0.000	0.000	0.000	0.000	0.000	0.000
Co	0.000	0.000	0.000	0.000	0.000	0.000	0.001	0.001	0.000	0.000
Ga	0.000	0.000	0.000	0.000	0.000	0.000	0.000	0.000	0.000	0.001
Zn Position	0.977	0.975	0.990	0.993	0.990	0.984	0.983	0.976	0.981	0.975